Exploring the molecular diversity and biomedicinal potential of marine invertebrates and South African actinomycetes for tuberculosis drug discovery

Thesis submitted for the award of Doctor of Philosophy degree in the department of Chemistry, University of Cape Town,

Kojo Sekyi Acquah

Supervisor: Prof. David W. Gammon

Department of Chemistry, University of Cape Town (UCT)

Co-supervisor: Prof. Denzil R. Beukes

School of Pharmacy, University of the Western Cape (UWC)

Co-supervisor: Dr. Paul R. Meyers

Department of Molecular and Cell Biology, University of Cape Town (UCT)

Co-supervisor: Prof. Digby F. Warner

Institute of Infectious Disease and Molecular Medicine, University of Cape Town (UCT)

March 2021

Declaration

I hereby declare that this thesis is my original work produced from research undertaken under supervision and has not been presented for a degree in this university or another university elsewhere for the award of any other degree.

Signed by candidate

…….

Kojo Sekyi Acquah

Declaration on the Inclusion of Publication

I confirm that I have been granted permission by the University of Cape Town's Doctoral Degrees Board to include the following publication in my PhD thesis, and where co-authorships are involved, my co-authors have agreed that I may include the publication:

> **Acquah, K.S.**; Beukes, D.R.; Warner, D.F.; Meyers, P.R.; Sunassee, S.N.; Maglangit, F.; Deng, H.; Jaspars, M.; Gammon, D.W. Novel South African Rare Actinomycete *Kribbella speibonae* Strain SK5: A Prolific Producer of Hydroxamate Siderophores Including New Dehydroxylated Congeners. *Molecules* 2020, 25, 2979. https://doi.org/10.3390/molecules25132979

Signature: Signed by candidate Date 6th April 2021

Student Name: Kojo Sekyi Acquah Student Number: ACQKOJ001

Dedication

In loving memory of my parents Mr. Charles Richmond Acquah and Madam Agnes Sarkwah.

Acknowledgements

I would like to thank my initial supervisor Dr. Suthananda N. Sunassee, for giving me the opportunity and setting me up to work on these two fascinating research projects for my PhD. My PhD study and this thesis is possible because of the supervision, support, direction, dedication, motivation, encouragement, and mentorship I received from my supervisors Prof. David W. Gammon, Prof. Denzil R. Beukes, Dr. Paul R. Meyers and Prof. Digby F. Warner for which I am eternally grateful.

I appreciate the supervision, support, mentorship, and warm reception I received from Prof. Marcel Jaspars, Dr. Hai Deng, Dr. Rainer Ebel and the students and scientists at the Marine Biodiscovery Center, School of Natural Sciences, University of Aberdeen before, during and after my doctoral research visits in 2017 and 2018.

I acknowledge Audrey Jordaan and Ronnett Seldon of the University of Cape Town's Molecular Mycobacteriology Research Unit for assistance with antimycobacterial assays and Lameeza Jakoet of the same Unit for administrative assistance.

I acknowledge Prof. Edith Antunes and the students and scientists at the Marine BioDiscovery Research Group of the University of the Western Cape for their assistance and support.

I thank all members of the UCT Department of Chemistry and Molecular and Cell biology, especially my lab mates Dr. Godwin Dziwornu, Dr. Daniel Watson and Christopher de Cerf for their assistance and camaraderie. My stay in Cape Town was fun and homely because of the love and support I received from my Ghanaian family at UCT (Dr. Godwin Dziwornu, Miss Henrietta Attram, Constance Korkor, Samuel Adadey, Richmond Akoto and Dr. Naomi Kumi).

I am very grateful for the financial support I received from the South African Medical Research Council through the Strategic Health Innovation Partnerships initiative (to Prof Digby Warner), Newton Advanced Fellowship Award (NA160057) (to Dr. Suthananda N. Sunassee and Prof. Marcel Jaspars), and the University of Cape Town.

Most importantly, I thank the almighty God for life, provision and good health throughout my studies. I am very grateful to my family and loved ones for the continuous love and support.

Abstract

Tuberculosis (TB) which is caused by *Mycobacterium tuberculosis* (Mtb), is the leading cause of death from a single infectious disease and remains a global health threat. Although there is medicine for treating TB, it still kills millions each year. This is due to a lengthy and demanding TB treatment regimen with associated problems of adverse drug-drug interactions and toxicities. Several resistant strains of Mtb, which are difficult and more expensive to treat, have also emerged. Therefore, there is a need to discover new potent and safe TB drugs to effectively treat Mtb with its resistant strains. Less explored and biodiversity-rich ecosystems such as the marine environment and South Africa (SA)'s fauna and flora have been a source of new bioactive natural products (NPs). A range of marine invertebrates and SA actinomycetes were therefore studied for the discovery of new antimycobacterial NPs.

Several organic and aqueous marine invertebrate extracts were screened for their *in vitro* inhibitory activity against the Mtb strain H37Rv. The chemical components of two out of 54 active extracts were dereplicated using ^{1}H NMR, HR-LCMS with GNPS molecular networking. The extracts were subsequently subjected to an activity-guided isolation process to yield heteronemin from *Hyrtios reticulatus* extract, and bengamides P and Q from *Jaspis splendens* extract. A new bengamide derivative was putatively identified in the molecular network of *Jaspis splendens* extract, and its structure predicted based on the similarity of its MS/MS fragmentation pattern to that of other bengamides. The isolated bioactive metabolites and semi-pure fractions exhibited antimycobacterial activity with MIC_{90} in the range of < 0.24 to 62.50 µg/mL. This is first report of antitubercular activity of bengamides P and Q.

In studies on actinomycetes, the organic extract of a liquid culture of the South African *Streptomyces* strain Muiz4Y exhibited antimycobacterial activity against *Mycobacterium aurum* strain A+ and Mtb strain H37Rv. HR-LCMS analysis of the crude extract for dereplication suggested the presence of new compounds. A bioactivity, spectroscopy and spectrometry guided isolation procedure led to the isolation of three new natural products, a β-carboline alkaloid (1-(1,2-dihydroxyethyl)-1,2,3,4-tetrahydro-β-carboline-3-carboxylic acid), a peptide (*N*-(2-phenylacetyl)-serine), and a glycosylated lactone (4-*O*-(β-glucopyranosyl)-5-(hydroxymethyl)-3-

(4-methylpentyl)-5,6-dihydro-2H-pyran-2-one), together with known compounds 3,6-bis(phenylmethyl)-2,5-piperazinedione and 2,4,6-triphenylhex-1-ene. The structures of the isolated compounds were elucidated based on spectroscopic methods including 1D and 2D NMR, MS, as well as by comparison with the relevant literature. Only 2,4,6-triphenylhex-1-ene exhibited antimycobacterial activity against Mtb strain H37Rv with an MIC_{90} of 5.8 µg/mL.

The novel rare South African Actinomycete *Kribbella speibonae* strain SK5 exhibited antimycobacterial activity against *Mycobacterium aurum* A+. Dereplicating the crude extract of a large-scale culture of strain SK5 using ^{1}H NMR, genome mining and HR-LCMS with GNPS molecular networking showed that it is a prolific producer of hydroxamate siderophores including new congeners. Two new analogues, dehydroxylated desferrioxamines, speibonoxamine and desoxy-desferrioxamine D_1, were isolated, together with four known hydroxamates, desferrioxamine D_1, desferrioxamine B, desoxy-nocardamine and nocardamine, and a diketopiperazine (DKP). The isolated compounds were characterized by the analysis of HRESIMS and 1D and 2D NMR data, as well as by comparison with the relevant literature. Three new dehydroxy desferrioxamine derivatives were tentatively identified in the molecular network of *K. speibonae* strain SK5 extracts, and structures were proposed based on their MS/MS fragmentation patterns. A plausible *spb* biosynthetic pathway was proposed. To the best of our knowledge, this is the first report of the isolation of desferrioxamines from the actinobacterial genus *Kribbella*. The isolated compounds were inactive against Mtb strain H37Rv and *Mycobacterium aurum* A+.

This study confirmed the marine environment as a source of new antimycobacterial NPs and established South African actinomycete as a source of new bioactive NPs.

Abbreviations

AI	Artificial Intelligence
AIDS	Acquired Immunodeficiency Syndrome
ADC	Antibody-Drug Conjugate
BCG	Bacille Calmette-Guérin
BGC	Biosynthetic Gene Cluster
CC	Column Chromatography
CE	Capillary Electrophoresis
COSY	Homonuclear Correlation Spectroscopy
DAD	Diode-Array Detection
DR	Drug Resistant
EI	Electron Impact
ELSD	Evaporative Light Scattering Detector
ESI	Electrospray Ionization
EtOAc	Ethyl Acetate
EMEA	European Medicine Agency
FDA	Food and Drugs Authority
FTIR	Fourier-Transform Infrared
FCC	Flash Column Chromatography
GC	Gas Chromatography
GNPS	Global Natural Product Social Molecular Networking
HSQC	Heteronuclear Single Quantum Coherence Spectroscopy

HMBC	Heteronuclear Multiple Bond Correlation
HPLC	High-Performance Liquid Chromatography
HIV	Human Immunodeficiency Virus
HR	High Resolution
IR	Infra-Red Spectroscopy
LC	Liquid Chromatography
Mtb	*Mycobacterium tuberculosis*
MDR	Multi Drug Resistant
MIC	Minimum Inhibition Concentration
MeOH	Methanol
MTC	*Mycobacterium tuberculosis* Complex
MALDI	Matrix-Assisted Laser Desorption/Ionization
MNP	Marine Natural Product
MS	Mass Spectrometry
NCI	National Cancer Institute
NP	Natural Product
NMR	Nuclear Magnetic Resonance Spectroscopy
NRPS	Non-Ribosomal Peptide Synthetase
OSMAC	One Strain Many Compounds
PKS	Polyketide Synthase
PDA	Photodiode-Array Detection
QTOF	Quadrupole Time of Flight

RI	Refractive Index
ROV	Remotely Operated Vehicle
TB	Tuberculosis
TDR	Totally Drug Resistant
TLC	Thin-Layer Chromatography
TOCSY	Total Correlation Spectroscopy
TOF	Time-of-Flight
TST	Tuberculin Skin Test
tr	Retention Time
SCUBA	Self-Contained Underwater Breathing Apparatus
SDG	Sustainable Development Goal
SPE	Solid-Phase Extraction
UN	United Nations
UV	Ultraviolet Light
uHPLC	Ultra-High-Performance Liquid Chromatography
VIS	Visible Light
WHO	World Health Organisation
XDR	Extensively Drug Resistant

Table of contents

List of Figures

List of Tables

Chapter One: Introduction

1.1 Background

Tuberculosis (TB) is an ancient infectious disease estimated to have been in existence for the past three million years.[1] The discovery of the causative organism, *Mycobacterium tuberculosis* (Mtb) by Robert Koch in 1882 gave hope, and was crucial in the development of the tuberculin skin tests in 1930, the Bacille Calmette-Guérin (BCG) vaccine in 1921, streptomycin in 1943 and other TB drugs in the ensuing decades for the diagnosis and eradication of TB.[2–4] Yet, TB still infects and kills millions around the world each year with about two billion people currently latently infected.[5] This necessitated the World Health Organisation (WHO) declaring TB a world emergency disease in 1993.[5] This is partly due to the ineffectiveness of the BCG vaccine (especially in adults) and the unique intrinsic ability of Mtb to develop resistance to TB drugs.[5,6] The lengthy treatment regimen coupled with heavy drug load and toxicities of TB drugs and concomitant use with non-TB (especially HIV) drugs further exacerbates the problem, as patients tend not to comply with TB treatment regimen, therefore making it possible for Mtb to become drug resistant.[5] This has resulted in the continuous development and emergence of drug-resistant strains of Mtb, including multidrug resistant (MDR), extensively drug resistant (XDR) and totally drug resistant (TDR) strains.[5] It is therefore imperative to discover and develop new, potent antitubercular drugs with novel mechanisms of action to effectively treat all the strains of Mtb and latent TB at a reduced treatment duration with fewer or no side effects.

Natural products (NPs) have historically been a good source of drugs and, for example, the main TB drugs used now are NPs or NP inspired.[7] However, NP drug discovery and development has recently declined compared to standard combinatorial synthetic chemistry methods as the development of the efficient high-throughput screening (HTS) technology was not compatible with NP drug discovery.[8] The main limitations of NP drug discovery have included the laborious and long purification processes associated with it, the slow and challenging process of identification and structure elucidation of pure bioactive compounds with high structural complexity,[9] and the problem of rediscovery of known compounds at the end of these time-consuming processes. In addition, the requirement for significant quantities of pure NPs to allow

for synthetic modification or further study of their structure-activity profiles often necessitates accessing further samples of the living organisms, which is often non-trivial for reasons associated with the ecological niches that they occupy.[9] However, recent innovations and technological advancements in purification, structure elucidation, accessing source organisms, chemical biology, genome sequencing and mining, dereplication, bioinformatic, cheminformatic and metabolomic tools like the Global Natural Product Social molecular networking (GNPS), have enhanced the competitiveness of NP drug discovery as combinatorial chemistry methods did not live up to expectations, because of its structurally limited screening libraries.[9] It is now clear that NP drug discovery with its promise of varied structural complexity and diversity will in fact provide an enhanced foundation for efficient combinatorial chemistry programs. Finally, it should be noted that the unique bioactivity with high selectivity and specificity associated with many NPs is related to their evolutionary origins in living organisms which are in competition with other organisms: their roles in survival and defence predisposes them towards modes of activities required in combatting human pathogens.[8]

The terrestrial environment has for a very long time been the primary source of bioactive NPs, with higher plants, for example, having a long history of being used to treat human diseases.[7,10] The serendipitous discovery of the antibiotic penicillin by Alexander Fleming in 1928 opened up microbial NP drug discovery and led to the golden era of novel antibiotic drug discovery, mostly from filamentous actinobacteria, also known as actinomycetes.[11] The actinomycetes are prolific producers of bioactive NPs and produce about two thirds of the antibiotics currently on the market.[12] The continuous re-isolation of known compounds from the terrestrial environment has led to the focus of NP drug discovery being shifted to unexplored areas. The ocean, which occupies over two thirds of the Earth's surface is endowed with the most diverse living organisms, and ironically relatively less explored for NP drug discovery.[13] Marine invertebrates, and especially those in the phylum Porifera, are prolific producers of novel bioactive metabolites and could serve as a rich source of novel antitubercular compounds. The U.S. National Cancer Institute (NCI) has, for example, since 1980 established an enormous repository of compounds and extracts for drug discovery, derived from their global collection of marine invertebrates.[14] Also, actinomycetes from marine sources, as well as other less explored areas and extreme

environments with hyper arid, high temperature and pressure conditions, have proven to be a good source of novel and/or rare species which secrete novel bioactive metabolites. South Africa, ranked as the third most biodiverse country in the world, has a rich and biodiverse collection of flora and fauna.[15] Although there have been reports of actinomycetes, including novel and rare species, isolated from South African soils, sediments, plants and animals including marine invertebrates, very few studies have been reported on the chemistry and bioactivity of metabolites from these species. Among the few NPs isolated from South African actinomycetes, the novel broad spectrum Gram-positive antibiotic, platensimycin produced by the South African *Streptomyces platensis* strain MA7327, has been reported to exhibit antimycobacterial activity against Mtb.[16] Also, preliminary work done in the laboratory of Dr Paul Meyers (University of Cape Town) isolated and identified some actinomycete strains which exhibited antimycobacterial activities against *Mycobacterium aurum*, *Mycobacterium bovis* and *Mycobacterium smegmatis*. South African actinomycetes could therefore be a good source of novel antitubercular agents.

1.2 Aims and Objectives

The main aim of this study was to screen an existing collection of South African actinomycetes, obtained from Dr Paul Meyers (University of Cape Town) together with extracts of marine invertebrates from the NCI collection for anti-mycobacterial activity, and to then use a range of bioanalytical, chemical, genomic and bioinformatics approaches to identify novel metabolites with activities meeting the requirement of antitubercular drug leads.

The specific objectives were divided into two parts. The first part was focused on South African actinomycetes and the second part on marine invertebrates.

South African actinomycetes

- Screen extracts of cultures of an existing collection of actinomycete strains against *M. aurum* strain A+ and *M. tuberculosis* strain H37Rv.
- Ascertain the genomic and biosynthetic potential of bioactive strains by genome mining.
- Obtain ^{1}H NMR and HR-LCMS data of active extracts to obtain their chemical profiles and perform subsequent dereplication to detect novel chemical entities.

- Employ a bioactivity guided isolation technique to isolate chemical entities responsible for antimycobacterial activity and concomitantly employ a spectrometric guided isolation technique to isolate new compounds.
- Obtain spectroscopic (UV, IR, 1D and 2D NMR) and spectrometric (ESI-MS) data to elucidate the structure of isolated bioactive compounds.

Marine invertebrates

- Screen several NCI marine invertebrate extracts against *M. tuberculosis* strain H37Rv.
- Confirm activity of bioactive extracts by rescreening them against *M. tuberculosis* strain H37Rv.
- Obtain ^{1}H NMR and HR-LCMS data of active extracts to ascertain their chemical profiles and perform a subsequent dereplication to detect novel chemical entities.
- Subject bioactive extracts to a bioactivity-guided isolation scheme to purify active metabolites.
- Obtain spectroscopic (UV, IR, 1D and 2D NMR) and spectrometric (ESI-MS) data to elucidate the structure of isolated bioactive compounds.

1.3 Structure and content of thesis

Chapter one provides a general introduction to the background and scope of the proposed research. The second chapter builds on this by providing a comprehensive literature review, in particular summarizing the state of knowledge of the disease TB, chemotherapeutic treatments of TB and then the role of natural product drug discovery as a source of new TB drugs, with a focus on marine invertebrates and actinomycetes. The chemistry and biological activity potential of South African actinomycetes is also reviewed. Chapters three to five present the results of the candidate's research, written in a manuscript format, with chapter three focusing on marine invertebrate natural products and chapters four and five on South African actinomycetes. It ends with an outlook and future work chapter.

Chapter three presents the results of screening 984 marine invertebrate extract samples sourced from the NCI against *M. tuberculosis* strain H37Rv and, in particular, the antimycobacterial activity of the 54 most active extracts. This is the first report of antimycobacterial activity for 44% of the species from which the extracts were obtained. Detailed studies of two of the active extracts are then discussed. This involved an appropriate and efficient dereplication process together with bioassay-guided isolation and purification of the active ingredients of extracts from *Hyrtios reticulatus,* which yielded heteronemin, and *Jaspis splendens*, which produced new derivatives of the bengamide class of compounds.

Chapter four reports the isolation and antimycobacterial activity of new secondary metabolites from the South African marine-derived actinobacterium, *Streptomyces* strain Muiz4Y.

Chapter five describes the use of genome mining, traditional dereplication, bioinformatics and cheminformatics techniques, such as the GNPS molecular networking, to ascertain the biosynthetic potential and chemical profile of the novel South African rare actinomycete *Kribbella speibonae* strain SK5. Strain SK5 produced several hydroxamate siderophores including new dehydroxylated congeners and diketopiperazines (DKPs). The biosynthetic pathway of the new hydroxamate siderophores is proposed.

1.4 References

1. Gutierrez, M. C., Brisse, S., Brosch, R., Fabre, M., Omaı¨s, B., Marmiesse, M., Supply, P., Vincent, V. Ancient Origin and Gene Mosaicism of the Progenitor of *Mycobacterium tuberculosis*. *PLoS Pathog.* **1**, (2005).

2. Gradmann, C., Kay, L., Mendelsohn, A. & Schlich, T. Robert Koch and the Pressures of Scientific Research : Tuberculosis and Tuberculin. *Med. Hist.* **45**, 1–32 (2001).

3. Luca, S., Mihaescu, T. History of BCG Vaccine. *Mædica - a J. Clin. Med.* **8**, 53–58 (2013).

4. Barberis, I., Bragazzi, N. L., Galluzzo, L. & Martini, M. The history of tuberculosis : from the first historical records to the isolation of Koch ' s bacillus. *J Prev Med Hyg* **58**, 9–12 (2017).

5. *WHO Global Tuberculosis Report 2019 (2019)*.

6. Smith, T., Wolff, K. A., Nguyen, L. Molecular Biology of Drug Resistance in *Mycobacterium tuberculosis*. *Curr Top Microbiol Immunol* **374**, 53–80 (2013).

7. Cragg, G. M. & Newman, D. J. Natural Products: A Continuing Source of Novel Drug Leads. *Biochim Biophys Acta* **1830**, 3670–3695 (2013).

8. Ortholand, J. & Ganesan, A. Natural products and combinatorial chemistry : back to the future. *Curr. Opin. Chem. Biol.* **8**, 271–280 (2004).

9. Lam, K. S. New aspects of natural products in drug discovery. *Trends Microbiol.* **15**, 280–289 (2007).

10. Petrovska, B. B. Historical review of medicinal plants' usage. *Pharmacogn. Rev.* **6**, 1–5 (2012).

11. Lyddiard, D., Jones, G. L. & Greatrex, B. W. Keeping it simple : lessons from the golden era of antibiotic discovery. *FEMS Microbiol. Lett.* **363**, 1–3 (2016).

12. Barka, E. A. *et al.* Taxonomy , Physiology , and Natural Products of Actinobacteria. *Microbiol Mol Biol Rev* **80**, 1–44 (2016).

13. Parkes, R. J. *et al.* Deep bacterial biosphere in Pacific Ocean sediments. *Nature* **371**, 410–413 (1994).

14. Thornburg, C. C. *et al.* NCI Program for Natural Product Discovery : A Publicly-Accessible Library of Natural Product Fractions for High-Throughput Screening NCI Program for Natural Product Discovery : A Publicly- Accessible Library of Natural Product Fractions for High- Throughp. *ACS Chem. Biol* (2018). doi:10.1021/acschembio.8b00389

15. https://www.biodiversityfinance.net/south-africa.

16. Martens, E. & Demain, A. L. Platensimycin and platencin : promising antibiotics for future application in human medicine. *J. Antibiot. (Tokyo).* 705–710 (2011). doi:10.1038/ja.2011.80

Chapter Two: Literature Review

2.1 Tuberculosis

2.1.1 Disease

Tuberculosis (TB) is a contagious airborne disease in humans and other primates caused mostly by *Mycobacterium tuberculosis* (Mtb), which is part of a group of genetically closely related Gram-positive mycobacterial strains called the *Mycobacterium tuberculosis* complex (MTC).[1–3] The other MTC members are *Mycobacterium bovis*, *Mycobacterium africanum*, *Mycobacterium microti*, *Mycobacterium caprae*, *Mycobacterium pinnipedii*, *Mycobacterium canetti*, *Mycobacterium mungi*, *Mycobacterium dassie*, *Mycobacterium oryx* and *Mycobacterium suricattae*.[4] Although these strains show high similarity in their 16S ribosomal ribonucleic acid (rRNA) sequences, they exhibit different pathogenic and phenotypic characteristics as well as host tropisms.[2,4] Not all MTC members are therefore known to cause disease in humans. Mtb generally causes TB in humans, but *M. bovis*, *M. africanum*, *M. canetti*, *M. microti* and *M. caprae*, have been isolated from some human TB patients. *M. bovis* affects primates, goats, cattle, and other bovines.[4] The zoonotic pathogen, *M. bovis*, is transmitted to humans through contaminated dairy products, meat and aerosols.[4] *M. caprae*, mostly found in central Europe, and *M. microti* also affects animals.[4] *M. africanum* and *M. canetti* affect some African patients or patients of African descent.[4]

Aerosols, called droplet nuclei, are generated and released into the air when an infected person with TB of the lungs speaks, coughs, sneezes, sings or shouts.[3] These droplet nuclei are 1– 5 microns in diameter and contain the tubercle bacilli.[3] The disease is transmitted when a person inhales infected droplet nuclei through the upper respiratory tract and into the alveoli of the lungs.[3] An immune response is initiated when macrophages engulf the tubercle bacilli to form a granuloma that keeps the bacilli contained and under control.[3] If an infected person's immune system suppresses the bacteria and makes the bacteria inactive, the disease will not manifest.[3] This is known as latent TB.[3] Latent TB is not contagious, and an infected person does not show the disease symptoms, but is at risk of developing active TB if their immune system is compromised.[3] About 5–10% of individuals with latent TB develop symptoms and clinical TB

infection in their lifetime.[1] Conditions that cause low immune resistance include diabetes, end-stage kidney disease, certain cancers, cancer treatment such as chemotherapy, immunosuppressive drugs taken to prevent organ transplant rejection and HIV/AIDS.[3] Active TB is contagious and develops when the immune system succumbs to the bacteria, and the bacteria multiply in the body, causing the development of symptoms.[3] TB symptoms include a persistent cough that lasts 3 weeks or longer with or without its associated bloody sputum, fever, chills, night sweats, loss of appetite and unexplained weight loss.[3,5] There are two types of active TB: lung or pulmonary TB and extrapulmonary TB.[3,5] Pulmonary TB affects the lungs, and extrapulmonary TB affects other parts of the body, including the brain, central nervous system, genitourinary tract, bones, and joints.[3] Extrapulmonary TB is characterized by considerably different symptoms based on the site of infection. Miliary or disseminated TB occurs when the tubercle bacilli spread through the bloodstream to other parts of the body, affecting both pulmonary and extrapulmonary areas.[3]

TB diagnosis starts with physical examination and evaluation of the patient's medical history and whether the patient has had exposure to TB infection or disease.[5] Still, proper diagnostic tests are required to confirm Mtb's presence or manifestation of the disease in the patient. Mtb in the body is detected and confirmed by the Tuberculin skin test (TST) and TB blood tests.[5] A positive response to these tests shows that one is infected with the bacteria either latently or actively. TST is the gold standard for the diagnosis of latent TB. To confirm the disease's manifestation in TB active patients, chest X-ray, sputum smear microscopy and bacterial culture are required for pulmonary TB but not extrapulmonary TB.[6] A wide range of tests, including CT scan, MRI scan or ultrasound scan, biopsy, laparoscopy of the affected part of the body and endoscopy as well as a lumbar puncture to collect cerebrospinal fluid for investigation are used to diagnose extrapulmonary TB.[7] However, these diagnostic tools and methods have limitations. Therefore, there is the development of several advanced rapid diagnostic tools, including Xpert MTB/RIF, Xpert Ultra and Truenat assays for the efficient detection and diagnosis of latent, active, drug-sensitive and drug-resistant TB.[1]

2.1.2 Epidemiology

TB is a world emergency disease and affects humans of all age groups and some animals on every part of planet earth.[1] It is contagious, and about one-third of the world population is latently infected and at risk of developing the disease.[1] About 5-10% of those latently infected develop the disease in their lifetime.[1] TB is an epidemic as millions contract and die of the disease each year. TB is part of the ten leading causes of death and tops the list of causes of death from a single infectious agent, although TB is curable and preventable.[1] About 63 million lives have been saved through proper TB diagnosis and treatment since 2000.[8] The United Nations Sustainable Development Goals (SDGs) have a target to end the TB epidemic by 2030 (SDG Target 3.3).[1] Progress has been made globally, as the TB incidence has fallen at about 2% per year and, for example, the TB incidence between 2015 and 2019 had a cumulative reduction of 9%.[8] However, this is not good enough as this does not even reach half of the End TB Strategy milestone of a 20% TB reduction between 2015 and 2020.[8] The End TB Strategy has defined milestones and targets for 2020, 2025, 2030 and 2035 to reduce TB cases and deaths.[1,8] There are also firm political and financial commitments with documented declarations, strategies and frameworks with defined targets by the WHO and the UN and its member states to eradicate the TB epidemic.[1,8]

In 2019, an estimated 10 million people contracted TB globally, out of which 5.6 million were men, 3.2 million women and 1.2 million children, with adult men accounting for the highest burden of 56%.[1] Among the 10 million people, 8.2% were people living with HIV.[1] The South-East Asian region, African region, and the Western Pacific Region of the WHO (Figure 2.1) accounted for the largest number of the new cases with 44%, 25% and 18%, respectively.[1] About 87% of these new TB cases were accounted for by the 30 high TB burden countries, eight of which accounted for two-thirds of the total number of the new TB cases (Figure 2.2).[1] India topped the list of these eight countries with 26%, followed by Indonesia (8.5%), China (8.4%), the Philippines (6.0%), Pakistan (5.7%), Nigeria (4.4%), Bangladesh (3.6%) and South Africa (3.6%).[1] With regards to mortality, 1.4 million people died from TB in 2019 (Figure 2.3). Close to 15% (208,000) of these deaths were people living with HIV/AIDS.[1] People living with HIV have compromised immune systems and easily develop active TB upon infection (18 times more likely than HIV-negative

individuals).[1] TB and HIV/AIDS are co-epidemics, and TB is a significant cause of mortality and morbidity among HIV-positive patients.[1] The WHO African region accounted for the highest-burden of HIV-associated TB.[1]

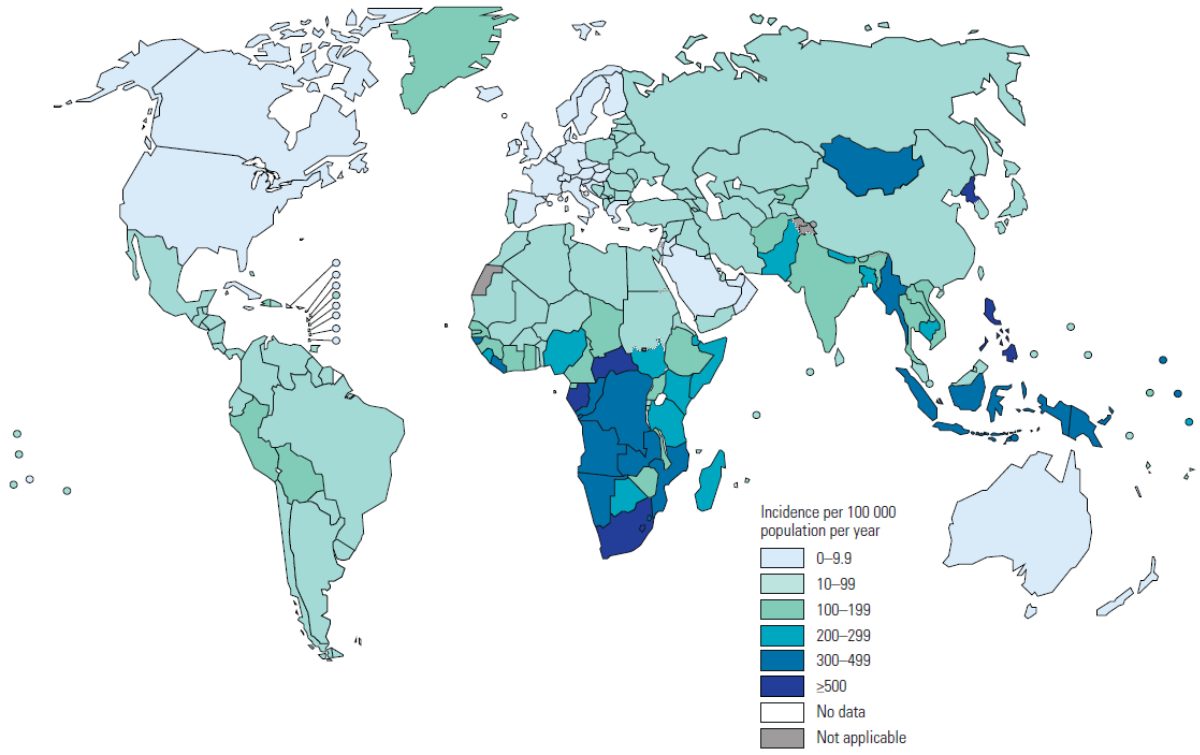

Figure 2.1: Estimated 2019 global TB incidence rates (Source: 2020 WHO Global TB Report).[1]

Apart from HIV/AIDS, social factors and other diseases also contribute to increased TB mortality and morbidity as TB is a social disease. These contributions include diabetes mellitus, immunosuppressive drug use, alcohol abuse, smoking, malnutrition and lack of education and awareness regarding the cause and transmission of TB.[9,10] Furthermore, poverty-related early marriages and large families, low quality of life, poor housing, overcrowding, and population explosion also increase TB incidence.[9]

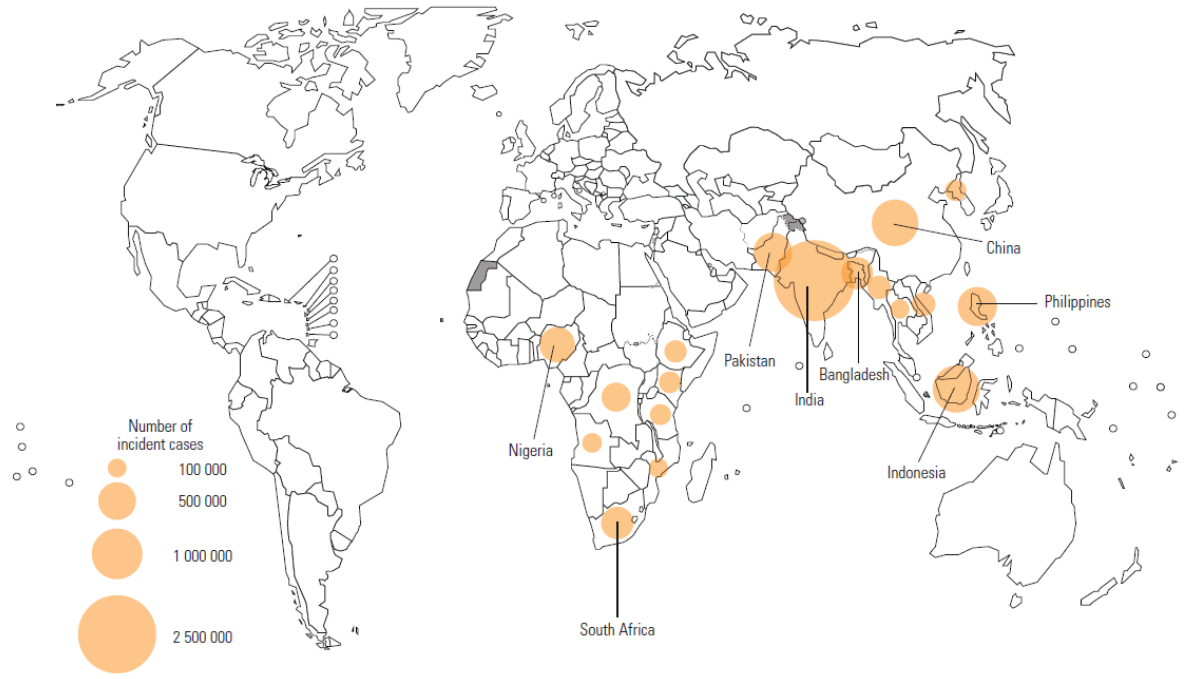

Figure 2.2: Countries with highest TB incident rate (at least 100,000 people infected) in 2019 (Source: 2020 WHO Global TB Report).[1]

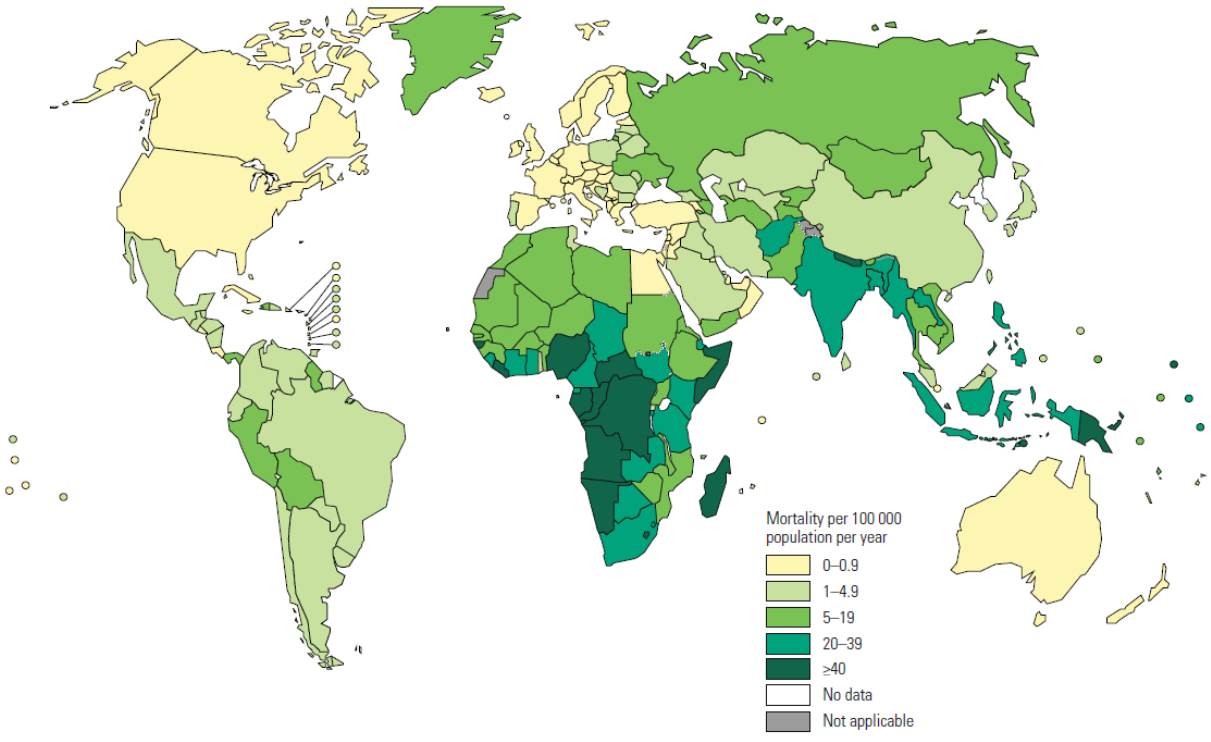

Figure 2.3: Estimated 2019 global TB mortality rates in HIV-negative people (Source: 2020 WHO Global TB Report).[1]

Drug-resistant TB, especially multidrug-resistant TB (MDR-TB), remains a public health crisis and a health security threat. MDR-TB is defined as TB caused by Mtb that is resistant to at least isoniazid **2.1** and rifampicin **2.2** (the two most potent TB drugs).In 2019, 206,030 people were infected with or developed multidrug- or rifampicin-resistant TB (MDR/RR-TB), a 10% increase for MDR/RR-TB from 186,883 in 2018.[1] And 12,350 people contracted extensively drug-resistant TB (XDR-TB). XDR TB is caused by Mtb that is resistant to isoniazid **2.1** and rifampin **2.2** plus any fluoroquinolone and at least one of the three injectable second-line drugs, namely, amikacin **2.13**, kanamycin **2.12** or capreomycin **2.14**. Three countries, India, China, and the Russian Federation, contribute about half of the global burden of MDR-TB.[1] Treatment of MDR-TB and XDR-TB is long and burdensome. Only 57% of MDR-TB patients are currently successfully treated.[1]

2.2 Prevention, Vaccination and Treatment of TB

2.2.1 Prevention and Vaccination

TB prevention begins with avoiding infection or transmission of Mtb from an infected person to a TB negative person. In the case of an infection, there are strategies to control and prevent infection progression to TB disease, including providing and monitoring TB prevention treatment until treatment is complete.[1,11,12] This is crucial to lessen the impact of TB disease and death. TB prevention also broadly encompasses campaign strategies to educate the general public on knowledge of TB transmission, the importance of treatment compliance and avoidance of stigmatization, which are necessary for the efficient management of outbreaks.[13] For example, a person diagnosed with TB, especially pulmonary TB, is advised to cough with their mouth covered with a handkerchief to reduce transmission. About two billion of the world's population is latently infected with TB, which is too high a number to be administered with TB prevention treatment.[1] Therefore, the initial focus of TB prevention and control are people at high risk of developing the disease, such as people living with HIV/AIDS and other immune compromising diseases and conditions.[1] The next high-risk group of importance are children below five years as their immune system is not adequately developed.[1] When one is diagnosed with TB disease, a proper contact tracing, even down to the patient's household, is undertaken with subsequent screening of

contacts to investigate those with infection.[1] Contacts confirmed with infection but who do not manifest the TB disease are given the TB prevention treatment and monitored until completion of treatment.[1] Contacts diagnosed with active TB are isolated and treated with monitoring until they become non-infectious. Health care workers are advised to use personal protective equipment and are routinely screened and provided with TB prevention treatment if infected.[1,14]

A positive result for the tuberculin skin test or the interferon-gamma release assays (IGRAs) is mandatory for initiating TB preventive treatment.[15] Children, especially below five years, who test negative, are vaccinated with the only licensed vaccine, Bacille Calmette-Guerin (BCG).[1] Although the BCG vaccine's efficacy against pulmonary TB is 50%, it has provided lifesaving protection against fatal forms of meningitis and miliary TB in young children.[16,17] The WHO recommends that babies get immunized with the BCG vaccine as soon as possible, especially in countries with a high disease burden.[1] In 2019, 147 countries reported BCG vaccination to the WHO. The BCG vaccine is not effective in adults, and there are currently no licensed or approved vaccines for immunization against TB in adults. Therefore, there is a need to discover potent and effective vaccines to prevent TB in the different human age groups (there are several vaccine candidates in various stages of clinical development).

The TB preventive treatment options recommended by the WHO include a weekly dose of rifapentine **2.6** and isoniazid **2.1** for three months (3HP), a daily dose of rifampicin **2.2** plus isoniazid **2.1** for 3 months (3HR), a daily dose of rifapentine **2.6** plus isoniazid **2.1** for 1 month (1HP), a daily dose of rifampicin **2.2** for 4 months (4R) and a daily dose of isoniazid **2.1** for 6 months (6H) or longer.[1] In 2019, 4.1 million people had TB preventive treatment, 3.5 million of which were people living with HIV.[1] The prevention and control of TB infection and disease, especially for people living with HIV, will be instrumental in achieving the WHO's End TB Strategy targets set for 2030 and 2035.[1]

2.2.2 Treatment of TB

TB treatment is long, burdensome and complicated. It has evolved extensively from the initial application of superficial, superstitious, and religious beliefs, including the royal touch practiced

in England and France, through the sanatorium cure used across Europe and the USA and various surgical procedures, to chemotherapy with the discovery and use of streptomycin **2.10**.[18] Many more anti-TB drugs have subsequently been discovered and are in use now.[19] These drugs have been grouped into the first- and second-line drugs based on their potency, safety, knowledge of their use and pharmacological class.[20] The first- and second-line drugs are used to treat drug-susceptible TB (DS-TB) and drug-resistant TB (DR-TB), respectively. An estimated 80% of TB patients are diagnosed with DS-TB, while 20% have DR-TB.[21]

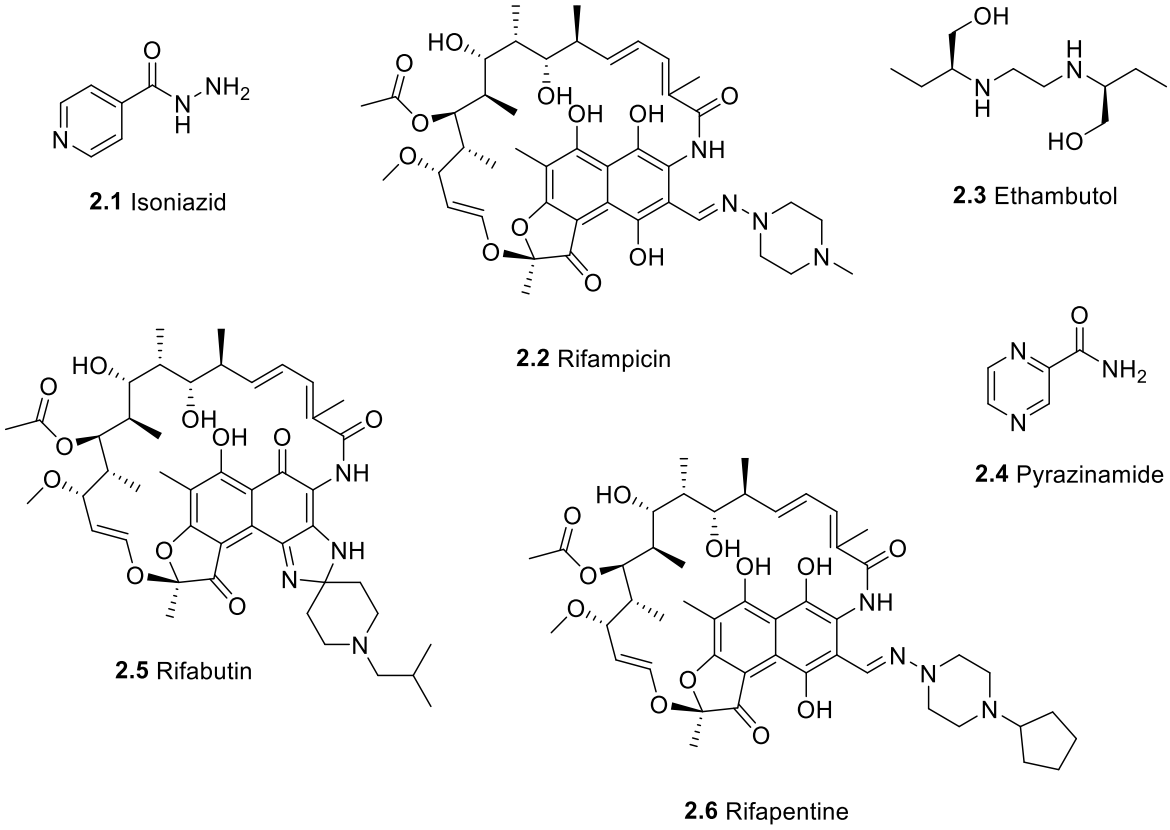

Figure 2.4: First line anti-TB drugs

Patients diagnosed with DS-TB are treated with the first-line oral drugs, which include isoniazid **2.1** (INH), rifampin **2.2** (RIF; also called rifampicin), ethambutol **2.3** (EMB) and pyrazinamide **2.4** (PZA) (Figure 2.4) for a minimum of six months.[1] Streptomycin **2.10**, which is administered parenterally, was a first-line drug but is not widely used now due to resistance. In the first two

months, called the intensive phase, new pulmonary TB patients are treated with INH, RIF, EMB and PZA and in the remaining four months, called the continuous phase, patients are treated with only INH and RIF.[1] This is a standard combination treatment regimen recommended by the WHO, but the dosages, frequency of administration and duration of treatment changes for HIV patients, patients with relapsed TB and patients with cavitary pulmonary TB.[1,6] Patients who effectively comply with the six-month combination therapy achieve over 95% cure rates.[22] The WHO's recommended treatment guidelines, called Directly Observed Treatment, Short course (DOTS), prescribe treatment regimens based on the patient's medical history and condition for the best TB management.[23] DOTS also requires the patient to take anti-TB drugs under the observation of a health worker or care provider. The WHO further recommends that a drug sensitivity test should be done before a treatment regimen is prescribed and the drugs formulated as a fixed dosed combination to avoid drug resistance and encourage treatment adherence.[24] It is essential to retest (X-ray, sputum smears and culture) patients during their TB treatment and after completing their TB treatment to ascertain whether the treatment regimen has been successful.

Although there is an effective treatment for the prevention, management and cure of drug-susceptible TB, the development and rapid emergence of drug-resistant strains of Mtb has eroded the significant gains made in ending the TB epidemic.[25] This is a major global public health concern. One of the primary reasons for the development of drug-resistant strains of Mtb is the non-adherence of patients to the treatment regimen. This is mostly due to the heavy drug burden and very long treatment duration. Also, due to the stigma associated with TB, just like HIV/AIDS, TB patients do not want to be seen visiting the TB section of health facilities for their medication, as there are designated sections for TB patients. Such patients tend to fail to comply with treatment.[26] Some healthcare workers' discriminatory behavior towards TB patients does not encourage TB patients to seek treatment. Mistakes or errors of physicians (human error) in therapy management, including inadequate and inappropriate treatment, also cause resistance.[27] Mtb can experience mutations in its genes and is able to develop resistance to anti-TB drugs through drug-efflux systems, the nature of the mycobacterial cell envelope, drug-target modification and drug modification and degradation.[28] There is also the development of drug-

tolerant and non-replicating Mtb in the granulomas and drugs' inability to get to some parts of granulomatous lesions.[29]

There are two main ways of developing drug-resistant TB, either through primary or acquired resistance. Primary resistance is when one is infected with a drug-resistant strain of Mtb, whereas acquired resistance, also known as secondary resistance, occurs when a drug-susceptible strain develops mutations or drug selection resistance in a person infected with DS-TB and with a history of first-line drug treatment due to improper or inadequate treatment. DR-TB cases are categorized into (1) mono-resistant TB, which is resistant to one first-line anti-TB drug only; (2) poly-resistant TB which is resistant to more than one first-line anti-TB drug, other than both isoniazid **2.1** and rifampicin **2.2**; (3) MDR TB which is resistant to at least both isoniazid **2.1** and rifampicin **2.2**; (4) XDR TB is MDR TB with resistance to any fluoroquinolone and at least one of three second-line injectable drugs (capreomycin **2.14**, kanamycin **2.12** and amikacin **2.13**); (5) rifampicin resistant (RR) TB is resistant to rifampicin **2.2** with or without resistance to other anti-TB drugs and includes any resistance to rifampicin **2.2**, in the form of mono-resistance, poly-resistance, MDR or XDR; and (6) totally drug-resistant TB (TDR-TB) or extremely drug-resistant TB is resistant to all first- and second-line anti-TB drugs.[30,31]

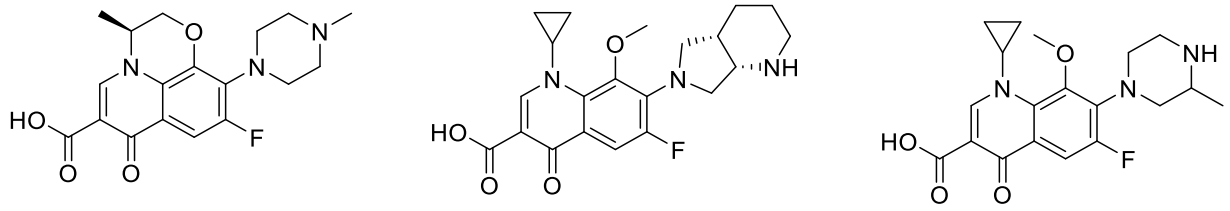

2.7 Levofloxacin **2.8** Moxifloxacin **2.9** Gratifloxacin

Figure 2.5: Second line anti-TB drugs Group A (fluoroquinolones)

DR-TB is treated with second-line drugs, and these drugs are categorized into four groups (A-D). Group A are the fluoroquinolones, made up of levofloxacin **2.7**, moxifloxacin **2.8** and gatifloxacin **2.9**. The second group (B) are injectable anti-TB drugs, and they include streptomycin **2.10**, kanamycin **2.12**, amikacin **2.13** and capreomycin **2.14**.[32] Group C contains oral bacteriostatic second-line anti-TB drugs, including ethionamide **2.15**, prothionamide **2.16**, cycloserine **2.18**,

terizidone **2.17**, linezolid **2. 20** and clofazimine **2.19**.[32] Group D is further divided into three subgroups (D1-D3).[32]

Group B

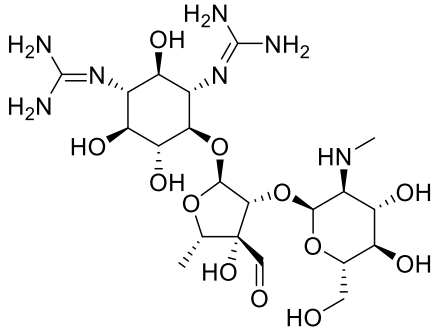

2.10 Streptomycin

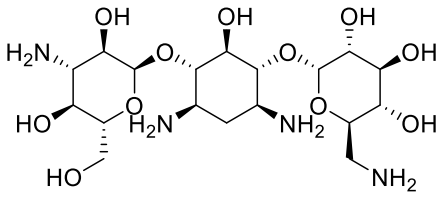

2.12 Kanamycin

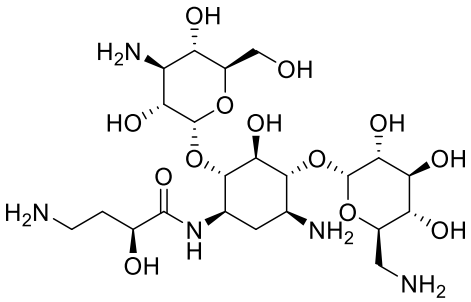

2.13 Amikacin

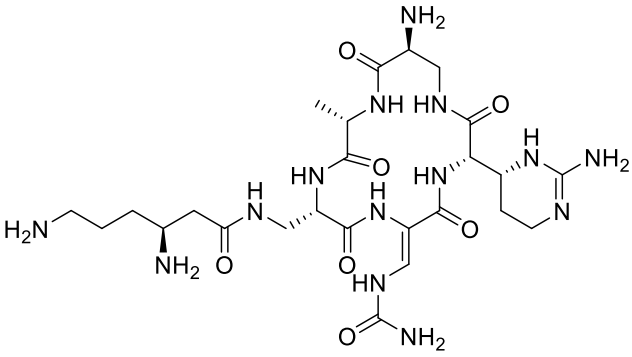

2.14 Capreomycin

Group C

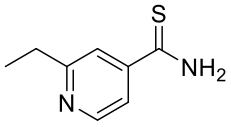

2.15 Ethionamide

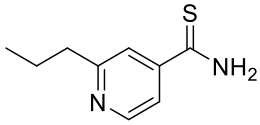

2.16 Prothionamide

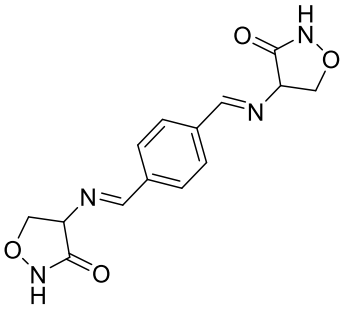

2.17 Terizidone

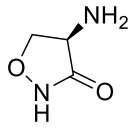

2.18 D-Cycloserine

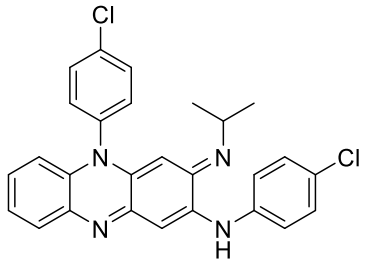

2.19 Clofazimine

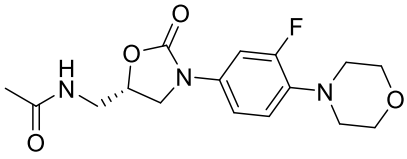

2.20 Linezolid

Figure 2.6: Second line anti-TB drugs Groups B and C

D1 comprises pyrazinamide **2.4**, ethambutol **2.3**, and high-dose isoniazid**2.1**.[32] Bedaquiline **2.21** and delamanid **2.22** make up D2, while D3 includes *p*-aminosalicylic acid **2.23**, amoxicillin **2.28**/clavulanate **2.26**, imipenem **2.24**/cilastatin **2.25**, meropenem **2.27** and thioacetazone **2.29**.[32]

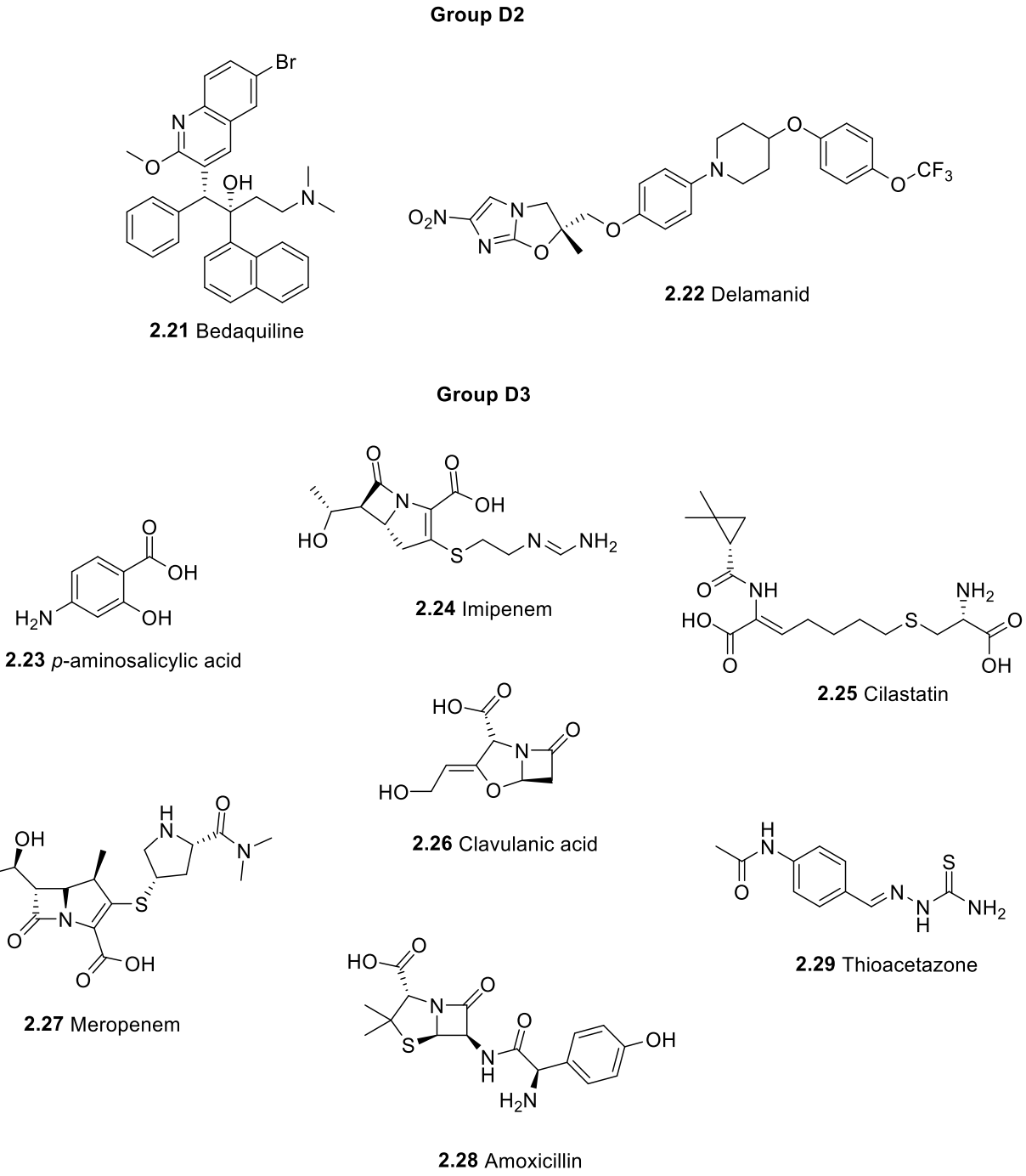

Figure 2.7: Second line anti-TB drugs Groups D2 and D3

The D group drugs are used to complement and strengthen MDR TB treatment. Treatment of DR-TB is more difficult, less effective, more complicated, and longer and requires more drugs than DS-TB. It takes a minimum of 18-20 months to treat a DR-TB patient.

MDR TB patients are treated with pyrazinamide **2.4** and four other effective second-line drugs, one from each of the four groups, in the intensive phase.[32] MDR TB patients are supposed to be screened for resistance against fluoroquinolones and second-line injectable anti-TB drugs. MDR TB patients infected with Mtb strains resistant to fluoroquinolones and second-line injectable anti-TB are given XDR TB treatment, which is even longer and requires even more drugs than MDR TB treatment does.

The anti-TB drugs elicit side effects in some patients under chemotherapeutic treatments. Some of the side effects, include nausea, vomiting, headache, dizziness, stomach upset, loss of appetite, skin rash, discoloration of body fluids like urine, sweat and tears, and sensitivity to the sun.[33] Still, there are more severe side effects such as blurred vision, easy bruising, slow blood clotting, depression, joint aches, seizures, abdominal pains, severe skin reactions, yellowish skin or eyes and a tingling sensation in hands and feet.[33] There are symptoms of disease conditions including arthralgia, hepatitis, gout, peripheral neuropathy, myelosuppression, hypothyroidism and a wide range of drug toxicities such as cardiotoxicity, nephrotoxicity, ototoxicity, ocular toxicity, hepatotoxicity and central nervous system (CNS) toxicity that develop due to toxicities from drugs or drug-drug interactions.[20,33] Therefore, patients undergoing TB chemotherapeutic treatment are monitored regularly for these side effects and toxicities from the anti-TB drugs for proper management of the disease. Treatment is discontinued in situations where there are adverse or severe side effects and toxicities.

2.2.3 Challenges of TB chemotherapy

TB treatment therapy is complex and involves many drugs, especially for DR-TB. Mtb is complex and requires drugs with different mechanisms of action to inhibit the growth and effectively kill replicating, slowly replicating and non-replicating forms of the pathogen.[34] Hence, the use of a minimum of four drugs. For example, isoniazid **2.1** effectively kills replicating forms, while

rifampin **2.2** is effective against both replicating and non-replicating forms of the pathogen by inhibiting its RNA synthesis.[34] This helps to reduce the length of treatment. Regardless, the current treatment regimen is long, with a minimum of six months for DS-TB and 18 months for DR-TB. It takes even more extended periods to complete treatment for XDR and TDR-TB.

The occurrence of drug-drug interactions between TB drugs and between TB drugs and medicines used to manage chronic diseases like HIV-AIDS is a major problem.[34] For example, ethambutol **2.3** and linezolid **2.20** both cause ocular toxicity. Using these two drugs together to treat DR-TB will cause an adverse effect of ocular toxicity stemming from both drugs' additive effect.[35] Also, isoniazid **2.1** and antiretrovirals can both cause peripheral neuropathy and hepatitis. Using both together to treat patients co-infected with TB and HIV will cause an enhanced effect of peripheral neuropathy and hepatitis.[36] Concomitant use of these drugs is therefore prohibited.

Furthermore, the use of TB drugs with other non-communicable chronic co-morbidities like diabetes mellitus increases the pill burden, thereby causing more toxicities and making TB treatment complicated and difficult.[37] Toxicities and side effects from some of these drugs leave permanent damage such as lung injury and kidney impairment to patients even after completing treatment.[38] There is still no available treatment for lung injury, which is a challenge.

The continuous emergence of Mtb strains resistant to anti-TB drugs is making DR-TB treatment more complex, costly, toxic and less-effective compared to DS-TB. Therefore, there is a pressing need to discover potent, safe and tolerable novel antitubercular drugs with novel mechanisms of action to shorten TB therapy duration; completely treat MDR, XDR, and TDR TB as well as latent TB. These drugs should be able to be co-administered safely with other antitubercular drugs and with anti-HIV drugs without any complications.

2.3 Natural product drug discovery

Living organisms continuously perform biochemical reactions, referred to as metabolism, vital for their growth, development and reproduction. The compounds or intermediates involved in and produced from these metabolic reactions are referred to as metabolites. Primary metabolites such as amino acids, carbohydrates, fatty acids, and nucleic acids are molecules that

arise from every living organism's primary metabolism and are essential for their existence.[39] On the contrary, secondary metabolites produced from secondary metabolism are not essential for the growth, development and reproduction of living organisms and are organism-specific.[39–41] The specific purpose or use of these metabolites is unknown, but it is believed that organisms produce these compounds to make them ecologically competitive, defend themselves and communicate with members of their kind (quorum sensing).[39,41,42] These secondary metabolites, also called natural products (NPs) or specialized metabolites, are structurally diverse small molecules with a wide range of biological activities.[41,43] Natural products have a long history of being used to treat human diseases and illnesses, among other applications. Most bioactive NPs and drugs have been isolated from plants, bacteria, fungi, and marine invertebrates.[41]

The use of NPs, mostly from plants, to treat various diseases, has been described in ancient folklore and documents, with the earliest records inscribed in cuneiform on clay tablets from Mesopotamia in 2600 BC.[44] The Egyptian Ebers Papyrus (2900 BC), the Chinese Materia Medica (1100 BC), Shennong Herbal (~100 BC) and the Tang Herbal (659 AD) are also documented records of the use of plant-based drugs.[44] There are also reports of the use, documentation and preservation of NPs by the Arabs, English, French, Germans, Greeks, Irish, Indians and Romans.[41,44] The medical encyclopedia referred to as the Canon of Medicine written by the Persian pharmacist, physician, philosopher and poet, Avicenna, became a standard medical text and was in use until 1650.[41,44] By 1815, the term "pharmacognosy", was coined from the Greek words φάρμακον pharmakon (drug) and γνῶσις gnosis (knowledge) and initially described the study of crude drugs in the form of teas, powders, poultices, tinctures, and formulations derived from plants and animal sources.[45] The American Society of Pharmacognosy now defines pharmacognosy as "the study of natural product molecules (typically secondary metabolites) that are useful for their medicinal, ecological, gustatory, or other functional properties". [46]

By the 19th century, NP drug discovery's focus had shifted to the isolation or purification of the active components or compounds from these traditional medicinal plants. The first compound to be isolated was the analgesic morphine **2.30**.[41,47] The alkaloid morphine **2.30** was isolated from opium poppy capsules, *Papaver somniferum*, in 1803 and commercially marketed in 1817.[48] This

was based on ethnopharmacological records of the medicinal use of poppy extracts by the Arabs, Ancient Greeks and Sumerians, with the Arabs describing opium as addictive.[48]

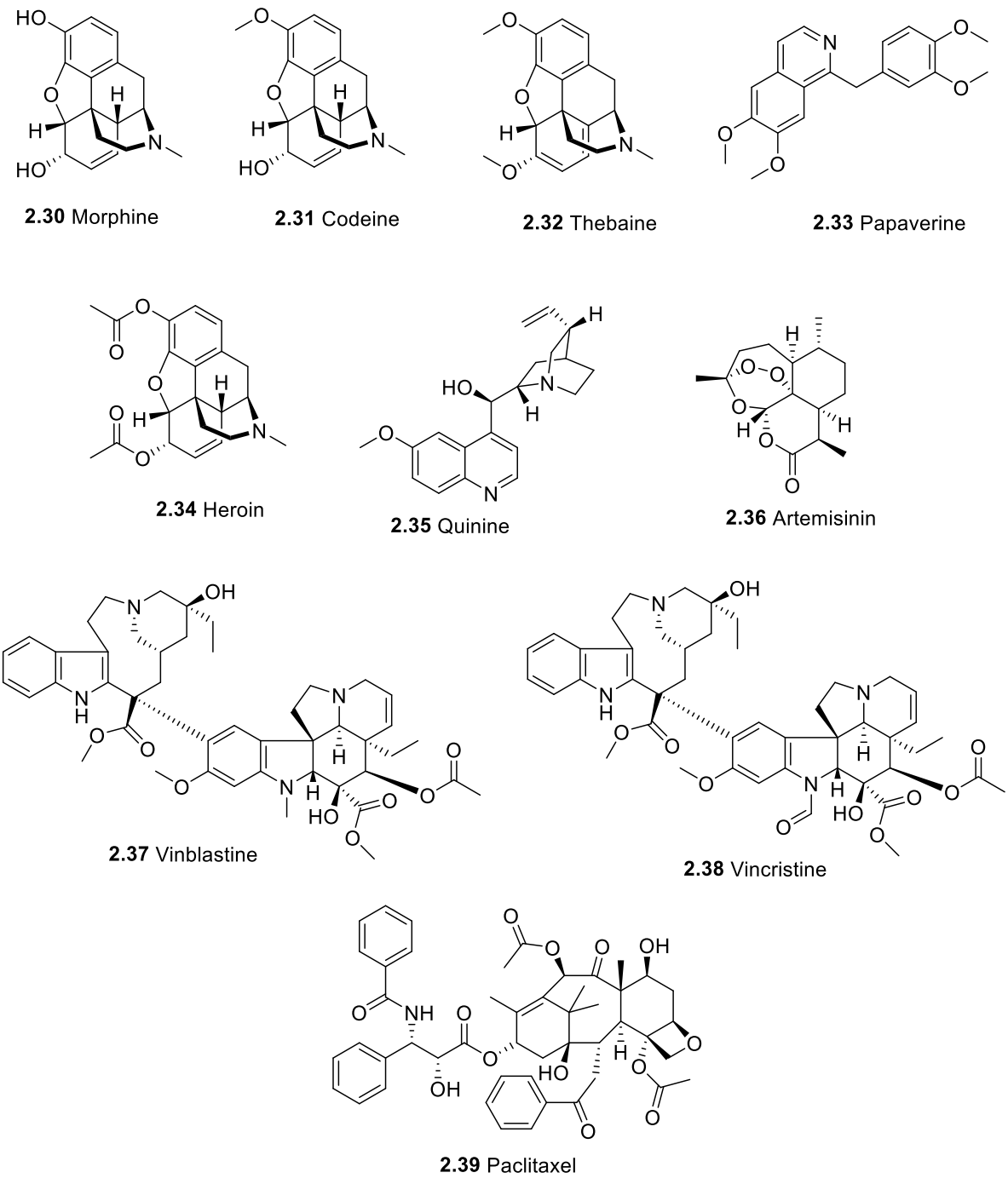

Figure 2.8: Some drugs from plant sources

Over 30 other bioactive alkaloids, including codeine **2.31** (analgesic and antitussive), thebaine **2.32** (precursor of opioids), and papaverine **2.33** (antispasmodic), have also been isolated from *P. somniferum*.[49] Also, the narcotic diacetylmorphine (heroin) **2.34** was derived from the crude extract of *P. somniferum*.[41]

Several other bioactive compounds and drugs, including quinine **2.35**, artemisinin and the vinca alkaloids, have been isolated from traditional medicinal plants based on ethnopharmacological or folkloric records. Quinine **2.35**, an antimalarial drug, was isolated from the bark of *Cinchona succirubra* Pav. ex Klotsch in 1820 because it had a long history of use for the treatment of malaria, fever, indigestion, mouth and throat diseases and cancer.[41,48]

The antimalarial, artemisinin **2.36** was isolated from the plant *Artemisia annua* in 1987 based on its use in traditional Chinese medicine to treat fever and chills.[50] Some artemisinin derivatives have been approved as antimalarial drugs, while others are in various clinical development stages.[51] The Madagascar periwinkle plant, *Catharanthus roseus*, although an ornamental plant, is beneficial for its medicinal properties. An investigation into its antidiabetic properties instead led to the isolation of the anticancer drugs vinblastine **2.37** in 1958 and vincristine **2.38** in 1961.[52] These drugs are used to treat various cancers, including acute lymphocytic leukemia, acute myeloid leukemia, bladder cancer, brain cancer, melanoma, Hodgkin's disease, neuroblastoma, lung cancer and testicular cancer.[52] Drug discovery then moved from having an ethnopharmacological basis to random, untargeted searches or screening, mostly, using bioassay-guided fractionation schemes.

A fascinating example is the isolation of the anticancer drug paclitaxel (taxol) **2.39** from the bark of the Pacific yew tree *Taxus brevifolia* in 1971 due to a National Cancer Institute (NCI)-funded plant screening program.[41,53] Paclitaxel is used to treat breast, bladder, cervical, melanoma, ovarian, lung, pancreatic, prostate, and esophageal cancers, as well as Kaposi's sarcoma.[54] Another approach was to isolate novel or interesting compounds based on their distinctive structures (as determined from UV, IR, MS, and NMR data) and later screen them against various disease targets.

2.3.1 Marine natural products (MNPs)

There are few ethnopharmacological records of using marine organisms to treat and/or prevent human diseases.[41] With success from the random screening of terrestrial flora and fauna to discover bioactive NPs, especially from less explored environments, the marine environment, which was relatively less explored, gained attention by 1950.[55,56] The oceans occupy more than 70% of the earth's surface and are endowed with extraordinarily diverse macro- and microorganisms compared to the terrestrial environment.[57] These marine organisms are unique, with most exclusive to the marine ecosystem since 32 out of the 34 fundamental phyla of life exist in the marine ecosystem while 17 occur on land.[57] These organisms biosynthesize and secrete secondary metabolites, which helps them adapt to the harsh marine ecosystem with a high salinity that undergoes constant variations in light, pressure, nutrient and temperature in both shallow and deep sea.[41,58] The marine macro-organisms, especially invertebrates, undergo a symbiotic association with microorganisms. They (together) produce potent cytotoxic secondary metabolites with high selectivity and specificity to immobilize or kill their predators and competitors, which gives them an advantage in an extremely competitive marine ecosystem.[59] Some of these chemicals have been found to be useful to humans, due to their various biological activities, especially in treating cancer.

The exploration of the ocean, which was initially inaccessible, began with the collection of colorful and conspicuous marine organisms such as algae, ascidians, bryozoans, tunicates, sponges, and soft corals, mostly in the intertidal zone by modern snorkeling and SCUBA (Self-Contained Underwater Breathing Apparatus) diving.[41] With technological advancement in these tools and the introduction of manned submersibles and remotely operated vehicles (ROVs), marine organisms have been sampled well beyond the intertidal zone.[41]

Over 28,500 structurally diverse and unique secondary metabolites with various biological activities have been isolated from the marine environment with the discovery of the antivirals spongothymidine **2.40** and spongouridine **2.41** from the crude extract of the Caribbean sponge, *Tethya crypta,* in the early 1950s as the first notable report.[55,56] These *C*-nucleosides **2.40** and **2.41** served as a structural scaffold for the development of the antiviral drug Vidarabine (Ara-A)

2.42 and the anticancer drug Cytarabine (Ara C) **2.43**.[60] Ara A and C are the first Food and Drug Authority (FDA) approved marine-derived drugs with approvals in 1976 and 1969, respectively.

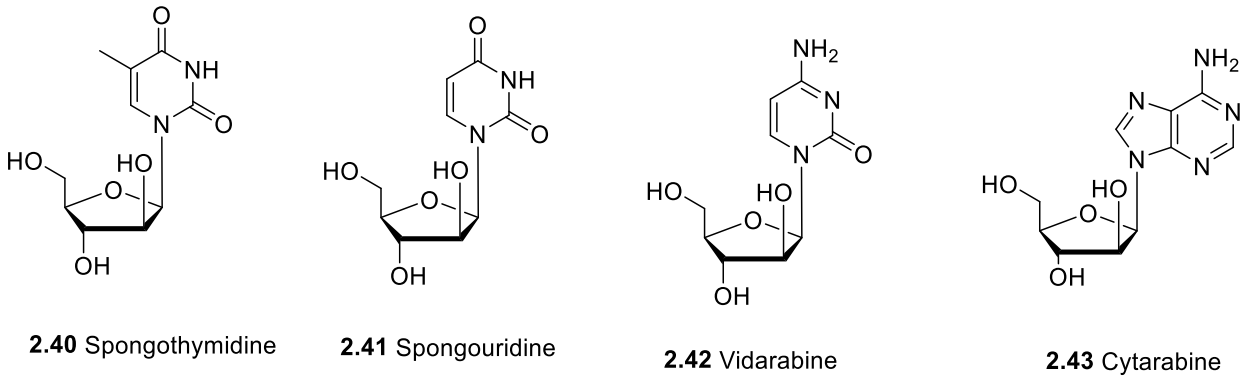

2.40 Spongothymidine **2.41** Spongouridine **2.42** Vidarabine **2.43** Cytarabine

Figure 2.9: *C*-nucleoside compounds and drugs from *Tethya crypta*.

From the global marine pharmaceutical pipeline, 12 more marine natural product (MNP) derived drugs have been approved to date, and 23 drug candidates are currently in various phases (I, II and III) of clinical development.[61] The 12 approved drugs are ziconotide **2.44**, omega-3-acid ethyl esters, eicosapentaenoic acid ethyl ester, omega-3-carboxylic acid, trabectedin **2.49**, eribulin mesylate **2.51**, brentuximab vedotin **2.53**, plitidepsin **2.57**, polatuzumab vedotin (DCDS-4501A) **2.54**, enfortumab vedotin-ejfv **2.55**, lurbinectedin **2.50** and belantamabmafodotin-blmf **2.56**.[61] Ziconotide **2.44**, also called SNX–111 or Prialt, is a synthetic form of an ω-conotoxin MVIIA peptide isolated from the venom of the fish hunting marine cone snail, *Conus magus*, in the early 1980s.[62] The FDA approved it in 2004 as an analgesic for treating chronic pain. Fish oil-derived omega-3-acid ethyl esters with ethyl esters of eicosapentaenoic acid **2.45** and docosahexaenoic acid **2.46** as major components were approved by the FDA in 2004 as an anti-hypertriglyceridemia drug.[60] This drug is marketed under the trade name Lovaza® formerly known as Omacor. Eicosapentaenoic acid ethyl ester **2.45** was approved in 2012 under the brand name Vascepa® to treat hypertriglyceridemia.[61] Omega-3-carboxylic acids are fish oil-derived from fatty acids with eicosapentaenoic acid **2.47** and docosahexaenoic acid **2.48** as the most abundant. It was approved in 2014 under the brand name Epanova® to treat hypertriglyceridemia.[61]

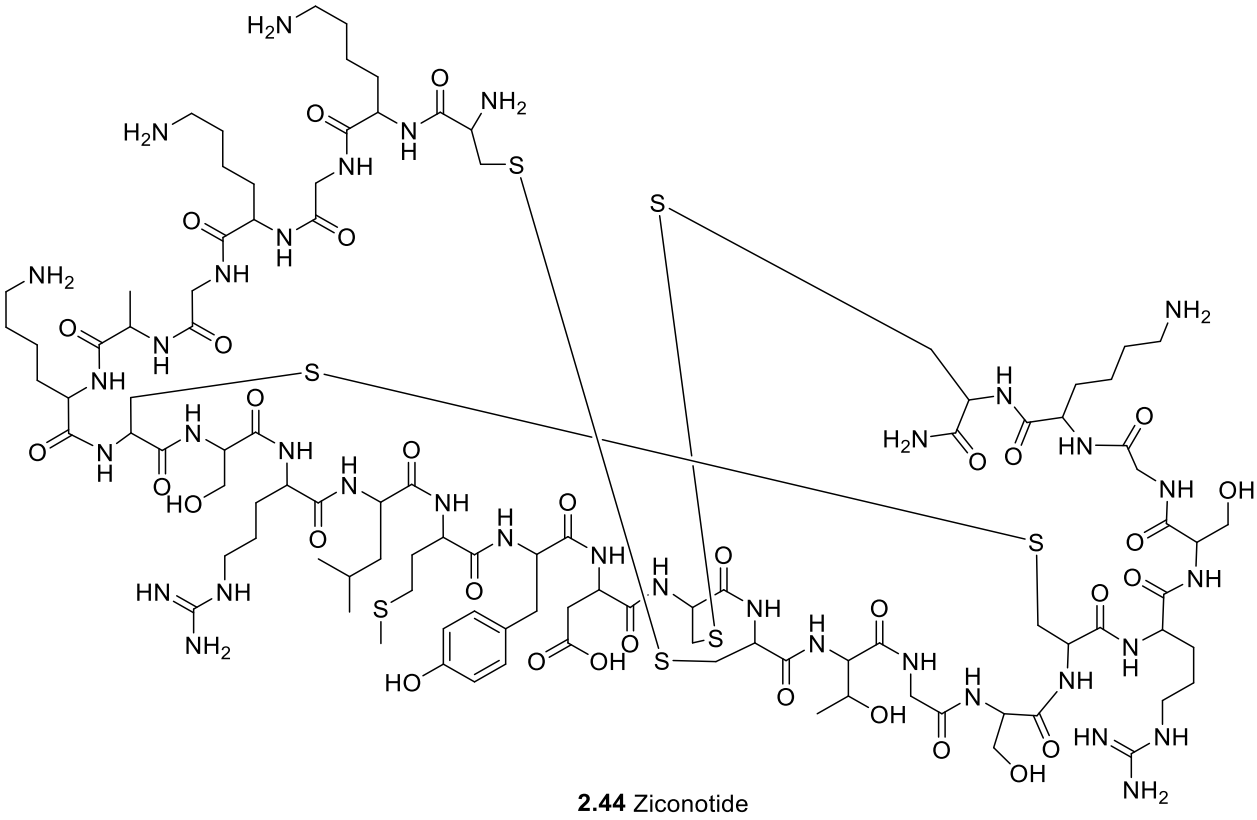

2.44 Ziconotide

Figure 2.10: Ziconotide isolated from *Conus magus*.

The antitumor agent, trabectedin **2.49**, also called Yondelis or ET-743, was originally isolated from the crude extract of the sea squirt *Ecteinascidia turbinate* in 1984.[63] The European Medicine Agency (EMEA) approved this drug in 2007 to treat soft-tissue sarcoma and ovarian cancer. Lurbinectedin **2.50**, a synthetic analogue of trabectedin **2.49**, was approved by the FDA in 2020 to treat metastatic small cell lung cancer.[61] Eribulin mesylate **2.51** (E-7389 or Halaven) is a synthetic derivative of the anticancer agent halichondrin B **2.52** initially isolated from the marine sponge *Halichondria okadai* in 1986.[61,64] This drug was approved in 2010 by the FDA to treat metastatic breast cancer.

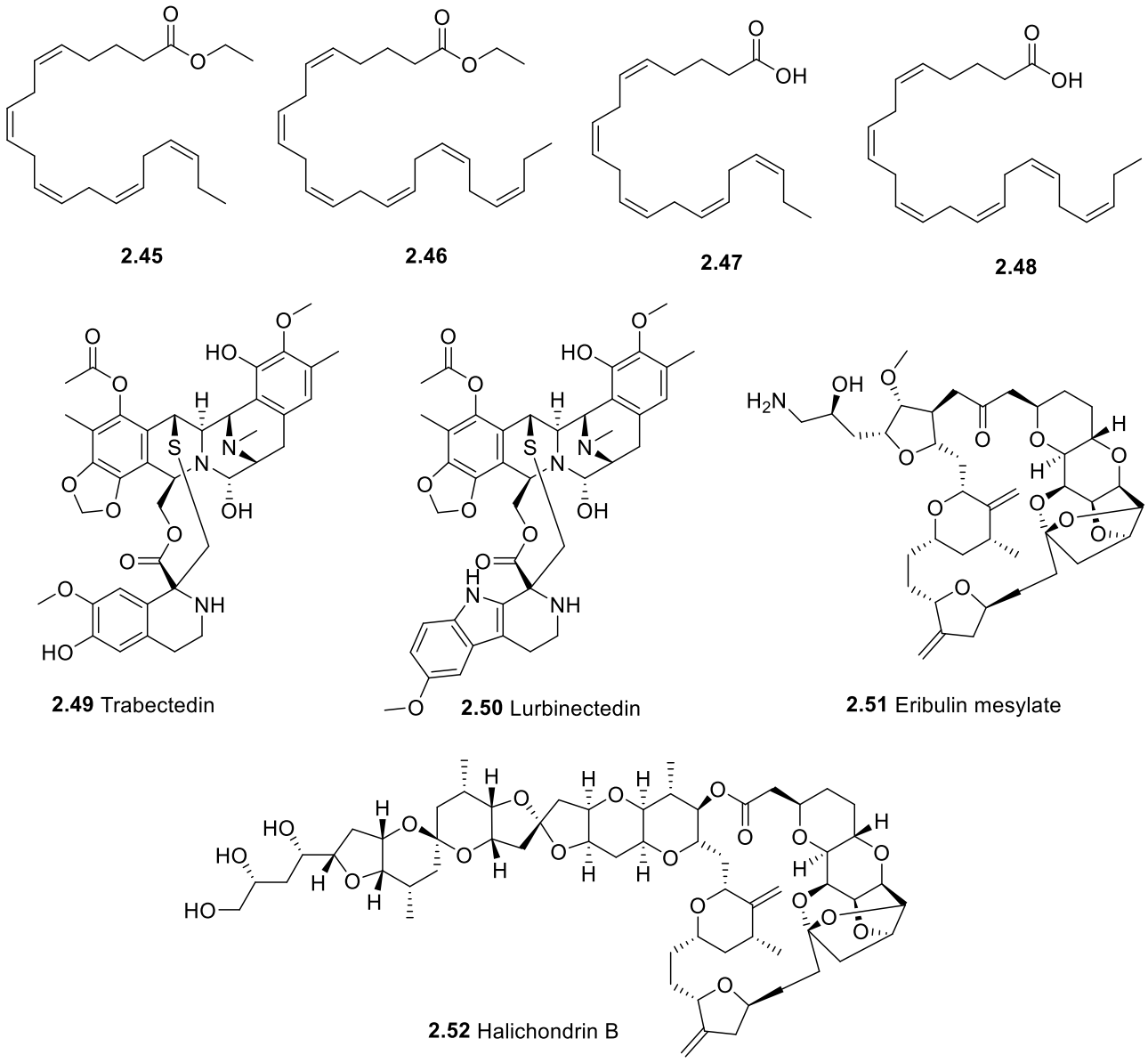

Figure 2.11: MNPs, MNP drugs and MNP derived drugs (chemical structures **2.45**-**2.52**)

Brentuximab vedotin **2.53** (SGN-35 or Adcetris) is an antibody-drug conjugate (ADC) and was developed from monomethyl auristatin E (MMAE), a synthetic analogue of the antineoplastic agent dolastatin 10 **2.57**.[60] This drug was approved by the FDA in 2011 to treat relapsed or refractory Hodgkin lymphoma and systemic anaplastic large cell lymphoma.[60] Two other ADCs, polatuzumab vedotin **2.54** (DCDS-4501A) and enfortumab vedotin-ejfv **2.55** were also developed from MMAE and approved by the FDA in 2019 for the treatment of cancer.[61,65] Polatuzumab

vedotin **2.54** is used to treat non-Hodgkin lymphoma, chronic lymphocytic leukemia, lymphoma, B-Cell lymphoma, and follicular lymphoma.[61] Enfortumab vedotin-ejfv **2.55** is used to treat metastatic urothelial cancer.[61] Another ADC, Belantamab mafodotin-blmf **2.56**, developed from monomethyl auristatin F (MMAF), also a synthetic analogue of dolostatin 10 **2.57**, was approved by the FDA in the year 2020 to treat relapsed/refractory multiple myeloma.[61,66] Although dolastatin 10 **2.57**, which was initially isolated from the sea hare *Dolabella auriculari* in 1972, was the most active antineoplastic agent at the time of its isolation, it never progressed past Phase II clinical trials.[60,67] However, several analogues of dolastatin 10 **2.57** are in various stages of clinical trial developments. Plitidepsin **2.58** (dehydrodidemnin B or Aplidin) was isolated from the Mediterranean ascidian *Aplidium albicans* and exhibited antitumor, antiviral and immunosuppressive activities.[68] Plitidepsin **2.58** was approved in 2018 in Australia to treat relapsed and refractory multiple myeloma.[61]

Ten out of the 14 approved marine-derived drugs and most marine-derived drug candidates in preclinical and clinical trials and the MNPs isolated have been reported to show cytotoxic and anticancer activity.[61] This could be attributed to the chemical defense role these MNPs play and the involvement of the US National Institutes of Health (NIH)/ National Cancer Institute (NCI), which sponsored most of the marine natural product drug discovery's greater focus on antitumor activity.[69,70] The NCI even developed a repository of extracts of marine invertebrates sampled worldwide to screen against its 60 human cancer cell lines.[71] There is no MNP derived antitubercular drug or antitubercular drug candidate in clinical trials, although some isolated MNPs have exhibited potent antitubercular activity. It is imperative to rescreen NCI's MNP repository and aggressively refocus MNP drug discovery on other disease targets like Mtb for tuberculosis drug discovery. About 75% of the MNP derived drugs and those in clinical trials found in the global marine pharmaceutical pipeline were obtained from marine invertebrates.[61,72,73]

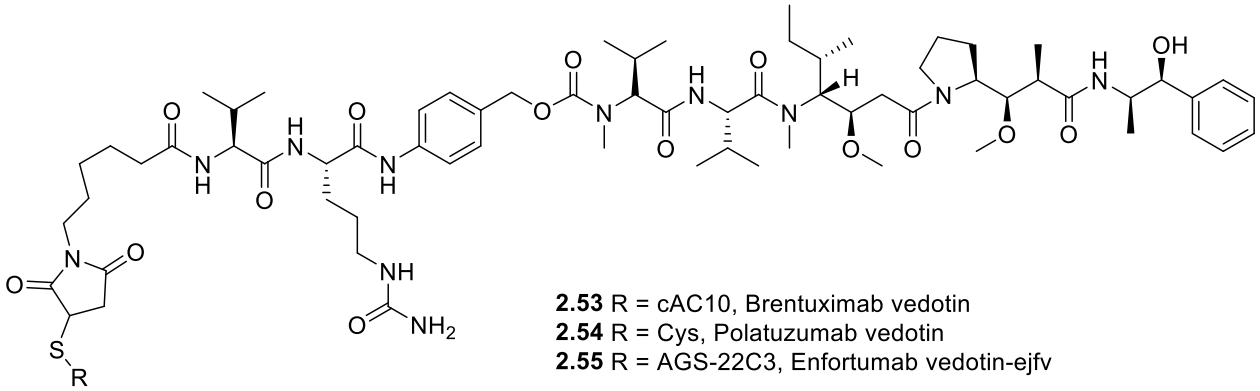

2.53 R = cAC10, Brentuximab vedotin
2.54 R = Cys, Polatuzumab vedotin
2.55 R = AGS-22C3, Enfortumab vedotin-ejfv

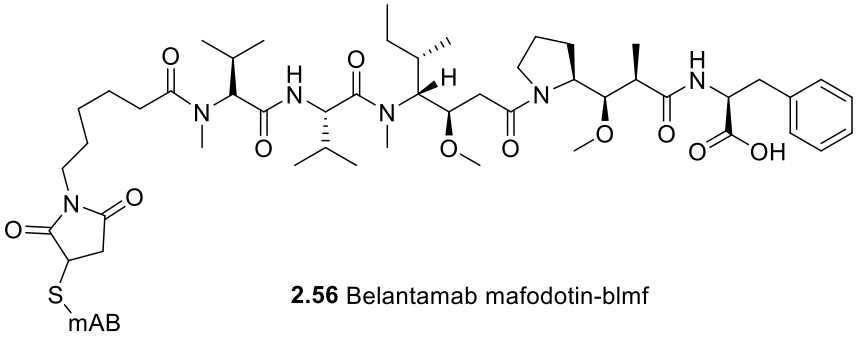

2.56 Belantamab mafodotin-blmf

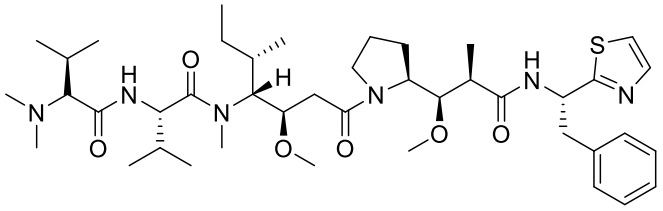

2.57 Dolastatin 10

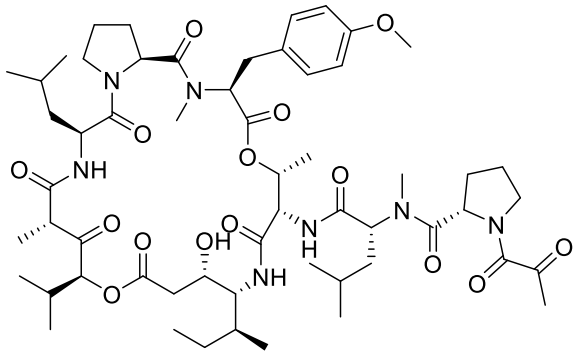

2.58 Plitidepsin

Figure 2.12: MNPs, MNP drugs and MNP derived drugs (chemical structures **2.53**-**2.58**)

2.3.1.1 Marine invertebrates

Marine invertebrates are marine animals without a backbone. With evolution, some have developed a hard exoskeleton or shell. The marine invertebrate phyla that have been explored for drug discovery include tunicates, cnidarians, echinoderms, molluscs, arthropods and sponges. The sponges are soft-bodied and sessile.[41] They possess pores within them that allow constant water to flow through their bodies to obtain oxygen, food and to get rid of waste since they do not have circulatory, digestive and nervous systems.[41] These invertebrates, especially the sponges, are vulnerable to attacks and predation from micro and macro marine organisms. They therefore biosynthesize and secret compounds that serve as chemical weapons to protect them from their competitors and predators to survive.[41,72] These compounds exhibit a wide range of biological activities.

This section of the literature review chapter will further highlight some MNPs with antimycobacterial activity isolated from marine sponges. Many compounds (over 170) of the alkaloid, terpenoid, peptide, quinone, pyrone, sterol, and lactone structural classes, with anti-TB properties, have been isolated from marine organisms.[73] Out of the over 170 compounds, 48.1% were isolated or derived from marine invertebrates.[73] These marine invertebrates were largely sponges, corals, molluscs and tunicates.[73] The sponges are the most prolific producers of marine bioactive compounds and accounted for about 42.7% of the anti-TB agents isolated from marine invertebrates.[73] Highlighted in Table 1 and Figures **2.13**-**2.15** are some sponge derived bioactive anti-TB metabolites. These MNPs have interestingly unique complex chemical structures, and an example is the manzamine class of compounds. The manzamines are polycyclic alkaloids with mainly a fused and bridged tetra- or pentacyclic ring system attached to a β-carboline moiety.[74] The first manzamine, manzamine A **2.59**, was isolated from the Okinawan sponge *Haliclona* sp. and reported in 1986.[75] Over 80 other manzamines and manzamine-related compounds have been isolated from several marine sponges collected from different geographical locations, including species of the genera *Acanthostrongylophora*, *Amphimedon*, *Cribrochalina*, *Ircinia*, *Pachypellina*, *Pellina*, *Petrosia*, *Prianos*, *Xestospongia* and *Xestospongiaashmorica*.[76,77]

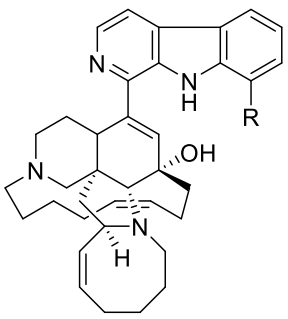

2.59 R = H, Manzamine A
2.60 R = OH, 8-Hydroxymanzamine A

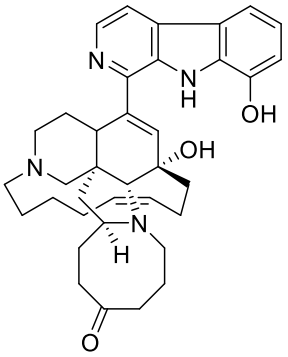

2.61 Manzamine F

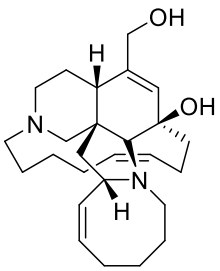

2.62 Ircinol A

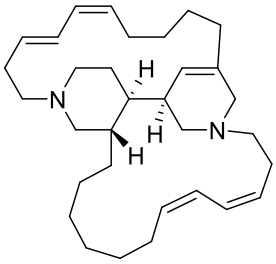

2.63 Halicyclamine A

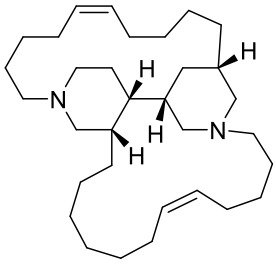

2.64 Haliclonacyclamine A

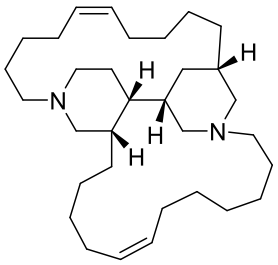

2.65 Haliclonacyclamine B

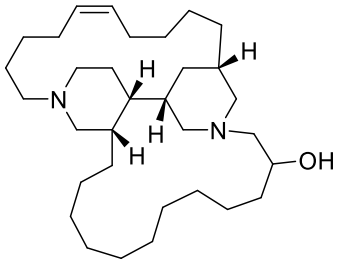

2.66 Hydroxyhaliclonacyclamine B

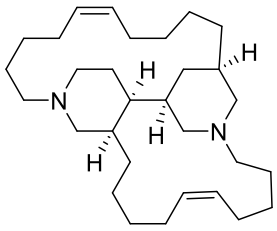

2.67 Neopetrosiamine A

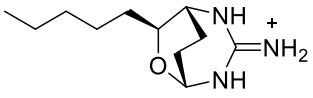

2.68 Monanchorin

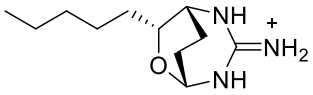

2.69 6-Epi-monanchorin

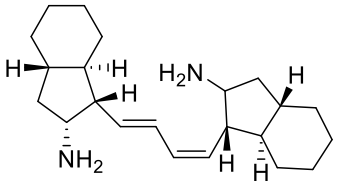

2.70 Halichondriamine A

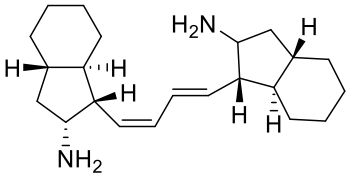

2.71 Halichondriamine B

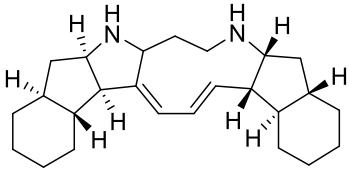

2.72 Papuamine

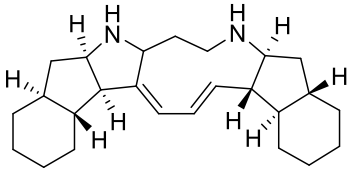

2.73 Haliclonadiamine

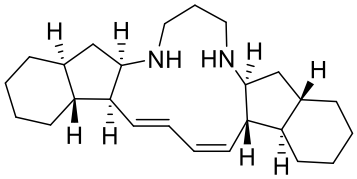

2.74 (10Z,12E)-Haliclonadiamine B

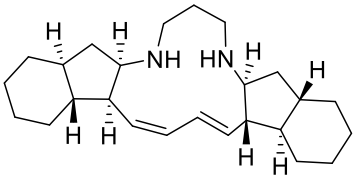

2.75 (10E,12Z)-Haliclonadiamine B

Figure 2.13: MNPs isolated from marine sponges with anti-Mtb activity (**2.59**-**2.75**)

The manzamines have shown good biological activities against various disease-causing pathogens and targets.[74] Manzamines A **2.58**, F **2.61**, 8-hydroxymanzamine **2.60** and ircinol A **2.62** exhibited potent activity against *M. tuberculosis* H37Rv with MICs of 1.64, 0.69, 2.84, and 4.61 µM, respectively.[73,75,78–80] Among the halicyclamine tetracyclic alkylpiperidine alkaloids isolated, halicyclamine A **2.63**, haliclonacyclamines A **2.64** and B **2.65**, and 22-hydroxyhaliclonacyclamine B **2.66** isolated from the Indonesian marine sponge *Haliclona* sp. exhibited strong antimycobacterial activity.[73,81–83] A bis-piperidine halicyclamine alkaloid neopetrosiamine A **2.67**, isolated from the Puerto Rican marine sponge *Neopetrosia proxima* was strongly active against *M. tuberculosis* strain H37Rv with a MIC of 17.05 µM.[84] Papuamine **2.72,** haliclonadiamine **2.73** and its derivatives (10Z,12E)-haliclonadiamine **2.74** and (10E,12Z)-haliclonadiamine **2.75**, halichondriamines A **2.70** and B **2.71**, and the bicyclic guanidine alkaloid, monanchorin **2.68** and 6-epi-monanchorin **2.69** isolated from the Okinawan marine sponge *Halichondria panacea* and other marine sponges were potently active against *M. smegmatis* with inhibitory zones of 7–16 mm at a concentration of 10 µg/disc.[73,85–88] Compound **2.75** was the most active with a 16 mm zone of inhibition at 10 µg/disc.[73] An anti-TB and cytotoxic extract of the Brazilian marine sponge *Pachychalina* sp. yielded ingenamine G **2.76** and cyclostellettamines A–I, **2.77-2.85** K **2.86** and L **2.87**.[89,90] Compounds **2.76**, **2.78, 2.79, 2.83** and **2.87** were active against *M. tuberculosis* H37Rv with a MIC range of 4.0-32 µg/mL. The Mexican sponge *Aplysina gerardogreeni* yielded the antimycobacterial bromotyrosine derivative, areothionin **2.88**.[91] Compound **2.88** was active against resistant strains of *M. tuberculosis* H37Rv at a MIC of 12.5 µg/mL.[91] The agelasines are cyclic diterpenoids with a 9-methyladeninium moiety exclusively produced by the sponge of the genus *Agelas*.[92] Among the agelasines isolated, agelasines D **2.90**, E **2.91** and F **2.92** have shown anti-Mtb activity. While agelasine E **2.91** showed weak inhibitory activity against *M. tuberculosis*, (þ)-agelasine D **2.90** was potent with 92% inhibition at 6.25 µg/mL, and agelasine F **2.92** was active against DR-Mtb at concentrations at a minimum of 3.13 µg/mL.[93,94] The polycyclic guanidine alkaloids batzelladines L **2.93** and N **2.94** isolated from the Jamaican sponge *Monanchora unguifera* showed potent activity against *M. tuberculosis* with MICs of 2.63 and 5.23 µM.[95] Heteronemin **2.89,** originally isolated from the Italian marine sponge *Heteronema erecta*

and subsequently isolated from several other marine sponges showed potent anti-Mtb activity with a MIC of 6.25 µg/mL.[96,97]

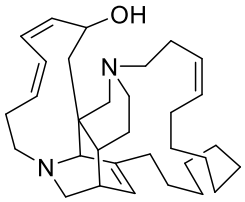

2.76 Ingenamine G

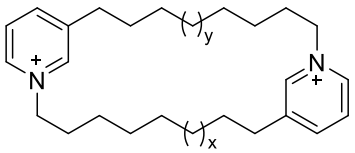

2.77 x = y = 5, Cyclostellettamine A
2.78 x = 5, y = 6, Cyclostellettamine B
2.79 x = y = 6, Cyclostellettamine C
2.80 x = 5, y = 7, Cyclostellettamine D
2.81 x = 6, y = 7, Cyclostellettamine E
2.82 x = y = 7, Cyclostellettamine F
2.83 x = 4, y = 5, Cyclostellettamine G
2.84 x = 3, y = 5, Cyclostellettamine H
2.85 x = 3, y = 6, Cyclostellettamine I
2.86 x = 3, y = 7, Cyclostellettamine K
2.87 x = 4, y = 7, Cyclostellettamine L

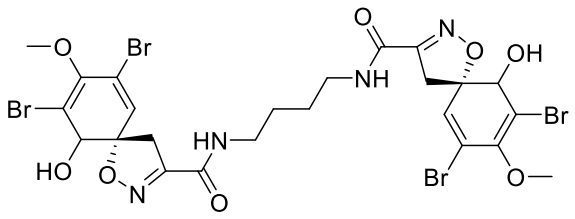

2.88 Areothionin

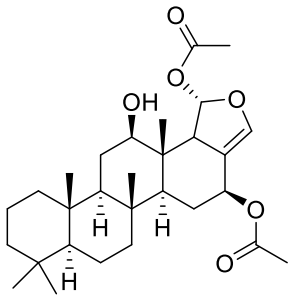

2.89 Heteronemin

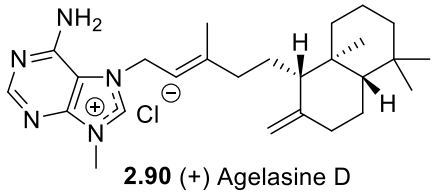

2.90 (+) Agelasine D

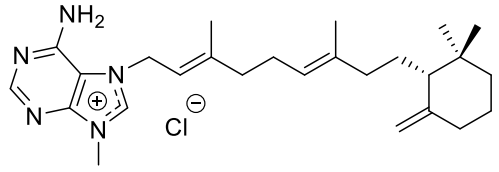

2.91 Agelasine E

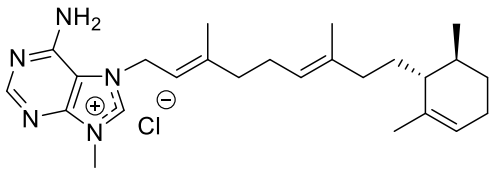

2.92 Agelasine F

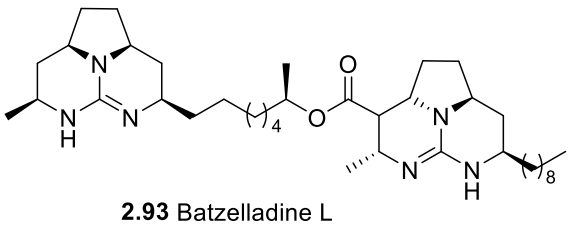

2.93 Batzelladine L

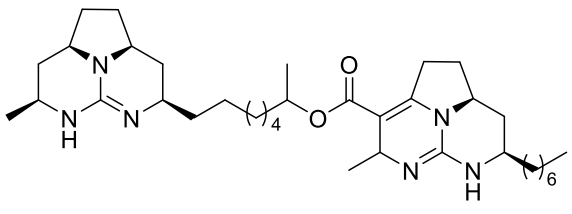

2.94 Batzelladine N

Figure 2.14: MNPs isolated from marine sponges with anti-Mtb activity (**2.76**-**2.94**)

The quinone sesquiterpenes puupehenone **2.95**, 15-cyanopuupehenone **2.96** and 15-cyanopuupehenol **2.97**, isolated from sponges of the genera *Verongida* and *Hyrtios*, exhibited potent activity against *M. tuberculosis* H37Rv with 99%, 90%, and 96% inhibition at 12.5 µg/mL.[98,99]

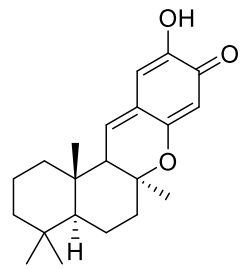

2.95 Puupehenone

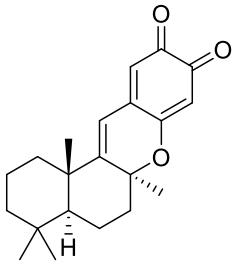

2.96 15-Cyanopuupehenone

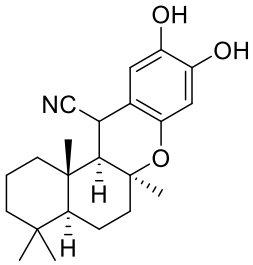

2.97 15-Cyanopuupehenol

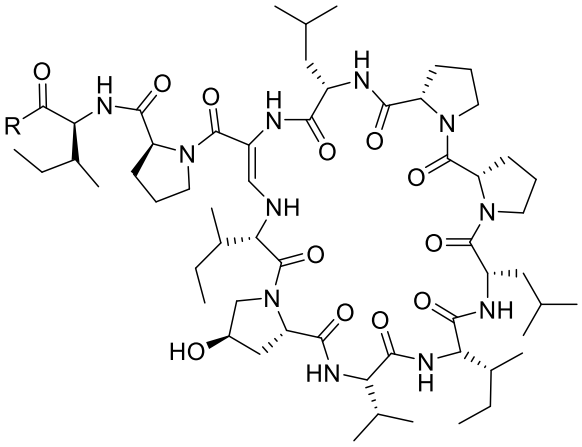

2.98 Callyaerins A, R =

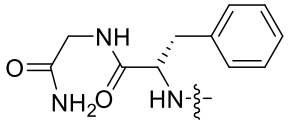

2.99 Callyaerins B, R =

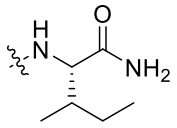

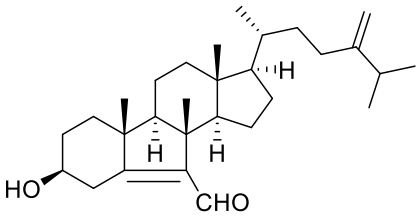

2.100 Parguesterol A

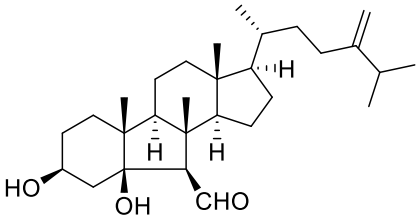

2.101 Parguesterol B

Figure 2.15: MNPs isolated from marine sponges with anti-Mtb activity (**2.95**-**2.101**)

The peptides callyaerins A **2.98** and B **2.99** isolated from the Indonesian sponge *Callyspongia aerizusa* exhibited potent activity against *M. tuberculosis* with MIC_{90}s of 2.00 and 5.00 µM, respectively.[73,100] The sterols parguesterols A **2.100** and B **2.101** isolated from the Caribbean

sponge *Svenzea zeai* were active against *M. tuberculosis* H37Rv with MICs of 18.93 and 26.05 μM.[101]

Table 2.1: Some sponge MNPs with anti-TB activity.

Structure No	Compound	Structural Class	Species	Ref
2.58-2.60	Manzamines	Alkaloids	*Acanthostrongylophora* sp.	73-80
2.63-2.75	Haliclonacyclamines	Alkaloids	*Haliclona* sp.	73, 81-83
2.766	Neopetrosiamine A	Alkaloids	*Neopetrosia proxima*	84
2.77-2.75	Haliclonadiamines, Halichondriamines A and B Papuamine	Alkaloids	*Halichondria panacea*	73, 85-88
2.76-2.87	Ingenamine G, Cyclostellettamines A-I, K, and L	Alkaloids	*Pachychalina* sp.	89, 90
2.88	Areothionin	Alkaloids	*Aplysina gerardogreeni*	91
2.90-2.92	(+)-Agelasine D	Alkaloids	*Agelas* sp.	92-94
2.93-2.94	Batzelladines	Alkaloids	*Monanchora unguifera*	95
2.89	Heteronemin	Terpenoids	*Heteronema erecta*	96, 97
2.95-2.97	Puupehenone (84) 15-Cyanopuupehenone 15-Cyanopuupehenol	Terpenoids	*Verongida* spp. *and Hyrtios* spp.	88, 89
2.98-2.99	Callyaerins	Peptides	*Callyspongia aerizusa*	73, 100
2.100-2.101	Parguesterols A and B	Sterols	*Svenzea zeai*	101

2.3.2 Microbial natural products

Plants, and mostly higher plants, have historically been used to treat numerous illnesses, and recently marine organisms, especially invertebrates, have also been the source of drugs for treating diseases. There are, however, problems with the (re-)supply of bioactive compounds from these source organisms. Gram quantities of a bioactive compound are typically needed for further studies, such as preclinical and clinical trials in the drug discovery pipeline. This means that more must be re-isolated from a large quantity of the source organism if it is difficult to synthesize or semi-synthesize this bioactive compound. While plant availability is generally seasonal, there are political and environmental restrictions on some rare species of plants. There are similar challenges with respect to collection of samples from the marine environment: special equipment is often required to access sufficient quantities and often within significant ecological constraints.

Conversely, it is easy to re-isolate large quantities of a bioactive compound from a microorganism since it only requires direct culturing of this organism on a large-scale using commercial fermenters. Samples from which these microbes are isolated are only collected once. With the advancement in technology and the reduced cost involved in the extraction and the subsequent sequencing of microbial genomic material, it is relatively easy to over-express the biosynthetic cluster responsible for producing a bioactive compound through a heterologous system (i.e. by cloning the biosynthetic genes into another microorganism).[102] Furthermore, microbial natural products are diverse with unique chemical scaffolds and various biological activities.[103] The serendipitous discovery of the breakthrough antibiotic penicillin from the fungus *Penicillium notatum* by Sir Alexander Fleming in 1929 redirected focus and gave microbial natural products prominence.[104] Fungi and bacteria, including actinobacteria, *Bacillus*, cyanobacteria, myxobacteria and *Pseudomonas* species, have been the primary source of microbial natural products.[103] The number of drugs from microbes is unmatched compared to drugs from other sources, with actinomycetes (filamentous actinobacteria) being the most prolific producers of them all.[103] Actinomycetes are responsible for producing about 45% of bioactive microbial metabolites.[103]

2.3.2.1 Actinomycetes

Actinobacteria are Gram-positive bacteria with high guanine and cytosine (G+C) content in their DNA. Many produce spores. They belong to the phylum Actinobacteria, which currently comprises 20 orders and more than 50 families.[105] This bacterial phylum is widely distributed in terrestrial, and fresh and marine aquatic environments. Some of them can thrive under extreme conditions, such as hyper-arid, high salinity, cold, high pressure, low pH (acidic) and heavy metal-contaminated ecosystems.[106] Actinomycetes are either free-living, and examples are soil-dwelling actinomycetes or living in association with other organisms like the plant commensals or those living in and/or on the surfaces of animals like ants, termites and marine invertebrates.[107–109] Some actinomycetes also serve as plant and animal pathogens.[108] Actinomycetes play diverse roles (sometimes in symbiosis with macro-organisms). They are of commercial value and find use in agriculture, biotechnology, and medicine. In agriculture, they are saprophytic and break down dead plant and animal remains, hastening decomposition.[107] They also aid in nitrogen fixation and are also known to produce plant growth promoters, insecticides, herbicides and fungicides.[108] In biotechnology, actinomycetes are used in treating human and industrial waste.[110] Actinomycete secondary metabolites are structurally diverse and have shown various biological activities, including antioxidant, anthelmintic, antifungal, enzyme inhibitory, antibacterial, anticancer, immunosuppressive and cardiovascular properties.[108,111,112] Antibiotics are the largest class of drugs discovered from actinomycetes, as actinomycetes produce about 70% of all naturally derived antibiotics currently in clinical use.[108]

Most of these antibiotics fall under the most significant drug scaffolds, including aminoglycosides, β-lactams, glycopeptides, macrolides, rifamycins and tetracyclines. Many of these antibiotics were discovered during the golden era of novel antibiotic drug discovery.[111] Among the antibiotics produced by actinomycetes are antimycobacterial agents or drugs. The first anti-TB drug ever discovered was the aminoglycoside streptomycin **2.10**. Streptomycin **2.10** was isolated from the actinomycete *Streptomyces griseus* in 1943.[113] Another *Streptomyces griseus* strain, 446-S3, produced the nucleoside antibiotic, capuramycin **2.102**, which exhibited potent antimycobacterial activity.[114,115] The kanamycins A-C **2.12, 2.103-2.104** are broad-spectrum aminoglycoside antibiotics isolated from *Streptomyces kanamyceticus* in 1957.[116] Kanamycin A

2.12, normally referred to as kanamycin, and its derivative amikacin **2.13** are used as second-line anti-TB drugs.[117]

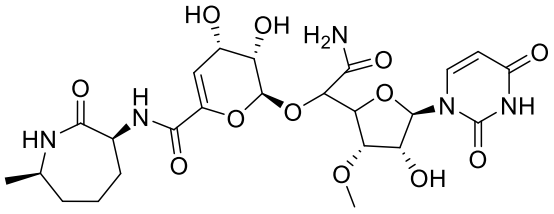

2.102 Capuramycin

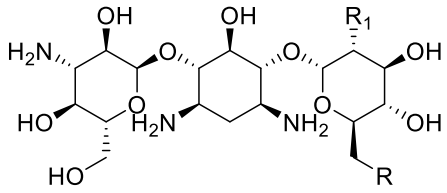

2.12 R = NH_2, R_1 = OH, Kanamycin A
2.103 R = R_1 = NH_2, Kanamycin B
2.104 R = OH, R_1 = NH_2, Kanamycin C

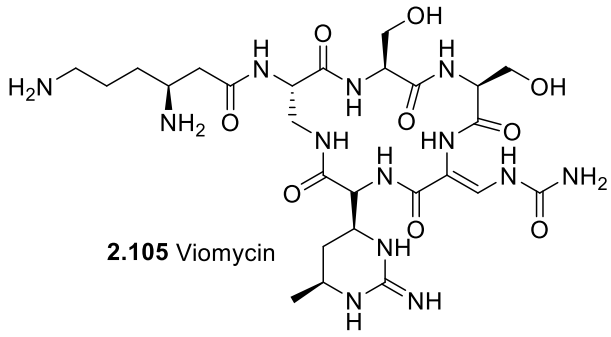

2.105 Viomycin

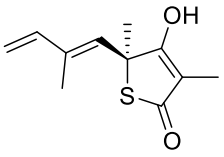

2.106 Thiolactomycin

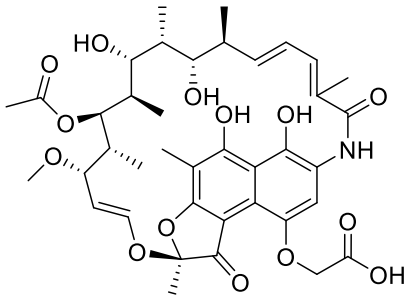

2.107 Rifamycin B

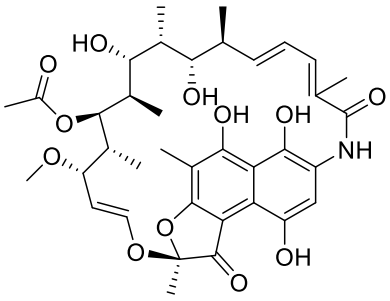

2.109 Rifamycin SV

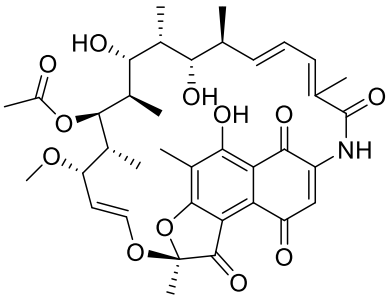

2.108 Rifamycin S

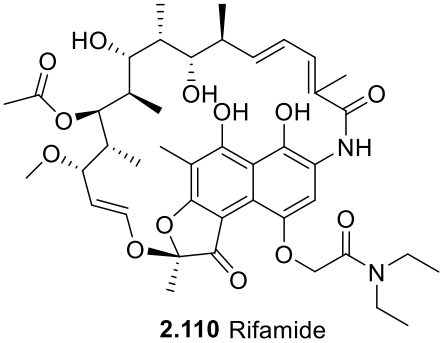

2.110 Rifamide

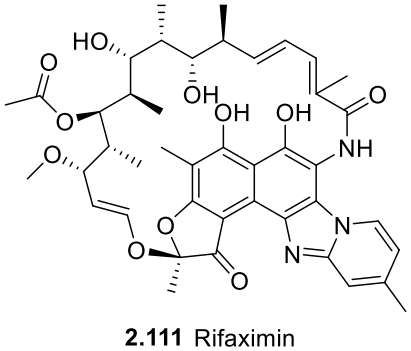

2.111 Rifaximin

Figure 2.16: Anti-TB drugs from actinomycetes (**2.102**-**2.111**)

Capreomycin is an antiphlogistic antibiotic, which is grouped with the second line anti-TB aminoglycoside drugs, was isolated from *Streptomyces capreolus* in 1960.[116] The tuberactinomycin class antibiotic, viomycin **2.105**, was replaced by the less toxic capreomycin in TB treatment.[118] Viomycin **2.105** was isolated in 1950 from the actinomycetes *Streptomyces puniceus* and exhibited potent antimycobacterial activity against Mtb.[119] The antibiotic cycloserine **2.18**, isolated from *Streptomyces orchidaceus*, was used as a second-line anti-TB drug.[116] The thiolactone antibiotic, thiolactomycin **2.106**, produced by the soil actinomycete, *Nocardia* sp. strain 2-200, showed antimycobacterial activity.[120] A French soil actinomycete, later correctly labeled *Amycolatopsis rifamycinica* isolated in 1957, yielded an ansamycin class of antibiotics called rifamycins.[121] The most stable pure isolate, rifamycin B **2.107**, was weakly active, but its oxidized and hydrolyzed analogue, rifamycin S **2.108**, exhibited potent activity.[122] Structural modifications of rifamycin S **2.108** yielded rifamycin SV **2.109** and later rifamide **2.110**, which entered clinical use intravenously.[122,123] Rifampin **2.2**, a 3-(4-methyl-1-piperazinyl)-iminomethyl derivative of rifamycin SV **2.109** was discovered after an intense structural modification study.[122,123] Rifampin **2.2** has been a core anti-TB drug, and it is administered orally.[123] Currently, three more rifamycin analogous, rifabutin **2.5**, rifapentine **2.6**, and rifaximin **2.111**, have been approved for (and are in) clinical use. Compounds **2.5** and **2.6** are anti-TB drugs, while **2.111** is used to treat irritable bowel syndrome and travelers' diarrhea in adults.[123]

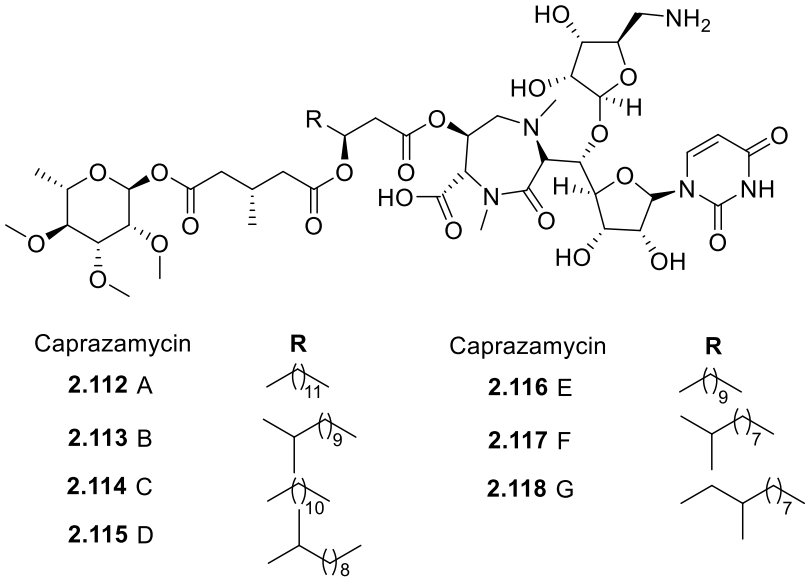

Figure 2. 17: Anti-Mtb drugs from actinomycetes (**2.112**-**2.118**)

A collection of lipo-uridyl class of antibiotics called caprazamycins A-G **2.112-2.118**, isolated from the fermentation broth of *Streptomyces* sp. MK730-62F2 was active against acid-fast bacteria, including Mtb and members of the *M. avium* complex.[124] It has been established that biodiversity-rich ecosystems serve as sources of novel actinomycetes from which novel secondary metabolites are produced.

2.3.2.2 Chemistry and bioactivity of metabolites from South African Actinomycetes

South Africa is the third most bio-diverse natural habitat on Earth.[125] Several novel actinomycete strains have been isolated from South African biodiversity-rich soils, sediments, flora and fauna both in the terrestrial and marine environments. These strains include species of the ubiquitous *Streptomyces* genus and the less isolated rare genera *Actinomadura*, *Actinosynnema*, *Amycolatopsis*, *Gordonia*, *Kribbella*, *Nocardia*, *Nonomuraea*, *Rhodococcus*, *Streptosporangium*, *Saccharopolyspora* and *Tsukamurella*.[126–134] Most of the research projects that led to the isolation of these strains and their metabolites were mainly drug discovery-based. However, some focused on the biology and metabolomic profiles of these strains. These strains and their metabolites displayed various biological activity, including antibacterial, antifungal, anticancer and antiplasmodial activities. This section of the literature review chapter highlights the secondary metabolites produced by actinomycete strains isolated from South African environments. It includes natural products isolated from species of the genus *Streptomyces* and rare actinomycetes isolated from South African soils and the South African termite *Macrotermes natalensis* and its fungal comb, through bioassay-guided and/or spectroscopic guided isolation schemes. It is worth mentioning that none of the research on the chemistry of metabolites from South African actinomycetes reported here was done in South Africa. These projects only collected samples from South Africa.

The first report of a South African actinomycete-derived secondary metabolite was a tetraene macrolide called pimaricin **2.119** (also known as natamycin, natacyn, tennecetin and E235), which was patented in 1958.[135,136] This antibiotic was first purified in 1955 from the extract of the culture broth of *Streptomyces natalensis*, isolated from a soil sample collected from Pietermaritzburg in KwaZulu-Natal province, South Africa.[136]

Table 2.2 : Secondary metabolites from South African actinomycetes and their biological activities.

Structure No.	Compound	Structural class	Bioactivity	Producing Species	Discovery tool	Ref
2.119	Pimaricin	Tetraene macrolide	Antifungal	*Streptomyces natalensis*		135-144
2.120-2.128	Altromycins	New anthraquinone pluramycin type	Antibacteria, antitumor and cytotoxicity	Strain AB 1246E-26	Antibiotic screening	145-149
2.129-2.169	Platensimycin, Platencin, their analogues and unrelated compounds	New ketolides	Antibacteria	*Streptomyces platensis* strain MA7327	Antisense screening	150-160
2.170-2.178	Natalamycin A, Reblastatin, Geldanamycin and its derivatives	Ansamycin macrolide	Antifungal	*Streptomyces* strain M56		161
2.179	17-Hydroxycyclooctatin		Cytotoxicity	*Streptomyces* sp. M56	LCMS based	162
2.180-2.193	Termisoflavones A-D and other Isoflavonoids	Isoflavonoids		*Streptomyces* sp. RB1	Antibiotic screening	163-164
2.194	1-*O*-(2-aminobenzoyl)-α-L-rhamnopyranoside (ABR)		Cytotoxicity	*Streptomyces* sp. RB1	Bioactivity	164
2.195-2.198	Dentigerumycin , Dentigerumycin C-D	Cyclic depsipeptide	Antifungal	*Streptomyces* sp. M41	Bioactivity and LCMS based	166
2.199-2.202	Rubterolones A-F	Tropolone alkaloids	Antifungal	*Actinomadura* sp. 5-2	Bioactivity and LCMS based	167
2.205-2.207	Natalenamides A–C	Cyclic tripeptides	Cytotoxicity	*Actinomadura* sp. RB99	LCMS based	168
2.208-2.222	Polychlorinated and Polybrominated analogous of Daidzein and Genistein	Isoflavanoid	Antibacteria and antifungal	*Actinomadura* sp. RB99	LCMS based	169
2.223	Fridamycin A	Type II polyketide synthase-derived	Antibiotic and antitumor	*Actinomadura* sp. RB99	LCMS based	170
2.224-2.227	Macrotermycins A-D	Glycosylated Polyketide macrolactams	Antifungal	*Amycolatopsis* sp. M39	Bioactivity and LCMS based	171

Pimaricin **2.119** was later also isolated from *Streptomyces gilvosporeus*, *Streptomyces chattanogenesis* and *Streptomyces lydicus*.[137–139] Pimaricin **2.119** was active against saprophytic and parasitic fungi and is therefore used as a pesticide.[140] Its mechanism of action is by binding

to a crucial constituent of the fungal cell wall called ergosterol, thereby inhibiting fungal growth.[141,142] Therefore, pimaricin **2.119** has a broad spectrum of fungal activity, with minimal toxicity to mammalian cells. It also displayed *in vitro* activity against numerous protozoa, including *Trypanosoma* and *Acanthamoeba*.[143,144] Pimaricin **2.119** is produced commercially and used as a fungicide in medicine and the food industry.[140] In medicine, it is used to treat keratitis, especially that caused by *Aspergillus fumigatus*, *Candida albicans* and *Acanthamoeba* sp.[140,144] It is also used to treat fungal infections caused by *Cephalosporium*, *Fusarium* and *Penicillium*; and has shown activity against *Alternaria*, *Colletotrichum*, *Curvularia*, *Lasiodiplodia*, *Scedosporium* and *Trichophyton*.[140] It is a food additive that has been used as a preservative to prevent fungal growth on foods such as cheese, sausages, yoghurt, fruits, meats, baked confectioneries and beverages for about half a century.[140]

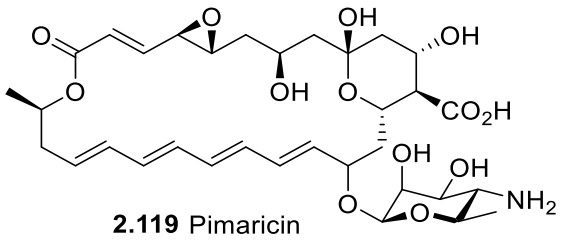

2.119 Pimaricin

Figure 2.18: Pimaricin from *Streptomyces natalensis*.

A soil microbial antibiotic screening project led to the isolation of actinomycete strain, AB 1246E-26, from a South African bushveld soil.[145] Although the genus of this actinomycete strain was not determined, preliminary characterization data narrowed the taxonomic assignment to either *Nocardia* or the defunct *Micropolyspora*.[145] Strain AB 1246E-26 showed activity against the highly antibiotic-sensitive strain of *Pseudomonas aeruginosa* K799/61 among other *P. aeruginosa* strains.[145,146] The organic extract of the whole fermentation broth of strain AB 1246E-26 was subjected to a bioactivity guided isolation procedure to yield the novel anthraquinone-derived class of antibiotics called altromycins.[146,147] The altromycins (A **2.120**- I **2.128**) are nine closely related members of the pluramycin class of compounds with a single epoxide substituent, an amino-disaccharide and/or a 6-deoxy-3-*O*-methylaltrose attached to the conjugated ring systems

of an anthraquinone-*γ*-pyrone core.[146–148] Altromycin B **2.121** was screened against 30 bacterial strains including *Staphylococcus aureus*, *Staphylococcus epidermidis*, *Micrococcus luteus*, *Enterococcus hirae*, *Streptococcus bovis*, *Streptococcus agalactiae, Streptococcus pyogenes, Escherichia coli*, *Enterobacter aerogenes*, *Klebsiella pneumoniae*, *Providencia stuartii*, *Pseudomonas aeruginosa*, *Pseudomonas cepacia* and *Acinetobacter sp.* clinical isolates.[145] Altromycin B **2.121** exhibited potent antibacterial activity against the clinical isolates of *Staphylococcus* and *Streptococcus* with a minimum inhibitory concentration (MIC) range of 0.39 to 3.12 µg/mL and 0.2 to 3.12 µg/mL, respectively, but displayed moderate to weak antibacterial activity against Gram-negative bacteria with a MIC range of 25 to >100 µg/mL.[145] The altromycins also showed cytotoxic activity against various cancer and tumor cell lines, including HeLa cells, human lung (A549), colon tumor (HCT-8), murine leukemia cell (P388) lines and ovarian sarcoma (M5076).[149]

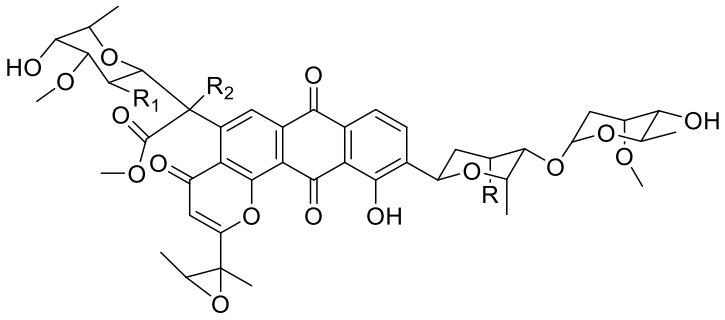

2.120 R = NHMe, R_1 = R_2 = OH, Altromycin A
2.121 R = $N(Me)_2$, R_1 = R_2 = OH, Altromycin B
2.122 R = NHMe, R_1 = H, R_2 = OH, Altromycin C
2.123 R = $N(Me)_2$, R_1 = H, R_2 = OH, Altromycin D
2.124 R = NHMe, R_1 = OH, R_2 = H, Altromycin E
2.125 R = $N(Me)_2$, R_1 = OH, R_2 = H, Altromycin F
2.126 R = NH_2, R_1 = OH, R_2 = OH, Altromycin G

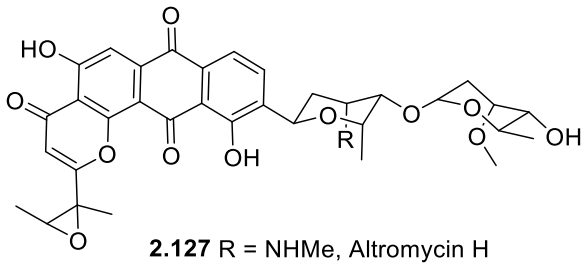

2.127 R = NHMe, Altromycin H
2.128 R = $N(Me)_2$, Altromycin I

Figure 2.19: Altromycins A-I (**2.120**-**2.128**) from South African actinomycetes strain AB 1246E-26.

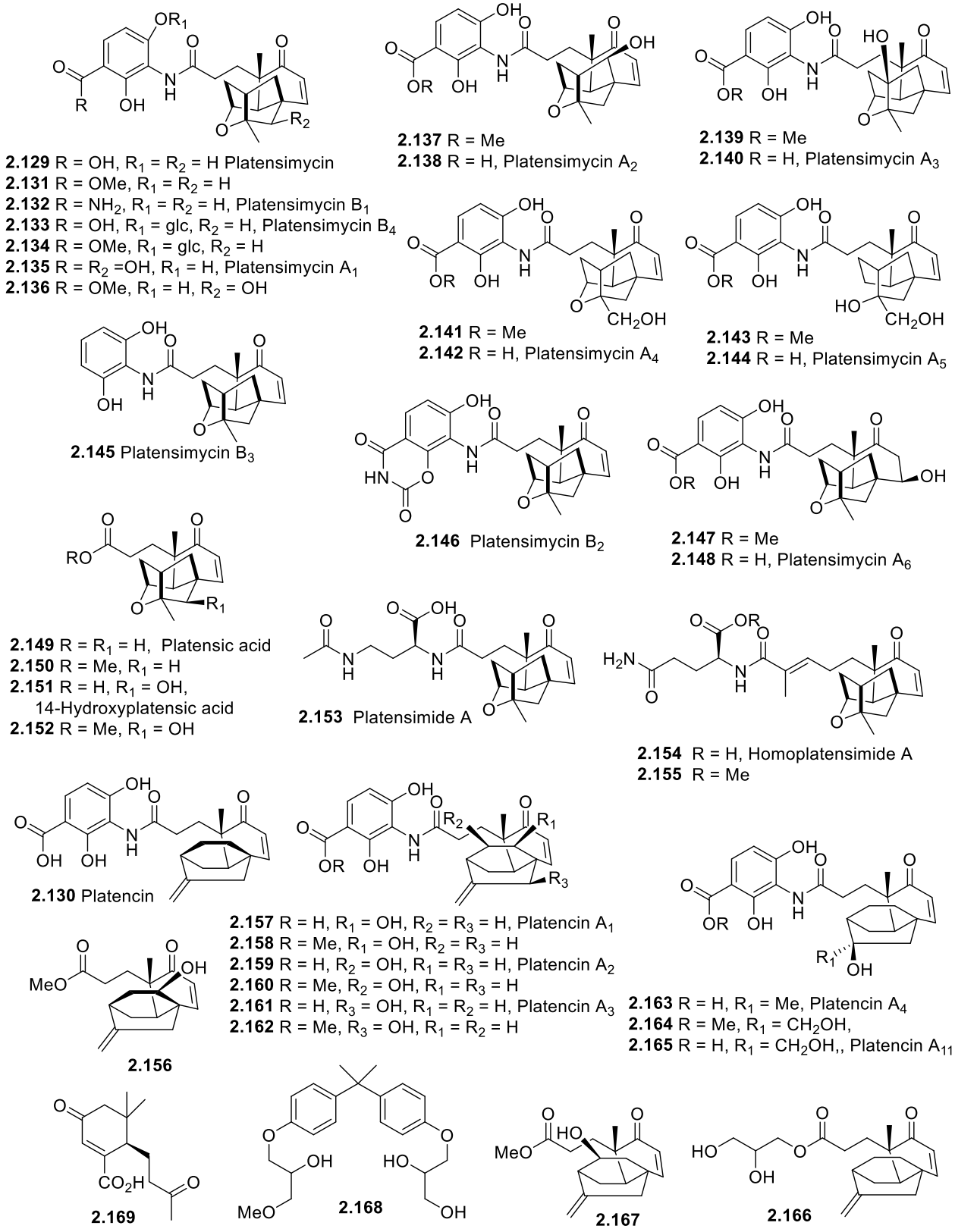

Figure 2.20: Secondary metabolites from South African actinomycetes (**2.129**-**2.169**)

In their search for antibiotics that inhibit the synthesis of bacteria fatty acids, which are essential for bacterial growth and propagation, researchers at Merck & Co., Inc., discovered the novel broad-spectrum Gram-positive antibiotic, platensimycin **2.129** from *Streptomyces platensis* strain MA7327, which was originally isolated from a soil sample collected in the Eastern Cape province of South Africa.[150] Several more strains of *Streptomyces platensis* have since been discovered. An organic extract of the fermentation broth of the South African *Streptomyces platensis* strain MA7327 was subjected to a unique antisense differential sensitivity whole-cell two-plate agar diffusion bioassay-guided fractionation process to yield platensimycin **2.129**.[150] Platensimycin **2.129** consist of a 3-amino-2,4-dihydroxybenzoic acid and a C-17 tetracyclic enone with an ether ring attached to an amide bond.[150,151] Another closely related compound, platencin **2.130**, was produced by *Streptomyces platensis* strain MA7339 using the same bioassay-guided fractionation process, although its biosynthetic gene cluster was also identified in strain MA7327.[152] Several other analogues, **2.131**-**2.167**, with modifications on or loss of the aromatic ring, modifications on the terpenoid and anilide moieties and a change in the length of the enone acid portion of platensimycin **2.129** and platencin **2.130** have also been isolated from strain MA7327.[153–160] Compounds **2.168** and **2.169**, which are structurally different from platensimycin **2.129** and platencin **2.130** were also isolated from strain MA7327.[153,154] It is worth to mention that other glycosylated analogues of platensimycin **2.129** and platencin **2.130** have been produced by engineered mutant strain *S. platensis* SB12600.[152] Platensimycin **2.129** selectively inhibits the elongation-condensing enzyme FabF of the bacterial fatty acid synthesis pathway, while platencin **2.130** equally inhibits both the initiation condensing (FabH) and elongation (FabF) enzymes.[151] Platensimycin **2.129**, platencin **2.130** and their analogues have shown potent in vitro activity against both cell-free and whole-cell systems including methicillin-resistant *Staphylococcus aureus*, vancomycin-resistant *Enterococcus* and *Mycobacterium tuberculosis*.[151] Although the isolated and synthesized analogues did not exhibit improved activity compared with compounds **2.129** and **2.130**, they provide important structure-activity relationship information to determine the pharmacophore of **2.129** and **2.130**.

In their quest to isolate biologically active metabolites from termite-associated actinobacteria, Kim et al., discovered that *Streptomyces* strain M56, isolated from the fungal comb material of a

South African *Macrotermes natalensis* Mn802 colony, exhibited potent broad-spectrum antifungal activity.[161] An activity guided isolation scheme resulted in the purification of the novel fused bicyclic ansa macrolide natalamycin A **2.170** alongside other ansa macrolides including reblastatin **2.171**, geldanamycin **2.172** and its derivates, 17-*O*-demethyl-geldanamycin **2.173**, 19-*S*-methylgeldanamycin **2.174**, 17-amino-17-demethoxy-geldanamycin **2.175**, methyl geldanamycinate derivative **2.176**, 17-amino-17-demethoxy-methyl geldanamycinate **2.177** and 19-[(1'S,4'R)-4'-hydroxy-1'-methoxy-2'-oxopentyl]geldanamycin **2.178**.[161] Although the fractions that yielded the isolated compounds showed strong antifungal activity against some strains; the natalamycins exhibited weak or no activity against *Saccharomyces cerevisiae* and other fungal isolates.[161]

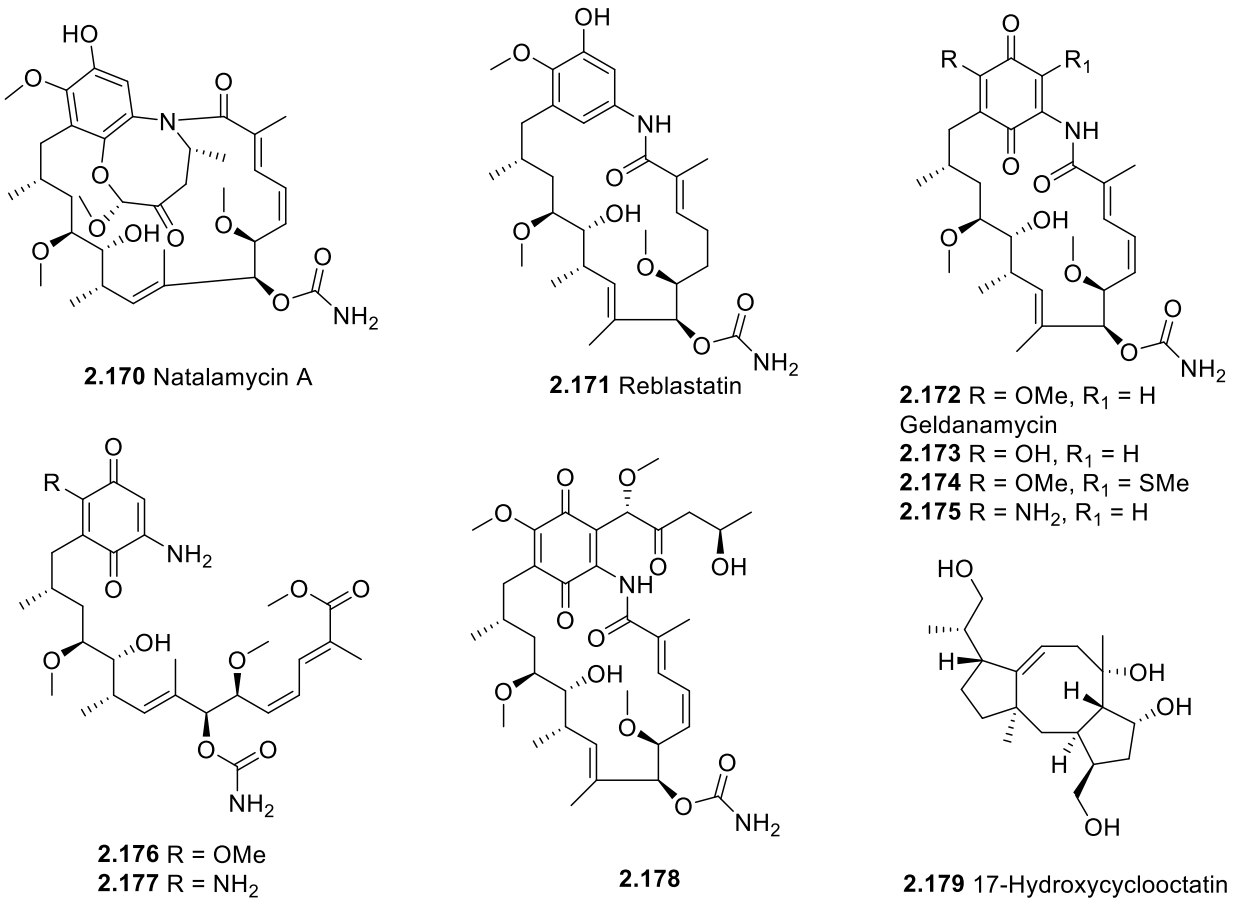

Figure 2.21: Secondary metabolites from South African actinomycetes (**2.170**-**2.179**)

An untargeted dereplication of the LCMS data of the methanol extract of *Streptomyces* strain M56 signified the presence of new metabolites.[162] The methanol extract of a large-scale culture of strain M56 was subjected to several chromatographic methods to yield the fused 5-8-5 tricyclic diterpene 17-hydroxycyclooctatin **2.179**.[162] Compound **2.179** is a potential ERα antagonist and exhibited weak cytotoxicity activity against MCF-7 human breast cancer cell lines with an IC_{50} value of 566.95 ± 0.48 µM at a concentration of 200 µM.[162]

Further studies on the metabolites of the actinobacteria in association with the fungus-growing South African termite *Macrotermes natalensis* for antimicrobial drug discovery led to the isolation of *Streptomyces* strain RB1 which exhibited biological activity against *Staphylococcus aureus* and human-pathogenic *Candida albicans*.[163] Purification of the methanol (MeOH) extract of strain RB1 yielded the new isoflavonoid glycosides, termisoflavone A **2.180**- C **2.182** and other isoflavonoids **2.184**-**2.188**, **2.190**-**2.192**.[163] The isolated compounds showed no antifungal and antibacterial activity when screened against *C. albicans*, *C. neoformans*, *S. aureus*, and *E. coli*, but compounds **2.187** and **2.191** ameliorated cisplatin-induced kidney cell damage to 80% of the control value at a cisplatin dose of 25 µM.[163] Further investigation of the MeOH extract of strain RB1 using LC/MS- and NMR-based dereplication strategies led to the identification and subsequent isolation of another new isoflavonoid glycoside, termisoflavone D **2.183**, together with the known isoflavonoids **2.184**, **2.185**, **2.187**, **2.189**-**2.191 and 2.193**.[164] Compound **2.187** displayed activity against glutamate-induced HT22 cells by preventing the accumulation of intracellular reactive oxygen species.[164] Another study exploring the termite associated actinobacteria for reno- and kidney-protective drug discovery found that the MeOH extract of *Streptomyces* sp. RB1 exhibited a protective effect against cisplatin-induced cytotoxicity.[165] A bioassay(LLC-PK1 cells)-guided isolation process yielded the renoprotective 1-*O*-(2-aminobenzoyl)-α-L-rhamnopyranoside (ABR) **2.194**.[165]

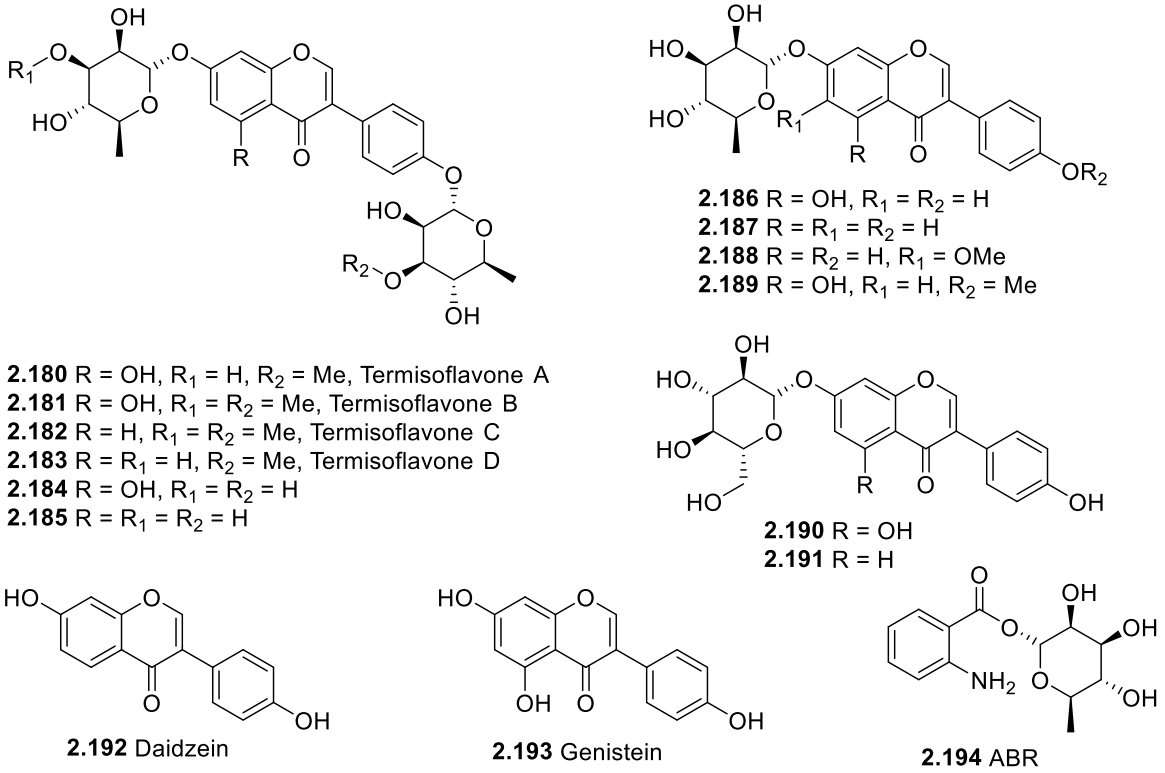

Figure 2.22: Secondary metabolites from South African actinomycetes (**2.180**-**2.194**)

Analyzing the chemical and metabolomic profile of actinobacteria derived from termite nest with an unbiased high-throughput high-performance liquid chromatography–high-resolution mass spectrometry based dereplication strategy revealed that *Streptomyces* sp. M41 isolated from the South African termite *Macrotermes natalensis*, produces new complex non-ribosomal peptide polyketide synthase (NRPS/PKS) hybrid compounds.[166] Chromatographic purification of a large scale culture of strain M41 interestingly yielded new analogues (two linear **2.195**-**2.196** and one cyclic **2.197**) of the cyclic depsipeptide dentigerumycin **2.198** and their biosynthesis was discussed.[166]

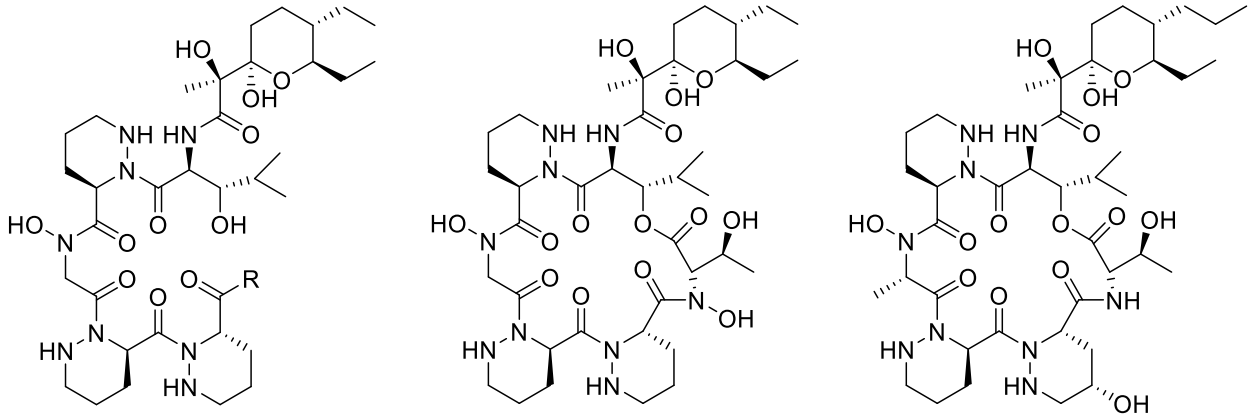

2.195 R = OH, Dentigerumycin C
2.196 R = NH_2, Dentigerumycin D

2.197 Dentigerumycin B

2.198 Dentigerumycin

Figure 2.23: Dentigerumycins A-D (**2.195**-**2.198**) from South African actinomycetes *Streptomyces* sp. M41

The rare actinomycete *Actinomadura* sp. 5-2, which was recovered from the gut of the South African fungus-growing termite *Macrotermes natalensis*, produced novel highly substituted tropolone alkaloids, rubterolones A-F **2.199**-**2.202**.[167] These compounds were detected by both bioactivity and HRMS based dereplication techniques, and subsequently isolated from the organic extract of a culture of strain 5-2.[167] Compounds **2.199**-**2.202** did not show any significant antifungal activity.[167] Another *Actinomadura* isolate, strain RB99, isolated from the surface of the South African worker termite *Macrotermes natalensis*, was discovered to produce novel bioactive compounds.[168] This was ascertained by dereplication of the liquid chromatography (LC)/ultraviolet (UV)/mass spectrometry (MS) data of the crude extract of the culture of strain RB99.[168] A spectrometry guided isolation technique was used to isolate three new cyclic tripeptides named natalenamides A **2.205**- C **2.207**.[168] The isolated compounds exhibited weak cytotoxicity when screened against HepG2 and HeLa/A549 cells.[168] Compound **2.207** showed significant activity against IBMX-mediated melanin synthesis in a dose-dependent manner.[168] Analyses of the high-resolution tandem mass spectrometry (HR-MS^2) data of the MeOH extract of strain RB99 and further exploration of the HR-MS^2 data on the Global Natural Product Social molecular networking platform showed that strain RB99 produces polyhalogenated isoflavanoids.[169] Seoung et al. proved that *Actinomadura* sp. RB99 can bio-transform the plant-based daidzein **2.192** and genistein **2.193** isoflavanoids in the ISP2 growth medium to

polyhalogenated derivatives.[169] Optimization of the growth medium (ISP2 augmented with NaCl or KBr) led to the production and subsequent MS-guided purification of eight polychlorinated analogous **2.208**-**2.215**, of which six were new, and seven novel polybrominated analogues **2.216**-**2.222**, of daidzein and genistein.[169] The isolated chlorinated analogues did not exhibit any antibacterial or antifungal activities when they were screened against *E. coli*, *S. aureus*, *S. epidermidis* and *C. albicans* but the brominated analogues **2.216** and **2.220** were active against *Helicobacter pylori*.[169] Additional analysis of the LCMS data of the MeOH extract of strain RB99 led to the detection and isolation of the antibiotic and antitumor agent fridamycin A **2.223** which is a type II polyketide.[170] Fridamycin A **2.223** showed good antidiabetic properties in 3T3-L1 adipocytes and could serve as a promising lead for type 2 diabetes drug discovery.[170]

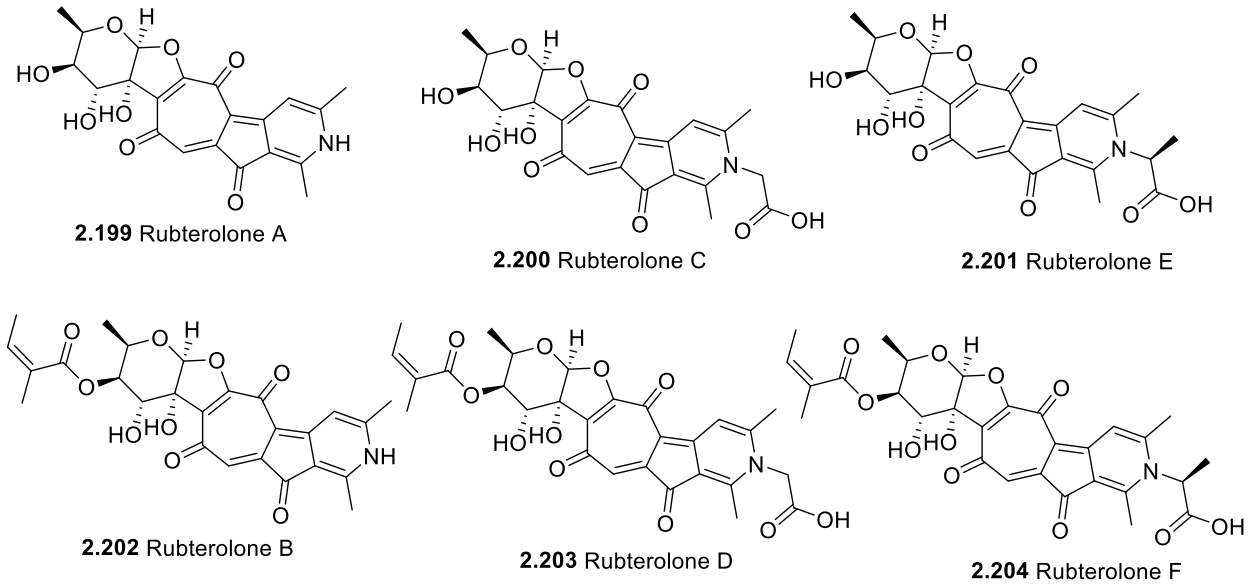

Figure 2.24: Rubterolones A-F (**2.199**-**2.204**) from South African actinomycetes *Actinomadura* sp. 5-2

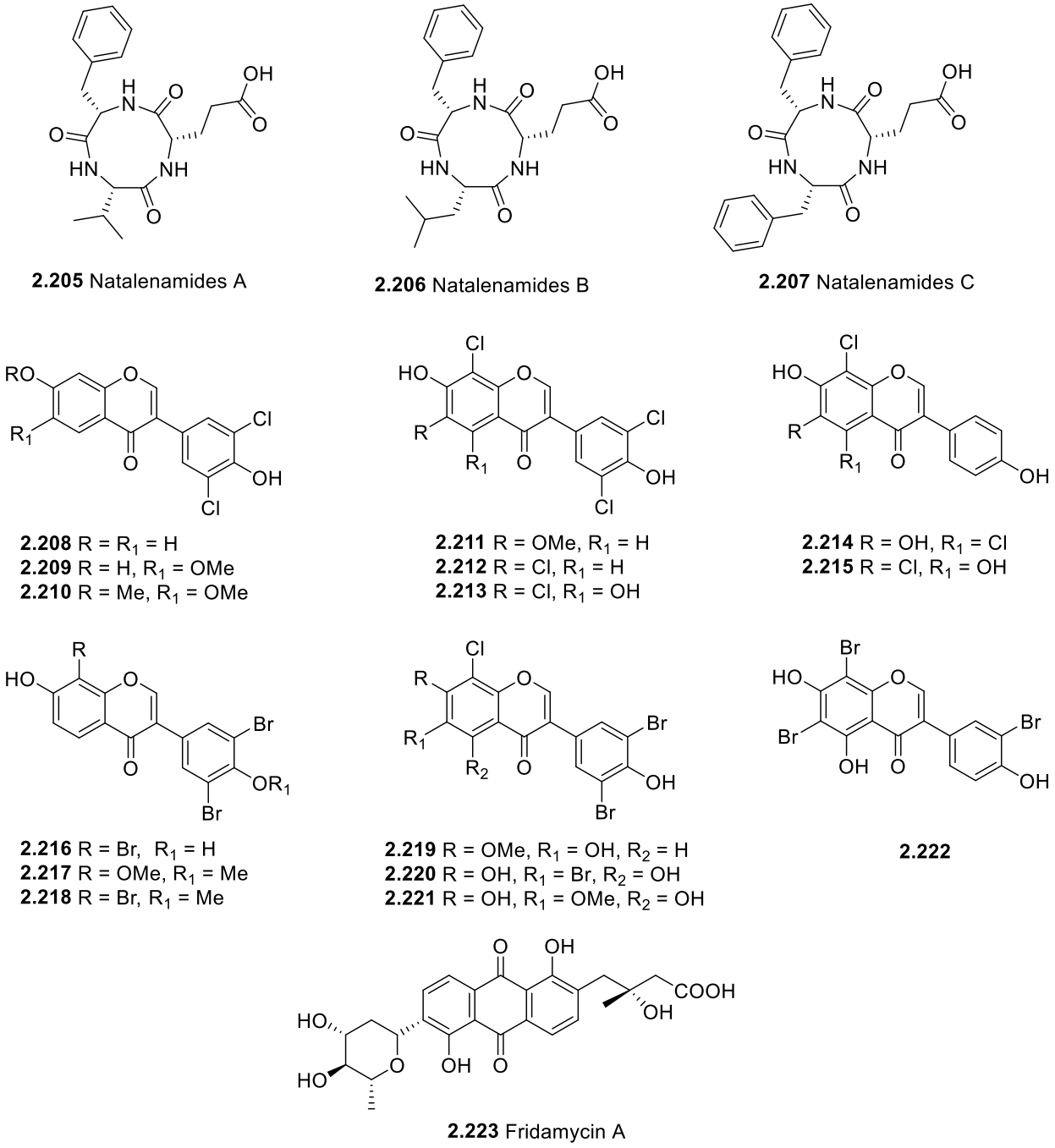

Figure 2.25: Secondary metabolites from South African actinomycetes (**2.205**-**2.223**)

Metabolomic and bioactivity profiling of termite associated actinomycetes led to the detection and subsequent isolation of four new 20-membered glycosylated polyketide macrolactams, named macrotermycins A **2.224**- D **2.227**, from the organic extract of the rare actinomycete, *Amycolatopsis* sp. M39.[171] Strain M39 was isolated from the South African termite *Macrotermes*

natalensis. Its organic crude extract exhibited a unique metabolomic profile and was active against the termite fungal garden competitor *Pseudoxylaria* spp.[171] Only compounds **2.224** and **2.226** were active against *Pseudoxylaria* sp.[171]

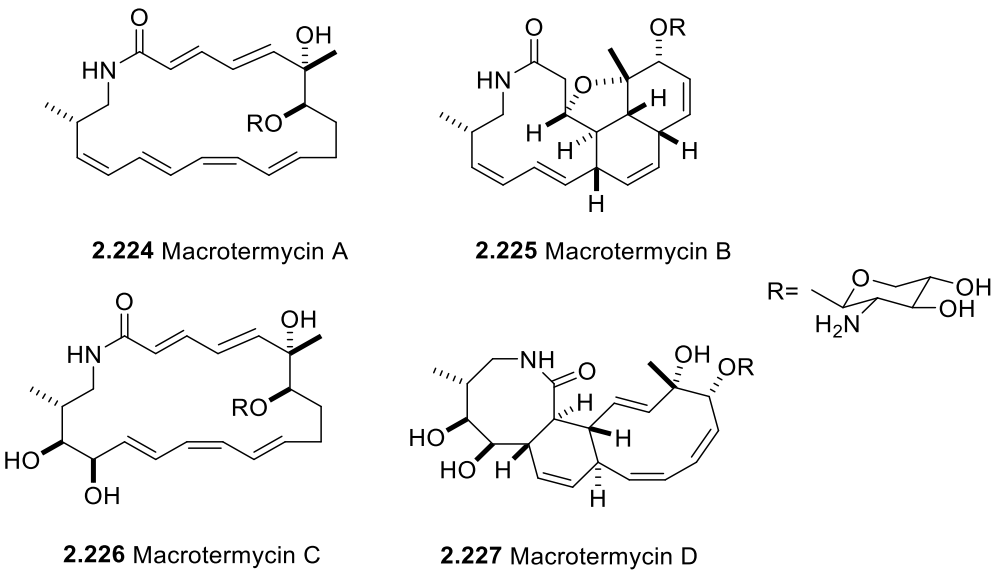

2.224 Macrotermycin A **2.225** Macrotermycin B

2.226 Macrotermycin C **2.227** Macrotermycin D

Figure 2.26: Macrotermycins A-D (**2.224**-**2.227**) from South African actinomycetes *Amycolatopsis* sp. M39

2.3.3 Screening and dereplication techniques

There are three major screening strategies used in drug discovery. The first is biological assay or bioactivity based, the second is chemical (spectrometric (MS), spectroscopic (UV, IR and NMR)) based and the third is genomic led but combinations of these methods are used.

The bioactivity-based screening technique involves screening NP crude extracts against disease-causing organisms or targets. A bioactive crude extract is subsequently subjected to a bioassay-guided fractionation and purification technique to isolate the bioactive metabolites. The essence of the fractionation and fraction screening process is to reduce the crude extract's complexity and lower the abundance or number of compounds per fraction to enable the rapid identification and purification of the single, active compounds. The bioactive compounds' structures are then elucidated by acquiring their spectroscopic and spectrometric data. There are two types of

biological assay approaches: whole-cell (WC) or phenotypic and target-based or genetics-driven approaches (TG).[172] The traditional WC approach involves testing the drug (extract or pure compound) against whole cells, isolated tissues or organs, or animals.[172] In contrast, the TG approach explores an essential enzyme or pathway, ideally specific to the disease-causing organism.[172] The advantage of the whole-cell approach is that the drug's permeability through the cell envelope of the disease-causing organism is established but not its mechanism of action, while the TG approach establishes the mechanism of action but not the permeability of the drug through the disease-causing organism's cell membrane.[173] Both approaches are useful for drug discovery, but the WC approach is better for NP screening projects because of the complexity of crude extracts and pure compounds, which may involve multiple mechanisms of action for activity. The best screening system incorporates both WC and TG, which is being developed and explored.[172] The biological assay-based screening method has been the traditional method by which many of the NP based drugs were discovered.[172] This process is long, expensive and laborious, although these limitations have to some extent been mitigated by the development and use of high-throughput screening systems, especially for TG.[172] Another primary concern is the frequent re-isolation of known or already reported compounds.

The chemical screening strategy screens and isolates compounds with interesting chemistry before testing to determine their bioactivity potential. Here the compounds are screened against a wide range of disease targets to determine which one they exhibit activity against, using the whole cell and/or target-based screening techniques. Chemical screening involves acquiring either UV, IR, NMR and/or MS data of the metabolites in the crude extract. UV helps establish if there are compounds with chromophores (conjugated double bonds), including phenolics, other aromatics and polyene systems. IR is useful in identifying the functional groups, while NMR establishes the carbon skeleton, positions of the protons, and presence and location of functional groups in the metabolites in the crude extract. MS gives the elemental composition, molecular weight, and formulae of the compounds in the crude extract. Phytochemical reagents can also be used to identify the functional groups or compound class of the metabolites in the crude extract. These data help determine the possible structural class of compounds in the crude extracts but do not determine what these compounds are.

These two screening methods are affected by the re-isolation of known metabolites, which is a significant problem in natural product drug discovery. Hence, it is preferable to employ early and accurate dereplication. Dereplication is a technique that allows the detection of known compounds in a crude extract early in the drug discovery and isolation process.[174] It involves acquiring spectroscopic and spectrometric data of the mixture of compounds in the crude extract and cross-checking these against information in databases to determine if they match any isolated compound.[174] The compounds in the crude extract need to be chromatographically separated for useful acquisition of reliable spectroscopic and spectrometric data.

The separation techniques widely used are thin-layer chromatography (TLC), gas chromatography (GC), liquid chromatography (LC), high-performance liquid chromatography (HPLC), ultra-high-performance liquid chromatography (uHPLC), capillary electrophoresis (CE), solid-phase extraction (SPE), column chromatography (CC) and flash column chromatography (FCC).[175] The detectors used to analyse these separations are UV/VIS (DAD or PDA), IR, MS (ESI, EI, MALDI, TOF, QTOF), NMR, ELSD, RI and X-RAY.[175] Technological advancement has led to the development of tandem analytical separation and detection systems. Several hyphenated methods comprising a combination of two (or more) separation and detection methods have been developed.[175] These include GC-MS, LC-PDA, LC-MS, LC-FTIR, LC-NMR, LC-NMR-MS, CE-MS, LC-UV-DAD, LC-MS-MS, LC-ESI-MALDI-TOF, LC-SPE-NMR, LC-SPE-NMR-MS-FTIR, LC-DAD-SPE-NMR, LC-UV-ESI-MS, LC-MS-ELSD, HPLC-DAD-HRESIMS, HPLC-DAD-MS-SPE-NMR, uHPLC-DAD-QTOF, uHPLC-DAD-QTOF-MS, uPHLC-MS-ELSD-PDA, uHPLC-MS-MS.[175]

Several databases are used for dereplication, including small in-house databases, proprietary commercially available databases, and free access databases.[175,176] These databases are curated from primary and secondary literature sources.[175,176] The databases available include CAS/SciFinder, PubChem, ChemSpider, ChEMBL, ChemBank, ChEBI, Dictionary of Natural Products, Dictionary of Marine Natural Products, MarinLit, AntiBase, AntiMarin, Metlin, Reaxy, KEGG, GNPS, NPAtlas, NaprAlert, MetaCyc, ReSpect, mzCloud, Massbank, NIST, NuBBEDB, NMRShiftDB, MIBiG, DrugBank and Norine.[175,176] These databases mostly contain analytical and physicochemical, spectroscopic or spectrometric properties of compounds, such as retention

time, molecular weight and formula, elemental composition, UV/VIS, IR, NMR, melting point, optical rotation, the taxonomy of source organism, biological activities, chemical structure and class of compound, and references.[175,176] Some of the databases are source, spectroscopic or spectrometric data specific, while others contain only NPs or both NPs and synthetic compounds.[176] MarinLit and Dictionary of Marine Natural Products only have information on MNPs. Antibase only contains NPs from micro-organisms and higher fungi. CAS/SciFinder, PubChem, ChemSpider and Reaxy contain information on both NPs and synthetic compounds. Massbank and mzCloud contains MS data of compounds, while NMRShiftDB is an NMR database. It is necessary and important to choose the appropriate database(s) for a specific study.

Chemical or metabolite profiling by direct dereplication where the molecular weight, possible formula, and UV data of each peak in an LCMS chromatogram of a NP crude extract is searched in a database, can sometimes be daunting and inefficient. The limitation with the direct search of the molecular mass and formula of each peak of the MS chromatogram in natural product databases is that smaller peaks or peaks unresolved from bigger peaks with the same retention time (tr) are often overlooked. It also does not show the structural relationship between the peaks in the chromatogram.[176] Therefore, there are computational, analytical, bioinformatic, cheminformatic and metabolomic tools, like the GNPS molecular network platform, that help address some of these challenges.[176,177]

The GNPS molecular networking platform is a free-to-access web-based metabolomics tool that connects or groups compounds of the same class or with structural similarity together as a molecular network or cluster based on similarity in their MS/MS fragmentation patterns.[177] Different LCMS and GCMS equipment or vendors (e.g., Agilent, Bruker, Thermo, and Waters) generate data in various formats that require different software to process.[176] To process data from different equipment on the GNPS molecular networking platform, the data must first be converted into a universal format (mzML or mzXML) using software such as ProteoWizard and MZmine 2.[177–179] Data generated or processed on the GNPS molecular networking platform can be viewed and analysed on the platform or using software called cytoscape.[177,180] The compounds are depicted as nodes connected by lines called edges. The thickness of the edge between two

nodes reflects how similar their fragmentation patterns are, indicating how closely related the structures of the compounds are, and this is calculated via cosine similarity scores.[177] This is useful in determining the structural relationship between nodes or compounds in a crude extract. The nodes can be annotated or dereplicated by querying against the GNPS database as well as other databases such as MassBank124 and NIST.[176,177] The GNPS database is publicly curated and its accuracy or confidence level is rated and needs to be verified.[176,177] Data generated from the same microbe but under different growth media and/or incubation conditions or from different organisms can be processed and analysed together at the same time. This is tremendously useful in metabolomic studies as it helps determine the production or not of specific metabolites under certain growth medium and conditions. It can also help establish whether species of the same genus produce the same or similar metabolites under the same condition.

Unlike traditional, direct dereplication techniques, the GNPS molecular networking platform and other ancillary softwares are computerized and use AI and algorithms to quickly and efficiently process raw MS data, dereplicate and show structural relationships between metabolites in an extract. With the analyses of the fragmentation pattern of compounds (nodes) from known and unknown compounds connected in a GNPS molecular network, predicting the unknown compounds' structures is possible even before isolation and purification. The limitation of the GNPS is that it does not incorporate retention time or abundance metrics in generating the molecular cluster.[176] Also, it is unable to connect compounds that differ by two distinct structural modifications together. Dereplication using a combination of MS/MS molecular networking and genome mining is a powerful technique in microbial natural product drug discovery.

The third technique which is mostly used in microbial natural product involves genome mining. Genome mining is a technique that involves comparing or checking the biosynthetic gene clusters (BGC) of a microbial genome sequence against publicly available databases containing either raw or annotated genome data made up of NP BGCs.[181] With this, the biosynthetic potential or the metabolites a microbe is capable of producing is determined. This process is computerized and automated and uses bioinformatic tools such as antiSMASH, PRISM and BiG-SCAPE.[181] AntiSMASH, for example, is an online BGC prediction and annotation tool which can predict non-

ribosomal peptide synthetase (NRPS) and polyketide synthase (PKS) substrate specificities and compare them to known BGCs in the MIBiG database.[182] AntiSMASH can predict molecular structures of NPs based on sequence data.[182] Genome mining helps identify silent or cryptic BGCs that cannot be expressed under normal laboratory growth conditions.[181] There are several techniques for awakening or activating these silent BGCs, including the OSMAC (one strain many compounds) approach, heterologous expression of the BGC, and knocking out or overexpressing regulatory genes of the BGC.[181]

With analytical and technological advancement in screening techniques, dereplication, genome mining and structure elucidation of NPs, NP drug discovery has become more appealing. Now, 1D and full 2D NMR data of NPs with quantities as small as 10–50 µg can be obtained on advanced NMR with higher field magnets and cryo-probes using very thin NMR tubes.[175] Computer-assisted structure elucidation techniques with dereplication of pure compounds using machine learning and cheminformatic tools like the NMR-based Small Molecule Accurate Recognition Technology (SMART 2.0), makes structure elucidation of complex molecules a lot easier.[183]

2.4 References

1. *WHO Global Tuberculosis Report 2020*.
2. Frothingham, R., Hills, H. G. & Wilson, K. H. Extensive DNA Sequence Conservation throughout the *Mycobacterium tuberculosis* Complex. *J. Clin. Microbiol.* **32**, 1639–1643 (1994).
3. Chapter 2: Transmission and Pathogenesis of Tuberculosis. Available at: https://www.cdc.gov/tb/education/corecurr/pdf/chapter2.pdf. (Accessed: 25th February 2021)
4. Farnia, P.Velayati, A. A. *Atlas of Mycobacterium Tuberculosis*. (2016).
5. https://www.cdc.gov/tb/publications/factsheets/testing/diagnosis.htm.
6. https://www.cdc.gov/tb/education/corecurr/pdf/chapter4.pdf.
7. https://www.nhs.uk/conditions/tuberculosis-tb/diagnosis/.

8. https://www.who.int/news-room/fact-sheets/detail/tuberculosis.

9. Lo¨nnroth, K., Jaramillo, E., Williams, B. G., Dye, C. & Raviglione, M. Drivers of tuberculosis epidemics : The role of risk factors and social determinants. *Soc. Sci. Med.* **68**, 2240–2246 (2009).

10. Hargreaves, J. R., Boccia, D., Evans, C. A., Adato, M. & Petticrew, M. The Social Determinants of Tuberculosis : From Evidence to Action. *Am. J. Public Health* **101**, 654–662 (2011).

11. Garfin, A. M. C. & Ohkado, A. A review of tuberculosis contact investigations in the poor urban areas of Manila, The Philippines. *Public Heal. Action* **6**, 220–225 (2016).

12. Egere, U. *et al.* Isoniazid preventive treatment among child contacts of adults with smear-positive tuberculosis in The Gambia U. *Public Heal. Action* **6**, 226–231 (2016).

13. https://www.cdc.gov/tb/education/corecurr/pdf/chapter6.pdf.

14. https://www.cdc.gov/tb/education/corecurr/pdf/chapter7.pdf.

15. Lalvani, A. & Pareek, M. Interferon gamma release assays: principles and practice. *Enferm. Infecc. Microbiol. Clin.* **28**, 245–252 (2010).

16. Brewer, T. F. Preventing Tuberculosis with Bacillus Calmette-Guerin Vaccine : A Meta-Analysis of the Literature. *Clin. Infect. Dis.* **31**, 64–67 (2000).

17. Khanna, P., Khanna, P. & Choudhary, S. Tuberculosis vaccine. *Hum. Vaccin. Immunother.* **10**, 420–422 (2014).

18. Barberis, I., Bragazzi, N. L., Galluzzo, L. & Martini, M. The history of tuberculosis : from the first historical records to the isolation of Koch ' s bacillus. *J PREV MED HYG* **58**, 9–12 (2017).

19. Nguta, J. M., Appiah-Opong, R., Nyarko, A. K., Yeboah-Manu, D. & Addo, P. G. A. Current perspectives in drug discovery against tuberculosis from natural products. *Int. J. Mycobacteriology* **4**, 165–183 (2015).

20. *World Health Organization.WHO Treatment Guidelines for Drug- Resistant Tuberculosis*.

(2016).

21. *World Health Organization. Drug-Resistant TB Surveillance and Response. Supplement to Global TB Report 2014; Geneva, 2014*.

22. https://www.who.int/tdr/publications/documents/incentives-disincentives-anti-tuberculosis.pdf.

23. https://www.who.int/tb/publications/dots-short-course/en/.

24. https://www.who.int/bulletin/archives/79(1)61.pdf.

25. https://www.afro.who.int/health-topics/tuberculosis-tb.

26. Naidu, T. *et al.* Major Depression and Stigma among Individuals with Multidrug-Resistant Tuberculosis in South Africa. *Am. J. Trop. Med. Hyg* **103**, 1067–1071 (2020).

27. https://www.who.int/tb/areas-of-work/drug-resistant-tb/xdr-tb-faq/en/.

28. Singh, R. *et al.* Recent updates on drug resistance in *Mycobacterium tuberculosis*. *J. Appl. Microbiol.* **128**, 1547--1567 (2019).

29. Kiran, D., Podell, B. K., Chambers, M. & Basaraba, R. J. Host-directed therapy targeting the *Mycobacterium tuberculosis* granuloma : a review. *Semin Immunopathol* **38**, 167–183 (2016).

30. https://www.who.int/tb/areas-of-work/drug-resistant-tb/types/en/.

31. Dheda, K., Limberis, J. D., Pietersen, E., Phelan, J., Esmail, A., Lesosky, M., Fennelly, K. P., te Riele, J., Mastrapa, B., Streicher, E. M., Dolby, T., Abdallah,, A. M., Ben-Rached, F., Simpson, J., Smith, L., Gumbo, T., van Helden, P., Sirgel, F. A., M, R. M. Outcomes , infectiousness , and transmission dynamics of patients with extensively drug-resistant tuberculosis and home-discharged patients with programmatically incurable tuberculosis : a prospective cohort study. *Lancet Respir Med* **5**, 269–81 (2017).

32. World Health Organization. WHO Treatment Guidelines for Drug- Resistant Tuberculosis; Geneva, 2016.

33. https://www.cdc.gov/tb/topic/treatment/adverseevents.htm.

34. Laurenzi, M., Ginsberg, A. & Spigelman, M. Challenges Associated with Current and Future TB Treatment. *Infect. Disord. - Drug Targets* **7**, 105–119 (2007).

35. Karuppannasamy, D., Raghuram, A. & Sundar, D. Linezolid-induced optic neuropathy. *Indian J. Ophthalmol.* **62**, 497–500 (2014).

36. Rangaka, M. X. *et al.* Isoniazid plus antiretroviral therapy to prevent tuberculosis : a randomised double-blind placebo-controlled trial. *Lancet.* **384**, 682–690 (2015).

37. Baghaei, P., Marjani, M., Javanmard, P., Tabarsi, P. & Masjedi, M. R. Diabetes mellitus and tuberculosis facts and controversies. *J. Diabetes Metab. Disord.* **12**, 1–8 (2013).

38. Wallis, R. S. *et al.* Tuberculosis — advances in development of new drugs , treatment regimens , host-directed therapies , and biomarkers. *Lancet Infect. Dis.* **16**, e34–e46 (2014).

39. Dewick, P. . *Medicinal Natural Products: A Biosynthentic Approach*. (John Wiley and Son: West Sussex, UK, 2002).

40. Maplestone, R.A.; Stone, M.J.; Williams, D. H. The evolutionary role of secondary metabolites—A review. *Gene* **115**, 151–157 (1992).

41. Dias, D. A., Urban, S. & Roessner, U. A Historical Overview of Natural Products in Drug Discovery. *Metabolites* **2**, 303–336 (2012).

42. Rice, S. A., McDougald, D., Kumar, N. & Kjelleberg, S. The use of quorum-sensing blockers as therapeutic agents for the control of biofilm-associated infections. *Curr. Opin. Investig. Drugs* **6**, 178–184 (2005).

43. Medema, M. H. Computational Genomics of Specialized Metabolism : from Natural Product Discovery to Microbiome Ecology. *mSystems* **3**, 1–5 (2017).

44. Cragg, G. M. & Newman, D. J. Biodiversity : A continuing source of novel drug leads. *Pure Appl. Chem.* **77**, 7–24 (2005).

45. Sarker, S. D. Pharmacognosy in modern pharmacy curricula. *Pharmacogn. Mag.* **8**, 91–92 (2012).

46. The American Society of Pharmacognosy. Available at: https://www.pharmacognosy.us/. (Accessed: 24th February 2021)

47. Schmitz, R. Friedrich Wilhelm Sertürner and the Discovery of Morphine. *Pharm. Hist.* **27**, 61–74 (1985).

48. Louis, S., Facts, M. O. & Kluwer, W. The Review of Natural Products . Eighth edition , edited by Ara DerMarderosian and John A . Beutler. **8285**, (2014).

49. D, D. E. P. & D, H. B. P. Application of Conventional and New Biotechnological Approaches for Improving of Morphinane Alkaloids Production. *J. Med. Plants* **9**, 33–50 (2010).

50. Miller, L. H., Su, X. Artemisinin : Discovery from the Chinese Herbal Garden. *Cell.* **146**, 855–858 (2012).

51. Ashley, E. A. & Ashley, E. A. Drugs in Development for Malaria. *Drugs* **78**, 861–879 (2018).

52. Johnson, I. S., Armstrong, J. G., Gorman, M., Burnett, J. P. The Vinca Alkaloids : A New Class of Oncolytic Agents. *Cancer Res.* **23**, (1963).

53. Cragg, G. M. Paclitaxel (Taxol®): A success story with valuable lessons for natural product drug discovery and development. *Med. Res. Rev.* **18**, 315–331 (1999).

54. Gallego-Jara, J., Lozano-Terol, G., Sola-Martínez, R. A., Cánovas-Díaz, M., de Diego Puente, T. A Compressive Review about Taxol®: History and Future Challenges. *Molecules* **25**, 1–24 (2020).

55. Binkley, F. The Isolation of a New Thymine Pentose from Sponges. *J. Biol. Chem* **72**, 2809–2810 (1950).

56. Bergmann, W. & Burke, D. C. Contribution to the Study of Marine Products. XXXIX. The Nucleosides of Sponges. III.1 Spongothymidine and Spongouridine. *J. Org. Chem.* **20**, 1501–1507 (1955).

57. Kijjoa, A. & Sawangwong, P. Drugs and Cosmetics from the Sea. *Mar. Drugs* **2**, 73–82 (2004).

58. Giordano, D. Bioactive Molecules from Extreme Environments. *Mar. Drugs* **18**, 1–7 (2020).

59. Leal, M. C. *et al.* Marine Microorganism-Invertebrate Assemblages: Perspectives to Solve the "Supply Problem" in the Initial Steps of Drug Discovery. *Mar. Drugs* **12**, 3929–3952 (2014).

60. Martins, A., Vieira, H., Gaspar, H. & Santos, S. Marketed Marine Natural Products in the Pharmaceutical and Cosmeceutical Industries: Tips for Success. *Mar. Drugs* **12**, 1066–1101 (2014).

61. Clinical Pipeline Marine Pharmacology. Available at: https://www.midwestern.edu/departments/marinepharmacology/clinical-pipeline.xml. (Accessed: 26th February 2021)

62. Bowersox, S. S. & Luther, R. Pharmacotherapeutic Potential of Omega- Conotoxin MVIIA (SNX-111), An N-Type Neuronal Calcium Channel Blocker found in the Venom of *Conus Magus*. *Toxicon* **36**, 1651–1658 (1998).

63. Rinehart, K. L. *et al.* Ecteinascidins 729, 743, 745, 759A, 759B, and 770: potent antitumor agents from the Caribbean tunicate *Ecteinascidia turbinata*. *J. Org. Chem.* **55**, 4512–4515 (1990).

64. McBride, A., Butler, S. K. Eribulin mesylate: A novel halichondrin B analogue for the treatment of metastatic breast cancer. *Am J Heal. Pharm* **69**, 745–755 (2012).

65. Shaer, D. Al, Musaimi, O. Al, Albericio, F. & Torre, B. G. De. 2019 FDA TIDES (Peptides and Oligonucleotides) Harvest. *Pharmaceuticals* **13**, (2020).

66. Markham, A. Belantamab Mafodotin : First Approval. *Drugs* **80**, 1607–1613 (2020).

67. Pettit, G. R. *et al.* The Isolation and Structure of a Remarkable Marine Animal Antineoplastic Constituent: Dolastatin 10. *J. Am. Chem. Soc.* **109**, 6883–6885 (1987).

68. Newman, D. J. & Cragg, G. M. Marine Natural Products and Related Compounds in Clinical and Advanced Preclinical Trials. *J. Nat. Prod* **67**, 1216–1238 (2004).

69. Newman, D. J. & Cragg, G. M. Drugs and Drug Candidates from Marine Sources : An Assessment of the Current " State of Play ". *Planta Med* **82**, 775–789 (2016).

70. Pereira, F. Expert Opinion on Drug Discovery Have marine natural product drug discovery efforts been productive and how can we improve their efficiency ? *Expert Opin. Drug Discov.* **14**, 717–722 (2019).

71. Thornburg, C. C. *et al.* NCI Program for Natural Product Discovery : A Publicly-Accessible Library of Natural Product Fractions for High-Throughput Screening NCI Program for Natural Product Discovery : A Publicly- Accessible Library of Natural Product Fractions for High- Throughp. *ACS Chem. Biol* (2018). doi:10.1021/acschembio.8b00389

72. Haefner, B. Drugs from the deep: marine natural products as drug candidates. *Drug Discov Today* **8**, 536–544 (2003).

73. Hou, X., Wang, C., Gerwick, W. H. & Shao, C. European Journal of Medicinal Chemistry Marine natural products as potential anti-tubercular agents. *Eur. J. Med. Chem.* **165**, 273–292 (2019).

74. Palem, J. R., Bedadala, G. R., Sayed, K. A. E. & Hsia, S. -c. Manzamine A as a Novel Inhibitor of Herpes Simplex Virus Type-1 Replication in Cultured Corneal Cells Manzamine A as a Novel Inhibitor of Herpes Simplex Virus Type-1 Replication in Cultured Corneal Cells. *Planta Med.* **77**, 46–51 (2011).

75. Sakai Ryuichi, Higa Tatsuo, Jefford, Charles W., B. G. Manzamine A, a Novel Antitumor Alkaloid from a Sponge. *J. Am. Chem. Soc.* **108**, 6404–6405 (1986).

76. Hu JF, Hamann MT, Hill R, K. M. The manzamine alkaloids. *Alkaloids Chem Biol* **60**, 207–85 (2003).

77. Peng, J. *et al.* Manadomanzamines A and B : A Novel Alkaloid Ring System with Potent Activity against Mycobacteria and HIV-1. *J. AM. CHEM. SOC.* **60**, 13382–13386 (2003).

78. Ichiba, T., Sakai, R., Kohomoto, S., Saucy, G. New Manzamine alkaloids from a sponge of the genus Xestospongia. *Tetrahedron Lett.* **29**, 3083–3086 (1988).

79. Ichiba, T., Corgiat, J. M., Scheuer, P. J. & Kelly-borges, M. 8-Hydroxymanzamine A, a ß-Carboline alkaloid from a sponge, *Pachypellina* sp.1. *J. Nat. Prod.* **57**, 168–170 (1994).

80. Tsuda, M., Kawasaki, N. & Kobayashi, J. Ircinols A and B , First Antipodes of Manzamine-Related Alkaloids from an Okinawan Marine Sponge. *Tetrahedron* **50**, 7957–7960 (1994).

81. Jaspars, M., Pasupathy, V. & Crews, P. A Tetracyclic Diamine Alkaloid, Halicyclamine A, from the Marine Sponge *Haliclona* sp1. *J. Org. Chem.* **59**, 3253–3255 (1994).

82. Clark, R. J. *et al.* The Haliclonacyclamines , Cytotoxic Tertiary Alkaloids from the Tropical Marine Sponge *Haliclona* sp. *Tetrahedron* **54**, 8811–8826 (1998).

83. Rai, M. A., IShida, S., Etiawan, A. S. & Obayashi, M. K. Haliclonacyclamines , Tetracyclic Alkylpiperidine Alkaloids , as Anti-dormant Mycobacterial Substances from a Marine Sponge of *Haliclona* sp . *Chem. Pharm. Bull.* **57**, 1136–1138 (2009).

84. Wei Xiaomei, Nieves Karinel, R. A. D. Neopetrosiamine A, biologically active bis-piperidine alkaloid from the Caribbean Sea sponge *Neopetrosia proxima*. *Bioorg Med Chem Lett* **20**, 5905–5908 (2010).

85. Baker, B. J., Scheuer, P. J., Shoolery, J. N. Papuamine , an Antifungal Pentacyclic Alkaloid from a Marine Sponge, *Haliclona* sp.1. *J. Am. Chem. Soc.* **110**, 965–966 (1988).

86. Abdjul, D. B., Yamazaki, H., Kanno, S., Takahashi, O., Kirikoshi, R., Ukai, K., Namikoshi, M. Haliclonadiamine Derivatives and 6- epi -Monanchorin from the Marine Sponge *Halichondria panicea* Collected at Iriomote Island. *J. Nat. Prod.* **79**, 1149−1154 (2016).

87. Meragelman, K. M., Mckee, T. C. & Mcmahon, J. B. Monanchorin , a Bicyclic Alkaloid from the Sponge *Monanchora ungiculata*. *J. Nat. Prod.* **6**, 1165–1167 (2004).

88. Fahy, E., Molinski, T. F., Harper, M. K., Sullivan, B. W. & Faulkner, D. J. Haliclonadiamine, an antimicrobial alkaloid from the sponge *Haliclona* sp. *Tetrahedron Lett.* **29**, 3427–3428 (1988).

89. Oliveira, J. H. H. L. De *et al.* Ingenamine G and Cyclostellettamines G - I , K , and L from the New Brazilian Species of Marine Sponge *Pachychalina* sp . *J. Nat. Prod.* **67**, 1685–1689 (2004).

90. De Oliveira, J. H.H. L., Seleghim, M. H. R., Timm, C., Grube, A., Köck, M., Nascimento, G. G. F., Martins, A. C. T., Silva, E. G. O., De Souza, A. O., Minarini, P. R. R., Galetti, F. C. S., Silva, C. L., Hajdu, E., Berlinck, R. G. S. Antimicrobial and Antimycobacterial Activity of Cyclostellettamine Alkaloids from Sponge *Pachychalina* sp. *Mar. Drugs* **4**, 1–8 (2006).

91. Encarnación-Dimayuga, R. Ramírez, M. R., Luna-Herrera, J. Aerothionin , a Bromotyrosine Derivative with Antimycobacterial Activity from the Marine Sponge *Aplysina gerardogreeni* (Demospongia). *Pharm. Biol.* **41**, 384–387 (2003).

92. Nakamura, H., Wu, H., Ohizumi, Y., Hirata, Y. AgelasinB-A, -B, C and -D, Novel Bicyclic Diterpenoids witb a 9-Methylandeninium unit possessing inhibitory effects on a NA, K-APTASE from the Okinawan sea sponge *Agelas* sp. *Tetrahedron Lett.* **5,N**, 2989–2992 (1984).

93. Mangalindan, G. C. *et al.* Agelasine F from a Philippine *Agelas* sp . Sponge Exhibits in vitro Antituberculosis Activity. *Planta Med.* **66**, 364–365 (2000).

94. Vik, A. *et al.* (+) -Agelasine D : Improved Synthesis and Evaluation of Antibacterial and Cytotoxic Activities. *J. Nat. Prod.* **69**, 381–386 (2006).

95. Hua, H. *et al.* Batzelladine alkaloids from the caribbean sponge Monanchora unguifera and the significant activities against HIV-1 and AIDS opportunistic infectious pathogens. *Tetrahedron* **63**, 11179–11188 (2007).

96. Kazlauskas, R., Murphy, P. T., Quinn, R. J., Wells, R. J. Heteronemin, a new Scalarin type Sesterterpene from the sponge *Heteronema erecta*. *Tetrahedron Lett.* 2634 (1976).

97. Sayed, K. A. El *et al.* Marine Natural Products as Antituberculosis Agents. *Tetrahedron* **56**, 949–953 (2000).

98. Nasu, S. S. *et al.* Puupehenone-Related Metabolites from Two Hawaiian Sponges , Hyrtios

spp. *J. Org. Chem.* **60**, 7290–7292 (1995).

99. Hamann, M. T., Scheuer, P. J., Kelly-borges, M. & Pierce, F. Biogenetically Diverse , Bioactive Constituents of a Sponge , Order Verongida : Bromotyramines and Sesquiterpene-Shikimate Derived Metabolites. *J. Org. Chem.* **58**, 6565–6569 (1993).

100. Ibrahim, S. R. M. *et al.* Bioorganic & Medicinal Chemistry Callyaerins A – F and H , new cytotoxic cyclic peptides from the Indonesian marine sponge *Callyspongia aerizusa*. *Bioorg. Med. Chem.* **18**, 4947–4956 (2010).

101. Wang, Y., Franzblau, S. G., Wei, X. & Rodrı, A. D. Novel ring B abeo-sterols as growth inhibitors of Mycobacterium tuberculosis isolated from a Caribbean Sea sponge , *Svenzea zeai*. *Tetrahedron Lett.* **48**, 8851–8854 (2007).

102. Corre, C. & Challis, G. L. New natural product biosynthetic chemistry discovered by genome mining. *Nat. Prod. Rep.* **26**, 977–986 (2009).

103. Bérdy, J. Bioactive microbial metabolites. *J. Antibiot. (Tokyo).* **58**, 1–26 (2005).

104. Lyddiard, D., Jones, G. L. & Greatrex, B. W. Keeping it simple : lessons from the golden era of antibiotic discovery. *FEMS Microbiol. Lett.* **363**, 1–3 (2016).

105. https://lpsn.dsmz.de/phylum/actinobacteria.

106. Merino, N. *et al.* Living at the Extremes : Extremophiles and the Limits of Life in a Planetary Context. *Front. Microbiol.* **10**, (2019).

107. Mayfield, C. I., Williams, S. T., Ruddick, S. M., Hatfield, H. L. Studies on the ecology of Actinomycetes in soil TV . Observations on the form and growth of Streptomycetes in soil. *soil Biol. Biochem. Vol.* **4**, 79–91 (1972).

108. Barka, E. A. *et al.* Taxonomy , Physiology , and Natural Products of Actinobacteria. *Microbiol Mol Biol Rev* **80**, 1–44 (2016).

109. Benndorf, R. *et al. Actinomadura rubteroloni* sp . nov . and *Actinomadura macrotermitis* sp . nov ., isolated from the gut of the fungus growing- - termite *Macrotermes natalensis*.

Int. J. Syst. Evol. Microbiol. **70**, 5255–5262 (2020).

110. Salwan, R. & Sharma, V. *The Role of Actinobacteria in the Production of Industrial Enzymes*. *New and Future Developments in Microbial Biotechnology and Bioengineering* (Elsevier B.V., 2018). doi:10.1016/B978-0-444-63994-3.00011-4

111. Genilloud, O. Natural Product Reports Actinomycetes : still a source of novel antibiotics. *Nat. Prod. Rep.* **34**, 1203–1232 (2017).

112. Taechowisan, T., Chaisaeng, S. & Phutdhawong, W. S. Antibacterial , antioxidant and anticancer activities of biphenyls from *Streptomyces* sp . BO-07 : an endophyte in *Boesenbergia rotunda* (L .) Mansf A . *FOOD Agric. Immunol.* **28**, 1330–1346 (2017).

113. Newman, D. J., Cragg, M. & Snader, K. M. The influence of natural products upon drug discovery. *Nat. Prod. Rep.* **17**, 215–234 (2000).

114. Seto, H., Otake, N., Sato, S., Yamaguchi, H., Takada, K., Itoh, M., Lu, H. S. M., Clardy, J. The structure of a new Nucleoside Antibiotic, Capuramycin. *Tetrahedron Lett.* **29**, 2343–2346 (1988).

115. Yamagguchi, H., Sato, S., Yoshida, S., Takada, K., Itoh, M., Seto, H., Otake, N. Capuramycin, a new Nucleoside Antibiotic taxonomy, fermentation, isolation and characterization. *J Antibiot* **39**, 1047–53 (1986).

116. R.S.VardanyanV.J.Hruby. Antimycobacterial Drugs. in *Synthesis of Essential Drugs* 525–534 (2006).

117. Noone, P. Use of antibiotics Aminoglycosides. *Br. Med. J.* 549–552 (1978).

118. Barkei, J. J., Kevany, B. M., Felnagle, E. A. & Thomas, M. G. Investigations into Viomycin Biosynthesis by Using Heterologous Production in Streptomyces lividans. *ChemBioChem* **10**, 366–376 (2009).

119. FINLAY, A. C. *et al.* Viomycin a new antibiotic active against Mycobacteria. *Am. Rev. Tuberc.* **63**, 1–3 (1951).

120. Slayden, R. A. *et al.* Antimycobacterial Action of Thiolactomycin : an Inhibitor of Fatty Acid and Mycolic Acid Synthesis. *Antimicrob. Agents Chemother.* **40**, 2813–2819 (1996).

121. Margalith, P. & Beretta, G. Rifomycin. XI. Taxonomic study on Streptomyces mediterranei nov. sp. *Mycopathol. Mycol. Appl.* **8**, 321–330 (1960).

122. Lancini, F. P. and G. Rifamycins. in *Antibiotic and Chemotherapy (Ninth Edition) 2010,* **2**, 326–333 (2010).

123. Maslow, M. J. & Portal-celhay, C. Mandell, Douglas, and Bennett's Principles and Practice of Infectious Diseases. in *Rifamycins* 339–349 (2015). doi:10.1016/B978-1-4557-4801-3.00027-8

124. Igarashi, M. *et al.* Caprazamycins , Novel Lipo-nucleoside Antibiotics , from *Streptomyces* sp . II . Structure Elucidation of Caprazamycins. *J. Antibiot.* **58**, 327–337 (2005).

125. https://www.biodiversityfinance.net/south-africa.

126. Rohland, J. & Meyers, P. R. *Streptomyces fractus* sp . nov ., a novel streptomycete isolated from the gut of a South African termite. *Antonie Van Leeuwenhoek* **107**, 1127–1134 (2015).

127. Cook, A. E., Roes, M. & Meyers, P. R. *Actinomadura napierensis* sp . nov ., isolated from soil in South Africa. *Int. J. Syst. Evol. Microbiol.* **55**, 703–706 (2005).

128. Everest, G. J., Roes-hill, M., Rohland, J., Enslin, S. & Meyers, P. R. antibiotic-producing actinobacteria isolated from South African soils. *J. Antibiot. (Tokyo).* **67**, 813–818 (2014).

129. Everest, G. J. & Meyers, P. R. *Kribbella hippodromi* sp . nov ., isolated from soil from a racecourse in South Africa. *Int. J. Syst. Evol. Microbiol.* **58**, 443–446 (2008).

130. Roes, M., Goodwin, C. M. & Ã, P. R. M. *Gordonia lacunae* sp . nov ., isolated from an estuary. *Syst. Appl. Microbiol.* **31**, 17–23 (2008).

131. Benndorf, R. *et al.* nov ., isolated from the gut of the fungus- - growing termite *Macrotermes natalensis*. *Int. J. Syst. Evol. Microbiol.* **70**, 5226–5234 (2020).

132. Meyers, P. R., le Roes, M. *Nonomuraea candida* sp . nov ., a new species from South African

soil. *Antonie Van Leeuwenhoek* **93**, 133–139 (2008).

133. Sibanda, T., Mabinya, L. V, Mazomba, N. & Akinpelu, D. A. Antibiotic Producing Potentials of Three Freshwater Actinomycetes Isolated from the Eastern Cape Province of South Africa. *Int. J. Mol. Sci.* **11**, 2612–2623 (2010).

134. Roes-hill, M. Le, Durrell, K., Prins, A. & Meyers, P. R. *Streptosporangium minutum* sp. nov., isolated from garden soil exposed to microwave radiation. *J. Antibiot. (Tokyo).* (2018). doi:10.1038/s41429-018-0036-0

135. Elsayed, E. A., Farid, M. A. & El-enshasy, H. A. Enhanced Natamycin production by Streptomyces natalensis in shake-flasks and stirred tank bioreactor under batch and fed-batch conditions. *BMC Biotechnol.* **19**, 1–13 (2019).

136. STRUYK, A. P. *et al.* Pimaricin, a new antifungal antibiotic. *Antibiot. Annu.* **5**, 878–885

137. CHEN, G-Q., LU, F-P., DU, L.-X. Natamycin Production by *Streptomyces gilvosporeus* Based on Statistical Optimization. *J. Agric. Food Chem. 2008,* **56**, 5057–5061 (2008).

138. Du, Y-L., Chen, S-F., Cheng, L-Y., Shem, X-L., Tian, Y., Li, Y.-Q. Identification of a Novel *Streptomyces chattanoogensis* L19 and Enhancing Its Nataycin Production by Overexpressing Positive Regulator ScnRII. *J. Microbiol.* **47**, 506–513 (2009).

139. Lu, C. G. *et al.* Identification of an antifungal metabolite produced by a potential biocontrol Actinomyces strain A01. *Brazilian J. Microbiol.* **39**, 701–707 (2008).

140. Aparicio, J. F., Barreales, E. G., Payero, T. D. & Vicente, C. M. Biotechnological production and application of the antibiotic pimaricin : biosynthesis and its regulation. *Appl Microbiol Biotechnol* **100**, 61–78 (2016).

141. Maria, Y. *et al.* Natamycin Inhibits Vacuole Fusion at the Priming Phase via a Specific Interaction with Ergosterol. *Antimicrob. Agents Chemother.* **54**, 2618–2625 (2010).

142. Welscher, Y. M. *et al.* Natamycin Blocks Fungal Growth by Binding Specifically to Ergosterol without Permeabilizing the Membrane . *J. Biol. Chem.* **283**, 6393–6401 (2008).

143. Rolon, M., Seco, E. M., Vega, C., Nogal, J. J., Escario, J. A., Gomez-Barrio, A., Malpartida, F. Selective activity of polyene macrolides produced by genetically modified Streptomyces on *Trypanosoma cruzi*. *Int. J. ofAntimicrobial Agents* **28**, 104–109 (2006).

144. Sunada, A. *et al.* In Vitro Evaluations of Topical Agents to Treat Acanthamoeba Keratitis. *Ophthalmology* **121**, 1–7 (2014).

145. Jackson, M. *et al.* Altromycins, Novel Pluramycin-like antibiotics I. Taxonomyof the producing organism, fermentation and antibacterial activity. *J. Antibiot. (Tokyo).* **43**, 223–8 (1984).

146. Brill, G. M., Mcalpine, J. B., Whittern, D. N. & Buko, A. M. Altromycins, Novel Pluramycin-like antibiotics II. Isolation and elucidation of structure. *J. Antibiot. (Tokyo).* **43**, 229–37 (1990).

147. Brill, G. M. *et al.* Altromycins E, F, G, H AND I; Additional Novel components of the Altromycin complex. *J. Antibiot. (Tokyo).* **47**, 1160–1164 (1994).

148. Hansen, M., Hurley, L. Altromycin B Threads the DNA Helix Interacting with Both the Major and the Minor Grooves To Position Itself for Site-Directed Alkylation of Guanine N7. *J. Am. Chem. Soc.* **117**, 2525–2533 (1995).

149. Anticancer drug discovery and develpoment: Natural Products and New Molecular Models. in (1991).

150. Singh, S. B. *et al.* Isolation , Structure , and Absolute Stereochemistry of Platensimycin , A Broad Spectrum Antibiotic Discovered Using an Antisense Differential Sensitivity Strategy. *J. AM. CHEM. SOC.* **128**, 11916–11920 (2006).

151. Martens, E. & Demain, A. L. Platensimycin and platencin : promising antibiotics for future application in human medicine. *J. Antibiot. (Tokyo).* 705–710 (2011). doi:10.1038/ja.2011.80

152. Yu, Z., Rateb, M. E., Smanski, M. J., Peterson, R. M. & Shen, B. Isolation and structural elucidation of glucoside congeners of platencin from *Streptomyces platensis* SB12600. *J.*

Antibiot. (Tokyo). 291–294 (2013). doi:10.1038/ja.2013.1

153. Zhang, C. *et al.* Platensimycin and Platencin Congeners from *Streptomyces platensis*. *J. Nat. Prod.* **74**, 329–340 (2011).

154. Zhang, C. *et al.* Bioorganic & Medicinal Chemistry Isolation , structure and biological activities of platencin A 2 – A 4 from *Streptomyces platensis*. *Bioorg. Med. Chem.* **18**, 2602–2610 (2010).

155. Herath, K. B. *et al.* Structure and Semisynthesis of Platensimide A , Produced by *Streptomyces platensis*. *Org. Lett.* **10**, 5–8 (2008).

156. Singh, S. B. *et al.* Isolation , enzyme-bound structure , and activity of platensimycin A 1 from *Streptomyces platensis*. *Tetrahedron Lett.* **50**, 5182–5185 (2009).

157. Zhang, C. *et al.* Isolation , structure and fatty acid synthesis inhibitory activities of platensimycin B 1 – B 3 from *Streptomyces platensis*. *Chem. Commun.* **40**, 5034–5036 (2008).

158. Zhang, C. *et al.* Isolation , structure and biological activities of platensimycin B 4 from *Streptomyces platensis*. *J. Antibiot. (Tokyo).* 699–702 (2009). doi:10.1038/ja.2009.106

159. Singh, S. B. *et al.* Bioorganic & Medicinal Chemistry Letters Isolation , enzyme-bound structure and antibacterial activity of platencin A 1 from *Streptomyces platensis*. *Bioorg. Med. Chem. Lett.* **19**, 4756–4759 (2009).

160. Jayasuriya, H. *et al.* Structure of homoplatensimide A : a potential key biosynthetic intermediate of platensimycin isolated from *Streptomyces platensis*. *Tetrahedron Lett.* **49**, 3648–3651 (2008).

161. Article, E. *et al.* Natalamycin A, an ansamycin from a termite- associated *Streptomyces* sp. *Chem. Sci.* **5**, 4333–4338 (2014).

162. Lee, S. R. *et al.* Absolute Configuration and Corrected NMR Assignment of 17-Hydroxycyclooctatin, a Fused 5−8−5 Tricyclic Diterpene. *J. Nat. Prod.* **83**, 354–361 (2019).

163. Kang, H. R. *et al.* Termisoflavones A–C, Isoflavonoid Glycosides from Termite- Associated *Streptomyces* sp. RB1. *J. Nat. Prod.* **79**, 3072–3078 (2016).

164. Line, H. T. C. *et al.* Chemical Identification of Isoflavonoids from a Termite-Associated *Streptomyces* sp . RB1 and Their Neuroprotective Effects in Murine Hippocampal HT22 Cell Line. *Int. J. Mol. Sci.* **19**, 1–13 (2018).

165. Lee, D., Kang, K. S. & Lee, H. Chemical Characterization of a Renoprotective Metabolite from Termite-Associated *Streptomyces* sp . RB1 against Cisplatin-Induced Cytotoxicity. *Int. J. Mol. Sci.* **19**, 1–10 (2018).

166. Wyche, T. P. *et al.* Linear Peptides Are the Major Products of a Biosynthetic Pathway That Encodes for Cyclic Depsipeptides. *Org. Lett.* **19**, 1772–1775 (2017).

167. Guo, H., Benndorf, R., Leichnitz, D., Klassen, J. L., Vollmers, J., Gorls, H., Steinacker, M., Weigel, C., Dahse, H-M., Kaster, A-K., de Beer, Z. W., Poulsen, M., Beemelmanns, C. Isolation, Biosynthesis and Chemical Modifications of Rubterolones A–F, Rare Tropolone Alkaloids from *Actinomadura* sp. 5-2. *Chem. Eur. J* **23**, 9338–9345 (2017).

168. Rb, T. A. *et al.* Natalenamides A–C, Cyclic Tripeptides from the Termite-Associated *Actinomadura* sp. RB99. *Molecules* **23**, 1–12 (2018).

169. Rb, A. *et al.* Polyhalogenation of Isoflavonoids by the Termite-Associated *Actinomadura* sp. RB99. *J. Nat. Prod.* **83**, 3102–3110 (2020).

170. Yoon, S., Lee, S. R., Hwang, J. Y. & Benndorf, R. Fridamycin A, a Microbial Natural Product, Stimulates Glucose Uptake without Inducing Adipogenesis. *Nutrients* **11**, 1–10 (2019).

171. Beemelmanns, C. *et al.* Macrotermycins A-D, glycosylated macrolactams from a termite-associated *Amycolatopsis* sp. M39. *Org Lett.* **19**, 1000–1003 (2018).

172. https://www.technologynetworks.com/drug-discovery/articles/phenotypic-versus-target-based-screening-for-drug-discovery-300037.

173. Chatterjee, A. K. & Yeung, B. K. S. Back to the Future : Lessons Learned in Modern Target-based and Whole- Cell Lead Optimization of Antimalarials. *Curr. Top. Med. Chem.* **12**, 473–

483 (2012).

174. Nuzillard, J. H. J. & Renault, J. Dereplication strategies in natural product research : How many tools and methodologies behind the same concept ? *Phytochem. Rev.* **16**, 55–95 (2017).

175. Gaudˆencio, S. P. Pereira, F. Dereplication : racing to speed up the natural products discovery process. *Nat. Prod. Rep.* **32**, 779–810 (2015).

176. Puckett, S. P., Chemistry, M. & Sciences, P. *Metabolomics and the Microbiome : Characterizing Molecular Diversity in Complex Microbial Communities*. *Comprehensive Natural Products III: Chemistry and Biology* (Elsevier Inc., 2020). doi:10.1016/B978-0-12-409547-2.14802-4

177. Networking, S. M. Perspective Sharing and community curation of mass spectrometry data with Global Natural Products Social Molecular Networking. *Nat Biotechnol* **34**, 828–837 (2016).

178. Holman, J. D. & Tabb, D. L., Mallick, P. Employing ProteoWizard to Convert Raw Mass Spectrometry Data. *Curr Protoc Bioinformatics.* **46**, 918–920 (2015).

179. Pluskal, T., Castillo, S., Villar-briones, A. & Ore, M. MZmine 2 : Modular framework for processing , visualizing , and analyzing mass spectrometry- based molecular profile data. *BMC Bioinformatics* **11**, (2010).

180. Otasek, D., Morris, J. H., Bouças, J., Pico, A. R. & Demchak, B. Cytoscape Automation : empowering workflow-based network analysis. *Genome Biol.* **20**, 1–15 (2019).

181. Albarano, L., Esposito, R., Ruocco, N., Costantini, M. Genome Mining as New Challenge in Natural Products Discovery Luisa. *Mar. Drugs* **18**, 1–17 (2020).

182. Blin, K. *et al.* antiSMASH 2 . 0 — a versatile platform for genome mining of secondary metabolite producers. *Nucleic Acids Res.* **41**, 204–212 (2013).

183. Reher, R. *et al.* A Convolutional Neural Network-Based Approach for the Rapid Annotation of Molecularly Diverse Natural Products. *J. Am. Chem. Soc.* **142**, 4114−4120 (2020).

Chapter Three: Screening of marine invertebrates identifies heteronemin and bengamides as potent antimycobaterial hits

3.1 Introduction

Tuberculosis (TB), which is caused by *Mycobacterium tuberculosis* (Mtb), remains a leading cause of death globally owing to a single infectious agent. Despite the availability of an effective anti-TB chemotherapy and a neonatal vaccine, an estimated 10 million people contracted TB and 1.4 million people died of the disease globally in 2019.[1] The current standard combination therapy carries a high pill burden (up to 4 separate anti-TB drugs are used), long duration (minimum of six months) of treatment and side effects or toxicities owing to concomitant use of mixtures of TB drugs and non-TB drugs (for example anti-HIV drugs).[1,2] Furthermore, delayed diagnosis, inappropriate treatment and non-adherence has led to the emergence of drug-resistant strains of Mtb which include multidrug-resistant (MDR), extensively drug resistant (XDR) and totally drug-resistant (TDR) strains of Mtb.[1,3] It takes a longer period (minimum of 24 months) and a lot more drugs to treat resistant strains of Mtb which comes at a high cost with severe side effects and low chance of complete cure.[3–5] There is therefore an urgent need to discover and develop new potent pan-active antitubercular drugs to effectively treat all Mtb strains with reduced treatment duration and fewer or no side effects.

Nature remains our primary source of drugs with the marine environment relatively less explored.[6] The ocean occupies over 70% of the Earth's surface and is uniquely rich in biodiversity. For their survival and existence, marine organisms, especially invertebrates, biosynthesize and secrete secondary metabolites to ward off competitors, predators and parasites.[7] These secondary metabolites have unique structural diversity with a high degree of stereochemical complexity and have shown a range of bioactivities including anticancer, antioxidant, antifungal, antiviral, antibacterial, anti-TB, anti-inflammatory, antimalarial, analgesic and antinematodal properties.[8,9] For example, the peptide, ziconotide, and the alkaloid, ecteinascidin-743, derived from the marine cone snail species, *Conus magus*, and sea squirt, *Ecteinascidia turbinate*, are drugs used to treat pain and cancer, respectively.[10,11] Marine natural products have promise of providing drug leads for the TB drug discovery pipeline and many anti-mycobacterial compounds

including the manzamines, halicyclamines, cyclostellettamines, batzelladines and callyaerins have already been isolated from marine organisms.[12]

Natural product drug discovery starts with screening of natural product extracts as the preliminary step to finding new lead compounds. As part of our continuous search for new anti-TB agents from marine invertebrates, we screened several marine natural product extracts obtained from the United States of America's National Cancer Institute (NCI).[13] The whole-cell approach was employed in preference to target-based and genetics-driven approaches given the unknown bioactive compositions of the extracts and the well-described difficulties in ensuring whole-cell activity against Mtb.[14] Herein, we report the initial screening of 984 organic and aqueous marine invertebrate extracts and the antimycobacterial activity results of 54 active extracts with the detection and isolation of the active components of two of the extracts. The extracts of the sponges, *Hyrtios reticulatus* and *Jaspis splendens*, were among the most active and were subjected to activity-guided fractionation to isolate the active ingredients. *Hyrtios reticulatus* yielded heteronemin **3.1** while *Jaspis splendens* produced the bengamide class of compounds. Bengamides have previously been shown to be potent antitubercular agents. To the best of our knowledge, this is the first report of antitubercular activity for bengamides P **3.2** and Q **3.3**.

3.2 Results and Discussion

3.2.1 Screening of marine invertebrate samples

An initial 984 organic and aqueous marine invertebrate extracts were screened for their *in vitro* inhibitory activity against a fully virulent *M. tuberculosis* H37Rv fluorescent reporter mutant[15,16] and the minimum inhibitory concentration required to inhibit 90% (MIC_{90}) and 99% (MIC_{99}) of the bacteria population was recorded. Of the 984 samples, 54 actives were identified and retested to confirm activity.

Table 3.1: Minimum inhibitory concentration (MIC_{90} and MIC_{99}) of marine invertebrate extracts against *M. tuberculosis* strain H37Rv and classification to species level of the marine invertebrates with their source country.

Country	**Phylum**	**Class**	**Order**	**Family**	**Genus**	**Species**	**NPID**	**MIC_{90}** (μg/mL)	**MIC_{99}** (μg/mL)
Mauritius	Porifera	Demospongiae	Astrophorida	Ancorinidae	*Jaspis*	*splendens (Dorypleres)*	C019765	2.4	4.5
	Porifera	Demospongiae	Dictyoceratida	Thorectidae	*Hyrtios*	*reticulatus*	C019725	51.0	72.0
South Africa	Porifera	Demospongiae	Poecilosclerida	Guitarridae	*Guitarra*	*fimbriata indica*	C018520	70.0	87.0
	Porifera	Demospongiae	Hadromerida	Suberitidae	*Aaptos*	*sp. 1*	C018442	71.0	83.0
	Porifera	Demospongiae	Verongida	Aplysinellidae	*Porphyria*	*pedunculata*	C018530	71.0	94.0
	Porifera	Demospongiae	Poecilosclerida	Hymedesmiidae	*Phorbas*	*sp. 1*	C018462	72.0	81.0
	Porifera	Demospongiae	Halichondrida	Heteroxyidae	*Higginsia*	*bidentifera*	C018466	72.0	83.0
	Porifera	Demospongiae	Halichondrida	Heteroxyidae	*Higginsia*	*sp. 1*	C018578	72.0	84.0
	Cnidaria	Hydrozoa	Leptothecatae	Aglaopheniidae	*Lytocarpia*	*formosa*	C018502	73.0	81.0
	Porifera	Demospongiae	Halichondrida	Halichondriidae	*Hymeniacidon*	*sp. 1*	C018470	73.0	84.0
	Porifera	Demospongiae	Poecilosclerida	Guitarridae	*Guitarra*	*fimbriata indica*	C018458	73.0	91.0
	Chordata	Ascidiacea	Aplousobranchia	Didemnidae	*Didemnum*	*obscurum*	C019906	1.6	1.7
	Porifera	Demospongiae	Halichondrida	Dictyonellidae	*Stylissa*	*sp. 1, n.sp.*	C019904	17.0	19.4
	Cnidaria	Anthozoa	Alcyonacea	Nephtheidae	*Drifa*	*sp. b (n.sp.)*	C018631	41.0	52.0
	Porifera	Demospongiae	Poecilosclerida	Raspailiidae	*Echinodictyum*	*sp. 1*	C018566	25.1	42.8
	Mollusca	Polyplacophora	Chitonida	Acanthochitonidae	*Acanthochitona*	*garnoti*	C018637	0.5	0.6
	Porifera	Demospongiae	Poecilosclerida	Isodictyidae	*Isodictya*	*sp. 2, n.sp.*	C018626	18.8	6.3
	Porifera	Demospongiae	Poecilosclerida	Tedaniidae	*Hemitedania*	*sp. 1*	C018538	18.7	9.3
	Porifera	Demospongiae	Halichondrida	Halichondriidae	*Halichondria*	*sp. 1*	C018460	13.8	12.2
Tanzania	Porifera	Demospongiae	Haplosclerida	Petrosiidae	*Neopetrosia*	*tuberosa cf.*	C015405	2.5	3.2
	Porifera	Demospongiae	Haplosclerida	Phloeodictyidae	*Oceanapia*	*ramsayi*	C015331	22.0	28.0
	Porifera	Demospongiae	Haplosclerida	Phloeodictyidae	*Oceanapia*	*sp. 3*	C015461	35.0	42.0
	Porifera	Demospongiae	Poecilosclerida	Chondropsidae	*Chondropsis*	*sp. 1*	C015479	58.0	64.0
	Chordata	Ascidiacea	Aplousobranchia	Polycitoridae	*Eudistoma*	*giganteum*	C015357	61.0	68.0
	Porifera	Demospongiae	Dictyoceratida	Thorectidae	*Aplysinopsis*	*elegans cf.*	C015228	2.5	2.6
	Mollusca	Gastropoda	Neogastropoda	Cypraeidae	*Cypraea*	*tigris*	C015272	47.9	57.9
	Porifera	Demospongiae	Poecilosclerida	Podospongiidae	*Diacarnus*	*ardoukobae*	C015180	70.8	81.2

Papua-New Guinea	Chordata	Ascidiacea	Aplousobranchia	Didemnidae	*Lissoclinum*	*badium*	C018795	2.6	3.1
	Porifera	Demospongiae	Dictyoceratida	Thorectidae	*Fascaplysinopsis*	*sp. 2*	C018781	7.9	16.5
	Porifera	Demospongiae	Haplosclerida	Petrosiidae	*Petrosia (Strongylophora)*	*corticata*	C018743	31.0	35.0
	Porifera	Demospongiae	Dictyoceratida	Dysideidae	*Dysidea*	*sp. 17*	C018675	32.0	36.0
	Porifera	Demospongiae	Haplosclerida	Chalinidae	*Haliclona (Gellius)*	*sp. 4*	C018717	36.0	57.0
	Porifera	Demospongiae	Dictyoceratida	Dysideidae	*Lamellodysidea*	*herbacea*	C018667	41.0	43.0
	Porifera	Demospongiae	Dictyoceratida	Thorectidae	*Carteriospongia*	*sp. 3*	C018787	48.0	70.0
	Porifera	Demospongiae	Dictyoceratida	Thorectidae	*Phyllospongia*	*sp. 7*	C018595	63.0	70.0
	Porifera	Demospongiae	Dictyoceratida	Thorectidae	*Aplysinopsis*	*elegans*	C018651	65.0	71.0
	Porifera	Demospongiae	Poecilosclerida	Mycalidae	*Mycale*	*setosa*	C018783	72.0	81.0
	Porifera	Demospongiae	Dictyoceratida	Spongiidae	*Spongia*	*sp. 5*	C018671	72.0	82.0
	Chordata	Ascidiacea	Aplousobranchia	Polyclinidae	*Synoicum*	*castellatum*	C018601	72.0	83.0
	Porifera	Demospongiae	Haplosclerida	Petrosiidae	*Neopetrosia*	*tuberosa cf.*	C018593	72.0	83.0
	Porifera	Demospongiae	'Lithistid'	Theonellidae	*Theonella*	*sp. 7*	C018729	73.0	83.0
	Porifera	Demospongiae	Dictyoceratida	Irciniidae	*Ircinia*	*arbuscula cf*	C018773	< 0.2	0.5
	Porifera	Demospongiae	Hadromerida	Suberitidae	*Aaptos*	*nigra*	C018695	58.3	51.4
	Porifera	Demospongiae	Agelasida	Agelasidae	*Agelas*	*oxeata cf.*	C018756	0.4	0.9
	Porifera	Demospongiae	'Lithistid'	Scleritodermidae	*Aciculites*	*oxtylota*	C018740	20.8	21.9
	Porifera	Demospongiae	'Lithistid'	Scleritodermidae	*Microscleroderma*	*herdmani*	C018684	23.7	30.6
	Porifera	Demospongiae	Haplosclerida	Callyspongiidae	*Callyspongia (Euplacella)*	*elongata cf.*	C018714	85.2	125.0
	Porifera	Demospongiae	Haplosclerida	Niphatidae	*Pachychalina*	*sp. 11*	C018694	17.9	46.5
	Porifera	Demospongiae	Astrophorida	Thrombidae	*Thrombus*	*sp. 1*	C018716	20.8	42.5
	Porifera	Demospongiae	Haplosclerida	Niphatidae	*Niphates*	*elegans*	C018720	23.8	91.3
Palau Islands	Porifera	Demospongiae	Halichondrida	Halichondriidae	*Topsentia*	*cavernosa*	C019960	71.9	78.9
	Porifera	Demospongiae	Hadromerida	Suberitidae	*Aaptos*	*nigra*	C019928	85.2	106.0
	Porifera	Demospongiae	Haplosclerida	Chalinidae	*Haliclona (Gellius)*	*sp. 4*	C020034	95.9	120.0
	Porifera	Demospongiae	Verongida	Aplysinellidae	*Porphyria*	*sp. 1, n.sp.*	C019898	113.0	125.0
Control	Rifampicin							0.02	0.03

A Scifinder (https://scifinder.cas.org/) search of the species of the marine invertebrates from which the 54 extracts were obtained revealed that this was the first report of antimycobacterial activity of 44% of the species. The 54 active extracts were from marine invertebrate samples collected from the territorial waters of Mauritius (Indian Ocean)- 2, South Africa (Indian and South Atlantic Oceans)- 17, Tanzania (Indian Ocean)- 8, Palau Island (Pacific Ocean)- 4, and Papua-New Guinea (Pacific Ocean)- 23. The invertebrates are of the phyla Porifera (46), Cnidaria (2), Chordata (4) and Mollusca (2). The actives displayed a MIC range between <0.24 and 125 µg/mL (Table 3.1) with 35% exhibiting good activity (MIC < 25 µg/mL), 28% moderate activity (MIC 25-65 µg/mL) and 37% weak activity (MIC 65-125 µg/mL). The extracts of the species belonging to the genera *Jaspis*, *Didemnum*, *Acanthochitona*, *Isodictya*, *Hemitedania*, *Neopetrosia*, *Aplysinopsis*, *Cypraea*, *Lissoclinum*, *Fascaplysinopsis*, *Ircinia* and *Agelas* exhibited the most potent activities with sub-10 µg/mL MICs. It is worth noting that a Scifinder search for these genera returned no reports of antimycobacterial activity, with the exception of the genera, *Didemnum*, *Neopetrosia*, *Lissoclinum*, *Ircinia* and *Agelas*. The diterpene alkaloids, agelasines, isolated from the genus *Agelas*, and the tetracyclic bis-piperidine alkaloid, neopetrosiamine A, isolated from *Neopetrosia proxima*, as well as crude extracts of species of the genera *Didemnum*, *Lissoclinum*, *Ircinia* and *Agelas*, have been reported to show antimycobacterial activities.[17–20] This reaffirms that marine invertebrates represent a potential source of anti-TB compounds.

3.2.2 Dereplication, Molecular Networking, Isolation and Structure elucidation

The actives were isolated using an activity-guided isolation procedure. First, the ^{1}H NMR spectra and HR-LCMS profiles were obtained for the bioactive extracts derived from the Mauritian marine sponges, *Hyrtios reticulatus* (SS10) and *Jaspis splendens* (SS2) – both of which were available in appreciable amounts. Next, the extracts were subjected to bioactivity-guided fractionation, using a normal phase solid phase extraction (SPE) procedure to yield five fractions (A-E) which were screened against the Mtb reporter strain.

The HR-LCMS profile of the extract of *Hyrtios reticulatus* (SS10) showed a major peak with *m/z* 511.3026 $[M + Na]^{+}$ which was identified as the antimycobacterial sesquiterpene, heteronemin **3.1**; this was confirmed by the ^{1}H NMR spectrum. Fractions A and B of SS10 were the most active

and had the same ^{1}H NMR spectrum and were therefore combined and further purified using normal phase column chromatography to yield the known compound, heteronemin **3.1,** as the most active ingredient. Heteronemin **3.1** was isolated as a white amorphous solid with a molecular formula of $C_{29}H_{44}O_6$ deduced from HRESIMS (observed $[M + Na]^+$ = 511.3026; calculated $[M + Na]^+$ = 511.3036; Δ = -1.96 ppm), corresponding to eight degrees of unsaturation (Figure S3.1). The structure of compound **3.1** was fully elucidated by analysis of HRESIMS, 1D and 2D NMR data and this was congruent with that reported in the literature (Figures S3.1-S3.6 and Table S3.1).[21,22]

The HR-LCMS/MS data of the extract of *Jaspis splendens* (SS2) was analyzed on the GNPS molecular networking platform.[23] Dereplication of the nodes showed molecular network families which are representative of the bengamide class of compounds and this was confirmed by the analysis of the ^{1}H NMR spectrum of SS2 (Figures 3.1-3.2, and Table S3.4). The bengamides are unique compounds with a core scaffold comprising a 2(R)-methoxy-3(R),4(S),5(R)-trihydroxy-8-methylnon-6(E)-enoyl moiety linked to an aminocaprolactam with its cyclic amide nitrogen free or methylated.[24] About 23 bengamides have been isolated with various structural variations, enabling grouping into structural classes.[25,26] The first type contains a hydroxylysine-derived caprolactam, with the OH at C-13 either unsubstituted (bengamides Y, Z) or acylated by a lipid unit (bengamides A, B, G–J, L–O), or by polyketide esters (bengamides C, D). The second type have the lysine-derived caprolactam (which therefore does not have an OH at C-13) but with the 5-OH acylated by the lipid unit (bengamides P–R) or not (bengamides E, E', F, F').[25,26] Some bengamides have the same molecular formulae and weight and are only differentiated by characteristic NMR signals. For example, bengamides J and M have the same molecular formula of $C_{33}H_{60}N_2O_8$ and weight 635.4228 $[M + Na]^+$ (Figures 3.2, Table S3.3).[24]

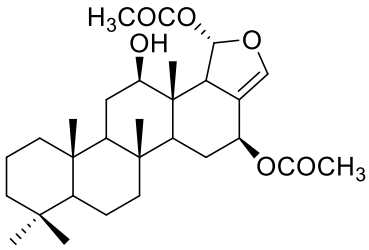

Heteronemin (3.1)

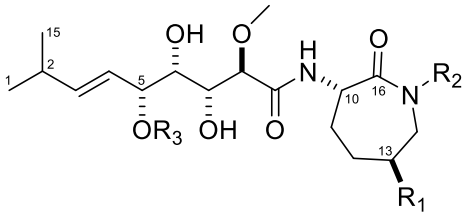

Bengamide	R_1	R_2	R_3
A (**3.8**)	$OCO(CH_2)_{12}CH_3$	H	H
B (**3.9**)	$OCO(CH_2)_{12}CH_3$	CH_3	H
C (**3.10**)	X	H	H
D (**3.11**)	X	CH_3	H
E (**3.12**)	H	H	H
F (**3.13**)	H	CH_3	H
G (**3.14**)	$OCO(CH_2)_{11}CH_3$	H	H
H (**3.15**)	$OCO(CH_2)_{11}CH_3$	CH_3	H
I (**3.16**)	$OCO(CH_2)_{13}CH_3$	H	H
J (**3.17**)	$OCO(CH_2)_{13}CH_3$	CH_3	H
L (**3.18**)	$OCO(CH_2)_{11}CH(CH_3)_2$	H	H
M (**3.19**)	$OCO(CH_2)_{11}CH(CH_3)_2$	CH_3	H
N (**3.20**)	$OCO(CH_2)_{10}CH(CH_3)_2$	H	H
O (**3.21**)	$OCO(CH_2)_{10}CH(CH_3)_2$	CH_3	H
P (**3.2**)	H	H	$CO(CH_2)_{12}CH_3$
Q (**3.3**)	H	CH_3	$CO(CH_2)_{12}CH_3$
R (**3.4**)	H	H	$CO(CH_2)_{14}CH_3$
S (**3.5**)	H	CH_3	$CO(CH_2)_{14}CH_3$
Y (**3.6**)	OH	H	H
Z (**3.7**)	OH	CH_3	H

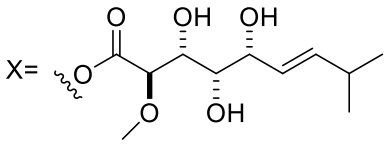

Figure 3.1: Structures of isolated compounds (**3.1**-**3.3**), predicted (**3.5**) and some known bengamides (**3.4, 3.6**-**3.21**)

Molecular cluster F1 contains the first class of bengamides with a lipid chain (Figure 3.2). The node with *m/z* 621.408 $[M + Na]^+$ corresponds to isomeric bengamides B **3.9**, I **3.16**, L **3.18** or O **3.21**, while the node with *m/z* 607.392 $[M + Na]^+$ corresponds to bengamides A **3.8**, H **3.15** or N **3.20** and the node with *m/z* 635.424 $[M + Na]^+$ to bengamides J **3.17** or M **3.19** (Figures 3.1 and 3.2). Family F2, which is constituted by four nodes, was dereplicated to be the second type of bengamides with a fatty acid chain, including bengamides P **3.2** (*m/z* 591.397 $[M + Na]^+$), Q **3.3** (*m/z* 605.413 $[M + Na]^+$) and R **3.4** (*m/z* 619.428 $[M + Na]^+$) which was linked to its new analogue **3.5** (node with *m/z* 633.445 $[M + Na]^+$) with a mass difference of 14 Da signifying methylation. From the biosynthesis of bengamides and a keen examination of isolated bengamide structures, the methylation would either be on the caprolactam ring nitrogen or an elongation of the lipid chain of **3.4**. Evaluation of the fragmentation patterns (Figure S3.23) of compounds **3.4** and **3.5** showed that, **3.5** is an *N*-methylated analogue of **3.4**. Compound **3.5** was therefore assigned the name bengamide S.

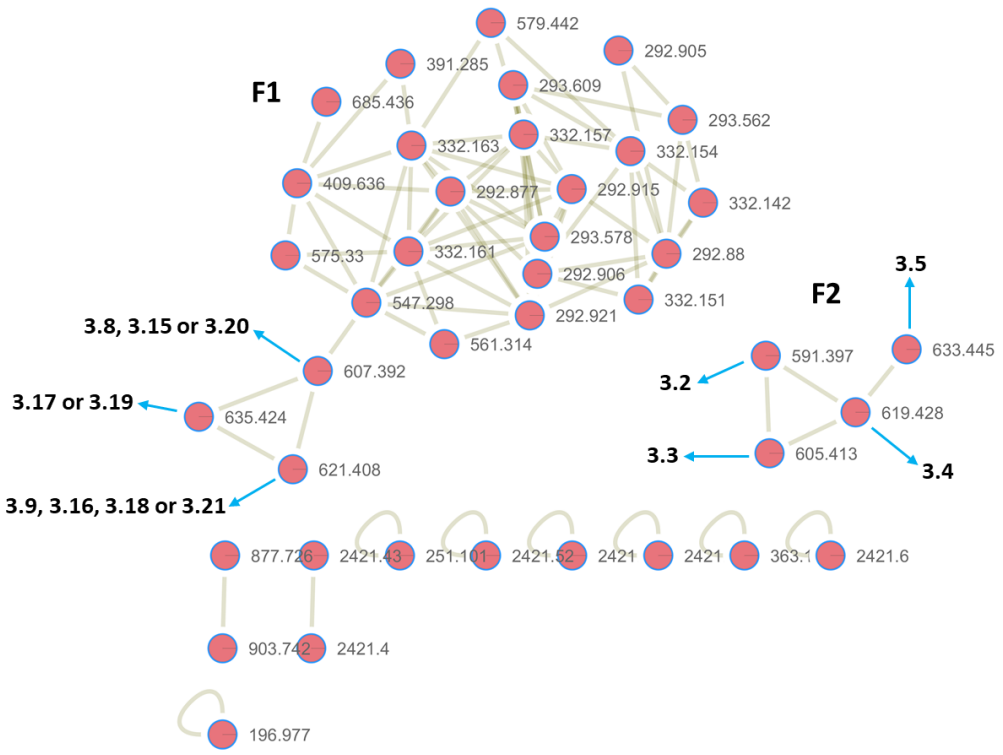

Figure 3.2**:** GNPS molecular network of the crude extract (SS2) of marine sponge *Jaspis splendens* containing some annotated nodes. Numbers in bold correspond to compounds shown in Figure 3.1.

Fractions B and C of SS2 exhibited the best activities with potent MIC_{90} values of <0.24 µg/mL and 0.23 µg/mL, respectively. Also, analyses of the HR-LCMS profiles and ^{1}H NMR spectra of active fractions B and C revealed they contained the bengamides. These fractions were therefore combined and subjected to normal phase column chromatography. ^{1}H NMR analysis of representative samples of the >150 fractions collected showed that they were mixtures of bengamides. However, fractions F94 and F100 were sufficiently homogeneous for their structures to be elucidated as compounds **3.2** and **3.3,** respectively. Compounds **3.2** and **3.3** had ^{1}H NMR signals characteristic of the second type of bengamides with a lipid chain located at C-5. The fact that this was attached to C-5 and not C-13 was evident from the downfield shift of the signal at δ_H 5.47 for the methine proton H-5 in the ^{1}H NMR spectrum, compared to the shielded signals for the diastereotopic C-13 methylene protons at δ_H 1.88 and 1.43. The structures of compounds **3.2** and **3.3** were fully elucidated by analyses of their HRESIMS, 1D and 2D NMR data and comparison with literature and confirmed to be bengamides P and Q respectively (Figures S3.7-S3.19 and Tables S3.2-S3.3).[24]

The ^{1}H NMR spectra of active fractions F107, F114 and F130 (Figures S3.20 – S3.22) showed characteristic signals for bengamides of both classes with a lipid chain. However, the main component of fraction F130 was the first type of bengamide, with a branched lipid chain and characteristic upfield signals in the ^{1}H NMR spectrum at δ_H 0.7-1.7 and a signal for an *N*-methyl group in the caprolactam ring (δ_H 3.13). It is proposed that this major component may be bengamide M **3.19** as a corresponding peak of *m/z* 635.423 $[M + Na]^+$ was identified in the HR-LCMS profile of fraction F130.

3.2.3 Antimycobacterial activity of isolated compounds and semi-pure fractions

Heteronemin **3.1** exhibited an MIC_{90} of 8.23 µg/mL against Mtb. Shown in the table 3.2 are antimycobacterial activity results of isolated pure compounds and the most active semi-pure fractions obtained from purification of fractions B and C of SS2. Fraction F114 showed the greatest activity with <0.24 µg/mL. Although bengamides have been isolated from the genus *Jaspis*, this is the first report of the detection and isolation of bengamides from *Jaspis splendens*, which is rather known to be a prolific producer of jasplakinolides.[25]

The bengamides are potent antitumor agents which target methionine aminopeptidase (MetAP).[25,26] Synthetic MetAP inhibitors based on the bengamide structural scaffold have been described with activity against the Mtb MetAPs (the bacillus encodes two isoforms, MetAP1a and MetAP1c), however the antimycobacterial potential (whole-cell or target -based) of natural bengamides is less explored.[27,28] There is a report of antimycobacterial activity of bengamide B **3.9**, which exhibited strong *in vitro* activity against *M. tuberculosis* and Mtb $MetAP_{1C}$ protein and was also non-toxic against human cell lines.[29] To our knowledge, this is the first report of antimycobacterial activity for the second type of bengamides with lipid chain, namely bengamides P **3.2** and Q **3.3**. This suggests that the bengamides are potential antitubercular leads and that all known natural analogs could be screened against Mtb to further aid in SAR and QSAR design and studies. Also, there appears to be value in further exploration of the Mtb MetAPs as potential drug targets.

Table 3.2: Minimum inhibitory concentration of bengamides P **3.2**, Q **3.3** and semi-pure fractions, obtained from purification of fractions B and C of SS2, against Mtb H37Rv cultured for 7 and 14 days.

Compound /Fraction	**MIC_{90} (µg/mL): 7 days**	**MIC_{90} (µg/mL): 14 days**
3.2	2.1	1.0
3.3	62.5	31.3
F107	1.1	0.7
F114	<0.2	<0.2
F130	0.7	0.5
Rifampicin	0.02	0.01

3.3 Materials and Methods

3.3.1 General experimental procedure

NMR spectra were obtained on a BRUKER Ascend 600 (Bruker, Billeria, MA, USA) cryoprobe prodigy at 600 MHz and 150 MHz for ^{1}H and ^{13}C nuclei, respectively. Chemical shifts were referenced using the corresponding undeuterated solvent signals in CD_3OD (δ_H 3.30, δ_C 47.61) and $CDCl_3$ (δ_H 7.25, δ_C 77.00). High resolution mass spectrometric data were obtained using a Thermo Instruments MS system (LTQ XL/LTQ Orbitrap Discovery, Thermo Scientific, Bremen, Germany) coupled to a Thermo Instruments HPLC system (Accela PDA detector, Accela PDA autosampler and Accela pump). The following conditions were used: capillary voltage 45 V, capillary temperature 260 °C, auxillary gas flow rate 10–20 arbitrary units, sheath gas flow rate 40–50 arbitrary units, spray voltage 4.5 kV, mass range 100–2000 amu (maximum resolution 30,000). All solvents used throughout were HPLC-grade and purchased from both Merck and Sigma-Aldrich. Column chromatography was carried out on silica gel 60 (Fluka 70–230 mesh, 63–200 µm, (Sigma-Aldrich, Buchs, Switzerland), and preparative TLC on silica gel 60 Analtech GF254 (20 × 20 cm, 2000 µm, Analtech Inc., Newark, DE, USA). Analytical TLC were performed on Merck silica gel 60 F254 (Merck KGaA, Darmstadt, Germany) and silica gel 60 RP-18 F254 plates and bands were visualized based on the UV absorbance at 254 nm and by heating after staining with ceric ammonium sulfate reagent.

3.3.2 Marine Invertebrate Samples

The screening consisted of 984 organic (MeOH/DCM) and aqueous extracts of marine invertebrate samples obtained from the National Cancer Institute (NCI), USA.[13]

3.3.3 Antimycobacterial Activity

The crude extracts, semi-pure and the isolated compounds were dissolved in DMSO and their minimum inhibition concentrations (MIC_{90}/MIC_{99} values) determined against the green fluorescent protein (GFP)-tagged Mtb H37Rv pMSp12::GFP bioreporter using the standard broth microdilution method developed by Collins et al.[15] Mtb H37Rv was cultured in the Middlebrook 7H9 broth medium supplemented with either albumin–dextrose complex, D-glucose, and Tween-

80 (7H9/ADC/Glu/Tw). The minimum concentration which inhibited the growth of 90% (MIC_{90}) or 99% (MC_{99}) of bacilli for the tested samples was scored visually at 1 week and 2 weeks post inoculation using the microplate Green Fluorescent Protein (GFP) and expressed in μg/mL. The fluorescence was measured with excitation at 485 nm and emission at 520 nm. Growth media and 5% dimethyl sulfoxide (DMSO) were used as a negative control, whereas rifampicin was used as a positive control.

3.3.4 Fractionation, Isolation and Purification of Active Compounds

The extracts SS2 and SS10 were subjected to an NCI DIOL SPE fractionation process. The organic extract (150 mg) was weighed and solubilized in 1.8 mL of 1:1 MeOH/CH_2Cl_2 and sonicated to mix. The mixture was loaded on a 2g DIOL SPE column and eluted stepwise, with solvent mixtures of increasing polarity (a column volume/solvent mixture of 6 mL): 9:1 hexane/CH_2Cl_2 (A), 20:1 CH_2Cl_2/EtOAc (B), 100% EtOAc (C), 5:1 EtOAc:MeOH (D), 100% MeOH (E). The fractionation process was repeated with 3 X 150 mg of extract and each fraction, from A to E, were combined and dried.

Fractions A and B of SS10 were combined and further purified through a normal phase column chromatography with an increasing polarity of a mixture of hexane/ EtOAc from 1:0 hexane/ EtOAc to 0:1 hexane/ EtOAC to yield compound **3.1** (17.01 mg) at solvent polarity of 7:3 Hexane/ EtOAc.

Fractions B and C of SS2 were also combined and subjected to a normal phase column chromatography with an increasing polarity of a mixture of hexane/ EtOAc from 1:0 hexane/ EtOAc to 0:1 hexane/ EtOAc to yield compounds **3.2** (3.08mg) and **3.3** (0.69 mg) at solvent polarity of 4:6 Hexane/ EtOAc and a mixture of bengamides.

Heteronemin **3.1**: white amorphous solid; For ^{1}H, ^{13}C NMR data, see Table S3.1 and Figures (S3.1-S3.6); HRESIMS (positive mode) m/z 511.3026 $[M + Na]^+$ Δ -1.96 ppm; calcd. for $C_{29}H_{44}O_6$.

Bengamide P **3.2**: colourless oil; For ^{1}H, ^{13}C NMR data, see Table S3.2 and Figures (S3.7-S3.12); HRESIMS (positive mode) m/z 591.3978 $[M + Na]^+$ Δ 2.03 ppm; calcd. for $C_{31}H_{56}N_2O_7$.

Bengamide Q **3.3**: colourless oil; For ^{1}H, ^{13}C NMR data, see Table S3.3 and Figures (S3.13-S3.19); HRESIMS (positive mode) m/z 605.4133 $[M + Na]^{+}$ Δ 1.82 ppm; calcd. for $C_{32}H_{58}N_2O_7$.

3.3.5 Dereplication and Molecular Networking

Raw LC–MS/MS data of sample SS2 was converted to mzXML format using the ProteoWizard tool MSconvert (version 3.0.10051, Vanderbilt University, United States).[30] The mzXML data was uploaded to the Global Natural Products Social (GNPS) Molecular Networking (MN) webserver3 (http://gnps.ucsd.edu) and analyzed using the MN workflow.[23] The data was filtered by removing all MS/MS fragment ions within +/- 17 Da of the precursor m/z. MS/MS spectra were window filtered by choosing only the top 6 fragment ions in the +/- 50Da window throughout the spectrum. The precursor ion mass tolerance was set to 0.02 Da and a MS/MS fragment ion tolerance of 0.02 Da. A network was then created where edges were filtered to have a cosine score above 0.7 and more than 3 matched peaks. Further, edges between two nodes were kept in the network if and only if each of the nodes appeared in each other's respective top 10 most similar nodes. Finally, the maximum size of a molecular family was set to 100, and the lowest scoring edges were removed from molecular families until the molecular family size was below this threshold. The spectra in the network were then searched against GNPS' spectral libraries. The library spectra were filtered in the same manner as the input data. All matches kept between network spectra and library spectra were required to have a score above 0.7 and at least 3 matched peaks. The output of the molecular network was visualized using Cytoscape version 3.7.2[31] and displayed using the settings “preferred layout” with “directed” style. The nodes (compounds) originating from the solvent control (MeOH) were excluded from the original network to enable visualization of only the compounds in SS2.

3.4 Conclusion

Marine natural products are a reliable source of potent antitubercular leads as this screening project identified 54 actives (MIC < 0.244 and 125 µg/mL) and 44% of the species from which these extracts were obtained are being reported for the first time for their antimycobacterial activity. ^{1}H NMR and HR-LCMS dereplication with GNPS molecular networking and a bioactivity-

guided isolation technique was employed to detect and isolate heteronemin and the bengamides (P and Q) as the respective active ingredients of the extracts of the Mauritian sponges *Hyrtios reticulatus* and *Jaspis splendens*. A new bengamide derivative was detected in the molecular network of SS2. The bengamides are potent antimycobacterial compounds and therefore need to be explored further. The isolation of promising active compounds from crude extracts with high and moderate activity gives enough reason to continue exploring these NCI marine invertebrate extracts for novel antitubercular leads.

3.5 References

1. *WHO Global Tuberculosis Report 2020*.

2. Snelll, N. J. C. The treatment of tuberculosis: current status and future prospects. *Expert Opin. Investig. Drugs* **7**, 545–552 (1998).

3. Nguta, J. M., Appiah-Opong, R., Nyarko, A. K., Yeboah-Manu, D. & Addo, P. G. A. Current perspectives in drug discovery against tuberculosis from natural products. *Int. J. Mycobacteriology* **4**, 165–183 (2015).

4. Riccardi, G. & Pasca, M. R. Trends in discovery of new drugs for tuberculosis therapy. *J. Antibiot. (Tokyo).* 655–659 (2014). doi:10.1038/ja.2014.109

5. Blanco, D., Perez-Herran, E., Cacho, M., Ballell, L., Castro, J., Del Río, R. G., Lavandera, J. L., Remuiñán, M. J., Richards, C., Rullas, J., Vázquez-muñiz, M. J. & Woldu, E. Mycobacterium tuberculosis Gyrase Inhibitors as a New Class of Antitubercular Drugs. *Antimicrob Agents Chemother* **59**, 1868–1875 (2015).

6. Cragg, G. M. & Newman, D. J. Natural Products: A Continuing Source of Novel Drug Leads. *Biochim Biophys Acta* **1830**, 3670–3695 (2013).

7. Paul, V. J. & Ritson-williams, R. Marine chemical ecology. *Nat. Prod. Rep.* **25**, (2008).

8. Patridge, E., Gareiss, P., Kinch, M. S. & Hoyer, D. natural products and their derivatives. *Drug Discov. Today* **21**, 204–207 (2016).

9. Gerwick, W. H., Moore, B. S. Lessons from the past and charting the future of marine natural products drug discovery and chemical biology. *Chem Biol* . **19**, 85–98 (2013).

10. Bowersox, S. S. & Luther, R. Pharmacotherapeutic potential of Omega- Conotoxin MVIIA (SNX-111), An N-TYPE neuronal calcium channel blocker found in the venom of *Conus Magus*. *Toxicon* **36**, 1651–1658 (1998).

11. Rinehart, K. L. *et al.* Ecteinascidins 729, 743, 745, 759A, 759B, and 770: potent antitumor agents from the Caribbean tunicate *Ecteinascidia turbinata*. *J. Org. Chem.* **55**, 4512–4515 (1990).

12. Hou, X., Wang, C., Gerwick, W. H. & Shao, C. European Journal of Medicinal Chemistry Marine natural products as potential anti-tubercular agents. *Eur. J. Med. Chem.* **165**, 273–292 (2019).

13. Thornburg, C. C. *et al.* NCI Program for Natural Product Discovery : A Publicly-Accessible Library of Natural Product Fractions for High-Throughput Screening NCI Program for Natural Product Discovery : A Publicly- Accessible Library of Natural Product Fractions for High- Throughp. *ACS Chem. Biol* (2018). doi:10.1021/acschembio.8b00389

14. Sass, P. Postgenomic strategies in antibacterial drug discovery. *Futur. Microbiol* **5**, 1553–1579 (2010).

15. Collins, L. A., Torrero, M. N. & Franzblau, S. G. Green Fluorescent Protein Reporter Microplate Assay for High-Throughput Screening of Compounds against Mycobacterium tuberculosis. *Antimicrob.Agents Chemother. Table* **42**, 344–347 (1998).

16. Abrahams, G. L. *et al.* Pathway-selective sensitization of *Mycobacterium tuberculosis* for target-based whole-cell screening. *Chem Biol.* **19**, 844–854 (2013).

17. Seleghim, M. H. R., Lira, S. P., Kossuga, M. H., Batista, T., Berlinck, R. G. S., Hajdu, E., Muricy, G., da Rocha, R. M., do Nascimento, G. G. F., Silva, M., Pimenta, E. F., Thiemann, O. H., Oliva, G., Cavalcanti, B. C., Pessoa, C., de Moraes, M. O., Gale, S. Antibiotic, cytotoxic and enzyme inhibitory activity of crude extracts from Brazilian marine invertebrates. *Braz J.*

Pharmacogn. **17**, 287–318 (2007).

18. Wei Xiaomei, Nieves Karinel, R. A. D. Neopetrosiamine A, biologically active bis-piperidine alkaloid from the Caribbean Sea sponge *Neopetrosia proxima*. *Bioorg Med Chem Lett* **20**, 5905–5908 (2010).

19. Arai, M., Yamano, Y., Setiawan, A. & Kobayashi, M. Identification of the Target Protein of Agelasine D , a Marine Sponge Diterpene Alkaloid , as an Anti-dormant Mycobacterial Substance. *ChemBioChem* **35145**, 117–123 (2014).

20. Mangalindan, G. C. *et al.* Agelasine F from a Philippine *Agelas* sp . Sponge Exhibits in vitro Antituberculosis Activity. *Planta Med.* **66**, 364–365 (2000).

21. Kazlauskas, R., Murphy, P. T., Quinn, R. J., Wells, R. J. Heteronemin, a new Scalarin type Sesterterpene from the Sponge *Heteronema erecta*. *Tetrahedron Lett.* 2634 (1976).

22. Bourguet-Kondracki, M. L., Martin, M. T., Debitus, C., Guyot, M. 12-epi-Heteroaemin : New Sesterterpene From Sponge the marine sponge *Hyrtios erecta*. *Tetrahedron Lett.* **35**, 109–110 (1994).

23. Networking, S. M. Perspective Sharing and community curation of mass spectrometry data with Global Natural Products Social Molecular Networking. *Nat Biotechnol* **34**, 828–837 (2016).

24. Thale, Z. *et al.* Bengamides Revisited : New Structures and Antitumor Studies. *J. Org. Chem.* 66, 1733–1741 (2001).

25. Garcí, C. & Sarabia, F. Chemistry and Biology of Bengamides and Bengazoles, Bioactive Natural Products from Jaspis Sponges. *Mar. Drugs* **12**, 1580–1622 (2014).

26. White, K. N., Tenney, K. & Crews, P. The Bengamides: A Mini-Review of Natural Sources, Analogues, Biological Properties, Biosynthetic Origins, and Future Prospects. *J. Nat. Prod.* **80**, 740−755 (2017).

27. Lu, J., Yuan, X., Yuan, H., Wang, W., Wan, B., Franzblau, S. G., Ye, Q. Inhibition of *Mycobacterium tuberculosis* methionine aminopeptidases by bengamide derivatives.

ChemMedChem **6**, 1041–1048 (2012).

28. Lu, J., Yuan, X. & Ye, Q. Structural analysis of inhibition of *Mycobacterium tuberculosis* methionine aminopeptidase by bengamide derivatives. *Eur. J. Med. Chem.* **47**, 479–484 (2012).

29. Quan, D. H. *et al.* Bengamides display potent activity against drug-resistant *Mycobacterium tuberculosis*. *Sci Rep* 1–10 (2019). doi:10.1038/s41598-019-50748-2

30. Holman, J. D. & Tabb, D. L., Mallick, P. Employing ProteoWizard to Convert Raw Mass Spectrometry Data. *Curr Protoc Bioinformatics.* **46**, 918–920 (2015).

31. Otasek, D., Morris, J. H., Bouças, J., Pico, A. R. & Demchak, B. Cytoscape Automation : empowering workflow-based network analysis. *Genome Biol.* 1–15 (2019).

Chapter Four: Isolation and Antimycobacterial activity of New Secondary Metabolites from the South African Marine Actinobacterium, *Streptomyces* strain Muiz4Y

4.1 Introduction

Tuberculosis (TB), which is caused by the rod-shaped Gram-positive bacterium, *Mycobacterium tuberculosis* (Mtb), is the leading cause of death by a single infectious disease.[1] The WHO 2020 Global TB report estimates that 10 million people contracted TB and 1.4 million people died of the disease in 2019.[1] Although there is an effective cure for drug-susceptible TB, the rapid development and emergence of drug resistant strains of Mtb is of great concern and continues to be a public health crisis.[1] Currently, there exist multi-drug resistant, extensively drug resistant and quite recently totally drug resistant strains of Mtb due to patients' non-compliance to treatment regimens as a result of the heavy drug load (four drugs: rifampicin, isoniazid, ethambutol and pyrazinamide) and long duration (a minimum of six months) of treatment.[2,3,4] It takes a longer period (over 24 months) with a different combination of drugs to treat patients infected with resistant strains of Mtb and the chances of curing these patients are lower than in those infected with drug-sensitive strains of Mtb.[1,3] There is therefore an urgent need for the discovery of new potent antimycobacterial drug scaffolds with novel mechanisms of action to completely cure patients infected with Mtb and all its resistant strains.

Natural products remain a key source of drug-like molecules, with microbes serving as an abundant source of bioactive metabolites.[5–7] The actinomycetes, filamentous members of the Gram-positive phylum *Actinobacteria*, have proven to be excellent producers of natural products with high chemical diversity and potent and selective biological activity.[8] Historically, actinomycetes have been an important source of antibiotics including antitubercular compounds. A very good example is the first antitubercular drug streptomycin, which was isolated from the actinobacterium *Streptomyces griseus*. Several other antitubercular compounds, including rifamycin, capreomycin, kanamycin, cycloserine, capuramycin, caprazamycin and thiolactomycin, have been isolated from other actinobacterial species.[9] Less explored biodiversity-rich ecosystems and extreme environments are a promising source of novel

actinobacteria species from which novel secondary metabolites with antitubercular activity could be isolated.

As part of a tuberculosis drug discovery programme focusing on actinomycetes, several actinomycete strains were isolated from plants, soil, and fresh water and marine sediment samples collected from the Western Cape Province of South Africa, which is considered a biodiversity hotspot. The organic extract of a liquid culture of *Streptomyces* strain Muiz4Y exhibited antimycobacterial activity against the non-pathogenic *Mycobacterium aurum* strain A^+ (quickly used as a surrogate for Mtb) and the virulent *Mycobacterium tuberculosis* strain H37Rv. Analysis of this extract by LCMS for dereplication using the Antibase (2017) database, gave no hits for several peaks suggesting the possible presence of new compounds (Figure S4.2).

A bioactivity, spectroscopy and spectrometry guided isolation scheme involving a modified Kupchan solvent partition method, a sequence of column chromatography and reverse phase HPLC, resulted in the isolation of a β-carboline alkaloid, 1-(1,2-dihydroxyethyl)-1,2,3,4-tetrahydro-β-carboline-3-carboxylic acid **4.1**, a peptide, *N*-(2-phenylacetyl)-serine **4.2**, a glycosylated lactone, 4-O-(β-glucopyranosyl)-5-(hydroxymethyl)-3-(4-methylpentyl)-5,6-dihydro-2H-pyran-2-one **4.3**, diketopiperazine 3,6-bis(phenylmethyl)-2,5-piperazinedione **4.4** and 2,4,6-triphenylhex-1-ene **4.5**. The structures were elucidated using 1D and 2D NMR spectroscopic and MS methods, as well as by comparison with relevant literature data. Although compounds **4.4** and **4.5** are known, **4.1**-**4.3** are new natural products. While compounds **4.1**-**4.4** did not show activity below 125 µg/mL, compound **4.5** exhibited antimycobacterial activity against *Mycobacterium tuberculosis* strain H37Rv with an MIC_{90} of 5.8 µg/mL. The isolation of the new tryptoline alkaloid **4.1** is an interesting discovery as very few alkaloids with a tryptoline core have been isolated from *Streptomyces* species except for BE-54017 (**4.6**) and the cladoniamides (A-G (**4.7-4.13**)) although β-Carboline alkaloids have been isolated from higher plants, marine invertebrates, fungi and some actinomycetes.[10–12] We have therefore proposed a biosynthetic pathway for compound **4.1** based on preliminary experiments and some precedents.[13]

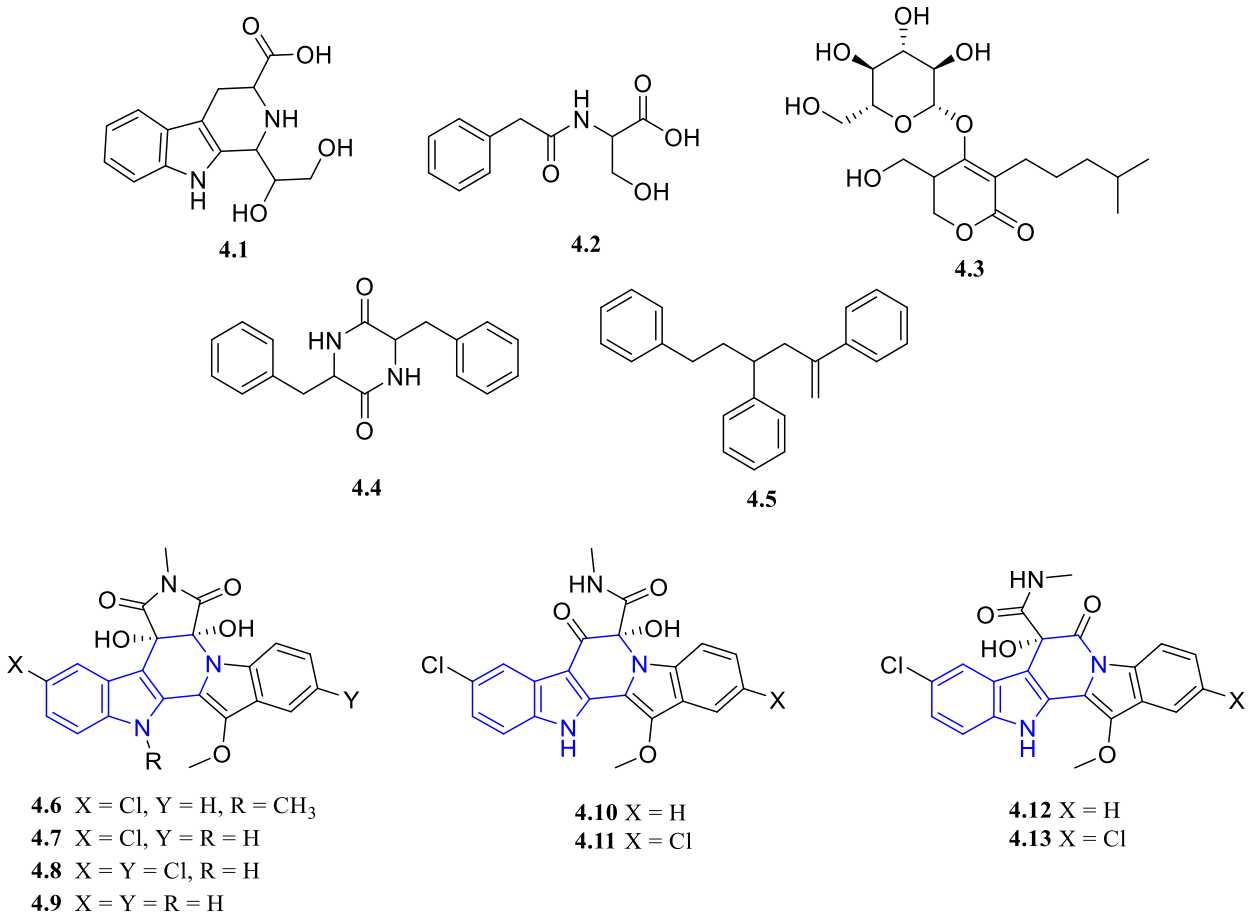

Figure 4.1: Structures of isolated metabolites **4.1-4.5** from *Streptomyces* strain Muiz4Y and compounds with tryptoline core including BE-54017 **4.6** and cladoniamide A-G (**4.7**-**4.13**) isolated from *Streptomyces* species.

4.2 Results and Discussion

4.2.1 Sediment Sample Collection

South Africa is endowed with biodiversity rich ecosystems both in the marine and terrestrial environment. False Bay, located in the Western Cape Province of South Africa, is rich in diverse marine fauna and flora. Sediments were collected from the False Bay coastline between Muizenberg and St. James in Cape Town, South Africa. *Streptomyces* strain Muiz4Y was isolated from one of the sediment samples.

4.2.2 Taxonomy of Strain

The closest phylogenetic relatives of strain Muiz4Y, based on pairwise 16S rRNA gene sequence similarities, were the type strains of *Streptomyces hygroscopicus* subsp. *glebosus* (100%), *Streptomyces libani* subsp. *rufus* (100%), *Streptomyces platensis* (99.9%), *Streptomyces caniferus* (99.9%), *Streptomyces nigrescens* (99.7%) and *Streptomyces libani* subsp. *libani* (99.7%).

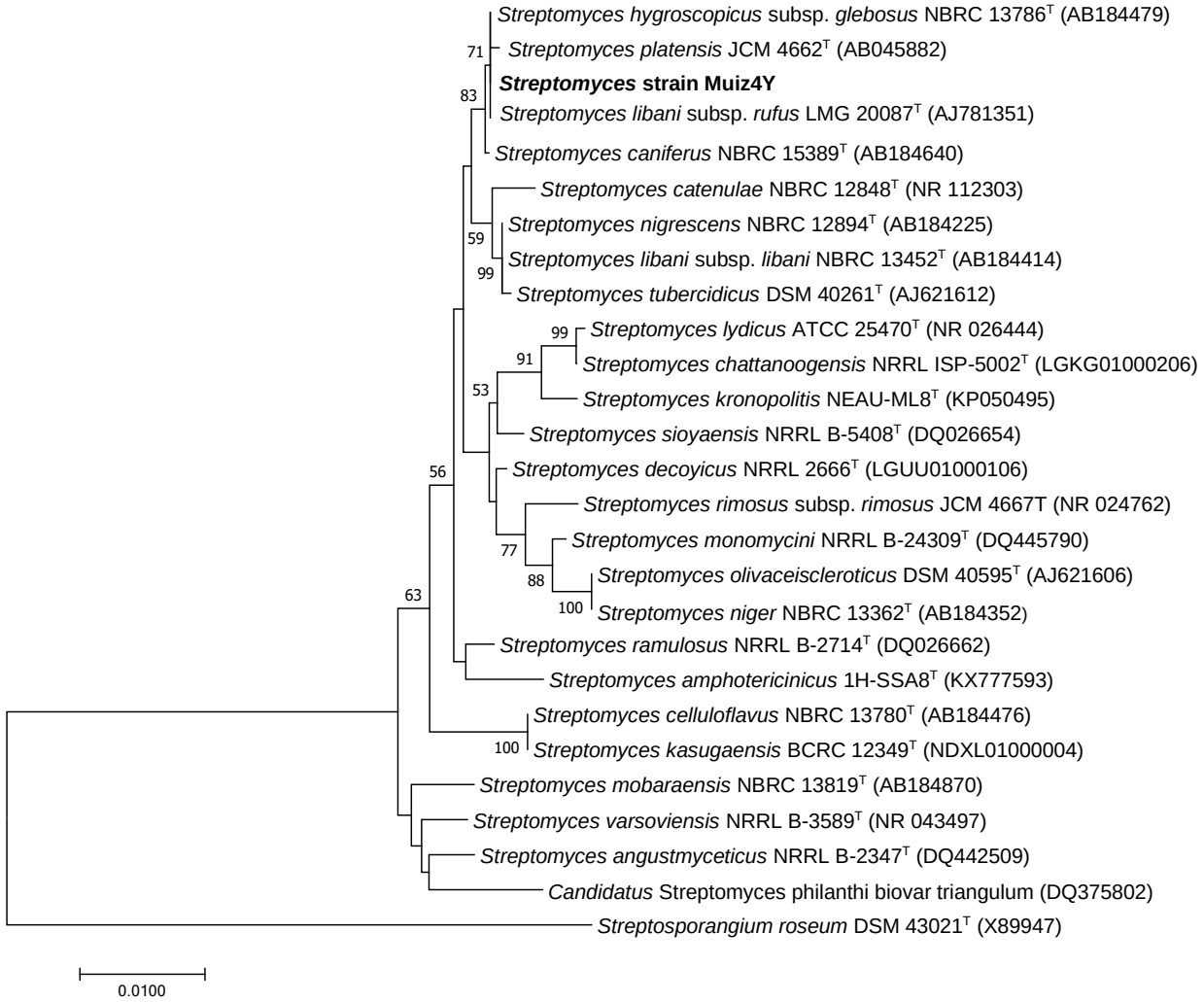

Figure 4.2: Neighbour-joining 16S rRNA gene phylogenetic tree showing the position of strain Muiz4Y amongst its closest relatives in the genus *Streptomyces*. The tree is based on 1428 nucleotides of common sequence. The bootstrap values are based on 1000 resampled datasets and only values ≥50% are shown. The scale bar represents 1 nt substitution per 100 nt. *Streptosporangium roseum* strain DSM 43021T was used as the outgroup.

A neighbour-joining phylogenetic tree, based on 16S rRNA gene sequences (Figure 4.2) showed that strain Muiz4Y clustered with the type strains of *S. hygroscopicus* subsp. *glebosus*, *S. platensis*, *S. libani* subsp. *rufus* and *S. caniferus* with moderate bootstrap support (83%).

4.2.3 Structure Elucidation

The structure of the known compounds, 3,6-dibenzyl-2,5-piperazinedione **4.4** and 2,4,6-triphenylhex-1-ene **4.5** were determined by analyses of their 1D and 2D NMR and HRESIMS data (Figure S4.6 and S4.24-S4.33) as well as comparison with that of literature.[14, 15,16]

Compound **4.1** was isolated as a white amorphous solid. The HRESIMS of this compound gave a molecular peak at m/z = 277.1190 $[M + H]^+$, Δ = 1.756 ppm and its sodium adduct at 299.1007 $[M + Na]^+$, which signified a molecular formula of $C_{14}H_{16}N_2O_4$ with eight degrees of unsaturation. Analysis of the ^1H, ^{13}C and multiplicity edited HSQC NMR spectra suggested the presence of five quaternary, seven methine, two methylene and no methyl carbons. The ^{13}C-NMR spectrum indicated the presence of 14 non-equivalent carbons including characteristic signals which supported the presence of a carboxylic acid (δ_C 172.8), eight aromatic carbons (δ_C 136.1, 132.6, 126.5, 120.7, 118.3, 117.3, 111.2 and 107.8) and four deshielded, sp^3 hybridized carbons (70.5, 62.9, 56.7, 54.6) that suggested attachment to O and N atoms. The presence of four aromatic protons at δ_H 7.42 (1H, d, *J* = 7.8 Hz, H-5), 6.98 (1H, t, *J* = 7.4, 7.4 Hz, H-6), 7.06 (1H, t, *J* = 7.5, 7.5 Hz, H-7) and 7.42 (1H, d, *J* = 8.0 Hz, H-8) confirmed the existence of a 1,2-disubstituted benzene ring and this was further confirmed by correlations in the HMBC spectrum from C-8a to H-8 and H-7, and C-4b to H-5 and H-6. The benzene ring was extended to an indole ring as inspection of the HMBC showed correlations from C-4a to H-5 and HN, C-9a to HN, C-8a to HN and C-4b to HN. The proton and carbon chemical shifts at positions 1' (δ_C 70.5, δ_H 4.18) and 2' (δ_C 62.9, δ_H 3.60, 3.54) suggested attachment to hydroxyl groups, and those in position 1 (δ_C 54.7, δ_H 4.43) suggested it was attached to an NH. These peaks formed a spin system as inspection of the COSY showed correlations between H-2'/H-1' and H-1'/H-1 (shown in Figure 4.3 below). The methine at C-1 of this moiety was attached to the indole ring at 9a as inspection of the HMBC showed correlations from C-9a to H-1 and H-1', and C-4a to H-1. The correlation in the COSY spectrum between H-3 and H-4 gave another spin system. The carboxylic acid carbon C-3' was attached to

C-3 of this moiety as there are HMBC correlations from C-3' to H-3 and H-4. This substructure was linked to the rest of the structure to form a tetrahydro-β-carboline (tryptoline) core, as the HMBC spectrum showed correlations from C-1 to H-3. This structure was consistent with the molecular formula and the degree of unsaturation derived from HRESIMS data. Although there is a report of synthesis of this compound, this is the first time it has been ever isolated from nature.[17] This compound is the saturated analogue (ring C) of dichotomine B **4.14**, isolated from the Chinese plant *Stellaria dichotoma* L. var. *lanceolata* Bge.[18]

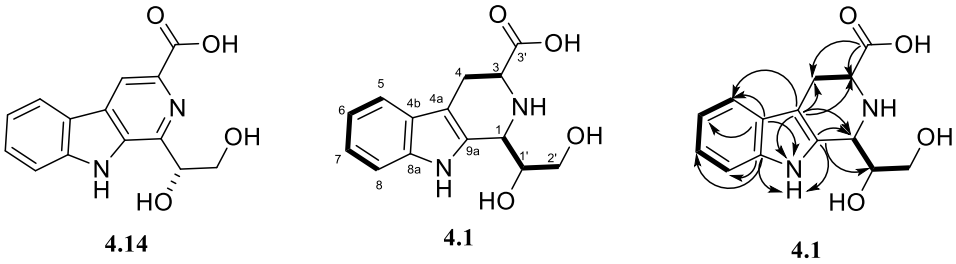

Figure 4.3: Dichotomine B **14** and **4.1** with COSY (▬) and key HMBC (→) correlations.

Table 4.1: ^{1}H, ^{13}C NMR data of **4.1** in DMSO. δ in ppm, *J* in Hz.

Position	^{13}C	^{1}H mult (J, Hz)
1	54.7, CH	4.43, m
2-N		
3	56.7, CH	3.62, m
4	24.6, CH_2	3.04, dd (3.7, 14.7) 2.69, m
4a	107.8, C	
4b	126.5, C	
5	117.3, CH	7.42, d (7. 8)
6	118.3, CH	6.98, t (7.4, 7.4)
7	120.7, CH	7.06, t (7.5, 7.5)
8	111.2, CH	7.36, d (8.0)
8a	136.1, C	
9-N		10.69, s
9a	132.6, C	
1'	70.5, CH	4.18 dd, (4.0, 7. 7)
2'	62.9, CH_2	3.60, m 3.54, dd (5. 5, 10.8)
3'	172.6, C	

Compound **4.2** was isolated as a white amorphous solid. The HRESIMS of this compound gave a molecular ion peak at m/z = 224.0922 $[M + H]^+$, Δ = 0.739 ppm, which signified a molecular formula of $C_{11}H_{13}NO_4$ and corresponded to six degrees of unsaturation. Analysis of the ^1H, ^{13}C and multiplicity edited HSQC spectra suggested the presence of three quaternary, six methine, two methylene and no methyl carbons. The methines with the ^{13}C chemical shifts 129.5, 128.6, 126.7 were found in the aromatic region and the corresponding protons of two of the carbons (δ_C 129.5, 128.6) integrated for 2 protons (H-5'/7' and H-4'/8') each. Inspection of the COSY spectrum showed correlations between the aromatic protons and this confirmed a mono-substituted benzene ring system. The benzene ring was extended into a benzyl as the methylene protons (H-2') correlated to the quaternary aromatic carbon C-3' and methine aromatic carbon C-4'/8' in the HMBC spectrum (as shown in Figure 4.4 below). Again, the HMBC spectrum showed correlations from the amide carbonyl carbon C-1' to the methylene protons (H-2') to establish a phenylacetyl moiety. Another spin system was observed as inspection of the COSY spectrum showed correlations between H-2, H-3 and HN. A carboxylic acid was attached to this moiety as HMBC spectrum showed correlations between the carboxylic acid carbon C-1 and the protons H-2, H-3 and HN to form serine. The phenylacetyl and serine moieties were linked together by an amide bond between the carbonyl C-1' of the phenylacetyl moiety and the NH of the serine to give *N*-(2-phenylacetyl)-serine **4.2**. This was confirmed by peaks from the phenylacetyl carbonyl carbon C-1' to serine protons HN, H-2. This is the first report of isolation of **4.2**, although the synthesis has been reported.[19]

Figure 4.4: Compound **4.2** with COSY (▬) and key HMBC (→) correlations.

Table 4.2: ^{1}H, ^{13}C NMR data of compound **4.2** in DMSO. δ in ppm, *J* in Hz.

Position	^{13}C	^{1}H mult (J, Hz)
1	172.5, C	
2	55.1, CH	4.25, dt (4.9, 4.9, 7.9)
3	61.9, CH_2	3.70, dd (5.3, 10.8) 3.61, m
4-N		8.18, d (7.8)
1'	170.7, C	
2'	42.3, CH_2	3.52, s
3'	136.8, C	
4'/8'	128.6, CH	7.29, m
5'/7'	129.5, CH	7.28, m
6'	126.7, CH	7.21, m

Compound **4.3** was isolated as a yellow amorphous solid. The HRESIMS of this compound gave a molecular ion peak at m/z = 391.1964 $[M + H]^+$, Δ = 0.151 ppm, which signified a molecular formula of $C_{18}H_{30}O_9$ and corresponded to four degrees of unsaturation.

Analysis of the ^{1}H, ^{13}C and multiplicity edited HSQC spectra suggested the presence of three quaternary, seven methine, six methylene and two methyl carbons. The ^{13}C NMR spectrum showed several peaks between 60 and 99 ppm, which suggested the presence of a sugar moiety. Inspection of the COSY NMR spectrum confirmed this, as there were correlations between the anomeric proton H-1' and H-2', H-2' and H-3', H-3' and H-4', H-4' and H-5', and H-5' and H-6' as shown in Figure 4.5 below. This was further confirmed by 1D TOCSY (H-1' to H-6') and 2D HSQC-TOCSY (H1'/C1' to C6') as shown in Figures S4.22 and S4.23 in supplementary material. It was difficult to determine the stereochemistry of the glucosyl moiety using its H-coupling constants because most of the ^{1}H NMR signals were overlapping. The sugar was therefore labelled as β-glucose, as the ^{13}C chemical shifts were consistent with the literature data for this diastereomer.[20] Another spin system was established from the COSY NMR spectrum, which showed correlations between H-7 and H-8, H-8 and H-9, and H-9 and H-10, and the methine H-10 also correlated with both H-11 and H-12 to form an isopentyl moiety. The isopentyl moiety was attached to the quaternary carbon C-2 (δ_C 105.3) and this carbon formed a double bond with the quaternary carbon at C-3 (δ_C 169.8). This was confirmed by correlations from C-2 to H-7 then C-3 to H-7 and H-8 as shown in the HMBC spectrum (Figure S4.21). The ^{1}H and ^{13}C NMR chemical

shift of H-5 (δ_C 68.0, δ_H 4.27/4.30) and H-6 (δ_C 61.9, δ_H 3.82) suggested attachment to alkoxy and hydroxyl groups respectively. Inspection of the COSY NMR spectrum showed correlation between H-5 and H-4, as well as H-4 and H-6. The carbonyl group was linked through an O to C-5 to form a lactone, as HMBC spectra showed correlations from C-1 to H-4 and H-5. The methine at position 4 was attached to the quaternary carbon at C-3 (δ_C 169.8) and the carbonyl carbon of the lactone was also attached to the quaternary carbon C-2 (δ_C 105.3) in the cyclic lactone ring. This was established by correlations from C-2 to H-4, H-5 and H-6, as well as C-3 to H-4 as shown in the HMBC spectrum. The anomeric oxygen was attached to the lactone ring at position 3, as the HMBC spectrum showed correlations from C-3 to H-1' to form 4-O-(β-glucopyranosyl)-5-(hydroxymethyl)-3-(4-methylpentyl)-5,6-dihydro-2H-pyran-2-one.

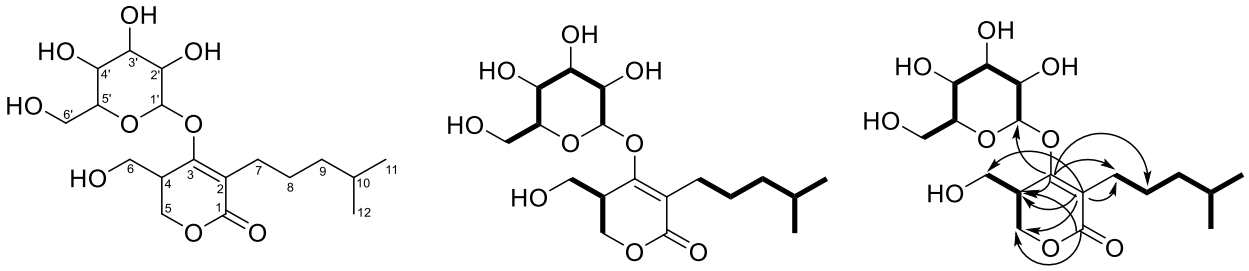

Figure 4.5: Selected COSY (—) and HMBC (→) data for compound **4.3**.

Table 4. 3: ^{1}H, ^{13}C NMR data of compound **4.3** in CD_3OD. δ in ppm, *J* in Hz.

Position	^{13}C	^{1}H mult (J, Hz)
1	172.6, C	
2	105.3, C	
3	169.8, C	
4	40.9, CH	3.43, m
5	68.0, CH_2	4.30, m 4.27, m
6	61.9, CH_2	3.82, dd (3.9, 10.7) 3.54, m
7	25.9, CH_2	3.12, m 2.76, m
8	25.9, CH_2	1.62, m
9	38.4, CH_2	1.31, dd (7.3, 14.7)
10	27.4, CH	1.60, m
11	21.6, CH_3	0.92, d (8.1)
12	21.5, CH_3	0.92, d (8.1)
1'	98.1, CH	5.01, d (7.4)
2'	73.4, CH	3.40, m
3'	76.7, CH	3.45, m
4'	69.7, CH	3.38, m
5'	77.2, CH	3.37, m
6'	60.9, CH_2	3.87, d (11.9) 3.70, d (9.54)

4.2.4 Biosynthesis of compound **4.1**

Based on the structure of **4.1** and the previous knowledge of the biosynthesis of bacterial β-carboline alkaloids[12,21], we speculate that **4.1** may have a similar biosynthetic machinery as marinacarbolines, of which the cyclization of β-carboline core is proposed to be catalysed by a new Pictet-Spengler (PS) enzyme, McbB.[12] It is proposed that McbB homologue in *Streptomyces* strain Muiz4Y will catalyse the PS reaction between tryptophan **4.15** and glyceraldehyde **4.16** to generate the imine intermediate **4.17**, followed by reduction to the amine product **4.1**.

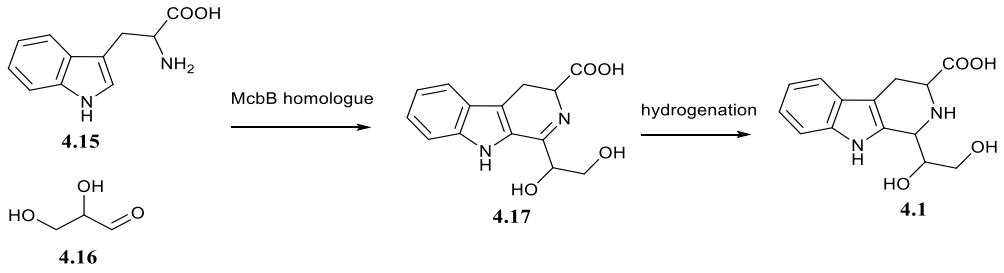

Figure 4.6: Proposed biosynthetic pathway of compound **4.1**

4.2.5 Antimycobacterial activity

Compounds **4.1**- **4.5** were screened for their *in vitro* inhibitory activity against *M. tuberculosis* strain H37Rv. Rifampicin was used as a reference standard and the minimum inhibitory concentration (MIC) was recorded. As shown in Table 4.4 below, all the compounds except compound **4.5**, showed very weak activity against *Mycobacterium tuberculosis* strain H37Rv. Compound **4.5** was active with an MIC_{90} of 5.8 µg/mL.

Table 4.4: Antimycobacterial activity of compounds **4.1**-**4.5** against *M. tuberculosis* strain H37Rv

Compound	MIC_{90} (µg/mL)
4.1	>125
4.2	>125
4.3	>125
4.4	>125
4.5	5.8
Rifampicin	0.002

4.3 Experimental

4.3.1 General experimental procedure

NMR spectra were obtained on a BRUKER Ascend 600 (Bruker, Billerica, MA, USA) Prodigy cryoprobe at 600 MHz and 150 MHz for ^{1}H and ^{13}C nuclei, respectively. DMSO-d_6 (δ_H 2.50, δ_C 39.7) was used for **4.1**, **4.2** and **4.4**, CD_3OD (δ_H 3.30, δ_C 49.0) for **4.3** and $CDCl_3$ (δ_H 7.25, δ_C 77.0) for **4.5**. High resolution mass spectrometric data were obtained using a Thermo Instruments MS system (LTQ XL/LTQ Orbitrap Discovery, Thermo Scientific, Bremen, Germany) coupled to a Thermo Instruments HPLC system (Accela PDA detector, Accela PDA autosampler and Accela pump). The following conditions were used: capillary voltage 45 V, capillary temperature 260 °C, auxillary gas flow rate 10–20 arbitrary units, sheath gas flow rate 40–50 arbitrary units, spray voltage 4.5 kV, mass range 100–2000 amu (maximum resolution 30,000). HPLC separations were carried out using Reverse phase Phenomenex Luna C18(2) (10µm, 250 x 10 mm) column connected to an Agilent Technologies 1200 series HPLC system equipped with an Agilent Technologies 1200 series quad pump and Agilent Technologies 1200 series DAD. Diaion HP-20 was obtained from Supelco, Bellefonte, USA. All solvents used throughout were HPLC-grade and

purchased from both Merck and Sigma-Aldrich. Sephadex LH-20 (25–100 µm) was purchased from GE Healthcare Bio-Sciences (Uppsala, Sweden). Column chromatography was carried out on silica gel 60 (Fluka 70–230 mesh, 63–200 µm, (Sigma-Aldrich, Buchs, Switzerland)), and preparative TLC on silica gel 60 Analtech GF_{254} (20 × 20 cm, 2000 µm, Analtech Inc., Newark, DE, USA). Analytical TLC were performed on Merck silica gel 60 F_{254} (Merck KGaA, Darmstadt, Germany) and silica gel 60 RP-18 F_{254} plates and bands were visualized by heating after staining with ceric ammonium sulfate reagent.

4.3.2 Isolation of species and screening

Streptomyces strain Muiz4Y was isolated from a marine sediment collected along the False Bay coastline between Muizenberg and St. James in Cape Town, South Africa.[22] The sediment sample was collected in sterile glass universals at a depth of about 5 cm below the sediment surface under 30 cm of sea water.[22] The sample was stored at 4 °C and processed within 24 hours of collection. Exactly 200 g of the sediment sample was added to 750 mL distilled water and autoclaved.[22] The autoclaved mixture was left on the bench for the sediment to settle. The supernatant was poured off, stored in a sterile container at 4 °C and used to supplement the media. The media used to culture the species was yeast extract-malt extract agar (ISP2 or YEME) which was prepared by weighing 4 g yeast extract, 10 g malt extract, 4 g d-glucose and 20 g agar in 1 L distilled water supplemented with 250 mL of the supernatant from the autoclaved water sediment mixture at a pH of 7.3.[22] The YEME agar medium was supplemented with 50 µg/mL cycloheximide and 10 µg/mL nalidixic acid to inhibit the growth of fungi and Gram-negative bacteria, respectively.[22] Approximately 0.1 g untreated sediment was added to 1 mL of sterile distilled water and vortexed for 1 min. The sample was serially diluted to 10^{-1}, 10^{-2} and 10^{-3} of the original volume in sterile distilled water and 100 µl of each dilution was spread-plated on YEME agar plates.[22] All isolation plates were incubated at 30 °C for up to 21 days. Different colonies were observed and actinobacteria were selected based on their colony morphologies.[22] Selected isolates were sub-cultured onto YEME agar plates without antibiotics using sterile toothpick and were incubated for 7 days at 30 °C.[22] Stock cultures of pure isolates were stored at -70 °C in 20% (v/v) glycerol. Pure isolates were cultured in 50 mL volumes of YEME broth (4 g yeast extract, 10 g malt extract, 4 g d-glucose in 1 L distilled water at a pH of 7.3) in 500 mL

Erlenmeyer flask at 30 °C with continuous shaking at 200 rpm for 4 days. The broth was filtered using glass wool. The aqueous culture broth was solvent partitioned with an equal volume of ethyl acetate and the cell mass was extracted with methanol. The methanol and ethyl acetate extracts were combined and dried under vacuum. The combined extract was screened against *M. aurum* A+ and *M. tuberculosis* H37Rv and subjected to HPLC/HRESIMS analysis. The extract was active against *M. aurum* A+ and *M. tuberculosis* H37Rv. Analysis of the HPLC/HRESIMS results revealed that some peaks including that with m/z 277.1187, 224.0922 and 390.1964 $[M + H]^+$ (Figure S4.2 in supplementary data) did not result in any relevant hits when the masses were entered as independent queries in the Natural Products Identifier AntiBase 2017 software to check whether these molecules were novel.

4.3.3 Phylogenetic analysis

Genomic DNA was extracted using the modified method of Everest et al. (2011)[23] and the 16S rRNA gene was amplified as described by Cook and Meyers (2003)[24]. The PCR product was purified using an ISOLATE II PCR and Gel Kit (Bioline, London, United Kingdom), sequenced by Macrogen Europe (Amsterdam, The Netherlands) and the sequences were assembled using DNAMAN version 5.2.9 (Lynnon BioSoft). The 16S rRNA gene sequence similarities between strain Muiz4Y and its closest phylogenetic relatives were calculated using the EzBioCloud server. [25] Sequences for phylogenetic analysis were aligned using Muscle [26] and all columns with missing data were deleted from the alignment to leave 1428nt of sequence common to all strains. A phylogenetic tree was constructed using the neighbour-joining method in MEGA version 7 [27], with Kimura's 2-parameter model used as the substitution model[28]. The robustness of the tree topology was assessed using the bootstrap method [29] with 1000 replicates.

4.3.4 Large scale fermentation

A stock culture of *Streptomyces* strain Muiz4Y (maintained in YEME with 20% (v/v) glycerol) was thawed, vortexed and inoculated into a 15 mL YEME broth in a 250 mL Erlenmeyer flask. After 4 days of incubation, the entire culture was inoculated into a 50 mL YEME broth in a 500 mL Erlenmeyer flask. This culture was incubated for 3 days and subsequently inoculated into 3 X 100 mL YEME broth in 1000 mL Erlenmeyer flasks and were incubated for another 4 days. Each 100

mL culture was then inoculated into a 1000 mL YEME broth in a 5000 mL Erlenmeyer flask and incubated for 18 days. Diaion HP-20 resin (50 g/L) was added under sterile conditions to the flasks after 18 days of culture and returned to the incubator for 6 hrs with shaking at 200 rpm. All incubations were done at 30 °C with continuous shaking at 200 rpm. At every stage, before sub-culture, the broth was checked for contamination by inoculating on an agar plate and Gram staining. The final, 3 L cultures were harvested and filtered under pressure using a piece of glass wool placed in a Buchner funnel. The filtrate was partitioned in a separating funnel with an equal volume of ethyl acetate. The cell mass mixed with Diaion HP-20 resin with adsorbed organics was extracted with methanol 3 X, then ethyl acetate 3 X and dichloromethane 3 X. All the organic extracts were combined and concentrated under reduced pressure to give 3.89 g of total crude extract (TCE).

4.3.5 Extraction, Isolation and Purification of compounds

The crude extract was suspended in 50 mL of distilled water and extracted three times with 50 mL of dichloromethane. The water layer was then extracted with the same volume of 2-butanol. The 2-butanol layer was also concentrated under reduced pressure, transferred into a vial and labelled as WB (591 mg). The dichloromethane extract was concentrated under reduced pressure, reconstituted in 50 mL 9:1 methanol water and extracted with an equal volume of hexane three times. The hexane fractions were combined and concentrated under reduced pressure, transferred into a vial and labelled as FH (125.8 mg). The polarity of the 9:1 methanol water fraction was adjusted to 1:1 and extracted with dichloromethane three times. The dichloromethane and 1:1 methanol water fractions were subsequently concentrated under reduced pressure, transferred into vials and labelled as FD (76.8 mg) and FM (32.9 mg) respectively. Fractions FH, FD, FM and WB were screen against *M. aurum* A+ and *M. tuberculosis* H37Rv; and subjected to HPLC/HRESIMS analysis. WB was subjected to size- exclusion column chromatography with Sephadex LH-20 and 1:1 methanol/dichloromethane mobile phase to yield eight fractions. Fraction 3 was subjected to a reverse phase HPLC separation and purification using a Phenomenex Luna C18 column (10µm, 250 x 10 mm, L × i.d.). Gradients of H_2O: MeOH (100% H_2O to 100% MeOH in 35 min) were used as eluent with a column flow rate set at 1.5 mL/min to afford compounds **4.1** (3.6 mg), **4.2** (4.2 mg) and **4.3** (3.0 mg). FD was also fractionated

using size- exclusion column chromatography with Sephadex LH-20 and 1:1 methanol/dichloromethane as the mobile phase. Nine fractions were collected. A solid precipitated out of fraction 6 and this was triturated with methanol to yield compound **4.4** (0.6 mg). FH was subjected to normal phase column chromatography with increasing polarity using a mixture of hexane/dichloromethane/ethyl acetate from 1:0 hexane/dichloromethane to 0:1 hexane/dichloromethane then from 1:0 dichloromethane/ethyl acetate to 0:1 dichloromethane/ethyl to afford compound **4.5** (2.4 mg).

1-(1,2-dihydroxyethyl)-1,2,3,4-tetrahydro-β-carboline-3-carboxylic acid **4.1**: pale yellow amorphous solid; UV (CH_3OH /0.1%HCOOH) 224, 272 nm; ^1H, ^{13}C NMR data, see Table 4.1; HRESIMS (positive mode) m/z 277.1183 $[M + H]^+$ and 299.1008 $[M + Na]^+$ Δ 1.756 ppm; calcd. for $C_{14}H_{16}N_2O_4$.

N-(2-phenylacetyl)-serine **4.2**: white amorphous solid; UV (CH_3OH /0.1%HCOOH) 226 nm; ^1H, ^{13}C NMR data, see Table 4.2; HRESIMS (positive mode) m/z 224.0922 $[M + H]^+$ and 246.0739 $[M + Na]^+$ Δ 0.739 ppm; calcd. for $C_{11}H_{13}NO_4$.

4-O-(β-glucopyranosyl)-5-(hydroxymethyl)-3-(4-methylpentyl)-5,6-dihydro-2H-pyran-2-one **4.3**: yellow amorphous solid; UV (CH_3OH /0.1%HCOOH) 226 nm; For 1H, 13C NMR data, see Table 4.3; HRESIMS (positive mode) m/z 391.1964 $[M + H]^+$ Δ 0.151 ppm; calcd. for $C_{18}H_{31}O_9$

3,6-dibenzyl-2,5-piperazinedione **4.4**: white amorphous solid; UV (CH_3OH /0.1%HCOOH) 230, 278 nm; ^1H, ^{13}C NMR data, see Figures S4.24 and S4.25; HRESIMS (positive mode) m/z 295.14483 $[M + H]^+$ and 317.1263 $[M + Na]^+$ Δ 1.036 ppm; calcd. for $C_{18}H_{18}N_2O_2$.

2,4,6-triphenalhex-1-ene **4.5**: colorless oil; ^1H, ^{13}C NMR data, see Figure S4.29 and S4.30; HRESIMS (positive mode) m/z 312.1862 $[M + H]^+$ Δ -1.032 ppm; calcd. for $C_{24}H_{24}$.

4.3.6 Antimycobacterial activity

The combined crude extracts and the isolated compounds were dissolved in DMSO and their minimum inhibition concentration against *M. tuberculosis* strain H37Rv was determined using the standard broth micro dilution method.[30] The lowest concentration of drug that inhibited

growth of more than 90% of the bacterial population was considered the MIC_{90}. Rifampicin was used as a reference standard.

4.4 Conclusion

In our quest to isolate novel antitubercular compounds from a South African actinomycete, we isolated three new natural products, 1-(1,2-dihydroxyethyl)-1,2,3,4-tetrahydro-β-carboline-3-carboxylic acid **4.1**, *N*-(2-phenylacetyl)-Serine **4.2**, 4-*O*-(β-glucopyranosyl)-5-(hydroxymethyl)-3-(4-methylpentyl)-5,6-dihydro-2H-pyran-2-one **4.3** alongside the known 3,6-bis(phenylmethyl)-2,5-piperazinedione **4.4** and 2,4,6-triphenalhex-1-ene **4.5** from *Streptomyces* strain Muiz4Y. This is an interesting discovery as very few alkaloids with a tryptoline core (**4.1**) have been isolated from the genus *Streptomyces*. The isolated compounds exhibited *in vitro* inhibitory activity against *Mycobacterium tuberculosis* strain H37Rv. Compounds **4.1**-**4.4** showed weak activity with MIC_{90}s of above 125 µg/mL, while compound **4.5** was active with an MIC_{90} of 5.8 µg/mL. This is the first report of antitubercular activity of **4.5**.

4.5 References

1. *WHO.Global Tuberculosis Report 2020*.
2. Nguta, J. M., Appiah-Opong, R., Nyarko, A. K., Yeboah-Manu, D. & Addo, P. G. A. Current perspectives in drug discovery against tuberculosis from natural products. *Int. J. Mycobacteriology* **4**, 165–183 (2015).
3. Riccardi, G. & Pasca, M. R. Trends in discovery of new drugs for tuberculosis therapy. *J. Antibiot. (Tokyo).* 655–659 (2014). doi:10.1038/ja.2014.109
4. Blanco, D., Perez-Herran, E., Cacho, M., Ballell, L., Castro, J., Del Río, R. G., Lavandera, J. L., Remuiñán, M. J., Richards, C., Rullas, J., Vázquez-muñiz, M. J. & Woldu, E. Mycobacterium tuberculosis Gyrase Inhibitors as a New Class of Antitubercular Drugs. *Antimicrob Agents Chemother* **59**, 1868–1875 (2015).
5. Cragg, G. M. & Newman, D. J. Natural Products: A Continuing Source of Novel Drug Leads. *Biochim Biophys Acta* **1830**, 3670–3695 (2013).

6. Katz, L. & Baltz, R. H. Natural product discovery: past, present, and future. *J. Ind. Microbiol. Biotechnol.* **43**, 155–176 (2016).

7. Bérdy, J. Bioactive microbial metabolites. *J. Antibiot. (Tokyo).* **58**, 1–26 (2005).

8. Raja, A., Prabakarana, P. Actinomycetes and Drug-An Overview. *Am. J. Drug Discov. Dev.* **1**, 75–84 (2011).

9. Ashforth, E. J. *et al.* Bioprospecting for antituberculosis leads from microbial metabolites. *Nat. Prod. Rep.* **27**, 1709–1719 (2010).

10. Nakase K, et al. Antitumor substance BE-54017 and its production. (2000).

11. Williams, D. E. *et al.* Cladoniamides A - G , Tryptophan-Derived Alkaloids Produced in Culture by Streptomyces uncialis. *Org. Lett.* **10**, 3501–3504 (2008).

12. Chen, Q. *et al.* Discovery of McbB , an Enzyme Catalyzing the b -Carboline Skeleton Construction in the Marinacarboline Biosynthetic Pathway **. *Angew. Chem. Int. Ed.* **52**, 9980–9984 (2013).

13. Sahashi, S. *et al.* Structural Basis for b -Carboline Alkaloid Production by the Microbial Homodimeric Enzyme McbB Article Structural Basis for b -Carboline Alkaloid Production by the Microbial Homodimeric Enzyme McbB. *Chem. Biol.* **22**, 898–906 (2015).

14. Zhang, H. *et al.* Protective e ff ects of diketopiperazines from Moslae Herba against in fl uenza A virus-induced pulmonary in fl ammation via inhibition of viral replication and platelets aggregation. *J. Ethnopharmacol.* **215**, 156–166 (2018).

15. Ellis, G. A., Wyche, T. P., Fry, C. G., Braun, D. R. & Bugni, T. S. Solwaric Acids A and B, Antibacterial Aromatic Acids from a Marine Solwaraspora sp. *Mar. Drugs* **12**, 1013–1022 (2014).

16. Ayer, W. A., Muir, D. J. & Chakravarty, P. Phenolic and Other Metabolites of Phellinus Pini , A Fungus Pathogenic to Pine. *Phytochemistry* **42**, 1321–1324 (1996).

17. Ronner, B. *et al.* Formation of Tetrahydro- -carbolines and -Carbolines during the Reaction

of L -Tryptophan with D -Glucose. *J. Agric. Food Chem.* **48**, 2111−2116 (2000).

18. Sun, B. *et al.* Structures of New -Carboline-Type Alkaloids with Antiallergic Effects from. *J. Nat. Prod* **67**, 1464–1469 (2004).

19. Carboni, C. *et al.* Preparation of D -amino acids by enzymatic kinetic resolution using a mutant of penicillin-G acylase from E . coli. *Tetrahedron: Asymmetry* **17**, 245–251 (2006).

20. Jansson, P., Kenne, L., Wildamin, G. Computer-assisted structural analysis of polysaccharides with an extended version of casper using 'H- and 13C- N.M.R. data*. *Carbohydr. Res.* **188**, 169–191 (1989).

21. Tanner, M. E. Increasing the Diversity of Known Pictet-Spenglerases. *Chem. Biol.* **22**, 806–807 (2015).

22. Kirby, B. M. Ph.D. Thesis,. University of Cape Town, 2007.

23. Everest, G. J., Cook, A. E., Kirby, B. M. & Meyers, P. R. Evaluation of the use of recN sequence analysis in the phylogeny of the genus Amycolatopsis. *Antonie Van Leeuwenhoek* **100**, 483–496 (2011).

24. Cook, A. E. & Meyers, P. R. Rapid identification of filamentous actinomycetes to the genus level using genus-specific 16S rRNA gene restriction fragment patterns Printed in Great Britain. *Int. J. Syst. Evol. Microbiol.* **53**, 1907–1915 (2003).

25. Yoon, S. *et al.* Introducing EzBioCloud : a taxonomically united database of 16S rRNA gene sequences and whole-genome assemblies. *Int J Syst Evol Microbiol* **67**, 1613–1617 (2017).

26. Edgar, R. C., Drive, R. M. & Valley, M. MUSCLE : multiple sequence alignment with high accuracy and high throughput. *Nucleic Acids Res.* **32**, 1792–1797 (2004).

27. Kumar, S., Stecher, G. & Tamura, K. MEGA7 : Molecular Evolutionary Genetics Analysis Version 7.0 for Bigger Datasets. *Mol. Biol. Evol.* **33**, 1870–1874 (2016).

28. Kimura, M. A Simple Method for Estimating Evolutionary Rates of Base Substitutions Through Comparative Studies of Nucleotide Sequences. *J. Mol. Evol.* **16**, 111–120 (1980).

29. Felsenstein, J. Confidence limits on phylogenies: an approach using the bootstrap. *Evolution (N. Y).* **39**, 783–791 (1985).

30. Id, M. G. *et al.* Cinnamoyl-Oxaborole Amides : Synthesis and Their in Vitro Biological Activity. *Molecules* **23**, 1–13 (2018).

Chapter Five: Novel South African Rare Actinomycete *Kribbella speibonae* Strain SK5: A Prolific Producer of Hydroxamate Siderophores including New Dehydroxylated Congeners

First author: Acquah, K. S.: 1 Conceptualization. 2) methodology. 3) investigation. 4) formal analysis. 5) data curation. 6) writing—original draft preparation.

Contributions: Beukes, D. R.: 1) Conceptualization. 2) methodology. 3) writing—review and editing. 4) supervision.

Warner, D. F.: 1) methodology. 2) writing—review and editing. 3) supervision.

Meyers, P. R.: 1) Conceptualization. 2) methodology. 3) resources 4) writing—review and editing. 5) supervision.

Sunassee, S. N.: 1) Conceptualization. 2) methodology. 3) resources 4) writing—review and editing. 5) supervision.

Maglangit, F.: 1) Helped with Formal analysis.

Deng, H.: 1) Helped with Formal analysis. 2) writing—review and editing.

Jaspars, M.: 1) Conceptualization. 2) methodology. 3) writing—review and editing. 4) supervision.

Gammon, D. W.: 1) Conceptualization. 2) methodology. 3) writing—review and editing. 4) supervision.

Novel South African Rare Actinomycete *Kribbella speibonae* Strain SK5: A Prolific Producer of Hydroxamate Siderophores including New Dehydroxylated Congeners

Kojo Sekyi Acquah [1], Denzil R. Beukes [2], Digby F. Warner [3,4,5], Paul R. Meyers [6], Suthananda N. Sunassee [1], Fleurdeliz Maglangit [7,8], Hai Deng [8], Marcel Jaspars [8] and David W. Gammon [1,*]

[1] Department of Chemistry, University of Cape Town, Rondebosch 7701, South Africa; ACQKOJ001@myuct.ac.za (K.S.A.); snsunassee@gmail.com (S.N.S.); david.gammon@uct.ac.za (D.W.G.)

[2] School of Pharmacy, University of the Western Cape, Bellville 7535, South Africa; dbeukes@uwc.ac.za (D.R.B.)

[3] SAMRC/NHLS/UCT Molecular Mycobacteriology Research Unit & DST/NRF Centre of Excellence for Biomedical TB Research, Department of Pathology, Faculty of Health Sciences, University of Cape Town, Observatory 7925, South Africa; digby.warner@uct.ac.za (D.F.W.)

[4] Institute of Infectious Disease and Molecular Medicine, Faculty of Health Sciences, University of Cape Town, Observatory 7925, South Africa

[5] Wellcome Centre for Infectious Diseases Research in Africa, University of Cape Town, Rondebosch 7701, South Africa

[6] Department of Molecular and Cell Biology, University of Cape Town, Rondebosch 7701, South Africa; paul.meyers@uct.ac.za (P.R.M.)

[7] College of Science, University of the Philippines Cebu, Lahug, Cebu City 6000, Philippines; 01fm16@abdn.ac.uk (F.M.)

[8] Marine Biodiscovery Centre, Department of Chemistry, University of Aberdeen, Old Aberdeen AB24 3UE Scotland, UK; h.deng@abdn.ac.uk (H.D.); m.jaspars@abdn.ac.uk (M.J.)

* Correspondence: david.gammon@uct.ac.za; Tel.: +27-21-650-2547

Received: 21 May 2020; Accepted: 9 June 2020; Published: 29 June 2020

Abstract

In this paper, we report on the chemistry of the rare South African Actinomycete *Kribbella speibonae* strain SK5, a prolific producer of hydroxamate siderophores and their congeners. Two new analogues, dehydroxylated desferrioxamines, speibonoxamine **5.1** and desoxy-desferrioxamine D_1 **5.2**, have been isolated, together with four known hydroxamates, desferrioxamine D_1 **5.3**, desferrioxamine B **5.4**, desoxy-nocardamine **5.5** and nocardamine **5.6**, and a diketopiperazine (DKP) **5.7**. The structures of **5.1**–**5.7** were characterized by the analysis of HRESIMS and 1D and 2D NMR data, as well as by comparison with the relevant literature. Three new dehydroxy desferrioxamine derivatives **5.8**–**5.10** were tentatively identified in the molecular network of *K. speibonae* strain SK5 extracts, and structures were proposed based on their MS/MS fragmentation patterns. A plausible *spb* biosynthetic pathway was proposed. To the best of our knowledge, this is the first report of the isolation of desferrioxamines from the actinobacterial genus *Kribbella*. The isolated compounds were inactive against *Mycobacterium tuberculosis* strain H37Rv.

Keywords: *Kribbella*; speibonoxamine; siderophore; hydroxamate; molecular networking; mass spectrometry

5.1 Introduction

Minerals are essential for the growth, development, and propagation of living organisms. Iron, a crucial element, is involved in various cellular processes including oxygen metabolism, electron transfer, DNA and RNA biosynthesis, and as a catalyst in enzymatic processes where it serves as a cofactor for many enzymes.[1] Microorganisms require iron for biofilm formation, and a lack of this mineral reduces the hydrophobicity of the microbial surface, leading to restriction in biofilm formation.[2] Although the Earth is endowed with copious amounts of iron, it is mostly in an insoluble oxidized form, $Fe(OH)_3$; there are insufficient amounts of the Fe(II) form to meet cellular needs. Plants and microorganisms overcome this limitation by producing Fe(III)-chelating

siderophores to scavenge and accumulate iron from soil, fresh and marine water, and sediments for absorption and subsequent reduction to the required Fe(II) form.[3]

Siderophores are low molecular weight compounds (200–2000 Da) produced by bacteria, fungi, and graminaceous plants under iron limiting conditions.[4] These compounds form complexes with Fe(III) in the extracellular environment, which are then taken up into the cell via specific high-affinity uptake proteins. Iron, in its soluble Fe(II) form, is subsequently liberated from the siderophore via a redox-mediated process.[3] Siderophores have agricultural, biological control, environmental and medicinal applications. In agriculture, they increase soil fertility by making Fe(II) readily available and aid in nitrogen fixation.[3] Siderophores from nonpathogenic microorganisms compete for iron with those produced by plant and fish fungal pathogens in soil and water habitats, respectively, thereby serving as biological control agents.[4] Since siderophores chelate other metal cations (divalent, trivalent, and actinides) in soil and water, they tend to reduce the level of metal contamination in the environment.[5] The siderophore, desferrioxamine B, isolated from several *Streptomyces* species, is used to remove excess iron in patients suffering from iron overload.[6] Furthermore, siderophores linked to antibiotics show a higher antibacterial potency compared to normal antibiotics due to an enhanced uptake using the siderophore-mediated iron active transport. Examples of siderophore-enhanced antibiotics are the natural albomycin (thioribosyl pyrimidine antibiotic and tri-hydroxamate siderophore) and the synthetic, FDA-approved cefiderocol (cephalosporin antibiotic and catechol siderophore).[6] Siderophores are also being explored in the synthesis of sideromycin (siderophore linked to antibiotics) for antibiotic drug discovery and have been explored in a “Trojan horse” approach to a novel anti-tuberculosis agent.[7,8]

There are over 500 reported siderophores belonging to a number of different structural classes, about 270 of which have been structurally characterized.[3,9] Siderophores are grouped into four classes, namely hydroxamates, catecholates, carboxylates, and siderophores with mixed ligands, based on characteristic functional groups.[10,11] The hydroxamates are typically made of *N*-hydroxy-*N*-succinyl-cadaverine units and normally use three pairs of N-OH and C=O to coordinate with iron in an octahedral geometry.[12] Desferrioxamines and ferrioxamines are good examples,

with over 20 known analogues identified to date, which have been mainly characterized by nuclear magnetic resonance (NMR) and extensive mass spectrometric (MS) methods.[13]

Species of the genus *Kribbella* are classified as rare actinomycetes since they are less frequently isolated than species of other actinomycete genera, especially *Streptomyces*, although they may not be rare in the environment.[14] *Kribbella* strains are rich sources of novel secondary metabolites; for example, the antifungal alkyl glyceryl ethers, kribelloside A–D, which are produced by *Kribbella* strain MI481-42F6, which was isolated from a soil sample collected in Japan.[15] Among the *Kribbella* species isolated, 31 have currently been fully characterized.[16] However, very few *Kribbella* strains have been investigated for their metabolite profiles and/or isolation of secondary metabolites.

Our research into South African bacterial strains for natural product molecules with antimycobacterial properties has led to the isolation of the rare actinomycete *Kribbella speibonae* strain SK5, which exhibited an antimycobacterial activity against *Mycobacterium aurum* strain A+.[17] Herein, we report the secondary metabolites isolated from *K. speibonae* strain SK5, including two new desferrioxamines, speibonoxamine **5.1** and desoxy-desferrioxamine D_1 **5.2**, four known hydroxamates **5.2**–**5.6** and a diketopiperazine (DKP) **5.7**. Although siderophores are ubiquitous among metabolites produced by actinomycete strains,[3] especially under iron-deficient conditions, this is the first report of the isolation of siderophores from an actinobacterium of the genus *Kribbella*.

5.2. Results and Discussion

The *K. speibonae* strain SK5 was isolated from a topsoil sample collected from Stellenbosch in the Western Cape Province of South Africa.[17] The strain was grown in an International *Streptomyces* Project medium 2 (ISP2) broth and an Amberlite XAD 16N resin was added after 14 days of incubation at 30 °C with constant shaking. Organic solvents, methanol (MeOH), ethyl acetate (EtOAc), and dichloromethane (CH_2Cl_2), were used sequentially to extract the organics from the combined resin and culture broth. Then, the MeOH, EtOAc, and CH_2Cl_2 extracts were subjected to a separate high-pressure liquid chromatography-diode array detection, high-resolution

electrospray mass spectrometry (HPLC-DAD/HRESIMS) analyses for chemical profiling (Figure S5.1). Further MS/MS and Global Natural Product Social (GNPS) molecular network analyses of the extracts revealed the presence of several siderophores and DKPs, some of which have not been reported previously (Figure S5.2). The MeOH, EtOAc, and CH_2Cl_2 extracts were combined and fractionated using a series of purification steps, including a modified Kupchan method[18], solid phase extraction (SPE), and HPLC to yield two new siderophores, speibonoxamine **5.1** and desoxy-desferrioxamine D_1 **5.2**, and four known hydroxamates, **5.3**–**5.6** and a DKP **5.7** (Figure 5.1).

5.2.1. Structure Elucidation

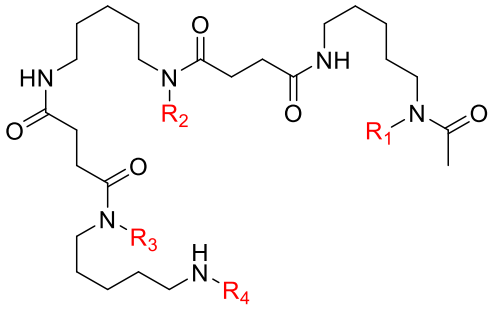

	R_1	R_2	R_3	R_4
Speibonoxamine **5.1**	H	H	H	$COCH_3$
desoxy-desferrioxamine D1 **5.2**	H	OH	OH	$COCH_3$
Desferrioxamine D1 **5.3**	OH	OH	OH	$COCH_3$
Desferrioxamine B **5.4**	OH	OH	OH	H

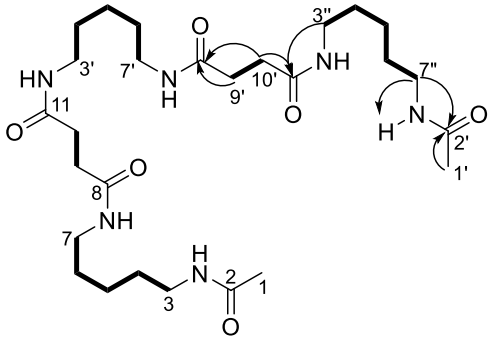

Speibonoxamine **5.1**

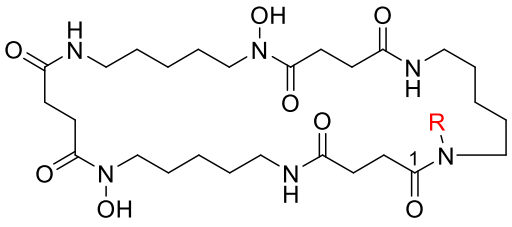

Desoxynocardamine **5.5** R = H
Desferrioxamine E / Nocardamine **5.6** R = OH

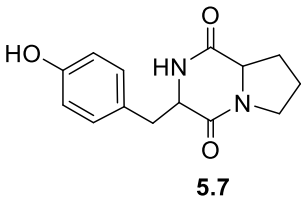

5.7

Hexahydro-3-((4-hydroxyphenyl)methyl)-pyrrolo[1,2-a]pyrazine-1,4-dione

Figure 5.1**:** Structures of isolated metabolites **5.1**–**5.7** from the *Kribbella speibonae* strain SK5, including depiction of Speibonoxamine **5.1** with COSY (—) and key heteronuclear multiple bond correlations (HMBC) (→) correlations.

The structures of the known compounds, desferrioxamine D_1 **5.3**, desferrioxamine B **5.4**, desoxynocardamine **5.5**, and nocardamine **5.6** were elucidated by comparison of the HRESIMS and NMR spectra with those reported in the literature (Figures S5.15–S5.27).[11,19-22] Compounds **5.3**–**5.6** belong to the hydroxamate class of siderophores.[3]

The molecular formula of compound **5.1,** isolated as a colourless amorphous solid, was deduced as $C_{27}H_{50}N_6O_6$ by HRESIMS (observed $[M + H]^+ = 555.3857$; calculated $[M + H]^+ = 555.3870$; $\Delta = 1.0$ ppm), indicating six degrees of unsaturation (Figure S5.3).

The ^{1}H-NMR of **5.1** in DMSO-*d*$_6$ showed only six signals (Figure S5.4), including four methylenes (δ_H 3.00, 2.27, 1.36, 1.22), one methyl (δ_H 1.77), and one NH (δ_H 7.77) with integrals of 12, 8, 12, 6, 6, and 6, respectively. The number of carbon atoms observed in the HRESIMS was five times higher than the number of signals observed in the ^{13}C-NMR spectrum (δ_C 171.7, 169.4, 38.9, 31.4, 29.3, 24.3). These results suggested that compound **5.1** had a symmetrical structure and/or repeating motifs. Analysis of the ^{1}H-^{1}H COSY spectrum together with integrals of the signals in the ^{1}H-NMR spectrum revealed two main spin systems, one of which consisted of three repeating motifs H-3 through H-7, H3′ through H-7′, and H-3″ through H-7″, and the other comprised two repeating motifs H-9 through H-10 and H-9′ through H-10′. Careful examination of the 1D NMR data and 2D NMR data suggested that the symmetrical structure of **5.1** consists of two succinyls, two acyl cadaverine (AC) units, and one cadaverine moiety, characteristic of a hydroxamate siderophore. The heteronuclear multiple bond correlations (HMBC) from H-7 (δ_H 3.00) to C-8 (δ_C 171.7) and H-3″ (δ_H 3.00) to C-11′ (δ_C 171.7) established the connectivity of the AC subunits to the succinyl groups. Furthermore, the cross peaks from H-3′ (δ_H 3.00) to C-11 (δ_C 171.7) and H-7′ (δ_H 3.00) to C-8′ (δ_C 171.7) established the attachment of the cadaverine moiety to the rest of the molecule.

The final structural analysis of **5.1** was confirmed by comparison with the spectroscopic data reported for desferrioxamine D_1 (**5.3**) in the literature,[21] which differs from **5.1** in the presence of *N*-hydroxy groups in the structure. Therefore, compound **5.1** represents a new non-hydroxylated desferrioxamine, which was named speibonoxamine after the producing organism, *Kribbella speibonae* strain SK5. This is the first report of a non-hydroxylated desferrioxamine.

Compound **5.1** may not be efficient in sequestering iron from the environment because of the lack of the hydroxamate moiety.

The molecular formula of compound **5.2**, also isolated as a colourless amorphous solid, was established as $C_{27}H_{50}N_6O_8$ by HRESIMS (observed $[M + H]^+$ = 587.3754; calculated $[M + H]^+$ = 587.3768; Δ = −2.1 ppm), indicating six degrees of unsaturation (Figure S5.9).

The mass of compound **5.2** was 32 mass units greater than **5.1** indicative of the presence of two additional oxygen atoms in the structure. Analysis of the ^{1}H-NMR data of **5.2** (Figure S5.10) revealed chemical shifts similar to those of **5.1**, except for signals at δ_H 1.50 (H-6 and H-6′) and 3.45 (H-7 and H-7′) as the most distinguishable change. The observed proton (δ_H 3.45) and carbon (δ_C 47.6) chemical shifts in **5.2** were more downfield than in **5.1** (δ_H 3.00, δ_C 38.9), indicating that the methylenes C-7 and C-7′ were deshielded by the adjacent *N*-hydroxy groups in **5.2**. Likewise, the methylene signals at (δ_H 1.50, δ_C 26.5) were downfield in **5.2** compared to that in **5.1** (δ_H 1.36, δ_C 29.3) because of the attachment of C-6 and C-6′ to the deshielded C-7 and C-7′ in **5.2**, respectively. Compound **5.2** was linked to desoxynocardamine (**5.5**) and desferrioxamine D_1 (**5.3**) in the GNPS molecular network with a mass difference of 2 and 16 Da, respectively (Figure S5.32) indicating that **5.2** is an acyclic analogue of **5.5** or dehydroxylated analogue of **5.3**. The structure of **5.2** was determined by analyses of the MS/MS fragmentation data together with a comprehensive interpretation of the 1D and 2D NMR data of **5.2** and comparison with literature data. Compound **5.2** is a new dehydroxy analogue of compound **5.3** and hence has been assigned the name desoxy-desferrioxamine D_1.[21]

5.2.2. Molecular Network Analysis

Dereplication of the metabolites produced by the *K. speibonae* strain SK5 was pivotal in the detection and isolation of the new compounds. Spectrometric data of the metabolites in the crude extract were searched against the natural product database, AntiBase (2017), with subsequent analysis of the data on the GNPS molecular networking platform[23], which grouped the compounds into clusters based on the similarity in MS/MS fragmentation patterns. Several known siderophores and DKPs were identified in the molecular network, including

desferrioxamine H **5.11**, ferrioxamine B **5.12**, ferrioxamine E **5.13**, ferrioxamine D_1 **5.14**, arthrobactin **5.15** and the DKP, hexahydro-3-(phenylmethyl)-pyrrolo[1,2-a]pyrazine-1,4-dione **5.16** (Figure S5.32).[13,19] Furthermore, three new dehydroxylated siderophores **5.8**–**5.10** were putatively identified in the molecular network, in addition to the new compounds, speibonoxamine **5.1** and desoxy-desferrioxamine D_1 **5.2**, isolated and reported in this study.

Compound **5.8** was linked to compound **5.2** when default parameters were used to generate the GNPS molecular network (Figure S5.33). Compound **5.8** (*m*/*z* 571.3807 $[M + H]^+$, $C_{27}H_{50}N_6O_7$) was identified as the dehydroxy analogue of **5.2** ($C_{27}H_{50}N_6O_8$) and the hydroxyl analogue of **5.1** ($C_{27}H_{50}N_6O_6$), as they have a mass difference of 16 Da and the same double bond equivalent (DBE) of six (Figure 5.2 and Table S5.1). Inspection of the fragment ions of compounds **5.1**, **5.2**, and **5.8** was very useful in assigning the position of the hydroxyl group, especially fragment ion 411.2596 ($C_{20}H_{35}O_5N_4^{\cdot}$), which was present in **5.1** and **5.8**, but absent in **5.2** (Figures S5.34–S5.36). Although the new compound **5.8** could not be isolated due to a paucity of material, its structure was proposed based on the MS/MS fragmentation data analysis and was assigned the name *di*desoxy-desferrioxamine D_1 (Figure 5.2).

Compound **5.9** (*m*/*z* 545.3654 $[M + H]^+$, $C_{25}H_{48}N_6O_7$) was linked to desferrioxamine B **5.4** in the GNPS molecular network and showed a mass difference of 16 Da (Figures 5.2 and S5.32). Compound **5.10** (*m*/*z* 529.3702 $[M + H]^+$, $C_{25}H_{48}N_6O_6$) was linked to **5.9** and had a mass difference of 16 Da. The MS/MS fragmentation patterns of **5.4**, **5.9**, and **5.10** were used to predict the structures of **5.9** and **5.10** (Figures S5.37–S5.39), and they were named as desoxy-desferrioxamine B and *di*desoxy-desferrioxamine B, respectively.

The results suggest that the *K. speibonae* strain SK5 is a prolific producer not only of hydroxamate siderophores, but also dehydroxylated and non-hydroxylated desferrioxamines. Although the presence of siderophores has been previously identified in the genomes of *Kribbella* species,[17,24] to our knowledge this is the first report of the isolation of hydroxamates from this genus.

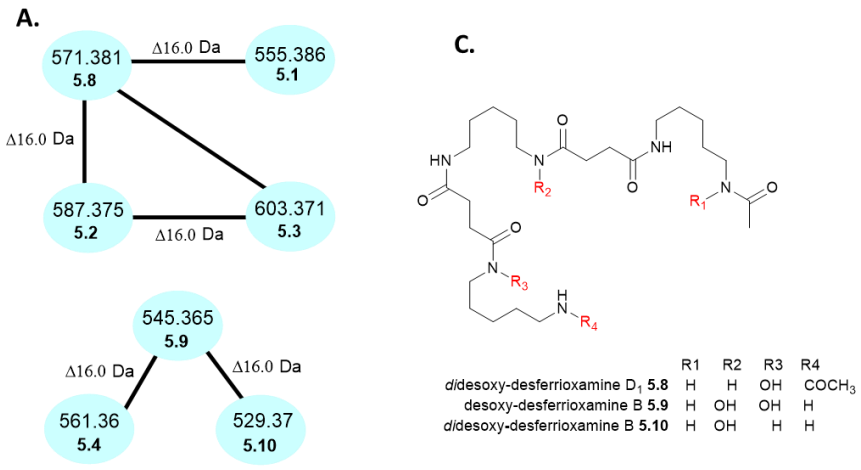

B.

Compound	Observed $[M+H]^+$	Molecular Formula	Calculated $[M+H]^+$	Δ ppm
Speibonoxamine **5.1**	555.3857	$C_{27}H_{50}N_6O_6$	555.3870	1.00
Desoxy-desferrioxamine D_1 **5.2**	587.3754	$C_{27}H_{50}N_6O_8$	587.3768	-2.09
Desferrioxamine D_1 **5.3**	603.3712	$C_{27}H_{50}N_6O_9$	603.3718	-0.69
*di*desoxy-desferrioxamine D_1 **5.8**	571.3807	$C_{27}H_{50}N_6O_7$	571.3819	-1.01
Desferrioxamine B **5.4**	561.3606	$C_{25}H_{48}N_6O_8$	561.3612	-1.05
desoxy-desferrioxamine B **5.9**	545.3654	$C_{25}H_{48}N_6O_7$	545.3663	-0.67
*di*desoxy-desferrioxamine B **5.10**	529.3702	$C_{25}H_{48}N_6O_6$	529.3714	-1.08

Figure 5.2: (**A**) Specific subnetwork analysis of the *K. speibonae* strain SK5; (**B**) putative dehydroxylated desferrioxamine analogues D_1 **5.8** and B **5.9**–**5.10**; (**C**) structures of plausible desferrioxamines **5.8**–**5.10** determined by the MS/MS fragmentation pattern.

5.2.3. Proposed Biosynthetic Pathway

Biosynthesis of the desferrioxamine class of hydroxamate siderophores has been elucidated in *Streptomyces* and is mediated by nonribosomal peptide synthetase-independent siderophore (NIS) synthetases.[9,10,25,26] Every NIS biosynthetic pathway identified to date contains at least one synthetase with a high sequence similarity to IucA/IucC and such synthetases have thus become the characteristic feature of these pathways.[10] In silico analysis of the annotated genome of the *K. speibonae* strain SK5 (GenBank accession number: SJJY00000000) identified the biosynthetic gene cluster (BGC) encoding the IucA/IucC synthetase that is likely responsible for producing **5.1**–**5.6** (Figure 5.3A, Table 5.1).

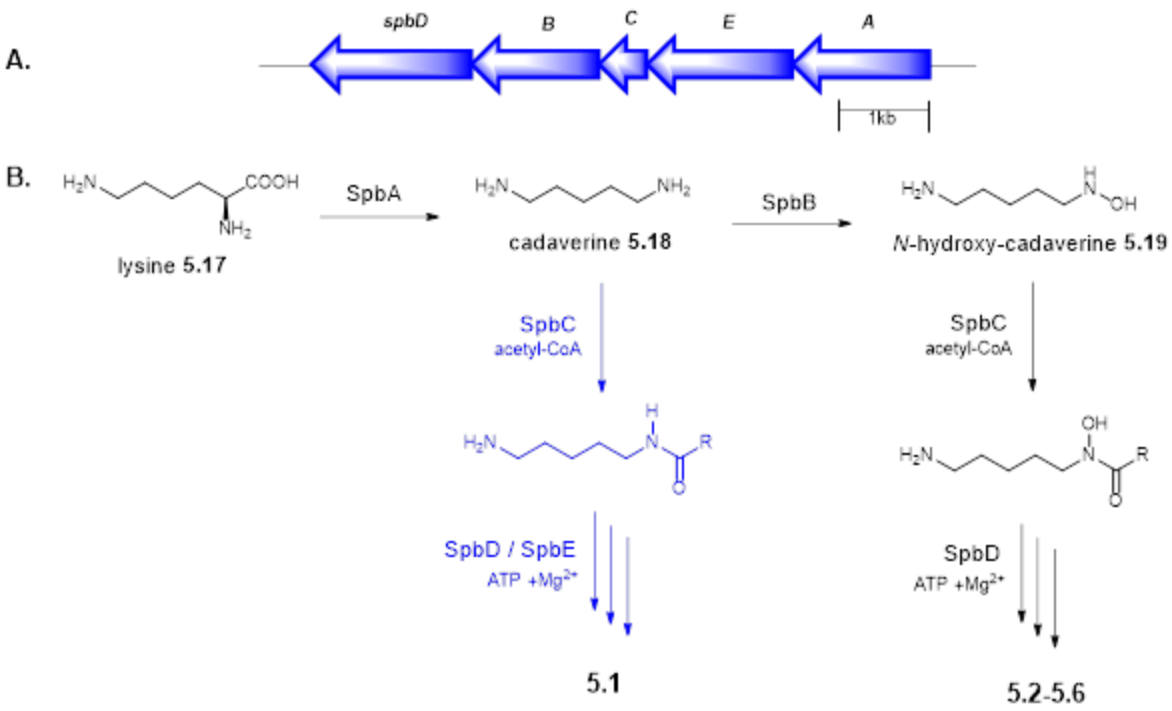

Figure 5.3: (**A**) Speibonoxamine (*spb*) biosynthetic gene cluster in the *K. speibonae* strain SK5; (**B**) proposed biosynthetic pathway of **5.1**–**5.6.**

The desferrioxamine (des) BGC in *Streptomyces coelicolor* strain M145 was proposed to comprise four genes, desABCD.[25] The spbA and spbB genes in the *K. speibonae* strain SK5 encode enzymes having a high sequence similarity to pyridoxal 5'-phosphate (PLP)-dependent decarboxylase and lysine-6-monooxygenase in Streptomyces strains, respectively.[27] These two enzymes are proposed to catalyze the decarboxylation of lysine **5.17** to form cadaverine **5.18** followed by hydroxylation to generate *N*-hydroxy-cadaverine **5.19** (Figure 5.3B). The acyltransferase, SpbC, is likely to catalyze the *N*-acylation of **5.19**,[9,25] which then undergoes ATP-dependent oligomerization and macrocylization catalyzed by SpbD and SpbE to produce the *N*-hydroxy-containing hydroxamate desferrioxamines **5.2**–**5.6**.[28]

The isolation of speibonoxamine **5.1** from *K. speibonae* strain SK5 suggests that the biosynthetic enzyme, *N*-acyl-CoA transferase SpbC, may display substrate promiscuity, binding not only to *N*-hydroxy-cadaverine **5.19** but also cadaverine **5.18**, the key difference between the biosynthesis of desferrioxamines and speibonoxamine **5.1**. It is proposed that the common decarboxylation intermediate, cadaverine **5.18,** undergoes spontaneous SpbC-catalyzed acylation, followed by

SpbD- and SpbE-catalyzed oligomerization of two molecules of succinate, two molecules of *N*-acetyl-cadaverine, and one molecule of cadaverine to generate **5.1**.

Table 5.1: Deduced functions of open reading frames (ORFs) in *spb* biosynthetic gene cluster (BGC).

Protein	Annotated Function	*Streptomyces* Homologue % Identity/% Similarity	Amino Acid Length
SpbD	IucA/IucC synthetase	74%/83%	565
SpbB	Lysine-6-monooxygenase	80%/88%	418
SpbC	Acyltransferase	67%/76%	156
SpbE	Siderophore synthetase	78%/84%	546
SpbA	PLP-dependent decarboxylase	86%/93%	495

5.2.4 Antimycobacterial activity

Although *K. Speibonae* strain SK5 exhibited a strong antimycobacterial activity against *Mycobacterium aurum* A+ in agar-overlay assays, a crude extract of its fermentation broth was inactive against *Mycobacterium aurum* A+ and *Mycobacterium tuberculosis* strain H37Rv. The isolated compounds did not exhibit any activity against *Mycobacterium tuberculosis* strain H37Rv.

5.3. Materials and Methods

5.3.1. General Experimental Procedures

NMR spectra were obtained on a BRUKER Ascend 600 (Bruker, Billerica, MA, USA) Prodigy cryoprobe at 600 and 150 MHz for ^{1}H and ^{13}C nuclei, respectively. DMSO-d_6 (δ_H 2.50, δ_C 39.7), CD_3OD (δ_H 3.30, δ_C 49.0), and $CDCl_3$ (δ_H 7.25, δ_C 77.00) were used for preparing samples for NMR experiments. High resolution mass spectrometric data were obtained using a Thermo Instruments MS system (LTQ XL/LTQ Orbitrap Discovery, Thermo Scientific, Bremen, Germany) coupled to a Thermo Instruments HPLC system (Accela PDA detector, Accela PDA autosampler, and Accela pump). The MS was run in a positive high-resolution mode (60,000) and MS/MS at a resolution of 7500 and a low-resolution negative mode. The following conditions were used: Capillary voltage 45 V, capillary temperature 260 °C, auxiliary gas flow rate 10–20 arbitrary units,

sheath gas flow rate 40–50 arbitrary units, spray voltage 4.5 kV, mass range 100–2000 amu (maximum resolution 30,000). HPLC separations were carried out using a reverse phase C18 ACE 10 µM 10 × 250 mm column connected to an Agilent Technologies 1200 series HPLC system equipped with an Agilent Technologies 1200 series quad pump and Agilent Technologies 1200 series DAD. The amberlite XAD 16N resin was obtained from Sigma-Aldrich, Johannesburg, South Africa. All solvents used throughout were of a HPLC-grade and purchased from both Merck and Sigma-Aldrich (Johannesburg, South Africa).

5.3.2. Isolation and Characterization of the Strain

The *K. speibonae* strain SK5 was isolated from a topsoil sample collected from the town of Stellenbosch in the Western Cape Province of South Africa using a newly developed *Kribbella*-selective medium.[17]

5.3.3. Fermentation

A liquid stock culture of the *K. speibonae* strain SK5 was inoculated into a 15 mL International *Streptomyces* Project medium 2 (ISP2) broth (yeast extract 4 g, malt extract 10 g, glucose 4 g, in 1 L H_2O, pH 7.3)[29] in a 250 mL Erlenmeyer flask and incubated for five days at 30 °C with shaking. Then, the entire culture was inoculated into a 50 mL ISP2 broth in a 500 mL Erlenmeyer flask and incubated at 30 °C with shaking for four days. This culture was subsequently split into three parts, which were used as the inocula for 3 × 100 mL ISP2 broths in 1000 mL Erlenmeyer flasks and incubated at 30 °C with shaking for four days. Then, each 100 mL culture was inoculated into a 1000 mL ISP2 broth in a 5000 mL Erlenmeyer flask and incubated at 30 °C with shaking. After 14 days of incubation, the Amberlite XAD 16N resin (50 g/L) was added under sterile conditions to each flask and further incubated for 6 h at 30 °C with shaking. Subsequently, the cultures were harvested and filtered under pressure using a piece of glass wool placed in a Buchner funnel. The filtrate was partitioned in a separating funnel with an equal volume of ethyl acetate. Then, the cell mass mixed with the Amberlite XAD 16N resin (containing the adsorbed organics) was extracted sequentially with MeOH (3×), then EtOAc (3×), and finally, CH_2Cl_2 (3×). All the organic extracts were concentrated under a reduced pressure to give 3.43 g of the MeOH extract, 0.51 g

of the EtOAc extract, and 0.19 g of the CH_2Cl_2 extract. The extracts were subjected to HPLC-DAD/HRESIMS analyses.

5.3.4. HPLC-DAD/HRESIMS Analyses

Chemical profiling of the MeOH, EtOAc, and CH_2Cl_2 extracts was performed by HPLC-DAD/HRESIMS analyses. Each extract (10 µL, 0.1 mg/mL in MeOH) was injected and chromatographically separated on a C18 reverse-phase HPLC column (ACE 10 µM 10 × 250 mm) using a linear gradient from 95% solvent A (0.1% formic acid in water) to 100% solvent B (0.1% formic acid in acetonitrile) for 25 min, followed by 100% B for 5 min at a flow rate of 1.5 mL/min. The DAD of the HPLC was scanned from 200–400 nm. The MS was run in a positive high-resolution mode (60,000) and MS/MS at a resolution of 7500 and a low-resolution negative mode. The Xcalibur software was used to process the raw data. The exact mass and molecular formula of each peak was entered as a single query in the commercially available AntiBase (2017) Natural Compound Identifier (https://www.wiley.com/en-us/AntiBase%3A+The+Natural+Compound+Identifier-p-9783527343591) to ascertain whether the data matched any compound in the database. The HPLC-DAD/HRESIMS profiles of the three extracts showed similar chemical profiles, hence they were combined to obtain 4.13 g.

5.3.5. Fractionation, Isolation, and Purification of Compounds

The combined crude extract (4.13 g) was suspended in 50 mL of distilled water and extracted with equal volumes of CH_2Cl_2 (three times). Then, the water layer was partitioned with the same volume of n-butanol (three times). The n-butanol layer (332.2 mg) was concentrated under a reduced pressure and fractionated on a C18 solid phase extraction (SPE) column using a stepwise elution of solvent mixtures of decreasing polarity (8 column volume/solvent mixture): 100% water (SPE1), 12.5% MeOH (SPE2), 25% MeOH (SPE3), 50% MeOH (SPE4), 100% MeOH (SPE5), and 100% MeOH containing 0.05% trifluoroacetic acid (SPE6). All fractions were subjected to the HPLC/HRESIMS analysis.

Fractions SPE2-4 were further purified by the reverse-phase HPLC analysis (C18, linear gradient 100% H_2O to 100% MeOH in 45 min, flow rate 1.5 mL/min). SPE2 yielded compounds **6.6** (19.3

mg) and **6.7** (0.8 mg), SPE3 yielded compounds **5.1** (1.2 mg), **5.2** (0.6 mg), **5.3** (1.2 mg), and **5.5** (0.8 mg), and SPE4 yielded **5.4** (0.5 mg).

Speibonoxamine **5.1**: Colorless amorphous solid; for ^{1}H, ^{13}C NMR data, see Table 5.2; HRESIMS (positive mode) *m/z* 555.3857 $[M + H]^+$ and 577.3672 $[M + Na]^+$ Δ 1.004; calcd. for $C_{27}H_{50}N_6O_6$.

Desoxy-desferrioxamine D_1 **5.2**: Colorless amorphous solid; ^{1}H, ^{13}C NMR data, see Table 5.2; HRESIMS (positive mode) *m/z* = 587.3754 $[M + H]^+$ and 609.3573 $[M + Na]^+$ Δ −2.092 ppm; calcd. for $C_{27}H_{50}N_6O_8$.

Desferrioxamine D_1 **5.3**: Colorless amorphous solid; ^{1}H NMR data, see Figure S5.16; HRESIMS (positive mode) *m/z* = 603.3708 $[M + H]^+$ and 625.3525 $[M + Na]^+$ Δ −0.685 ppm; calcd. for $C_{27}H_{50}N_6O_9$.

Desferrioxamine B **5.4**: Colorless amorphous solid; ^{1}H NMR data, see Figure S5.18; HRESIMS (positive mode) *m/z* = 561.3602 $[M + H]^+$ and 583.3415 $[M + Na]^+$ Δ −1.049 ppm; calcd. for $C_{25}H_{48}N_6O_8$.

Desoxynocardamine **5.5**: Colorless amorphous solid; ^{1}H NMR data, see Figure S5.20; HRESIMS (positive mode) *m/z* = 585.3602 $[M + H]^+$ and 607.3418 $[M + Na]^+$ Δ −0.391 ppm; calcd. for $C_{27}H_{48}N_6O_8$.

Nocardamine **5.6**: Colorless amorphous solid; ^{1}H, ^{13}C NMR data, see Figures S5.22–S5.23; HRESIMS (positive mode) *m/z* = 601.3552 $[M + H]^+$ and 623.3359 $[M + Na]^+$ Δ −0.161 ppm; calcd. for $C_{27}H_{48}N_6O_9$.

Hexahydro-3-((4-hydroxyphenyl)methyl)-pyrrolo[1,2-a]pyrazine-1,4-dione **5.7**: Colorless amorphous solid; ^{1}H NMR data, see Figures S5.28–S5.31; HRESIMS (positive mode) *m/z* = 261.1237 $[M + H]^+$ and 283.1655 $[M + Na]^+$ Δ 1.459 ppm; calcd. for $C_{14}H_{16}N_2O_3$.

Table 5.2: ^{1}H and ^{13}C-NMR data of speibonoxamine **5.1** and desoxy-desferrioxamine D_1 **5.2** in DMSO-d_6.

	Speibonoxamine 5.1		Desoxy-Desferrioxamine D_1 5.2	
Position	**^{13}C**	**^{1}H, Mult. (*J*, Hz)**	**^{13}C**	**^{1}H, Mult. (*J*, Hz)**
1, 1′	23.1, CH_3	1.77, s	23.1, CH_3	1.78, s
2, 2′	169.4, C	-	169.4, C	-
3, 3′, 3″	38.9, CH_2	3.00, t (6.15)	38.9, CH_2	3.00, m
4, 4′, 4″	29.3, CH_2	1.36, m	29.3, CH_2	1.38, dd (7.14, 14.24)
5, 5′, 5″	24.3, CH_2	1.22, m	24.0, CH_2	1.23, m
6, 6′	29.3, CH_2	1.36, m	26.5, CH_2	1.50, m
6″	29.3, CH_2	1.36, m	29.3, CH_2	1.38, dd (7.14, 14.24)
7, 7′	38.9, CH_2	3.00, t (6.15)	47.6, CH_2	3.45, t (6.96, 6.96)
7″	38.9, CH_2	3.00, t (6.15)	38.9, CH_2	3.00, m
8	171.7, C	-	172.4, C	-
8′	171.7, C	-	171.7, C	-
9	31.4, CH_2	2.27, s	28.1, CH_2	2.58, m
9′	31.4, CH_2	2.27, s	29.8, CH_2	2.40, t (6.89, 6.89)
10	31.4, CH_2	2.27, s	31.4, CH_2	2.27, m
10′	31.4, CH_2	2.27, s	30.4, CH_2	2.28, m
11	171.7, C	-	174.4, C	-
11′	171.7, C	-	171.2, C	-
NH		7.77		7.77

5.3.6. Molecular Networking

Raw data obtained from the LC-MS/MS system were converted to a mzXML format using the ProteoWizard tool MSconvert (version 3.0.10051, Vanderbilt University, Nashville, TN, USA).[31] All mzXML data were uploaded to the Global Natural Products Social (GNPS) molecular networking (MN) webserver3 (http://gnps.ucsd.edu) and analyzed using the MN workflow.[23] The data were filtered by removing all MS/MS fragment ions within +/− 17 Da of the precursor *m*/*z*. MS/MS spectra were window filtered by choosing only the top six fragment ions in the +/− 50 Da window throughout the spectrum. The precursor ion mass tolerance was set to 0.02 Da and a MS/MS fragment ion tolerance of 0.02 Da. Then, a network was created where edges were filtered to have a cosine score above 0.7 and more than three matched peaks. Further, edges between two nodes were kept in the network if and only if each of the nodes appeared in each other's respective top 10 most similar nodes. Finally, the maximum size of a molecular family was set to 100, and the lowest scoring edges were removed from molecular families until the molecular

family size was below this threshold. The spectra in the network were then searched against GNPS' spectral libraries. The library spectra were filtered in the same manner as the input data. All matches kept between the network spectra and library spectra were required to have a score above 0.7 and at least three matched peaks. The output of the molecular network was visualized using the Cytoscape version 3.7.2 (https://cytoscape.org/)[31] and displayed using the settings "preferred layout" with "directed" style. The nodes (compounds) originating from the culture medium and solvent control (MeOH) were excluded from the original network to enable visualization of only the *K. speibonae* strain SK5 metabolites derived from the MeOH, EtOAC, and CH_2Cl_2 extracts of the cultures.

5.3.7 Antimycobacterial activity

The combined crude extracts and the isolated compounds were dissolved in DMSO and their minimum inhibition concentration against *M. tuberculosis* strain H37Rv was determined using the standard broth micro dilution method.[32] The lowest concentration of drug that inhibited growth of more than 90% of the bacterial population was considered the MIC_{90}. Rifampicin was used as a reference standard.

5.4. Conclusions

The *K. speibonae* strain SK5 is a prolific producer of hydroxamate (desferrioxamine) siderophores and their dehydroxy analogues. Two new desferrioxamines, speibonoxamine and desoxy-desferrioxamine D_1, four known hydroxamates, and a DKP were isolated from *K. speibonae* strain SK5. Furthermore, several new and known siderophores were identified in the *K. speibonae* strain SK5 extracts, and their plausible structures were determined by the MS/MS fragmentation analysis. This is the first report of siderophores isolated from the genus *Kribbella*. The proposed speibonoxamine pathway (Figure 6.3B) suggests a biosynthetic machinery distinct from that reported for desferrioxamine biosynthesis. The isolated compounds did not show antimycobacterial activity.

Author Contributions: Conceptualization, S.N.S., M.J., P.R.M., D.W.G., and D.R.B.; methodology, S.N.S., M.J., P.R.M., D.R.B., D.W.G., D.F.W., and K.S.A.; investigation, K.S.A.; formal analysis,

K.S.A., H.D., and F.M.; resources, S.N.S. and P.R.M.; data curation, K.S.A. and F.M.; writing—original draft preparation, K.S.A.; writing—review and editing, S.N.S., M.J., P.R.M., D.R.B., D.W.G., D.F.W., and H.D.; supervision, S.N.S., D.W.G., and D.R.B.; project administration, S.N.S and D.W.G.; funding acquisition, S.N.S. and D.F.W. All authors have read and agreed to the published version of the manuscript.

Funding: The authors acknowledge funding for this research from the South African Medical Research Council (SAMRC) through the Strategic Health Innovation Partnerships (SHIP) initiative (to D.F.W.), Newton Advanced Fellowship Award (NA160057) (to S.N.S. and M.J.), and the University of Cape Town (to K.S.A.).

Conflicts of Interest: The authors declare no conflict of interest. The funders had no role in the design of the study, in the collection, analyses, interpretation of data, in the writing of the manuscript, or in the decision to publish the results.

5.5 References

1. Butler, A.; Theisen, R.M. Iron(III)–siderophore coordination chemistry: Reactivity of marine siderophores. *Coord. Chem Rev.* **254**, 288–296 (2011).
2. Weinberg, E.D. Suppression of bacterial biofilm formation by iron limitation. *Med. Hypotheses* **63**, 863–865 (2004).
3. Hider, R.C.; Kong, X. Chemistry and biology of siderophores. *Nat. Prod. Rep.* **27**, 637 (2010).
4. Ahmed, E.; Holmström, S.J.M. Siderophores in environmental research: Roles and applications. *Microb. Biotechnol.* **7**, 196–208 (2014).
5. Rajkumar, M.; Ae, N.; Narasimha, M.; Prasad, V.; Freitas, H. Potential of siderophore-producing bacteria for improving heavy metal phytoextraction. *Trends Biotechnol.* **28**, 142–149 (2010).
6. Wu, J.Y.; Srinivas, P.; Pogue, J.M. Cefiderocol: A Novel Agent for the Management of Multidrug-Resistant Gram-Negative Organisms. *Infect Dis. Ther.* **9**, 17–40 (2020).
7. Miller, M.J.; Walz, A.J.; Zhu, H.; Wu, C.; Moraski, G.; Ute, M.; Tristani, E.M.; Crumbliss, A.L.; Ferdig, M.T.; Checkley, L.; et al. Design, Synthesis, and Study of a Mycobactin - Artemisinin

Conjugate That Has Selective and Potent Activity against Tuberculosis and Malaria. *J. Am. Chem. Soc.* **133**, 2076–2079 (2011).

8. Braun, V.; Pramanik, A.; Gwinner, T.; Köberle, M.; Bohn, E. Sideromycins: Tools and antibiotics. *BioMetals* **22**, 3–13 (2009).
9. Maglangit, F.; Alrashdi, S.; Renault, J.; Trembleau, L.; Victoria, C.; Tong, M.H.; Wang, S.; Kyeremeh, K.; Deng, H. Characterization of the promiscuous *N*-acyl CoA transferase, LgoC, in legonoxamine biosynthesis. *Org. Biomol. Chem.* **18**, 2219–2222 (2020).
10. Carroll, C.S.; Moore, M.M. Ironing out siderophore biosynthesis: A review of non-ribosomal peptide synthetase (NRPS)-independent siderophore synthetases. *Crit. Rev. Biochem. Mol. Biol.* **53**, 356–381 (2018).
11. Maglangit, F.; Tong, M.H.; Jaspars, M.; Kyeremeh, K.; Deng, H. Legonoxamines A-B, two new hydroxamate siderophores from the soil bacterium, Streptomyces sp. MA37. *Tetrahedron Lett.* **60**, 75–79 (2019).
12. Barry, S.M.; Challis, G.L. Recent advances in siderophore biosynthesis. *Curr. Opin. Chem. Biol.* **13**, 205–215 (2009).
13. Pluháček, T.; Lemr, K.; Ghosh, D.; Milde, D.; Novák, J.; Havlíček, V. Characterization of microbial siderophores by mass spectrometry. *Mass Spectrom. Rev.* **35**, 35–47 (2016).
14. Subramani, R.; Sipkema, D. Marine Rare Actinomycetes: A Promising Source of Structurally Diverse and Unique Novel Natural Products. *Mar. Drugs* **17**, 249 (2019).
15. Igarashi, M.; Sawa, R.; Yamasaki, M.; Hayashi, C.; Umekita, M.; Hatano, M.; Fujiwara, T.; Mizumoto, K.; Nomoto, A. Kribellosides, novel RNA 5’ -triphosphatase inhibitors from the rare actinomycete Kribbella sp. MI481-42F6. *J. Antibiot. (Tokyo).* **70**, 582–589 (2017).
16. Parte, A.C. LPSN - List of prokaryotic names with standing in nomenclature (Bacterio.net), 20 years on. *Int. J. Syst. Evol. Microbiol.* **68**, 1825–1829 (2018), https://lpsn.dsmz.de/genus/kribbella
17. Curtis, S.M.; Norton, I.; Everest, G.J.; Pelser, J.G.; De Kock, M.C.; Meyers, P.R. Development of a *Kribbella*-specific isolation medium and description of *Kribbella capetownensis* sp. nov. and *Kribbella speibonae* sp. nov., isolated from soil. *Antonie van Leeuwenhoek* **113**, 617–628 (2020).

18. Zhang, Q.W.; Lin, L.G.; Ye, W.C. Techniques for extraction and isolation of natural products: A comprehensive review. *Chinese Med. (UK)* **13**, 1–26 (2018).
19. Feistner, G.J.; Stahl, D.C.; Ann, H. Proferrioxamine Siderophores of Erwinia Amylovora. A Capillary Liquid Chromatographic/Electrospray Tandem Mass Spectrometric Study. *Org. Mass Spectrom.* **28**, 163–175 (1993).
20. Lee, H.S.; Hee, J.S.; Kyoung, H.J.; Tae, S.K.; Oh, K.B.; Shin, J. Cyclic peptides of the nocardamine class from a marine-derived bacterium of the genus Streptomyces. *J. Nat. Prod.* **68**, 623–625 (2005).
21. Ueki, M.; Suzuki, R.; Takamatsu, S.; Takagi, H.; Uramoto, M.; Ikeda, H.; Osada, H. Nocardamin Production by Streptomyces avermitilis. *Actinomycetologica* **23**, 34–39 (2009).
22. Fang, Q.; Maglangit, F.; Wu, L.; Ebel, R.; Kyeremeh, K.; Andersen, J.H.; Annang, F.; Pérez-Moreno, G.; Reyes, F.; Deng, H. Signalling and Bioactive Metabolites from Streptomyces sp. RK44. *Molecules* **25**, 1–13 (2020).
23. Wang, M.; Carver, J.J.; Phelan, V. V; Sanchez, L.M.; Garg, N.; Peng, Y.; Nguyen, D.D.; Watrous, J.; Kapono, C.A.; Luzzatto-Knaan, T.; et al. Sharing and community curation of mass spectrometry data with Global Natural Products Social Molecular Networking. *Nat. Biotechnol.* **34**, 828–837 (2016).
24. Pukall, R.; Lapidus, A.; Del Rio, T.G.; Copeland, A.; Tice, H.; Cheng, J.F.; Lucas, S.; Chen, F.; Nolan, M.; Labutti, K.; et al. Complete genome sequence of Kribbella flavida type strain (IFO 14399 T). *Stand. Genomic Sci.* **2**, 186–193 (2010).
25. Ronan, J.L.; Kadi, N.; Mcmahon, S.A.; Naismith, J.H.; Alkhalaf, L.M.; Challis, G.L.; Challis, G.L. Desferrioxamine biosynthesis: Diverse hydroxamate assembly by substrate- tolerant acyl transferase DesC. *R. Soc. Publ. 373*, (2018) doi:10.1098/rstb.2017.0068
26. Kadi, N.; Song, L.; Challis, G.L. Bisucaberin biosynthesis: An adenylating domain of the BibC multi-enzyme catalyzes cyclodimerization of N-hydroxy-N-succinylcadaverine. Chem. Commun. 5119–5121, (2008) doi.org/10.1039/B813029A
27. Barona-Gómez, F.; Wong, U.; Giannakopulos, A.E.; Derrick, P.J.; Challis, G.L. Identification of a cluster of genes that directs desferrioxamine biosynthesis in Streptomyces coelicolor M145. *J. Am. Chem. Soc.* **126**, 16282–16283 (2004).

28. Rütschlin, S.; Böttcher, T. Dissecting the Mechanism of Oligomerization and Macrocyclization Reactions of NRPS-Independent Siderophore Synthetases. *Chem. A Eur. J.* **24**, 16044–16051 (2018).
29. Shirling, E.B.; Gottlieb, D. Methods for Characterization of *Streptomyces* species. *Int. J. Syst. Bacteriol.* **16**, 313–340 (1966).
30. Holman, J.D.; Tabb, D.L.; Mallick, P. Employing ProteoWizard to Convert Raw Mass Spectrometry Data. *Curr Protoc Bioinforma.* **46**, 1–7 (2014).
31. Otasek, D.; Morris, J.H.; Bouças, J.; Pico, A.R.; Demchak, B. Cytoscape Automation: Empowering workflow-based network analysis. *Genome Biol.* **20**, 1–15 (2019).
32. Id, M. G. *et al.* Cinnamoyl-Oxaborole Amides : Synthesis and Their in Vitro Biological Activity. *Molecules* **23**, 1–13 (2018).

Sample Availability: Samples of the compounds are not available from the authors.

Chapter Six: Outlook and Future Work

Tuberculosis is a global pandemic where the treatment regimen is known to be lengthy and complicated, and therefore often ineffective. These realities, together with the occurrence of drug-resistant strains of *M. tuberculosis*, continue to stimulate the search for potent and safe drugs. As discussed extensively in the literature review section of this thesis, natural products have historically been and still are a major source of drugs. Technological advancement in genome mining, dereplication, purification, structure elucidation and biological assays have made natural product drug discovery more efficient and therefore more appealing. Less explored and biodiverse ecosystems have proven to be a prolific source of novel bioactive natural products.

The marine environment, which is relatively less explored compared to the terrestrial environment, has been a source of structurally unique and complex bioactive secondary metabolites. To date, fourteen drugs have been developed and approved for clinical use from marine natural products (MNPs) and many more are in different stages of development and clinical trials. However, none of the approved drugs is an anti-TB drug. This is in part because a significant proportion of marine natural product drug discovery has been funded by the United States' National Cancer Institute (NCI), with a consequent focus on cancer. MNPs have potential for TB drug discovery. This project focused on obtaining baseline data on the antimycobacterial antibiotic potential of the NCI's enormous collection of marine invertebrate crude extracts, investigating some of these extracts for bio-active NPs, and on investigating another little-explored source of active NPs, the South African actinobacteria.

Out of 54 active extracts in the NCI collection screened, this is the first report of antimycobacterial activity for 44% of the invertebrate species from which the extracts were derived. Some extracts exhibited potent activities with sub-10 µg/mL MICs. These bioactive extracts can easily be accessed from the NCI using their NPIDs. With proper dereplication techniques, these active extracts could be prioritized and the bioactive components isolated. Indeed, this strategy was employed in the present work and the bioactive components of two of the extracts, which were available in sufficient amounts, were isolated. Extracts of the Mauritian marine sponges, *Hyrtios*

reticulatus and *Jaspis splendens* were dereplicated using ^{1}H NMR and HRESIMS with the Global Natural Product Social (GNPS) molecular networking platform. The *H*. *reticulatus* extract contained and yielded the known antimycobacterial, heteronemin. The *J*. *splendens* extract contained the bioactive bengamide class of compounds, including some new analogues. Bengamides P and Q were isolated, and their structures elucidated while the structure of a new analogue was predicted based on its MS/MS fragmentation pattern (Chapter three). Antimycobacterial activity for bengamides P and Q is reported for the first time.

With the class of bengamides having been shown to include potent antimycobacterial compounds, further exploration of these is warranted. There is preliminary evidence that the NCI's *J*. *splendens* extract contains new structural variants of the bengamides, and the promising activity justifies separation and isolation of these. Together with the known compounds, these could be screened in whole cell assays for antimycobacterial activity. This could aid in SAR and QSAR design and studies.

The isolation of promising active compounds from crude extracts with high and moderate activity gives enough reason to continue exploring these NCI marine invertebrate extracts for novel antitubercular leads.

Actinomycetes are unmatched with regards to bioactive secondary metabolites from microbial sources. South Africa has a rich biodiversity of organisms and has been the source of novel and rare actinomycetes. These are less explored for drug discovery, although they have been the source of novel bioactive compounds including some antimycobacterial agents. Two South African actinomycetes (one *Streptomyces* strain and one novel rare *Kribbella* strain), which showed antimycobacterial activity, were studied further.

Dereplication of the crude extract of *Streptomyces* strain Muiz4Y showed that it produced compounds which did not match any known structures in available databases. Three new compounds were isolated including a β-carboline alkaloid, a peptide, and a glycosylated lactone, together with the known diketopiperazine and a triphenylhexene (Chapter four). The structure proposed for the glycosylated lactone is novel but awaits confirmation by synthesis or other

analytical techniques. The observation that few β-carboline alkaloids have been isolated from *Streptomyces* strains led to the proposal of a biosynthetic pathway for this alkaloid. The triphenylhexene was the only active compound isolated from *Streptomyces* strain Muiz4Y.

The rare *Kribbella* speibonae strain SK5 exhibited potent antimycobacterial activity against *Mycobacterium aurum* A+ in agar-overlay assays. Dereplication of the crude extract of a large-scale fermentation of this strain using ^{1}H NMR and HRESIMS data, together with GNPS molecular networking showed it to be a prolific producer of hydroxamate siderophores including new dehydroxylated analogues (Chapter five). Although the crude extract was inactive, the siderophores were isolated and found to include two new variants. One of these is the non-hydroxylated desferrioxamine D_1 analogue which we named speibonoxamine. The isolation of this compound gave more insight into the biosynthesis of the desferrioxamines. A biosynthetic pathway was proposed for speibonoxamine.

Genome mining of strain SK5 showed that it has the potential to produce a range of interesting metabolites including lanthipeptides, NRPS and PKS type compounds. An OSMAC approach is being employed to elicit the production of the bioactive compounds from strain SK5 and the *Streptomyces* strain Muiz4Y as well. These strains are also being cultured on solid agar to determine if this will elicit the production of the bioactive compounds detected by genome mining. The option of adding elicitors, such as cerium ions and bacterial cells, such as *Mycobacterium aurum* A+, to the cultures of these actinomycetes strains should also be considered.

This study reaffirmed the marine environment, especially marine invertebrates, as a viable source of potent novel antimycobacterial natural products and established that South African actinomycetes are a less explored treasure-chest for the discovery of novel bioactive metabolites for TB drug discovery.

Appendix

Appendix for Chapter Three

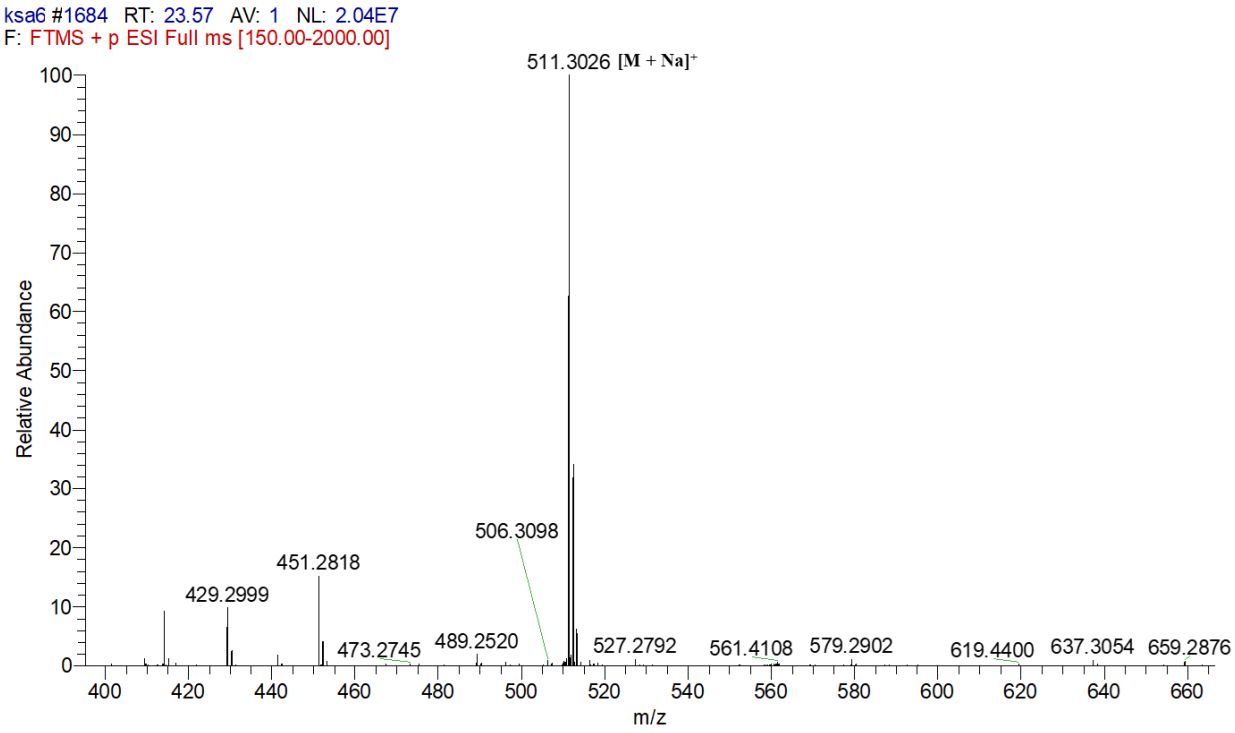

Figure S3.1. HR-ESI-MS spectrum of heteronemin **3.1**

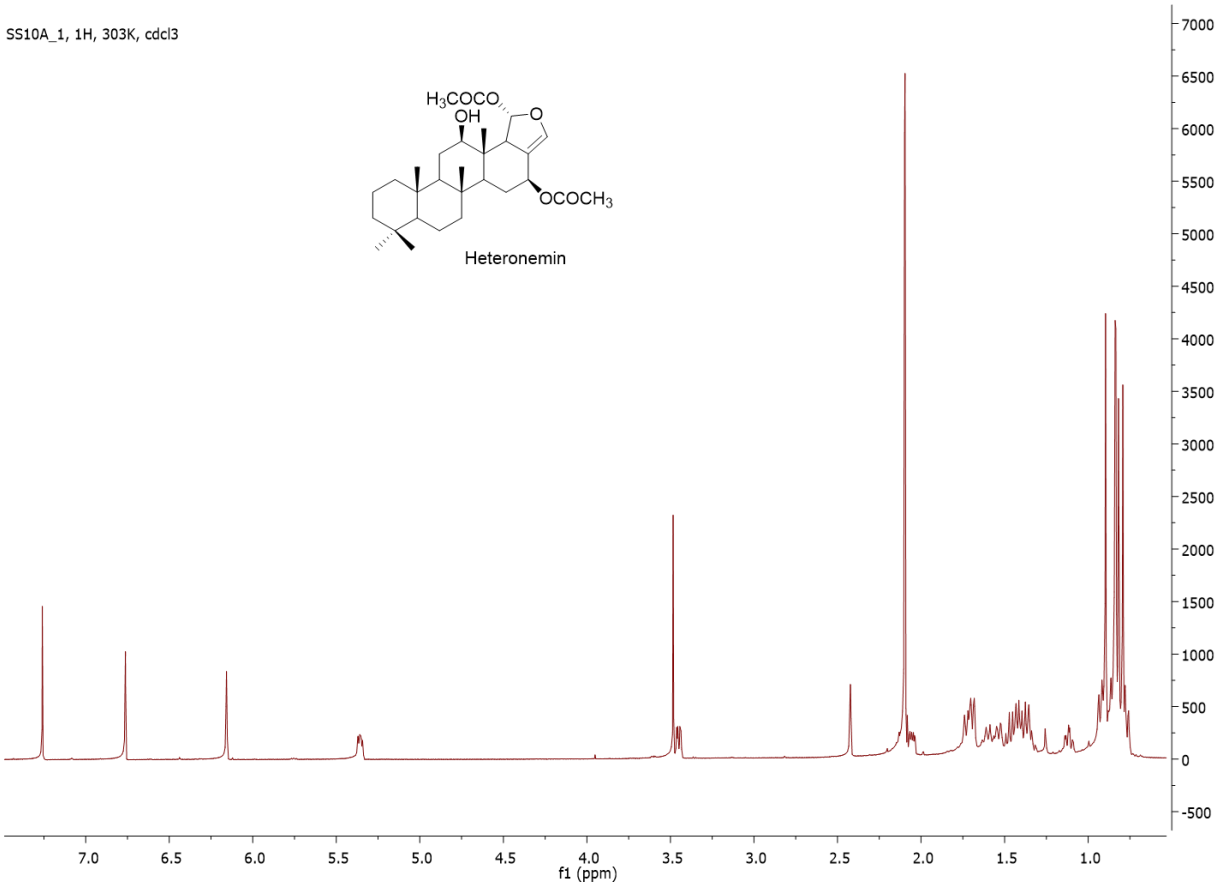

Figure S3.2. ^{1}H-NMR spectrum (600MHz, $CDCl_3$, 303K) of heteronemin **3.1**

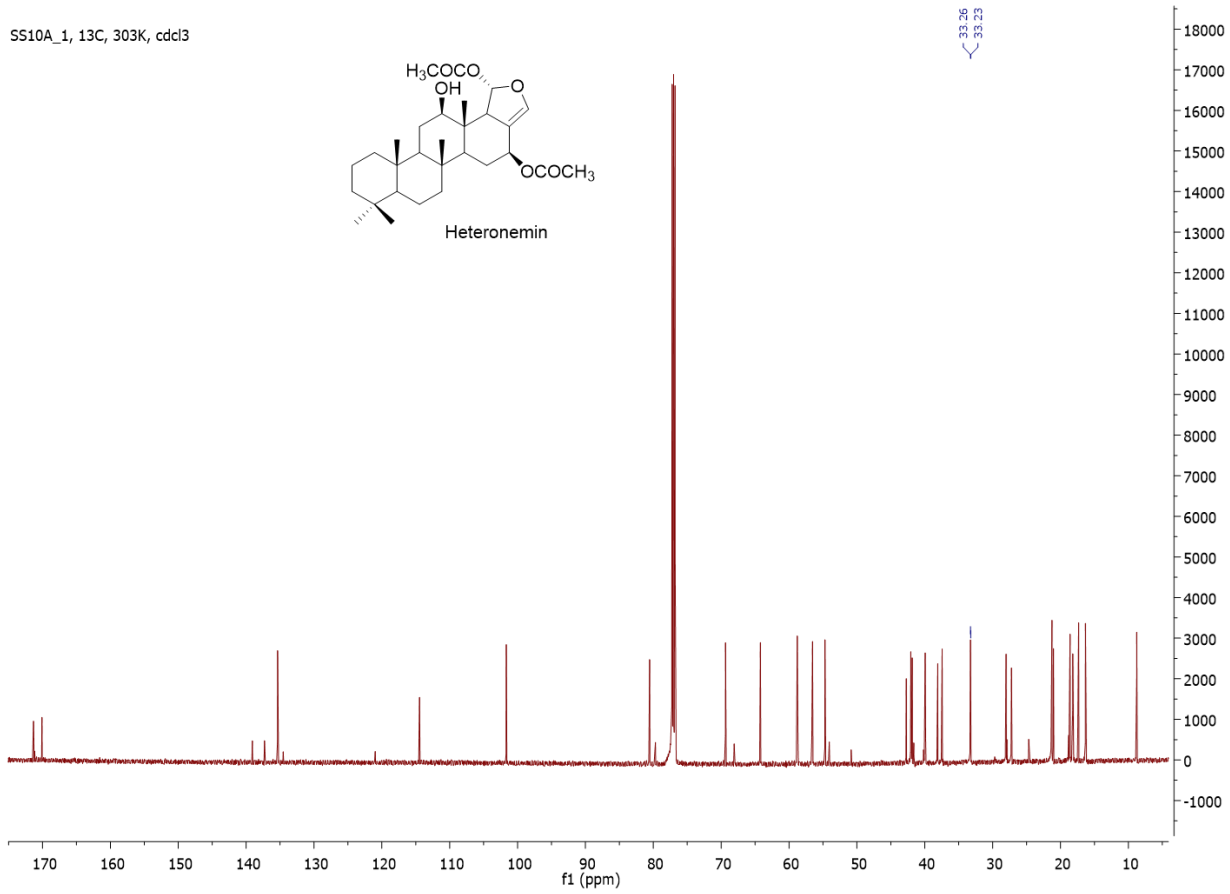

Figure S3.3. ^{13}C-NMR spectrum (150MHz, $CDCl_3$, 303K) of heteronemin **3.1**

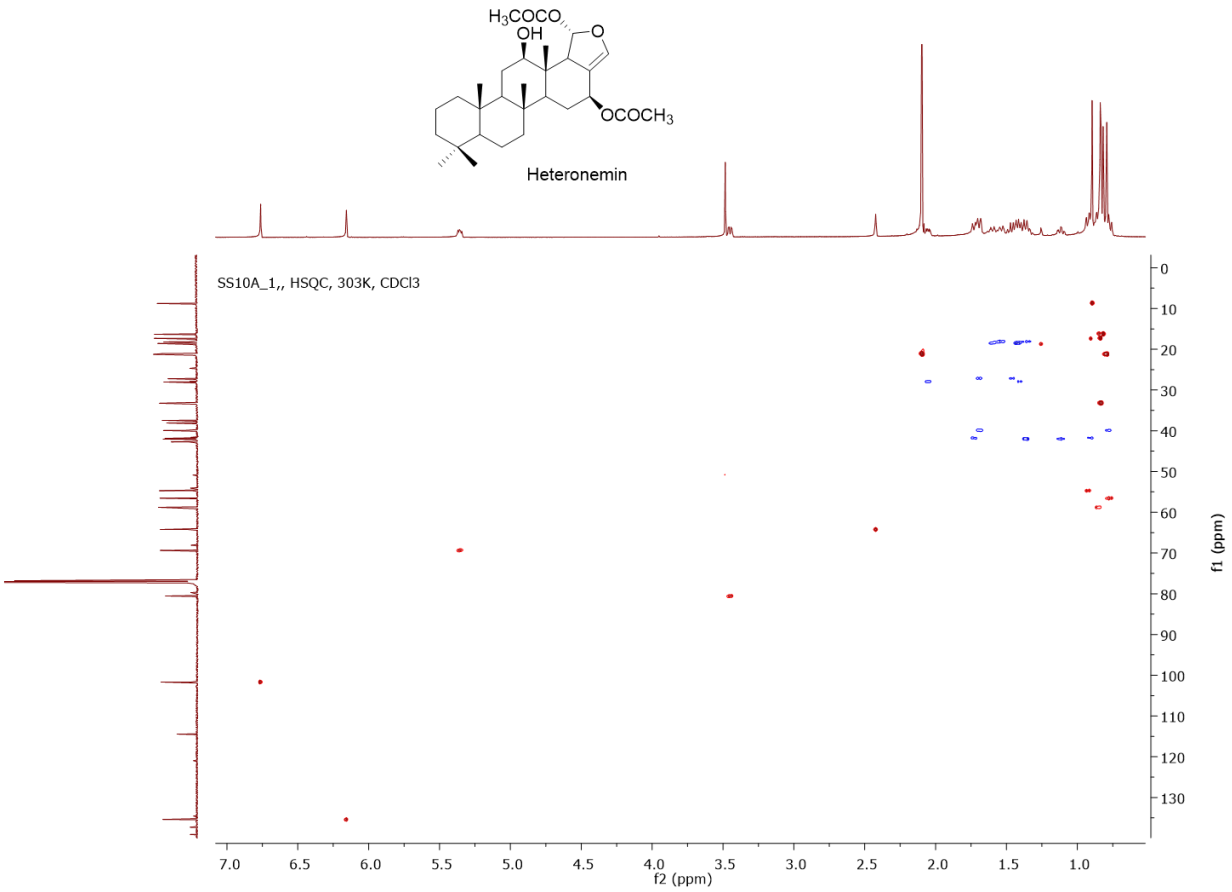

Figure S3.4. HSQC NMR spectrum (600MHz, $CDCl_3$, 303K) of heteronemin **3.1**

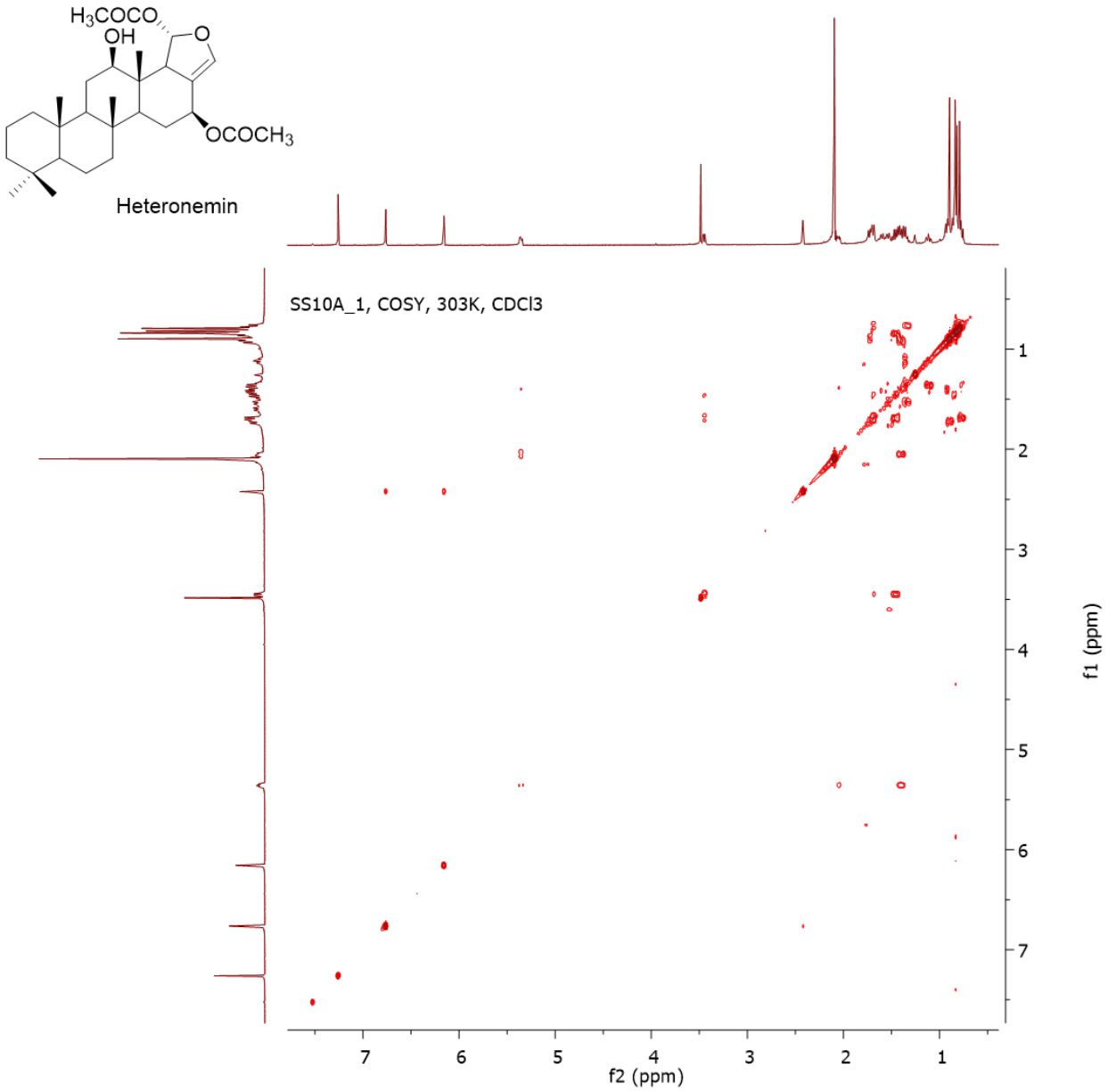

Figure S3.5. ^{1}H-^{1}H COSY spectrum (600MHz, $CDCl_3$, 303K) of heteronemin **3.1**

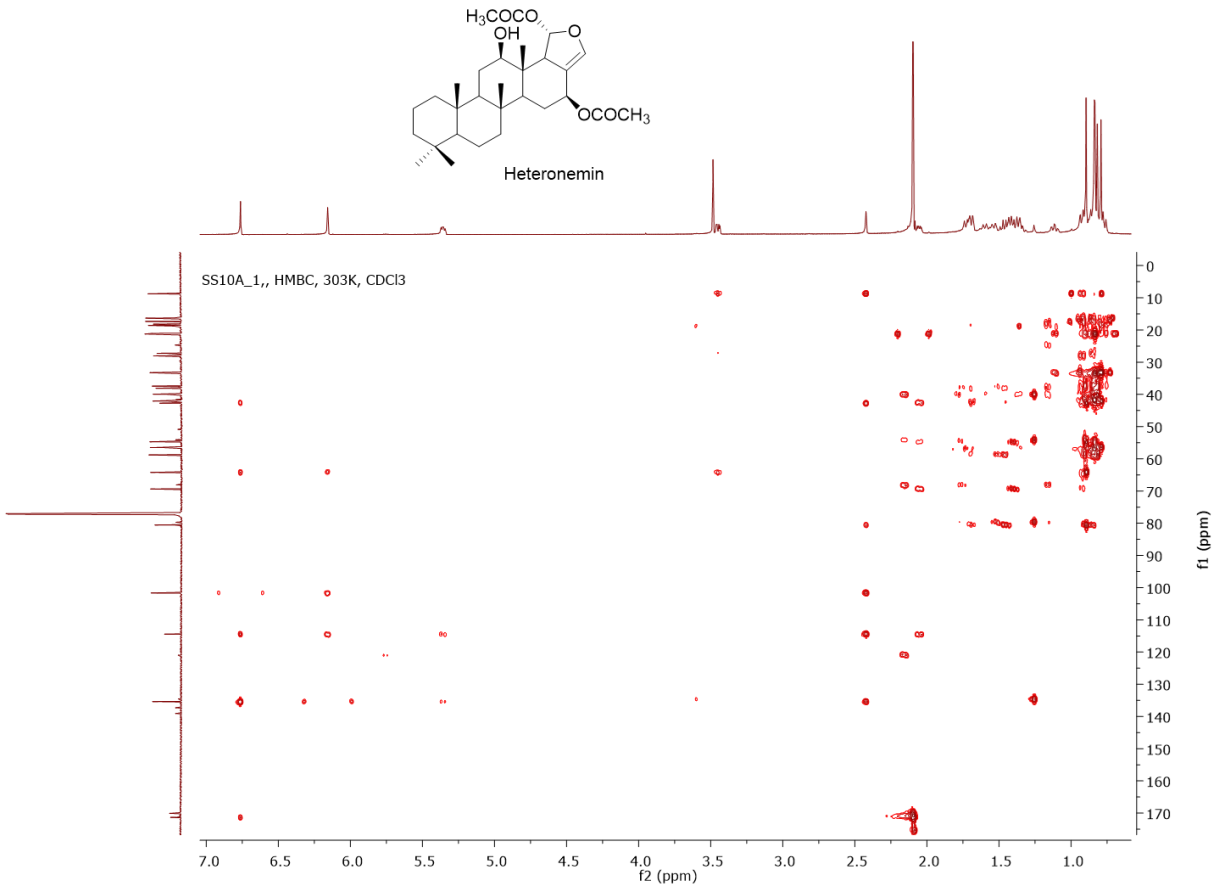

Figure S3.6. HMBC NMR spectrum (600MHz, $CDCl_3$, 303K) of heteronemin **3.1**

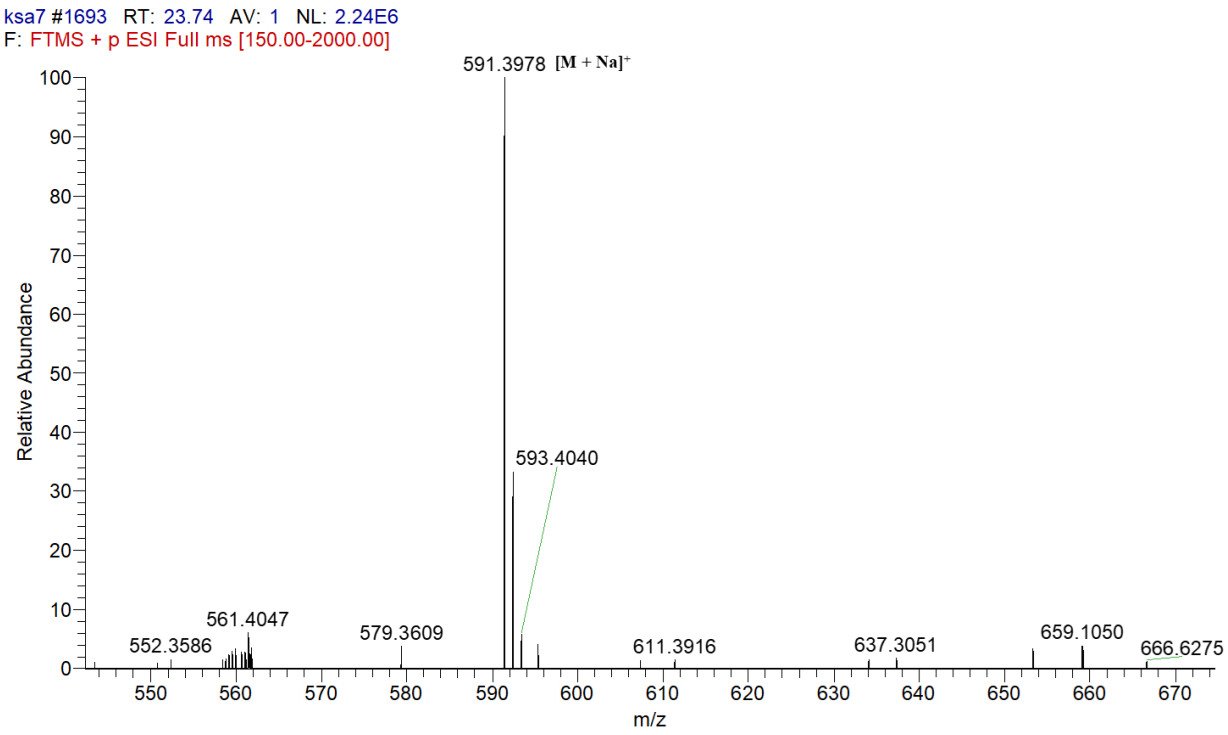

Figure S3.7. HR-ESI-MS spectrum of bengamide P **3.2**

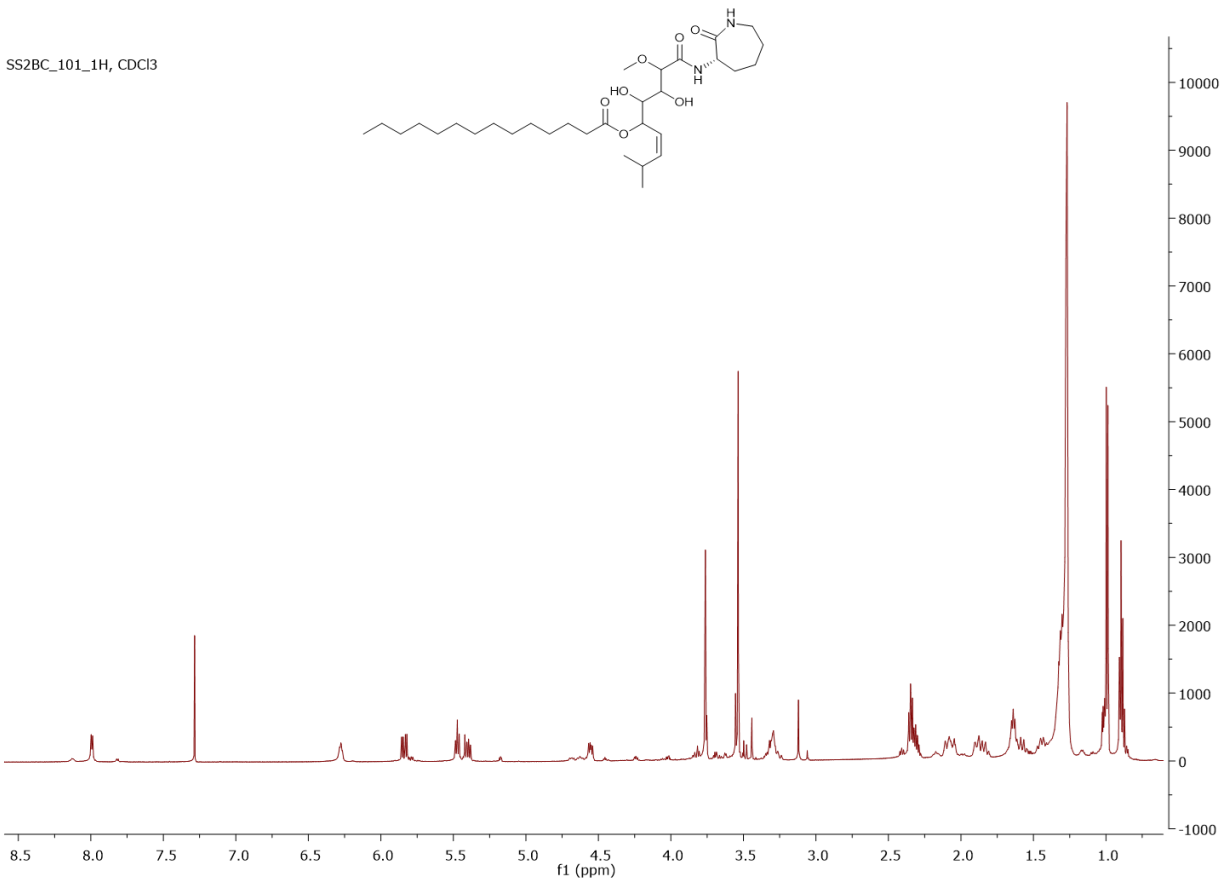

Figure S3.8. ^{1}H-NMR spectrum (600MHz, $CDCl_3$, 303K) of bengamide P **3.2**

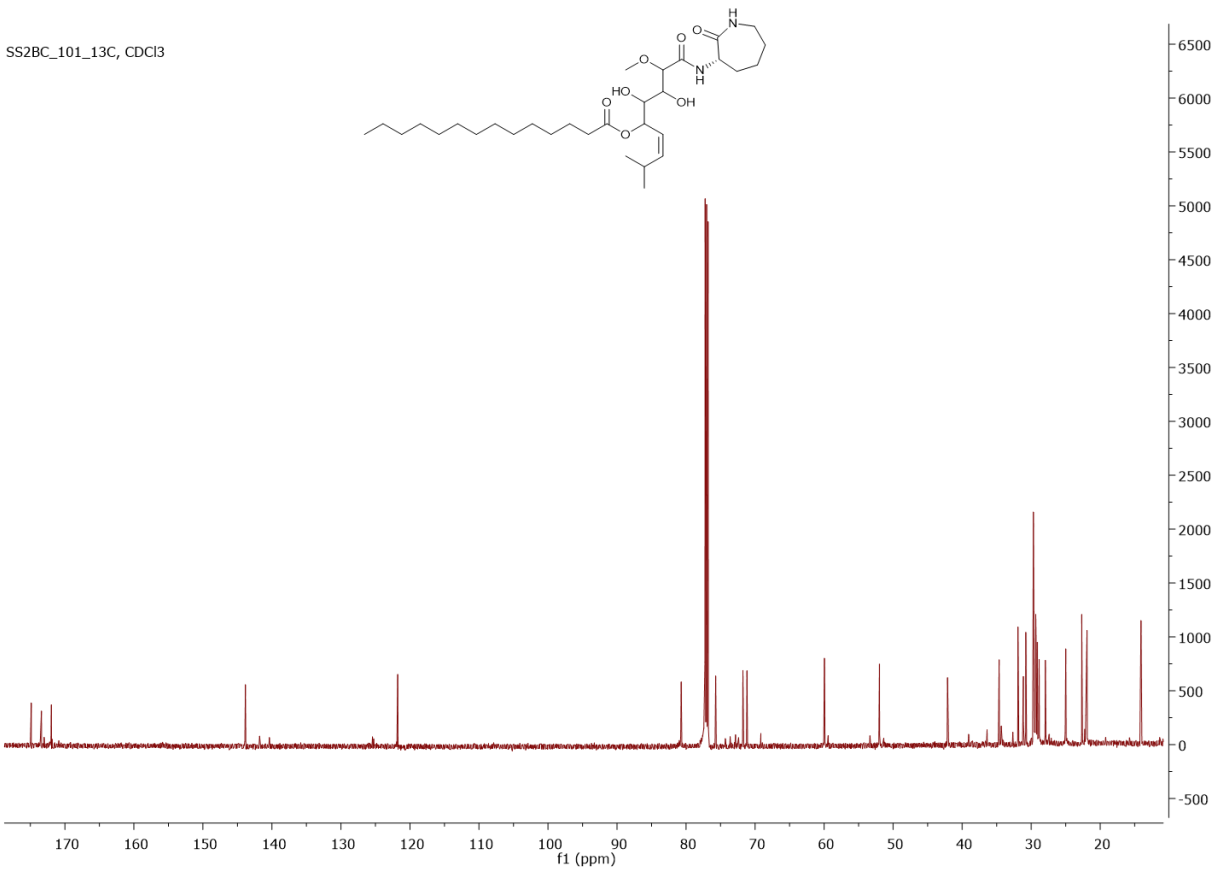

Figure S3.9. ^{13}C-NMR spectrum (150MHz, $CDCl_3$, 303K) of bengamide P **3.2**

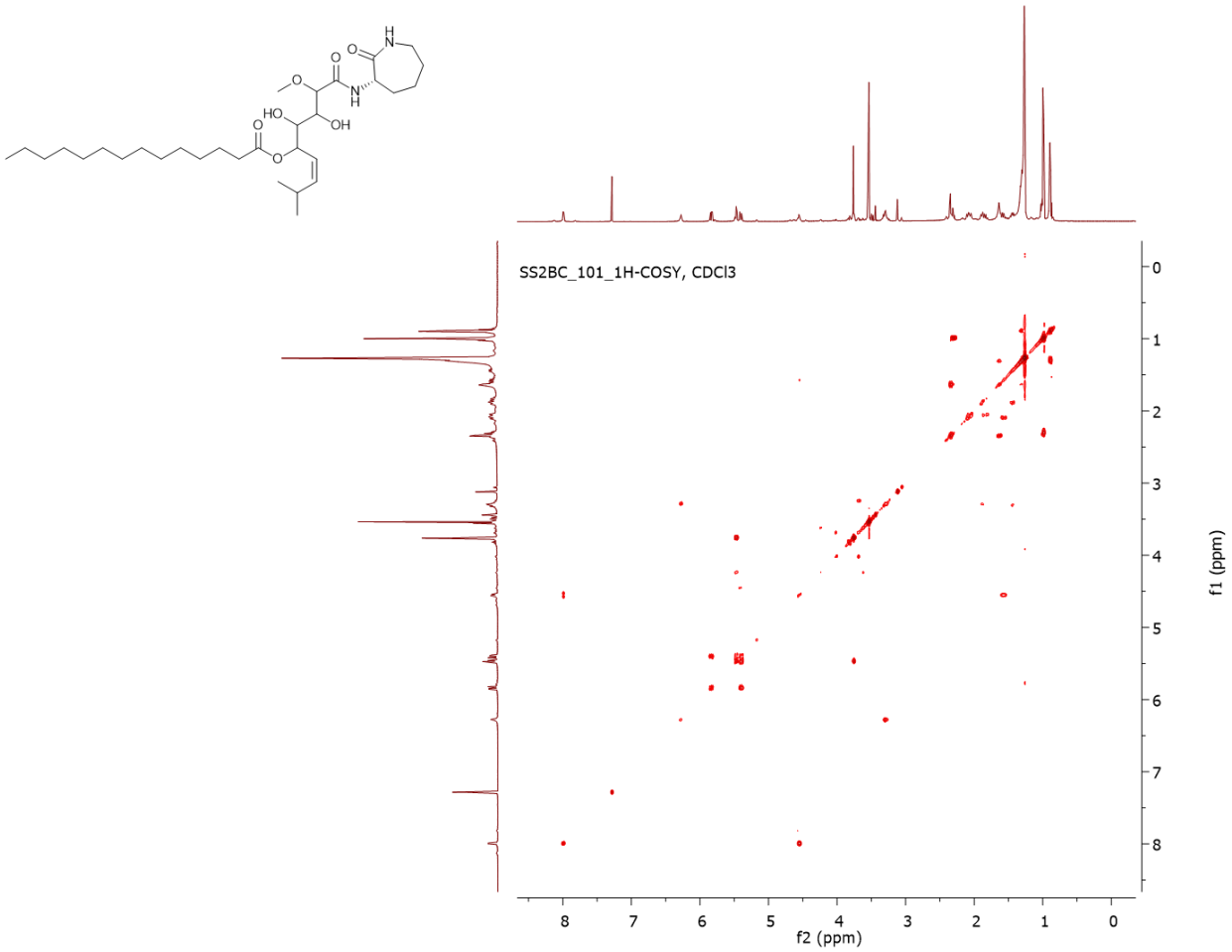

Figure S3.10. ^{1}H-^{1}H COSY spectrum (600MHz, $CDCl_3$, 303K) of bengamide P **3.2**

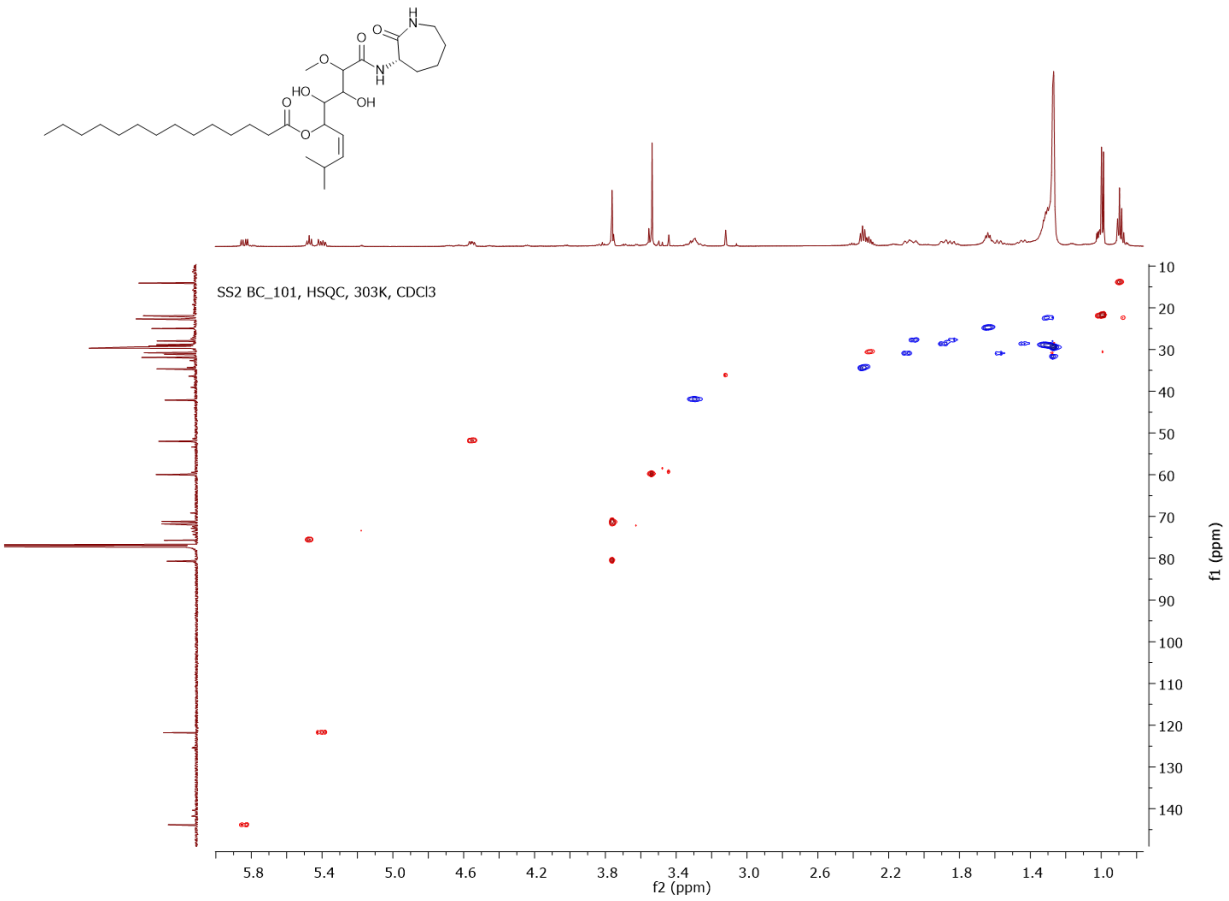

Figure S3.11. HSQC NMR spectrum (600MHz, $CDCl_3$, 303K) of bengamide P **3.2**

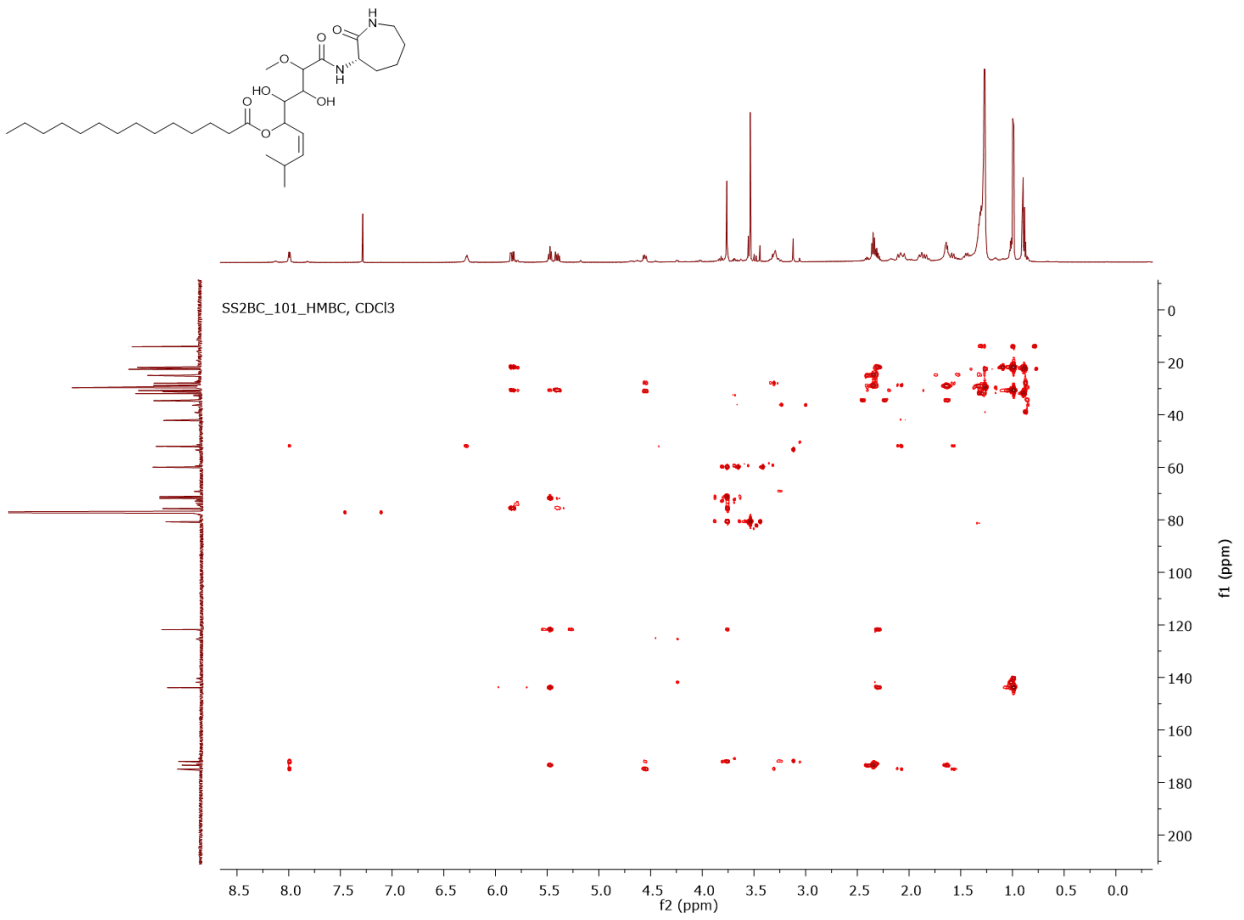

Figure S3.12. HMBC NMR spectrum (600MHz, $CDCl_3$, 303K) of bengamide P **3.2**

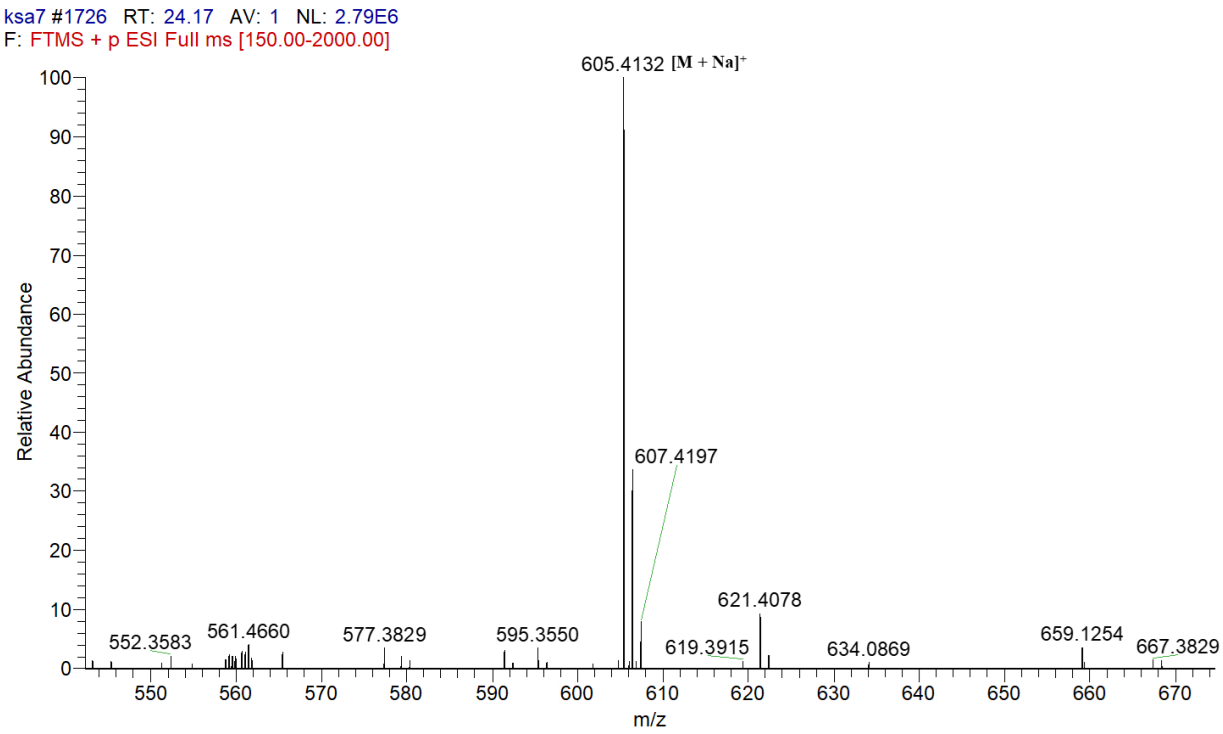

Figure S3.13. HR-ESI-MS spectrum of bengamide Q **3.3**

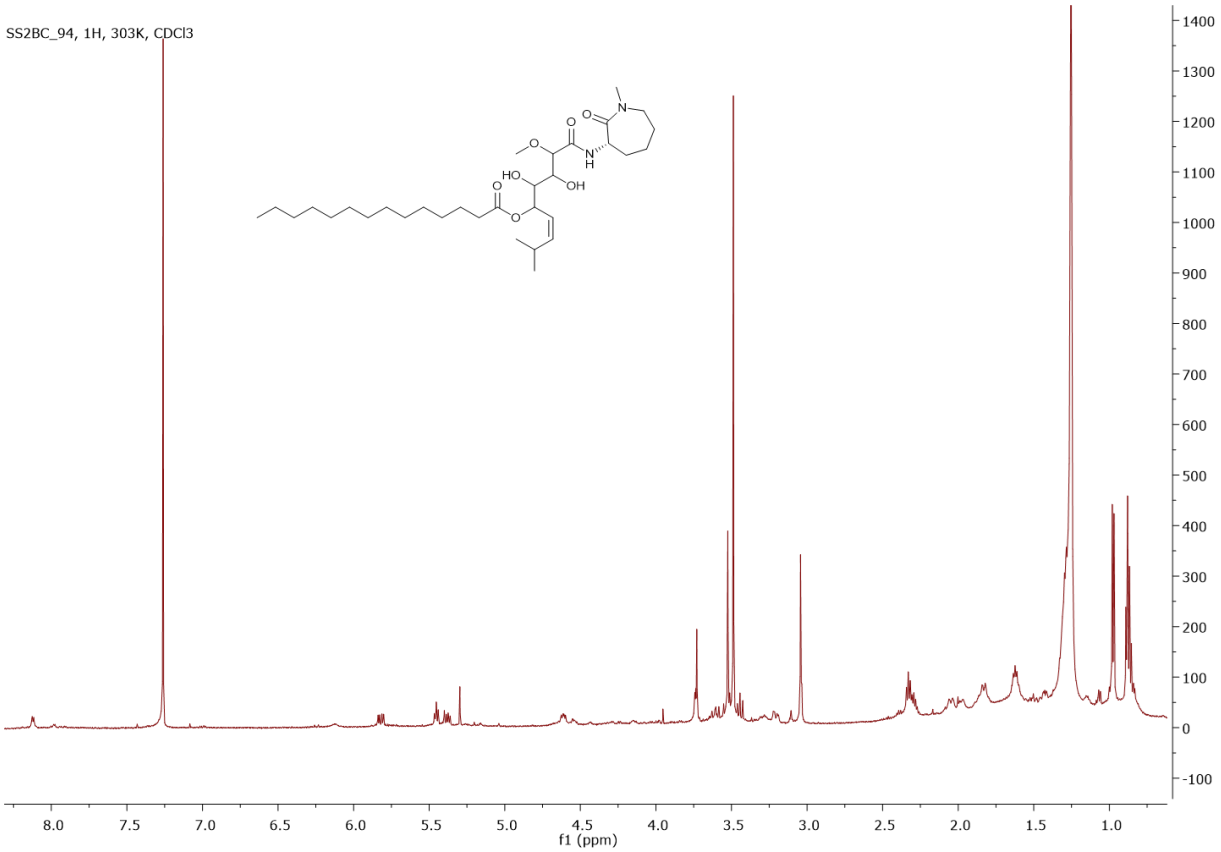

Figure S3.14. ^{1}H-NMR spectrum (600MHz, $CDCl_3$, 303K) of bengamide Q **3.3**

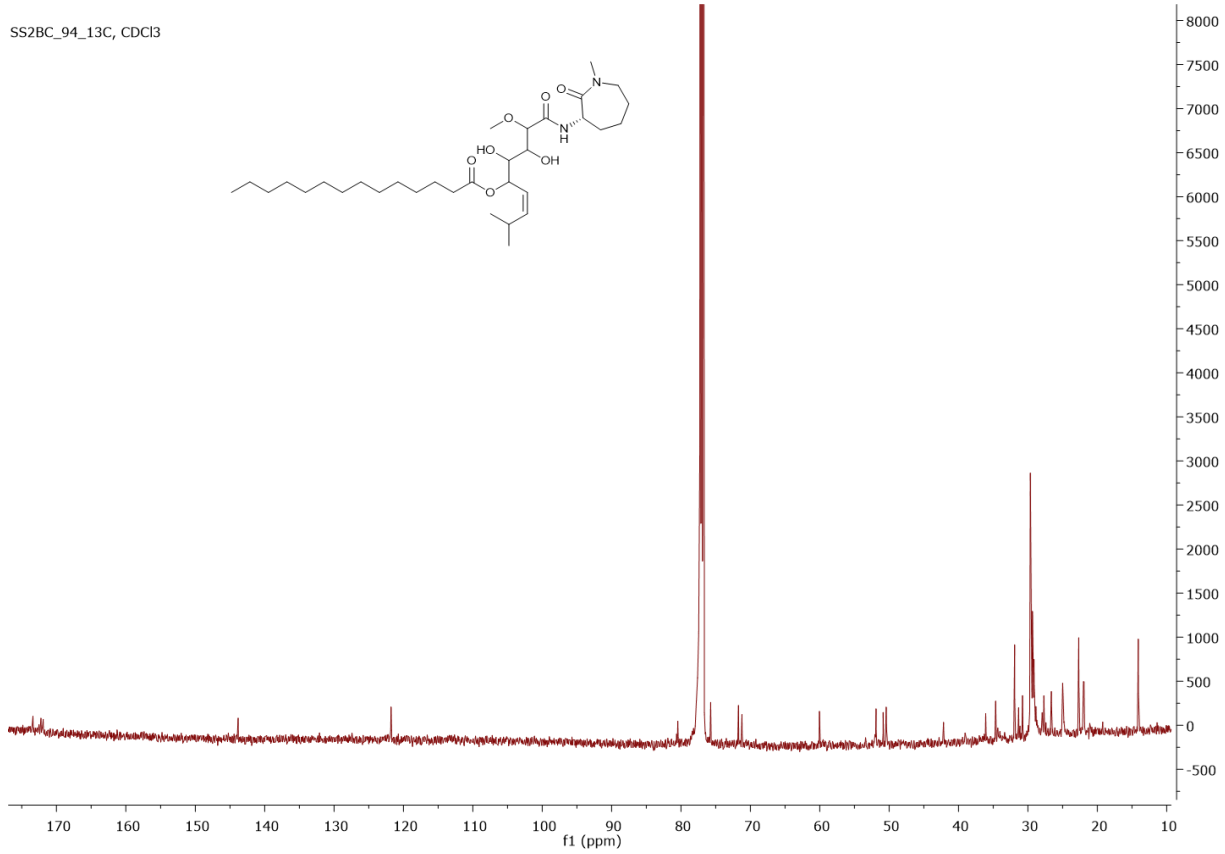

Figure S3.15. ^{13}C-NMR spectrum (150MHz, $CDCl_3$, 303K) of bengamide Q **3.3**

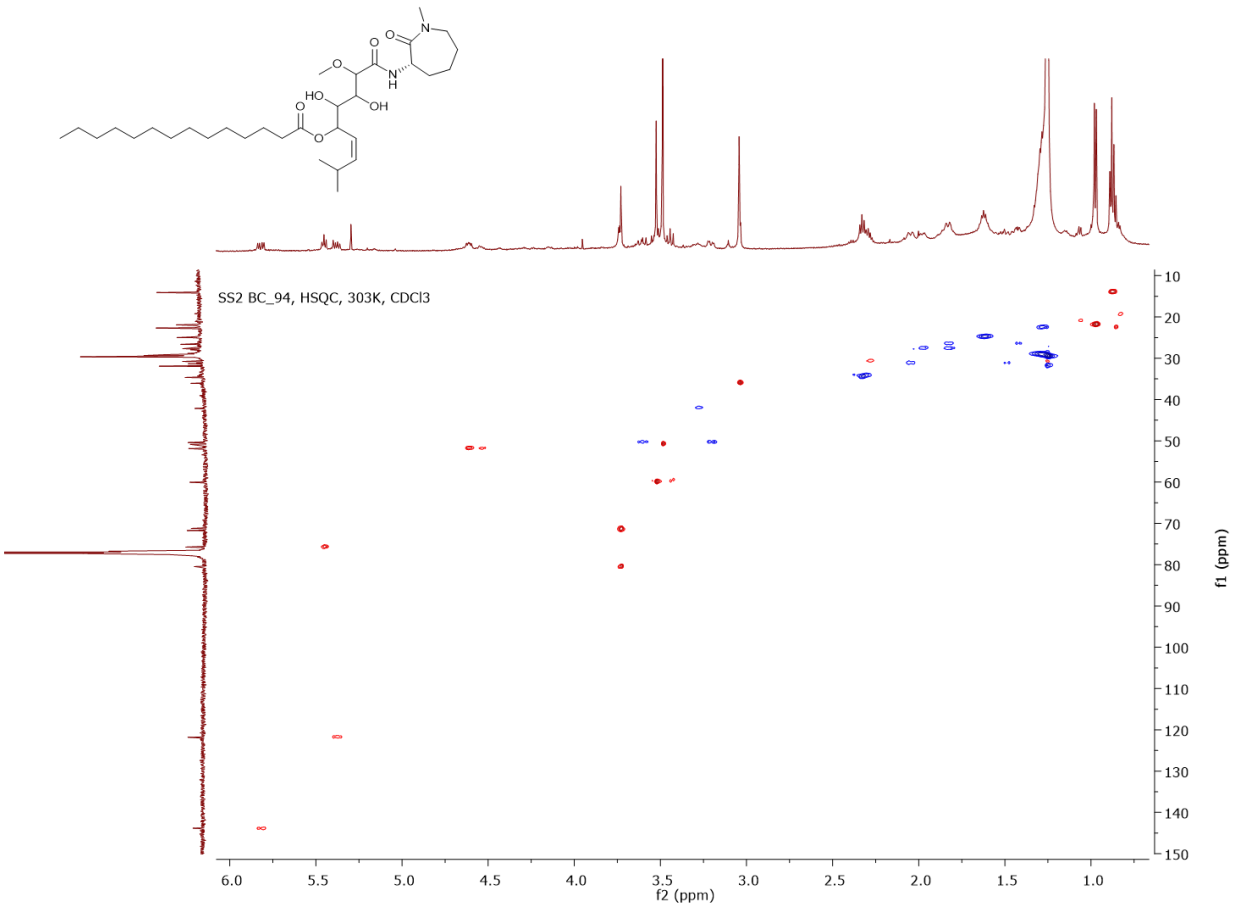

Figure S3.16. HSQC NMR spectrum (600MHz, $CDCl_3$, 303K) bengamide Q **3.3**

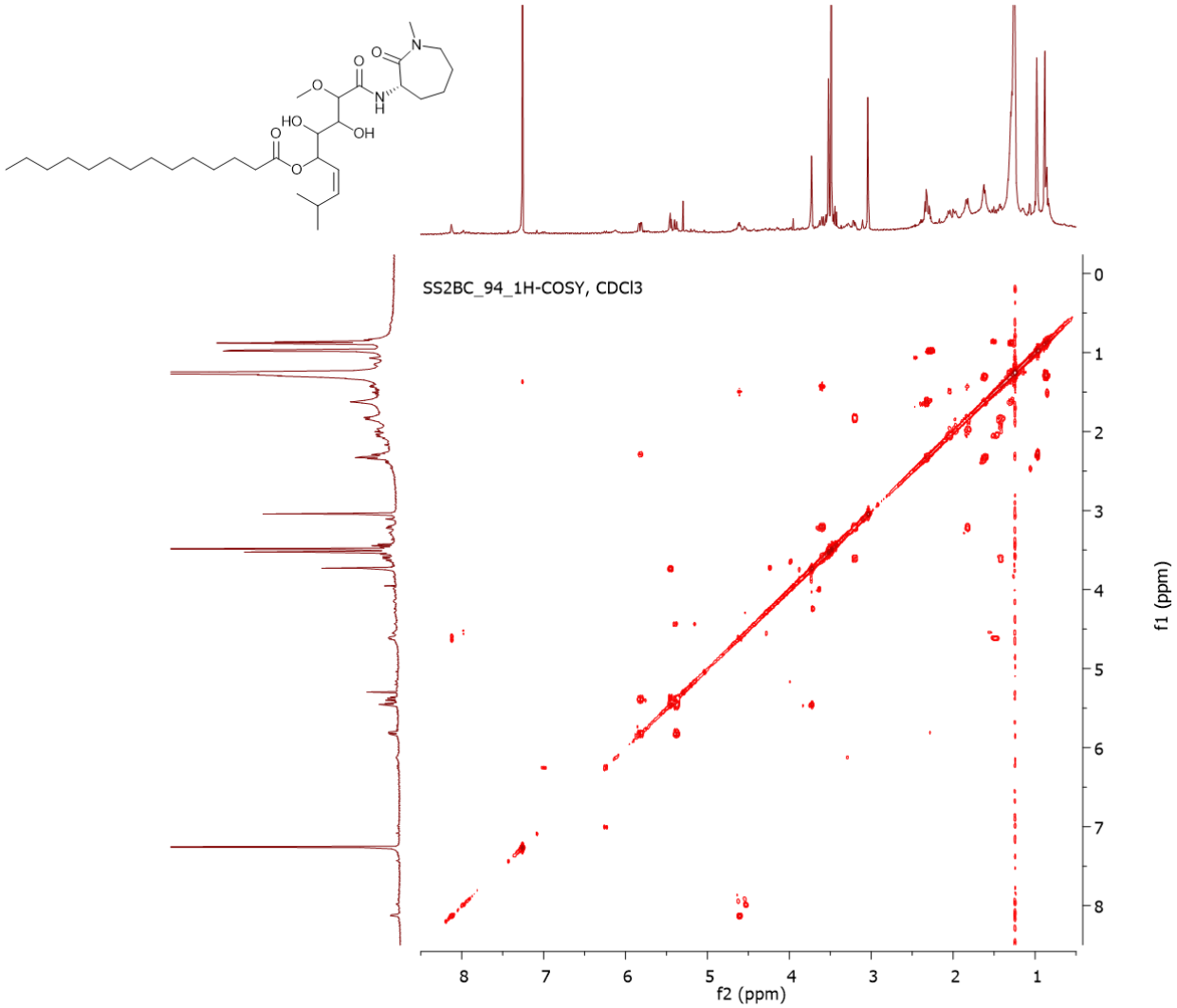

Figure S3.17. ^{1}H-^{1}H COSY spectrum (600MHz, $CDCl_3$, 303K) of bengamide Q **3.3**

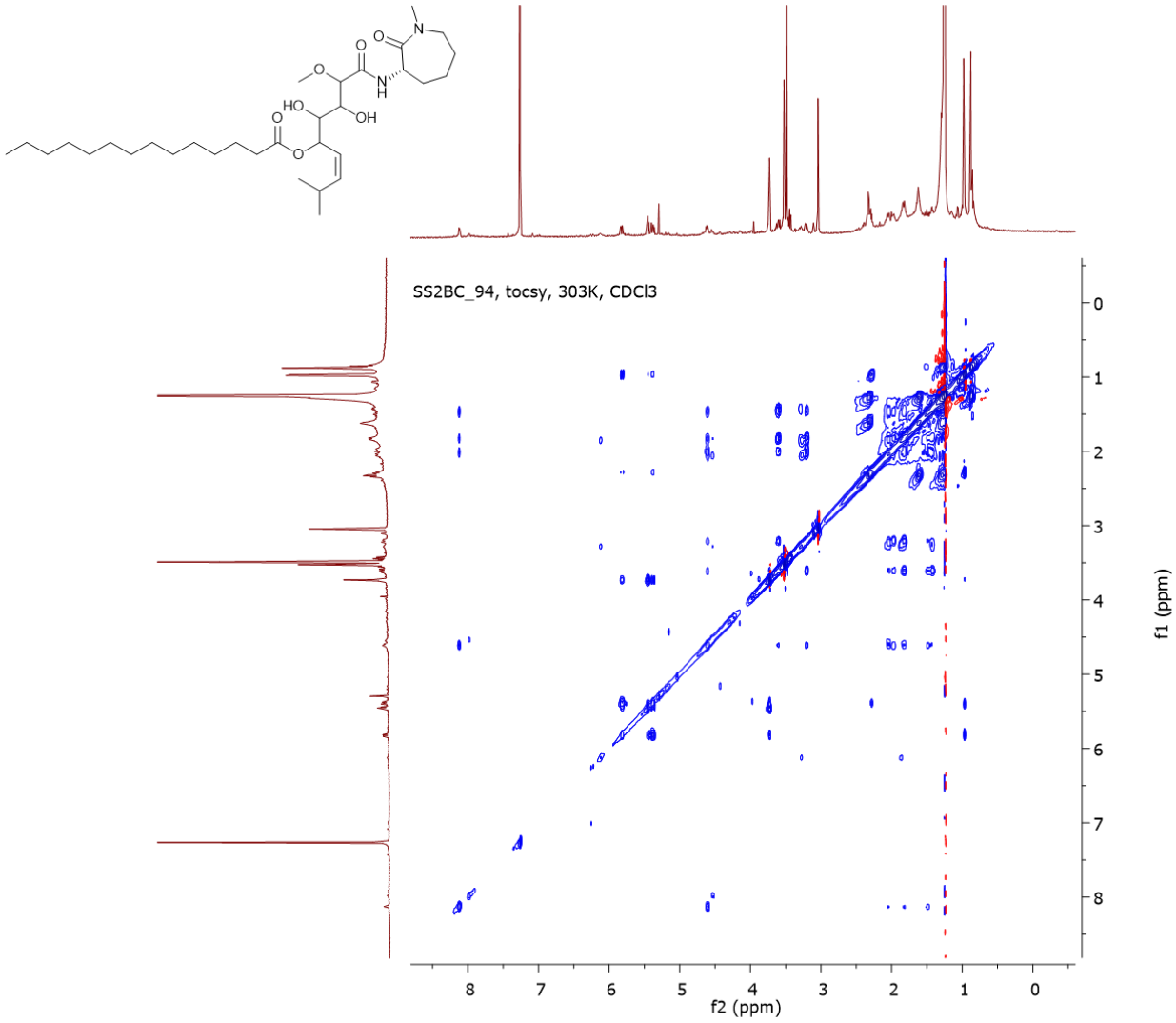

Figure S3.18. ^{1}H-^{1}H TOCSY spectrum (600MHz, $CDCl_3$, 303K) of bengamide Q **3.3**

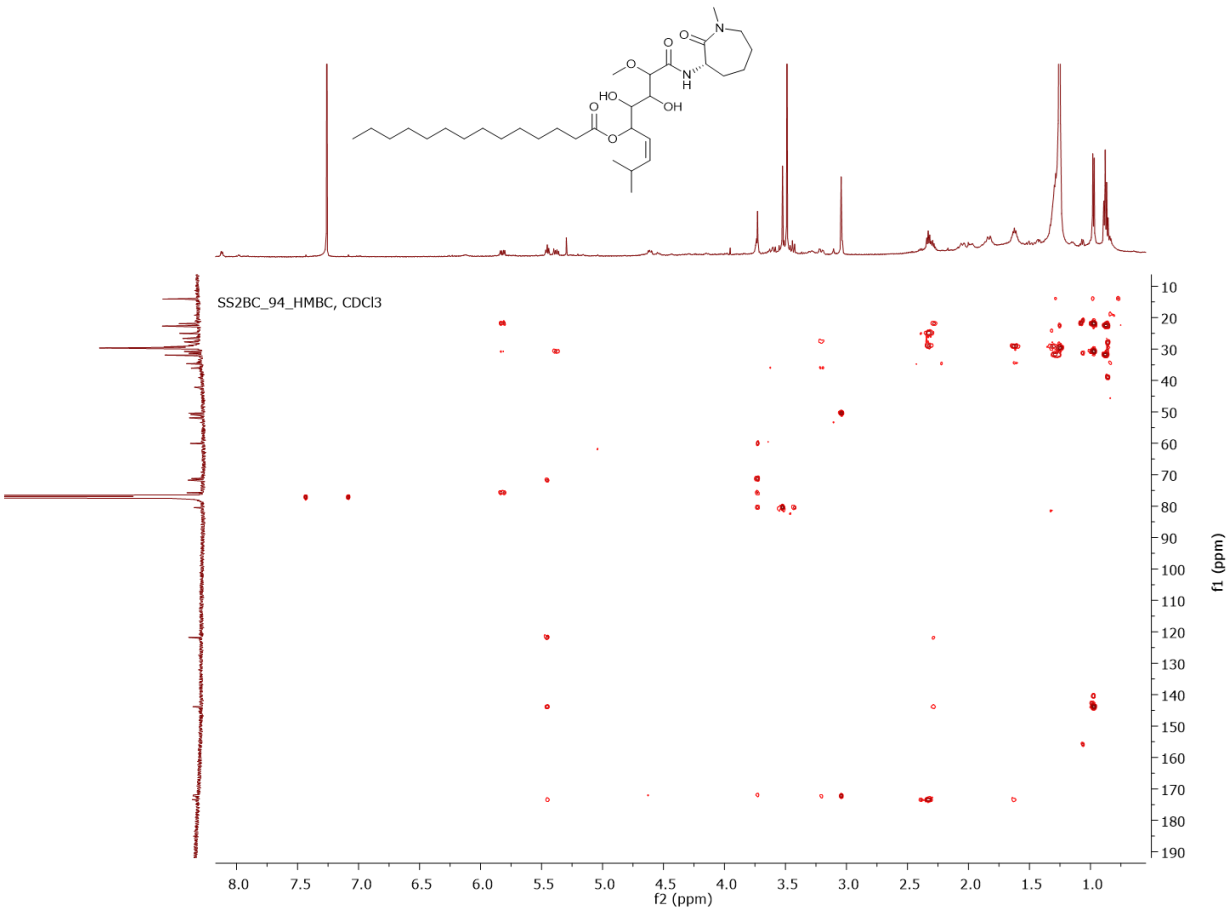

Figure S3.19. HMBC NMR spectrum (600MHz, $CDCl_3$, 303K) of bengamide Q **3.3**

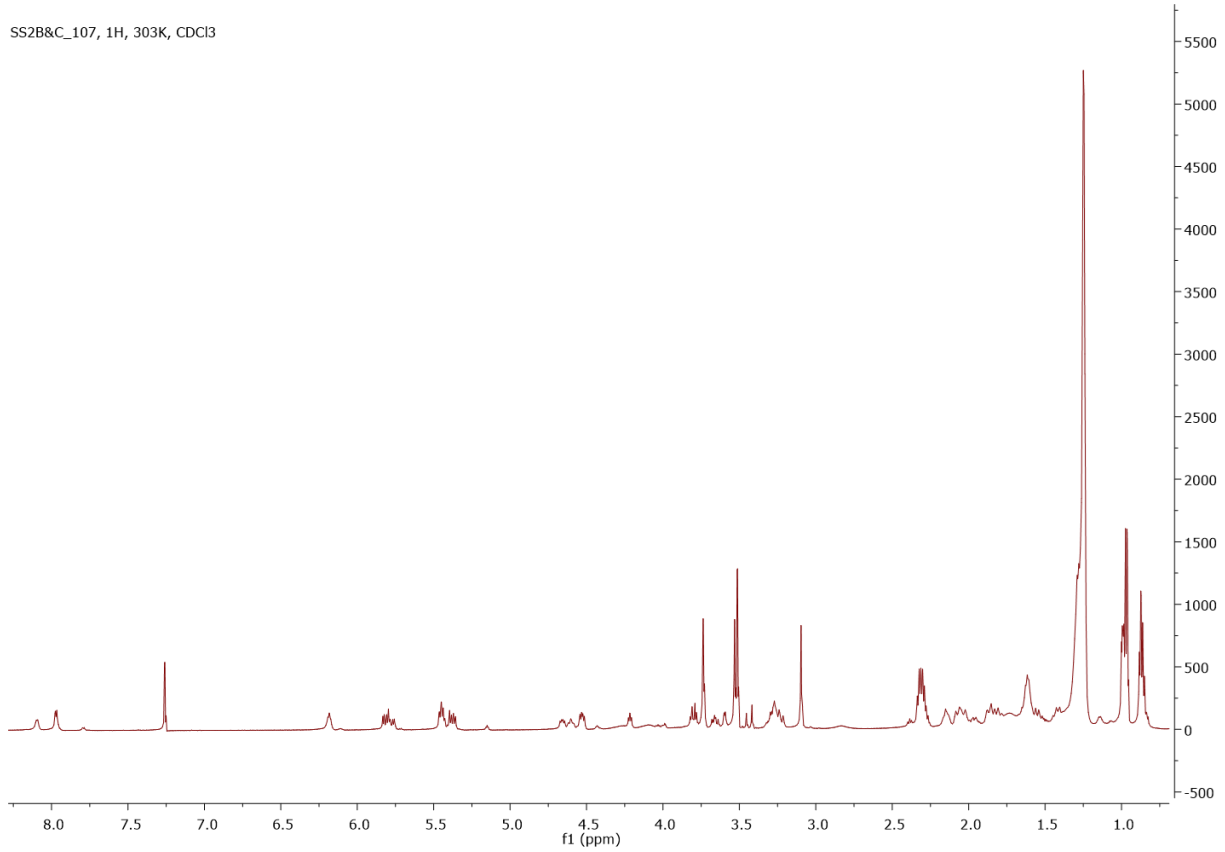

Figure S3.20. ^{1}H-NMR spectrum (600MHz, $CDCl_3$, 303K) of F107

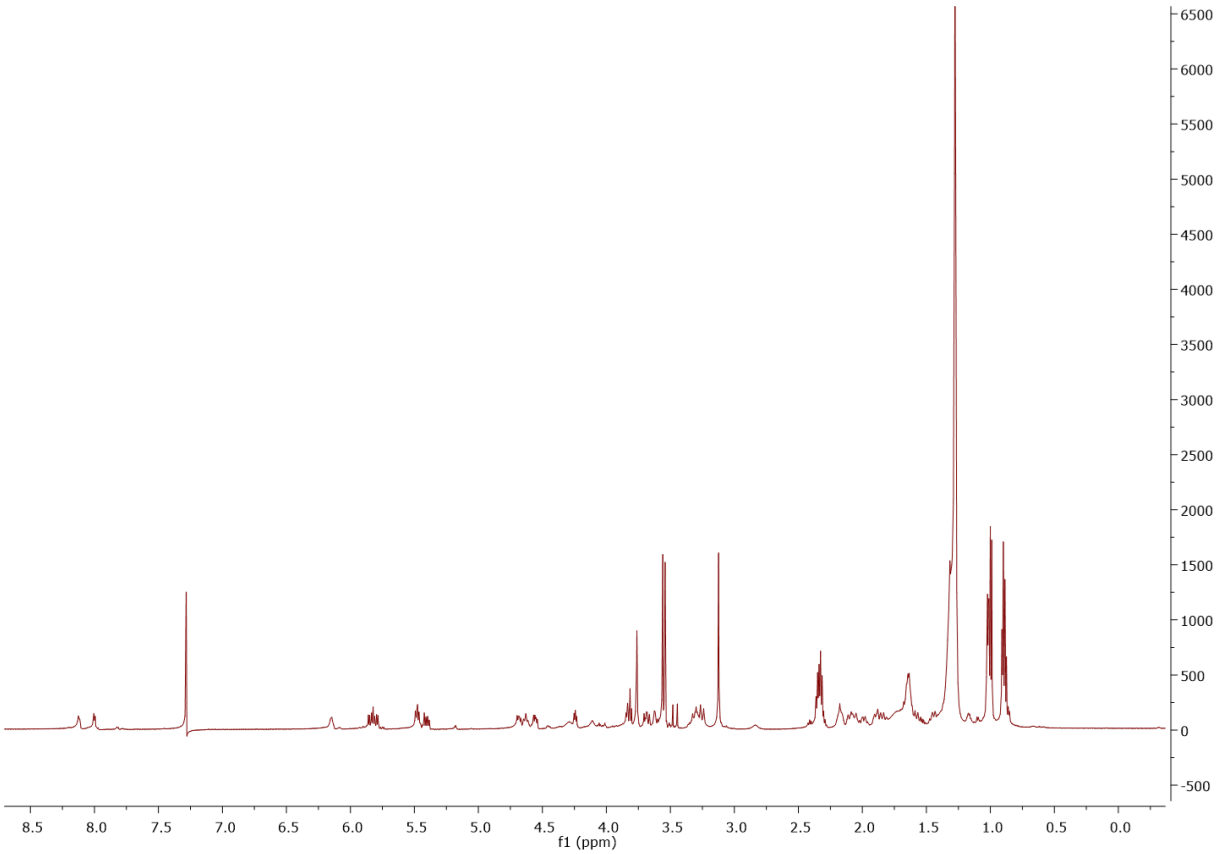

Figure S3.21. ^{1}H-NMR spectrum (600MHz, $CDCl_3$, 303K) of F114

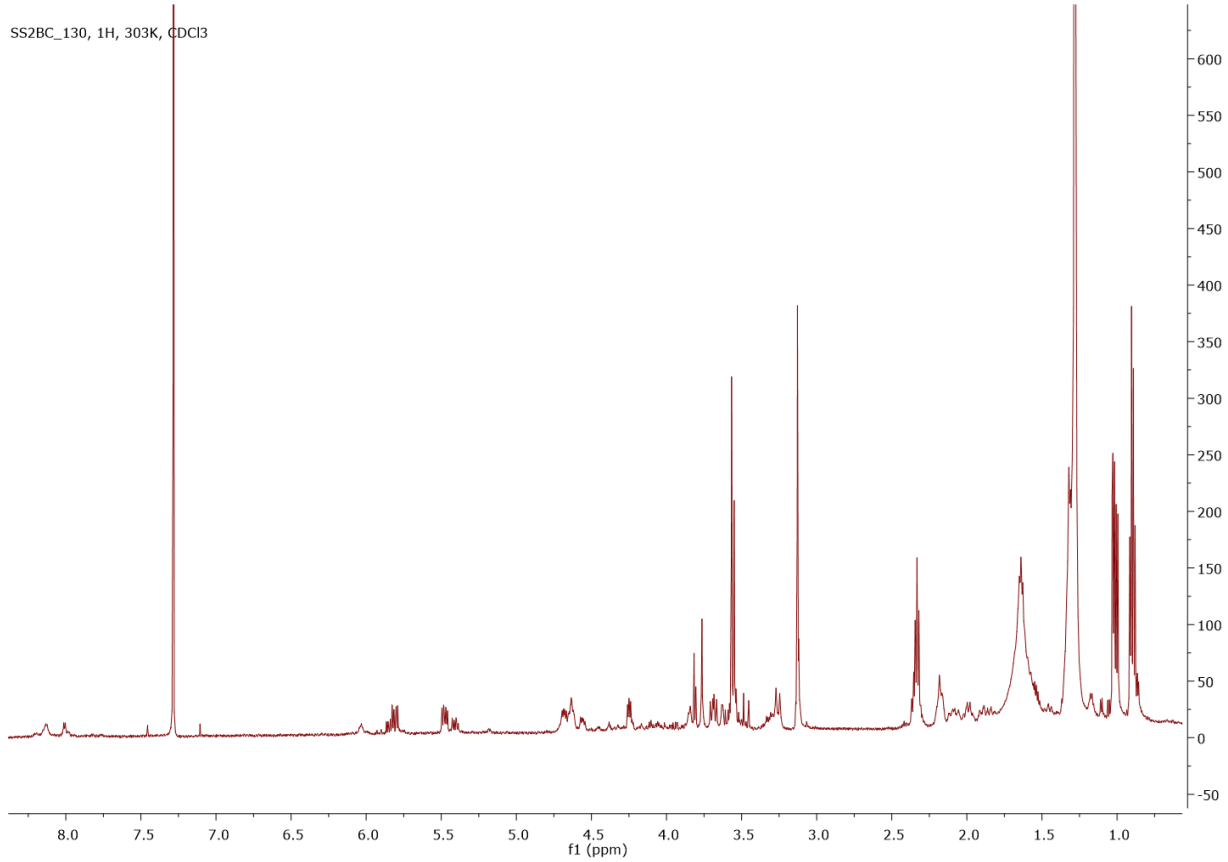

Figure S3.22. ^{1}H-NMR spectrum (600MHz, $CDCl_3$, 303K) of F130

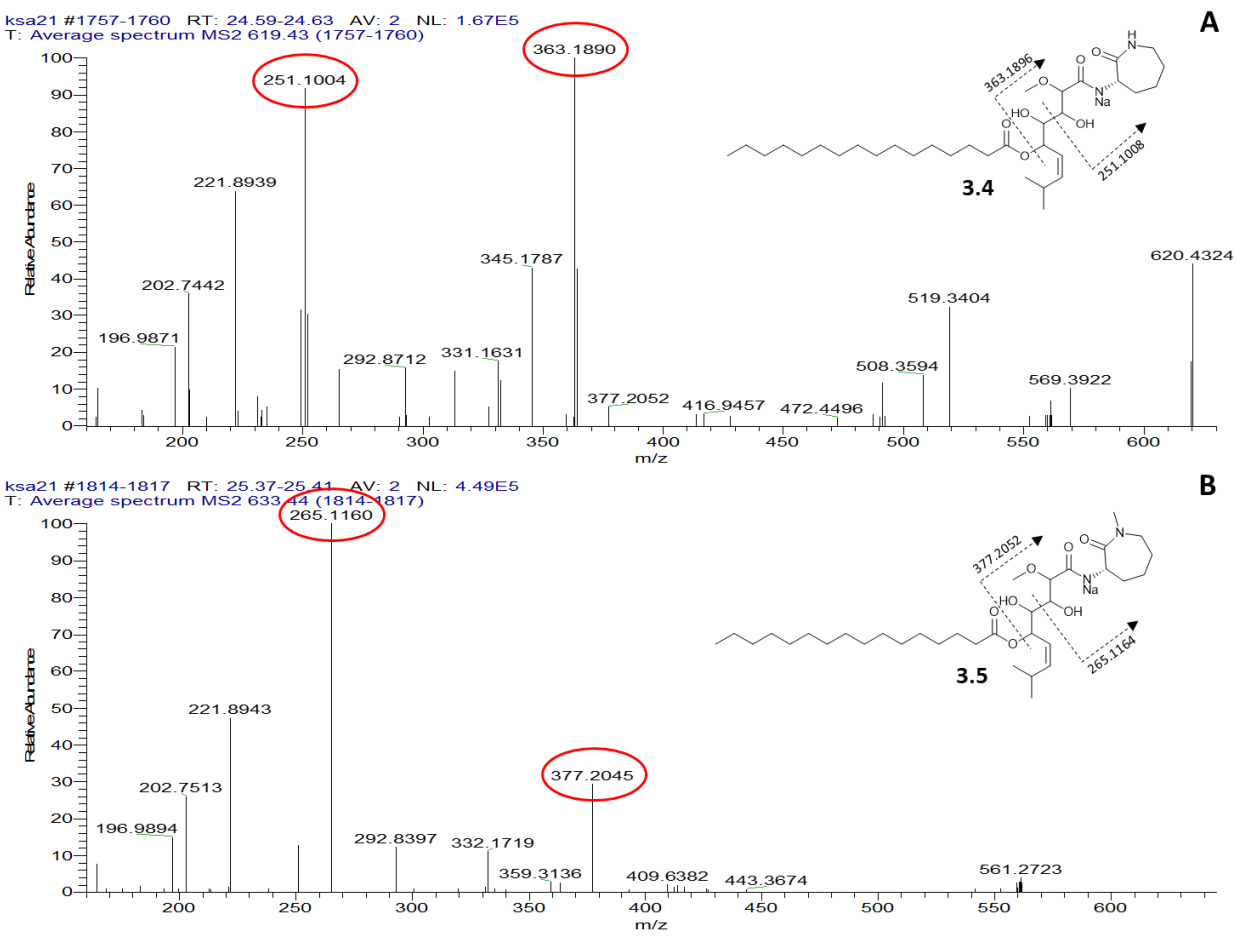

Figure S3.23. MS/MS fragmentation pattern of bengamide R **3.4** (A) and bengamide S **3.5** (B) with fragment ions circled in red showing methylation is on the nitrogen of the caprolactam ring.

Table S3.1. ^{13}C and ^{1}H chemical shifts of Heteronemin **3.1** isolated and that reported in literature.

	Isolated		Literature[1,2]	
Position	^{13}C	^{1}H, mult. (*J*, Hz)	^{13}C	^{1}H, mult. (*J*, Hz)
1	39.9	1.69 0.78	39.9	
2	18.2	1.53 1.36	18.2	
3	42.1	1.37 td J=4.03, 13.45, 13.51 1.11	42.0	
4	33.2		33.2	
5	56.5	0.78	56.5	
6	18.6	1.60 1.42	18.6	
7	41.9	1.73 0.91	41.8	
8	37.4		37.4	
9	58.8	0.78	58.8	
10	38.1		38.1	
11	27.2	1.69 1.46	27.2	
12	80.6	3.45 dd *J*=3.99, 11.37	80.5	3.44, dt, J =3.8.11.3
13	42.7		42.7	
14	54.8	0.92	54.7	
15	28.0	2.05 1.40	28.0	
16	69.4	5.36 dd J=6.06, 10.43	69.3	5.38 (dd,J = 4,10Hz)
17	114.4		114.4	
18	64.2	2.42	64.2	2.42
19	101.7	6.76 d *J*=1.38	101.6	6.77 (d, J= 1.3 Hz)
20	135.4	6.15 t *J*=1.93	135.3	6.17 (t, J = 2 Hz)
21	33.3	0.84	33.2	0.87
22	21.3	0.79	21.3	0.77
23	16.3	0.82	16.3	0.79
24	17.3	0.82	17.3	0.81
25	8.8	0.90	8.8	0.81
OAc	21.4	2.09	21.2	2.07
OAc	21.0	2.09	21.0	2.07
CO	171.3		171.3	
CO	170.1		170.1	

Table S3.2. ^{13}C and ^{1}H chemical shifts of bengamide P **3.2** isolated and that reported in literature.

	Isolated		Literature[3]	
Position	^{13}C	^{1}H, mult. (*J*, Hz)	^{13}C	^{1}H, mult. (*J*, Hz)
17	174.9		175.1	
16	173.3		173.6	
9	172.0		172.2	
3	143.8	5.84 (1H, dd, J= 6.47, 15.42 Hz)	144.1	5.83 (1H, dd, J= 6.5, 16.0 Hz)
4	121.8	5.40 (1H, dd, J= 7.84, 15.41 Hz)	122.0	5.39 (1H, dd, J= 7.5, 16.0 Hz)
8	80.7	3.76 (1H, bs)	80.8	3.74 (1H, bs)
5	75.7	5.47 (1H, t= 7.60 Hz)	75.9	5.47 (1H, t= 7.5 Hz)
7	71.8	3.75 (1H, bs)	72.0	3.74 (1H, bs)
6	71.2	3.75 (1H, bs)	71.4	3.74 (1H, bs)
13	28.8	1.88 (1H, m) 1.43 (1H, m)	29.1	1.86 (1H, m) 1.43 (1H, m)
OMe	60.0	3.53 (3H, s)	60.2	3.53 (3H, s)
10	52.0	4.55 (1H, m)	52.2	4.54 (1H, m)
14	42.1	3.29 (2H, m)	42.3	3.29 (2H, m)
18	34.6	2.34 (2H, t, J=7.32)	34.9	2.34 (2H, t, J=7.5)
12	27.9	2.05 (1H, m) 1.84 (1H, m)	28.2	2.07 (1H, m) 1.86 (1H, m)
28	31.9	1.27 (2H, m)	32.1	1.26 (2H, m)
2	30.9	2.30 (1H, m)	30.0	2.34 (1H, m)
20-27	30.8-29.1	1.27 (16H, m)	30.0-29.3	1.26 (16H, m)
11	31.1	2.09 (1H, m) 1.56 (1H, m)	31.4	2.07 (1H, m) 1.60 (1H, m)
19	25.0	1.64 (2H, m)	25.2	1.60 (2H, m)
29	22.8	1.28 (2H, m)	22.9	1.26 (2H, m)
1,15	21.9, 22.0	0.99 (6H, d J=6.88 Hz)	22.1,22.2	0.98 (6H, d J=7.0 Hz)
30	14.1	0.88 (3H, t J=7.08 Hz)	14.3	0.89 (3H, t J=7.0 Hz)

Table S3.3. ^{13}C and ^{1}H chemical shifts of bengamide Q **3.3** isolated and that reported in literature.

	Isolated		Literature[3]	
Position	^{13}C	^{1}H, mult. (J, Hz)	^{13}C	^{1}H, mult. (J, Hz)
17	173.4		173.6	
16	172.2		172.4	
9	171.9		172.1	
3	143.8	5.82 (1H, dd, J=6.47, 15.42 Hz)	144.0	5.83 (1H, dd, J=6.5, 16.0 Hz)
4	121.8	5.38 (1H, dd, J=7.92, 15.39 Hz)	122.0	5.39 (1H, dd, J=7.5, 16.0 Hz)
8	80.4	3.74 (1H, bs)	80.6	3.74 (1H, bs)
5	75.7	5.45 (1H, t, J=7.64 Hz)	75.9	5.46 (1H, t, J=7.5 Hz)
7	71.7	3.72 (1H, bs)	71.9	3.74 (1H, bs)
6	71.2	3.72 (1H, bs)	71.4	3.74 (1H, bs)
13	26.6	1.82 (1H, m) 1.42 (1H, m)	27.9	1.84 (1H, m) 1.47 (1H, m)
OMe	60.1	3.50 (3H, s)	60.3	3.54 (3H, s)
10	51.6	4.61 (1H, m)	50.6	4.62 (1H, m)
NMe	36.1	3.03 (3H, s)	36.3	3.05 (3H, s)
14	50.4	3.60 (1H, dd, J=15.50, 11.51) 3.21 (1H, dd, J=5.45, 15.53)	52.1	3.62 (1H, dd, J=15.5, 11.5) 3.22 (1H, dd, J=5.5, 15.5)
18	34.7	2.32 (2H, m)	34.9	2.34 (2H, t, J=7.5)
12	27.7	1.97 (1H, m) 1.82 (1H, m)	26.8	2.02 (1H, m) 1.84 (1H, m)
28	31.9	1.25 (2H, m)	32.1	1.26 (2H, m)
2	30.8	2.28 (1H, m)	31.0	2.34 (1H, m)
20-27	29.7-29.2	1.26 (16H, m)	29.9-29.3	1.26 (16H, m)
11	31.4	2.04 (1H, m) 1.49 (1H, m)	31.5	2.02 (1H, m) 1.63 (1H, m)
19	25.0	1.62 (2H, m)	25.2	1.63 (2H, m)
29	22.7	1.27 (2H, m)	22.9	1.26 (2H, m)
1,15	22.0, 21.9	0.97 (6H, d J=6.74 Hz)	22.2-22.1	0.98 (6H, d J=6.5 Hz)
30	14.3	0.87 (3H, t J=6.81 Hz)	14.3	0.89 (3H, t J=6.5 Hz)

Table S3.4. Compounds isolated and tentatively identified in the molecular cluster of the crude extract (SS2) of the sponge *Jaspis splendens* with their corresponding masses (observed and calculated), molecular formulae (MF), and mass error (ID (Δ ppm))

Compound	m/z ($[M+Na]^+$) Observed	m/z ($[M+Na]^+$) Calculated	MF	ID Δ ppm
Bengamide P **3.2**	591.3978	591.3966	$C_{31}H_{56}N_2O_7$	2.03
Bengamide Q **3.3**	605.4133	605.4122	$C_{32}H_{58}N_2O_7$	1.82
Bengamide A **3.8** Bengamide N **3.20** Bengamide H **3.15**	607.3928	607.3915	$C_{31}H_{56}N_2O_8$	2.14
Bengamide R **3.4**	619.4286	619.4279	$C_{33}H_{60}N_2O_7$	1.13
Bengamide B **3.9** Bengamide I **3.16** Bengamide L **3.18** Bengamide O **3.21**	621.4084	621.4071	$C_{32}H_{59}N_2O_8$	2.09
Bengamide J **3.17** Bengamide M **3.19**	635.4233	635.4228	$C_{33}H_{60}N_2O_8$	0.78
Bengamide S **3.5**	633.4446	633.4455	$C_{34}H_{62}N_2O_7$	-1.42

References

1. Kazlauskas, R., Murphy,, P. T., Quinn, R. J., Wells, R. J. Heteronemin, a new Scalarin type Sesterterpene from the Sponge Heteronema erecta. *Tetrahedron Lett.* 2631–2634 (1976).

2. Bourguet-Kondracki, M. L., Martin, M. T., Debitus, C., Guyot, M. 12-epi-Heteroaemin : New Sesterterpene From Sponge the marine sponge Hyrtios erecta. *Tetrahedron Lett.* **35**, 109–110 (1994).

3. Thale, Z. *et al.* Bengamides Revisited : New Structures and Antitumor Studies. *J. Org. Chem.* 66, 1733–1741 (2001).

Appendix for Chapter Four

Figure S4.1. *Streptomyces* strain Muiz4Y growing on an ISP2 agar plate.

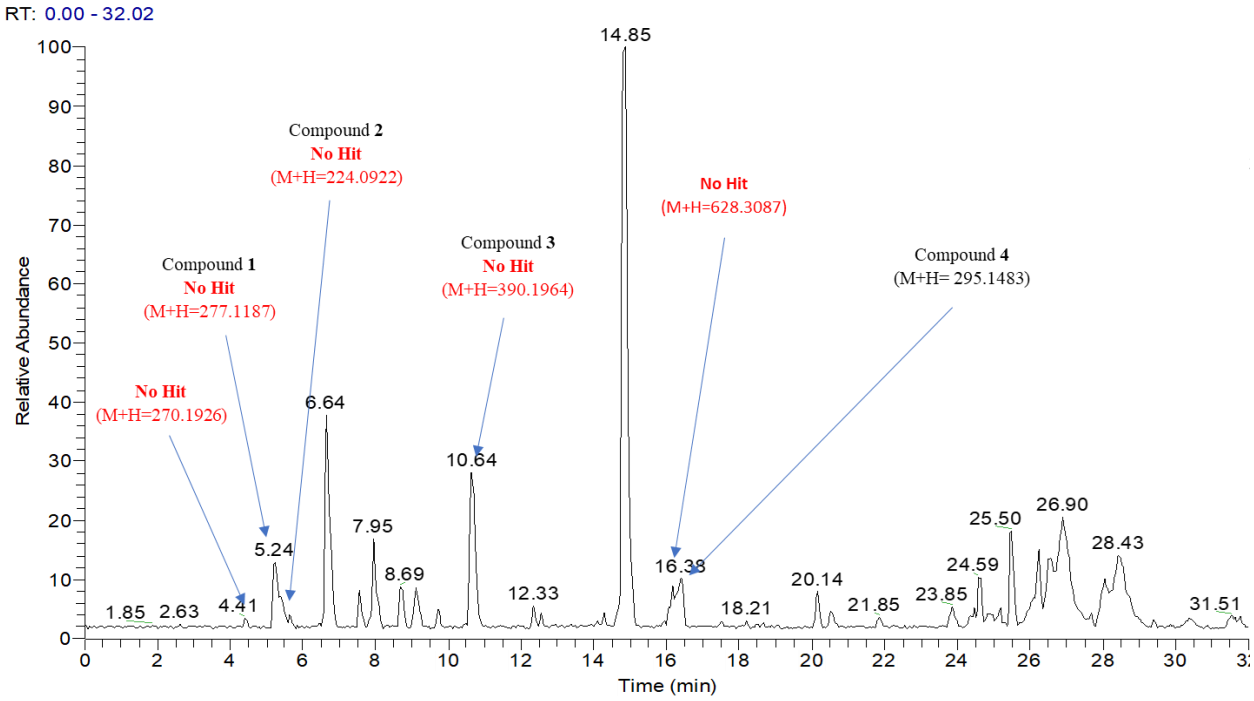

Figure S4.2. Dereplication: MS window of LCMS profile showing peaks, exact masses and retention times for compounds. Those in red gave no hits when the masses were entered in the natural product database Antibase.

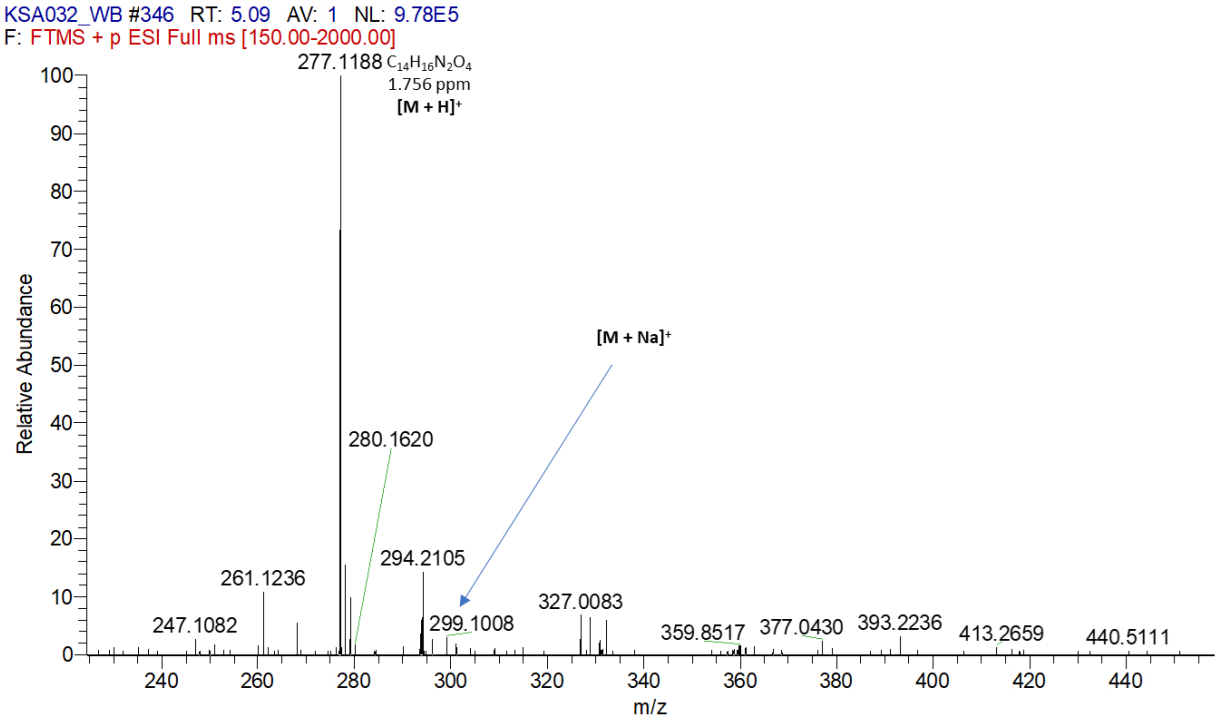

Figure S4.3. HR-ESI-MS spectrum of compound **4.1**

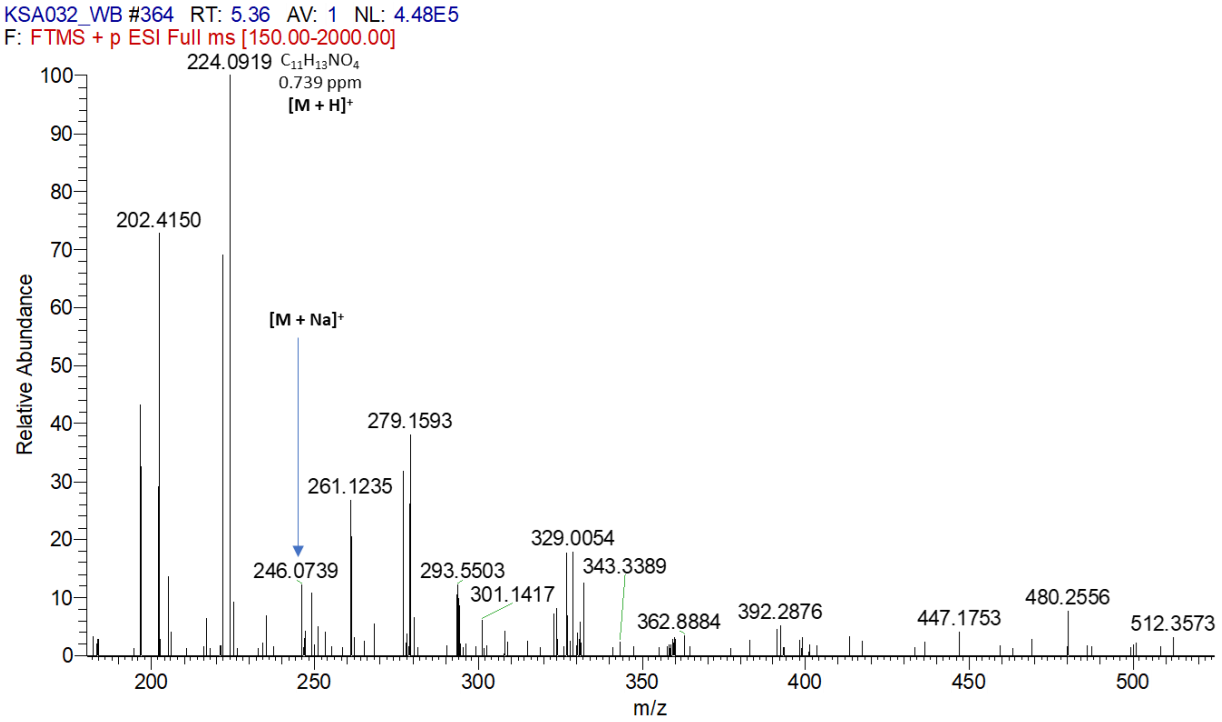

Figure S4.4. HR-ESI-MS spectrum of compound **4.2**

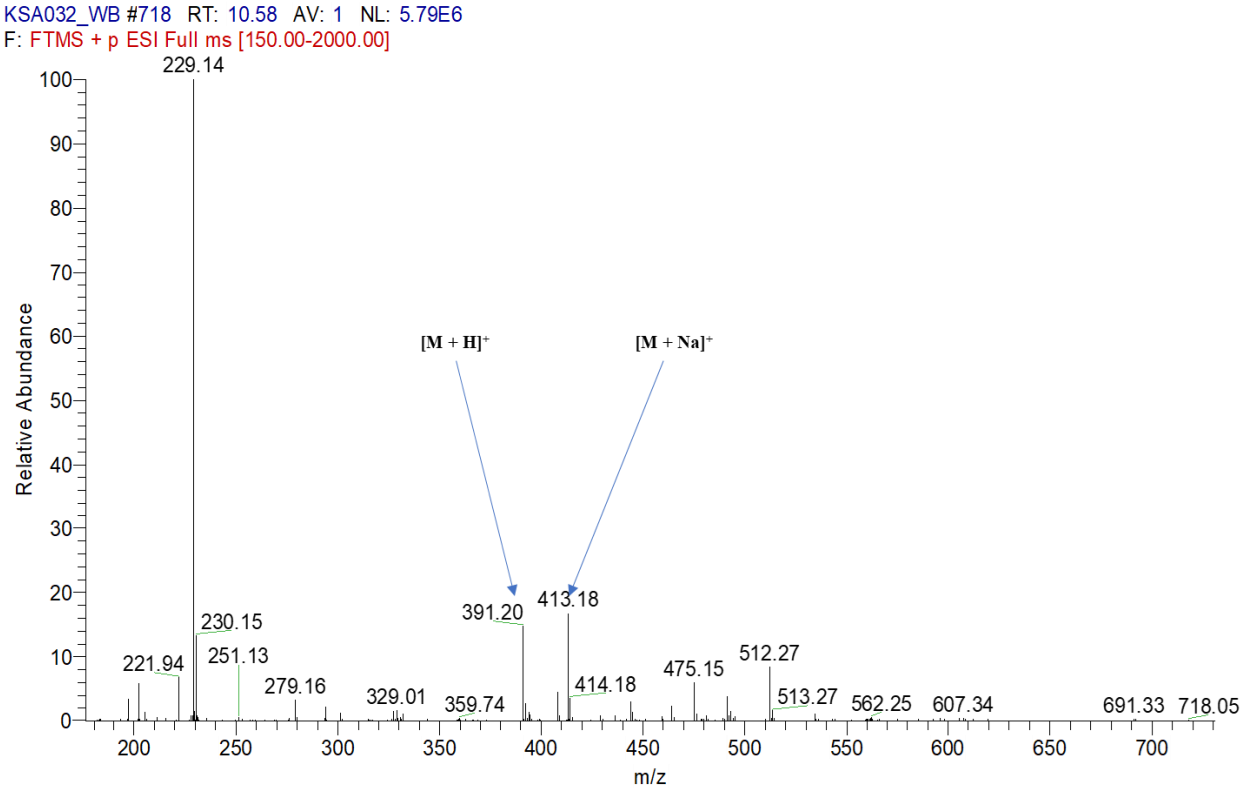

Figure S4.5. HR-ESI-MS spectrum of compound **4.3**

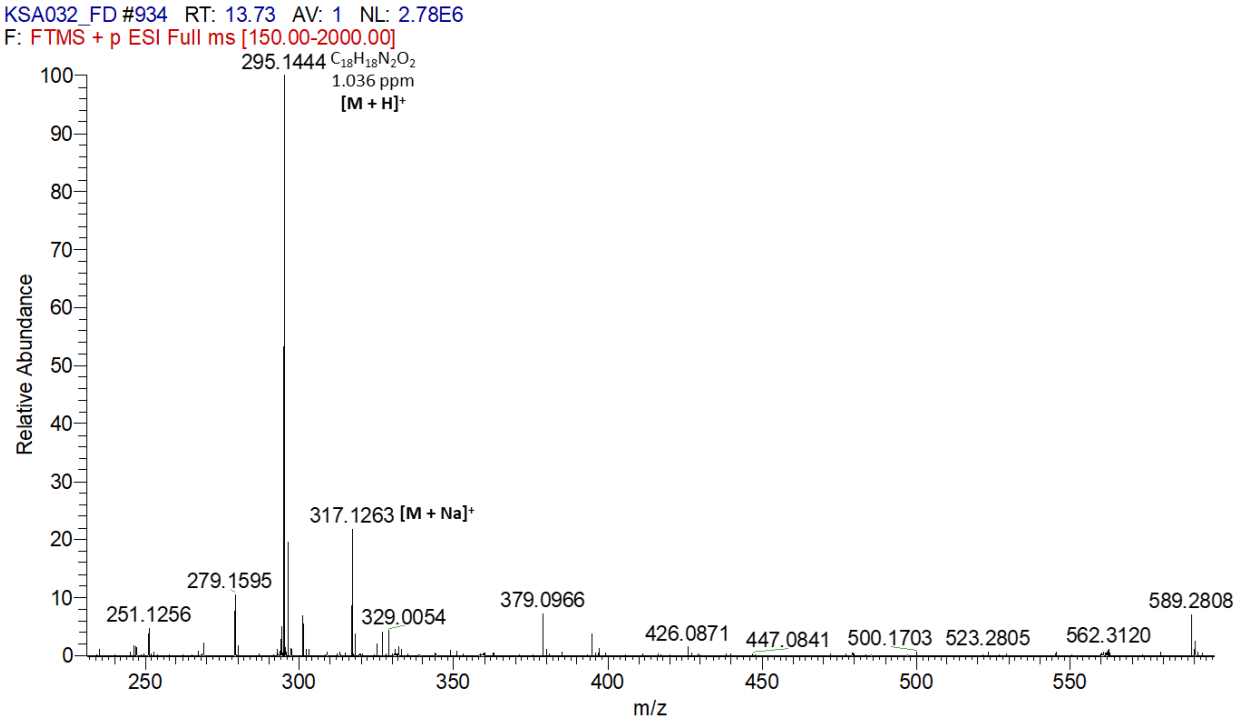

Figure S4.6. HR-ESI-MS spectrum of compound **4.4**

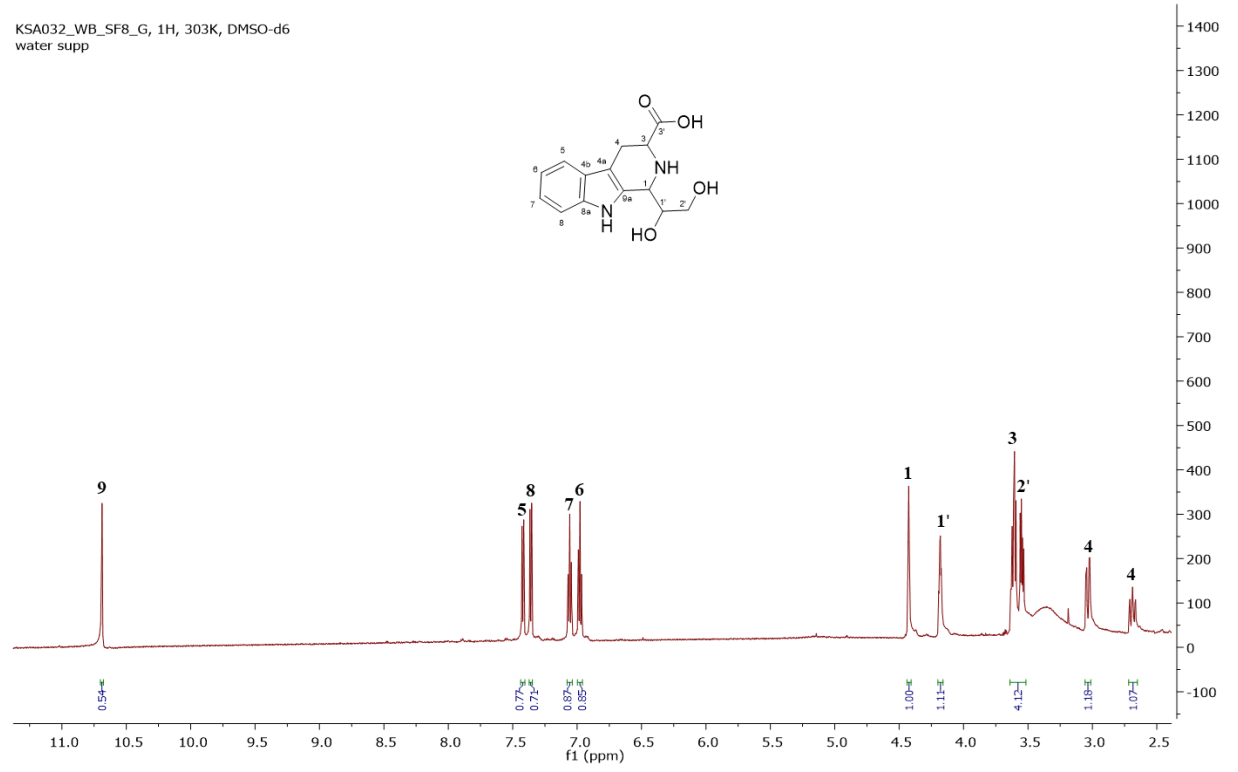

Figure S4.7. ^{1}H-NMR spectrum (600MHz, DMSO-d_6, 303K) of compound **4.1**

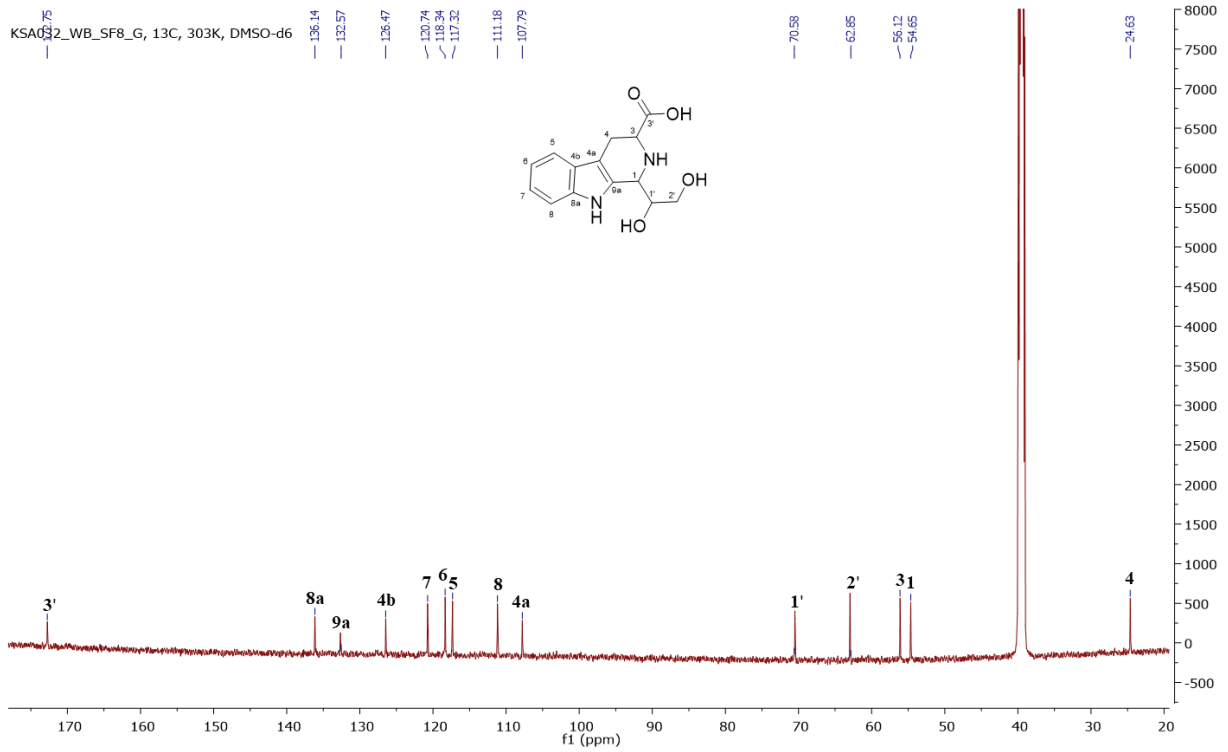

Figure S4.8. ^{13}C-NMR spectrum (150MHz, DMSO-d_6, 303K) of compound **4.1**

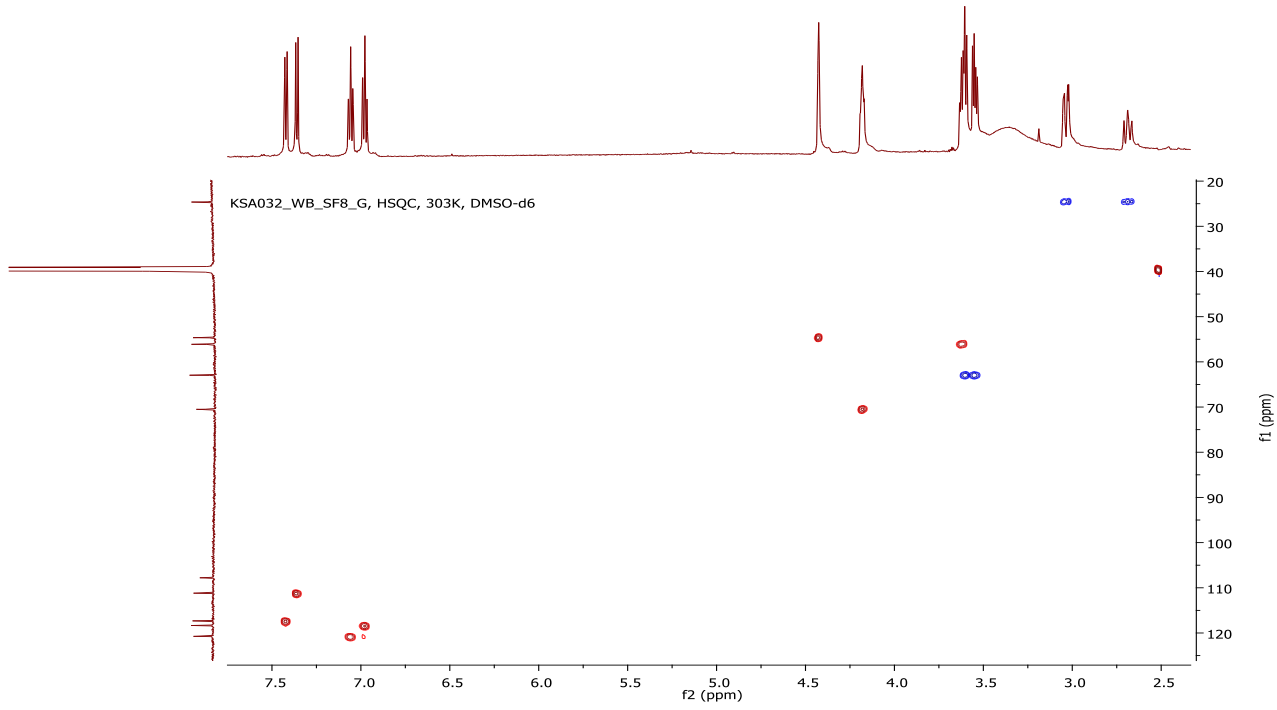

Figure S4.9. HSQC-DEPT NMR spectrum (600MHz, DMSO-d_6, 303K) of compound **4.1**

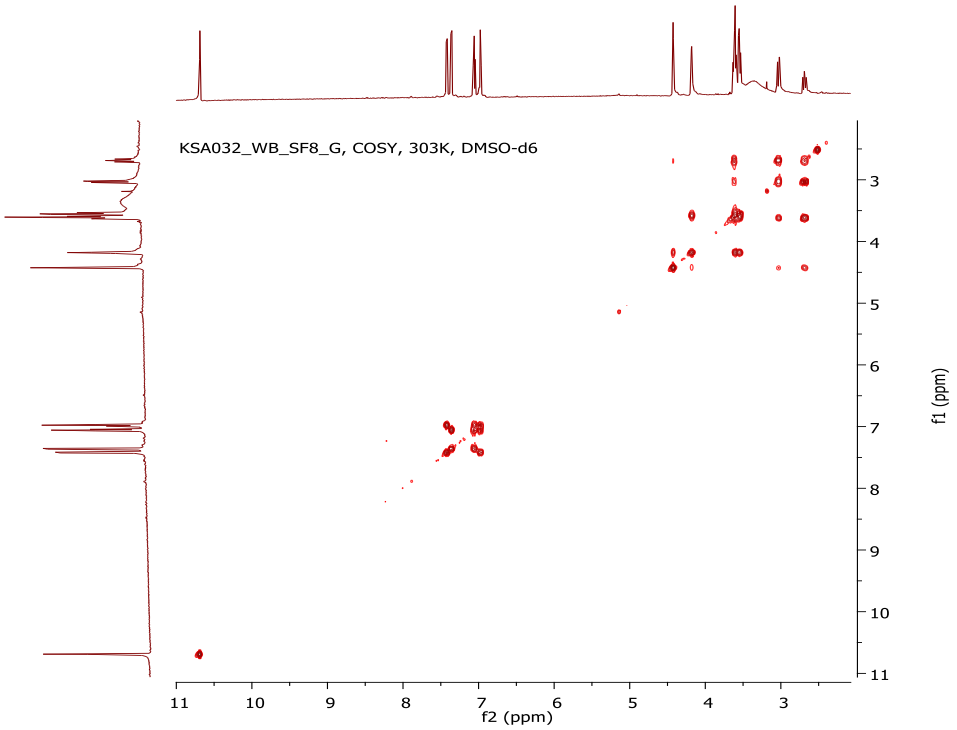

Figure S4.10. ^{1}H-^{1}H COSY spectrum (600MHz, DMSO-d_6, 303K) of compound **4.1**

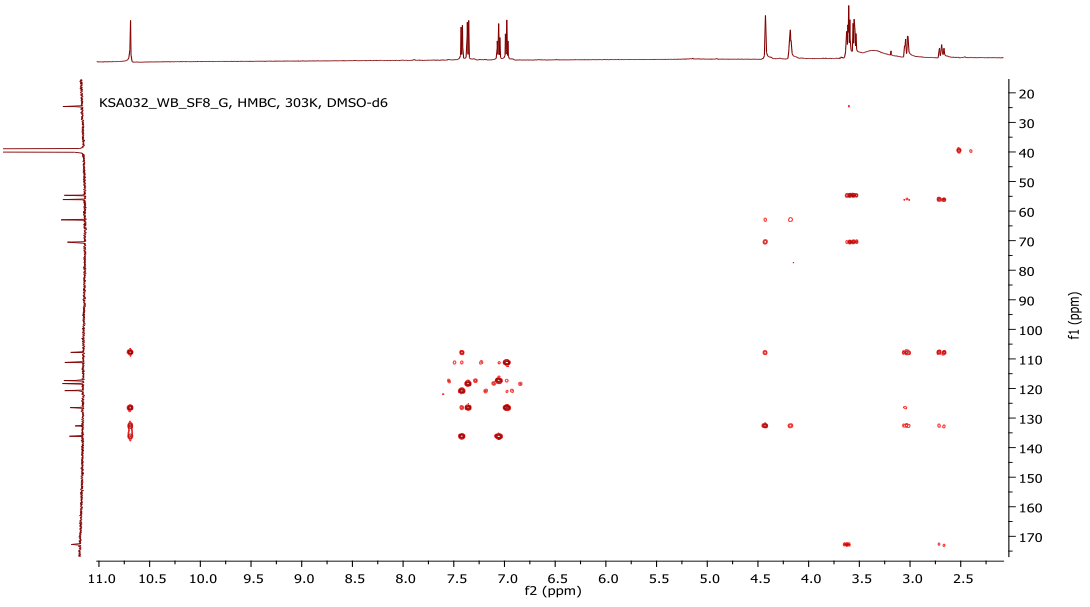

Figure S4.11. HMBC NMR spectrum (600MHz, DMSO-d_6, 303K) of compound **4.1**

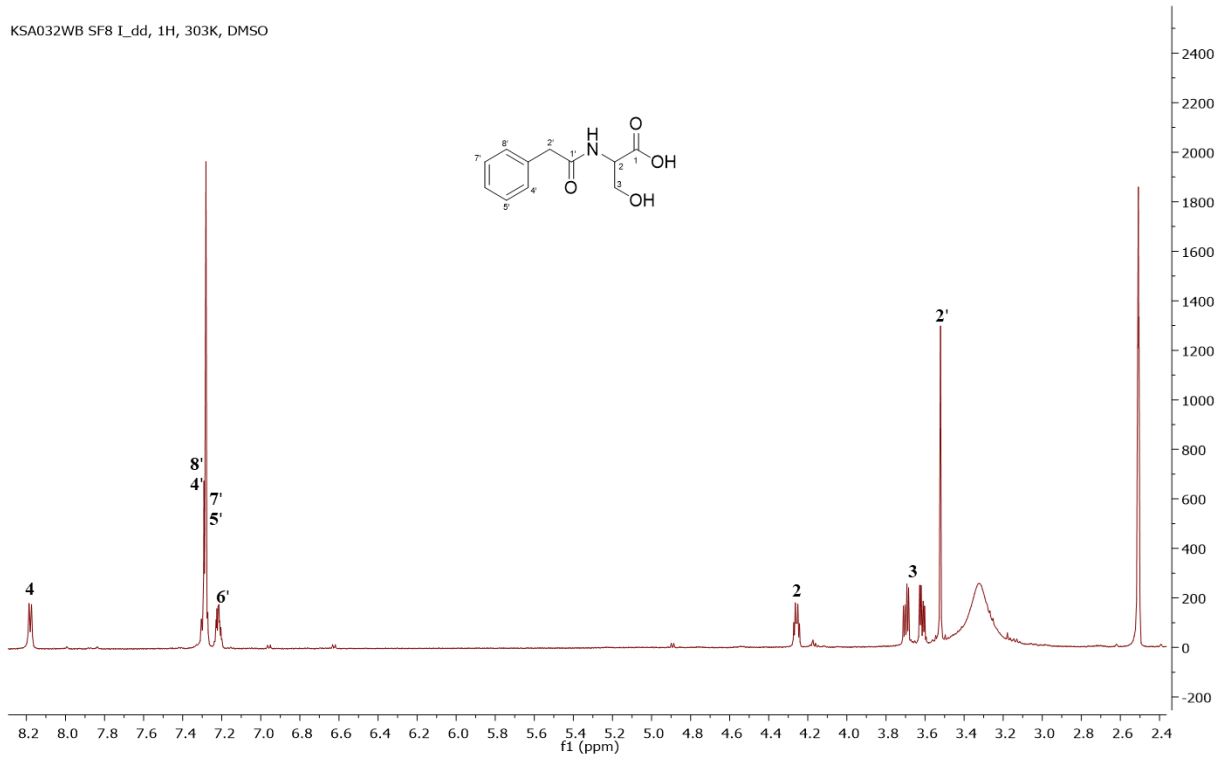

Figure S4.12. ^{1}H-NMR spectrum (600MHz, DMSO-d_6, 303K) of compound **4.2**

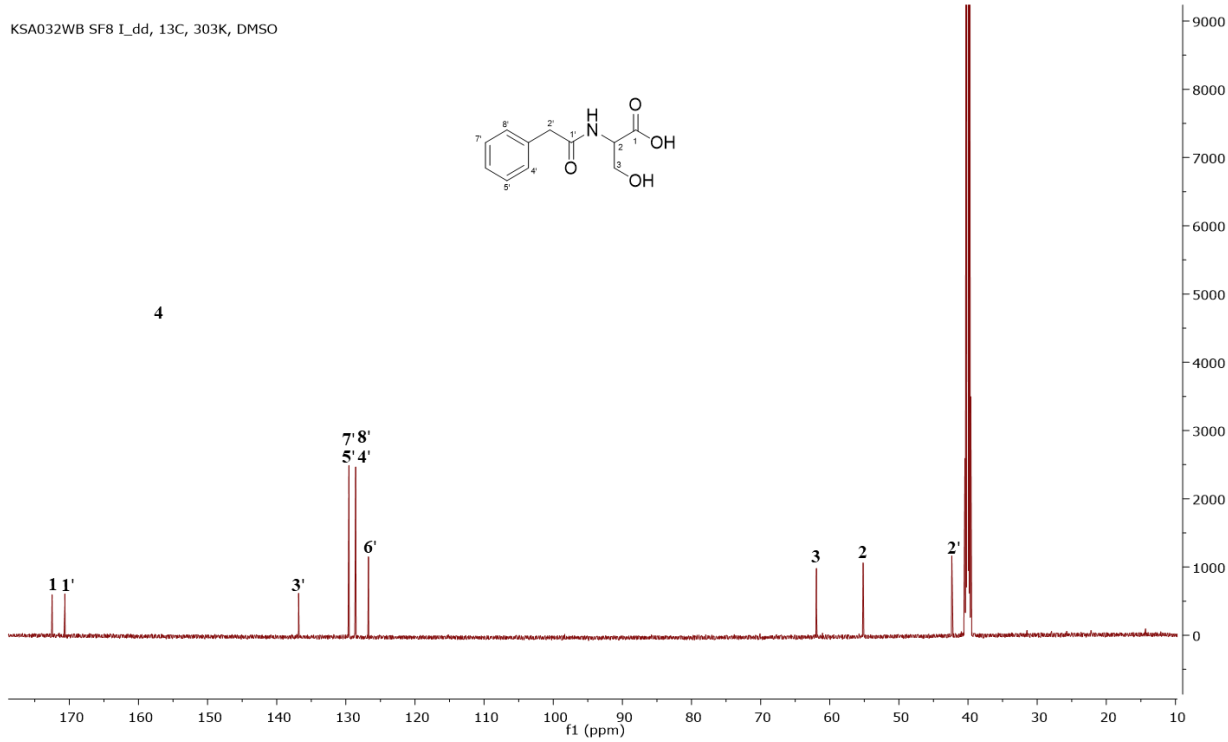

Figure S4.13. ^{13}C-NMR spectrum (150MHz, DMSO-d_6, 303K) of compound **4.2**

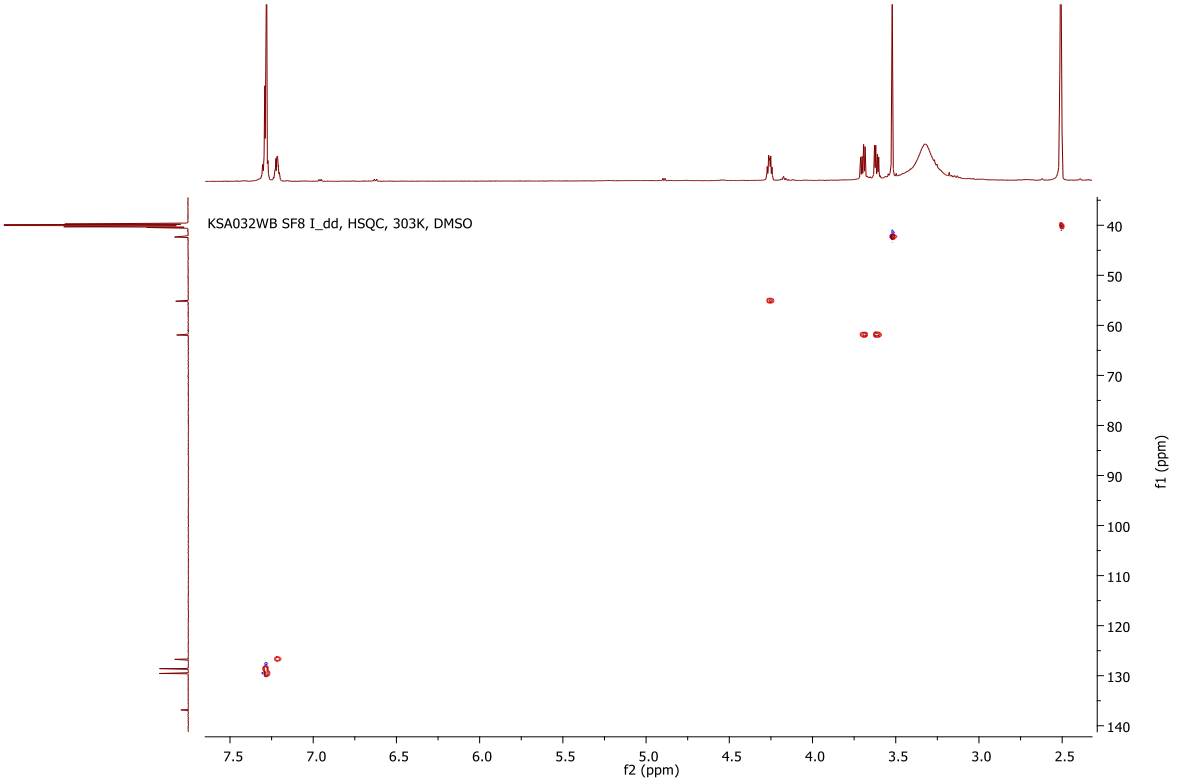

Figure S4.14. HSQC NMR spectrum (600MHz, DMSO-d_6, 303K) of compound **4.2**

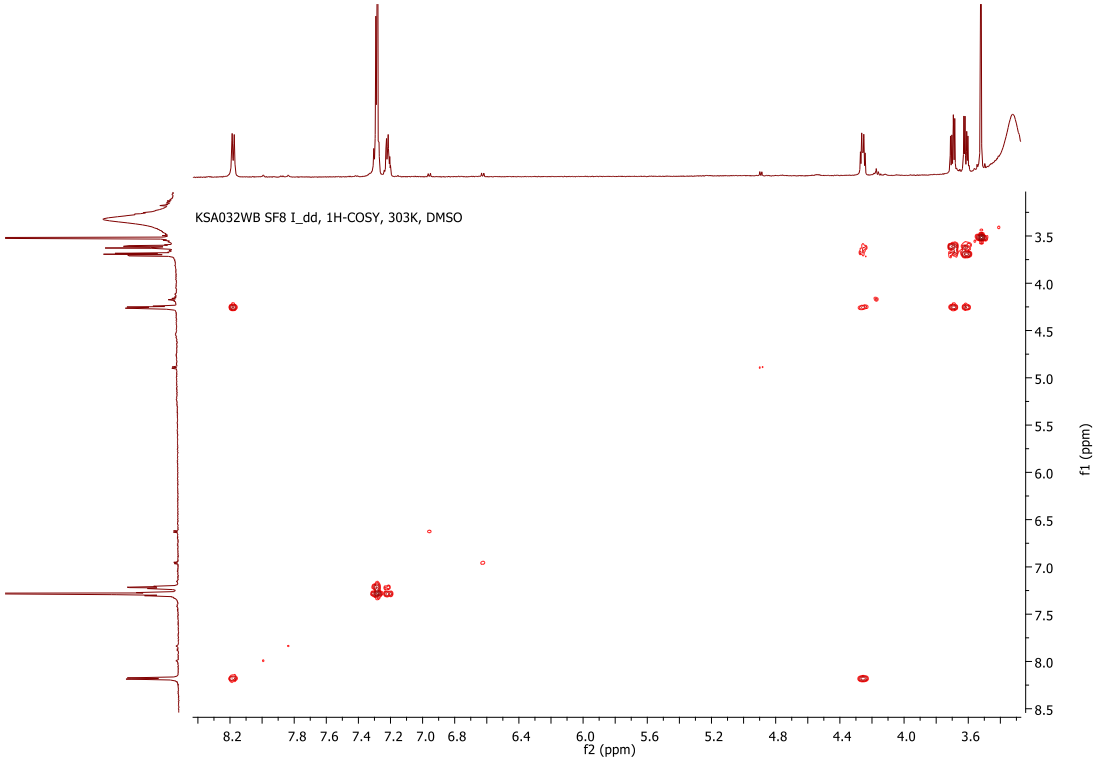

Figure S4.15. ^{1}H-^{1}H COSY spectrum (600MHz, DMSO-d_6, 303K) of compound **4.2**

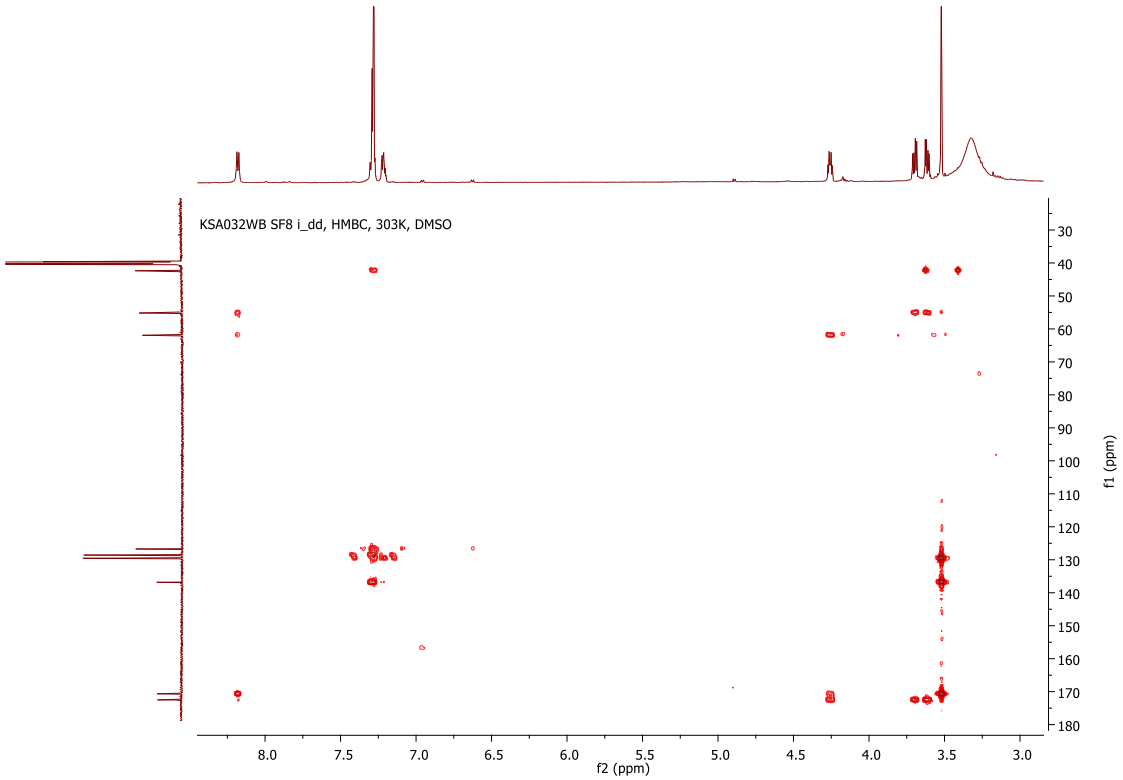

Figure S4.16. HMBC NMR spectrum (600MHz, DMSO-d_6, 303K) of compound **4.2**

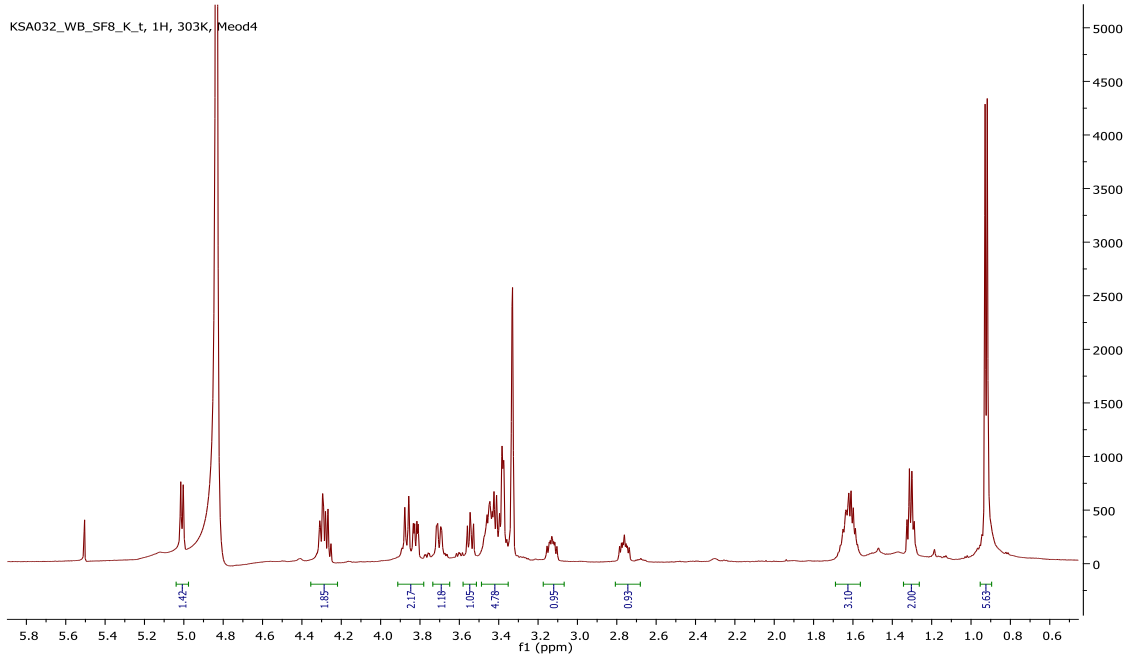

Figure S4.17. ^{1}H-NMR spectrum (600MHz, MeOD, 303K) of compound **4.3**

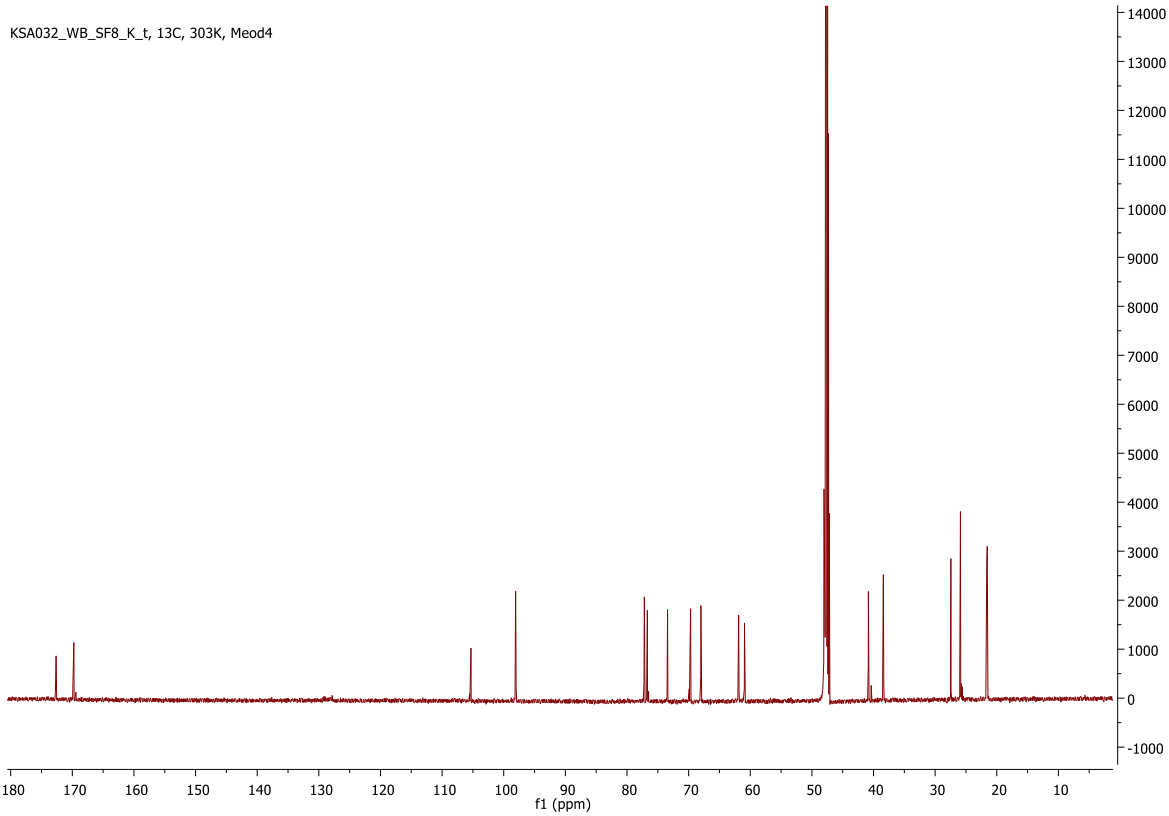

Figure S4.18. ^{13}C-NMR spectrum (150MHz, MeOD, 303K) of compound **4.3**

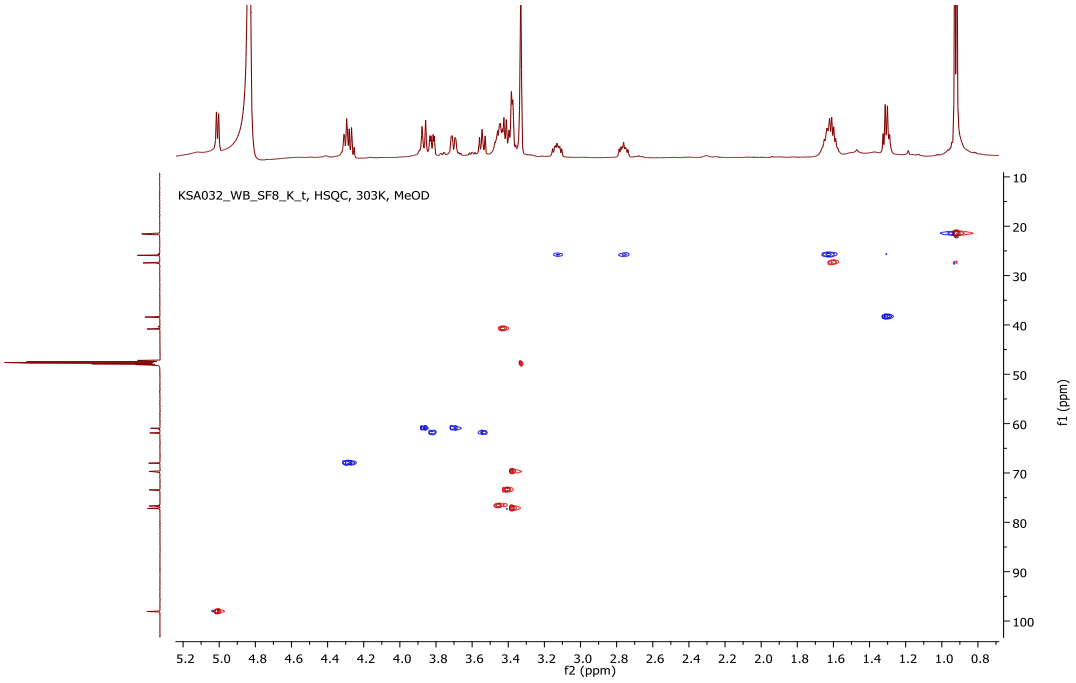

Figure S4.19. HSQC-DEPT NMR spectrum (600MHz, MeOD, 303K) of compound **4.3**

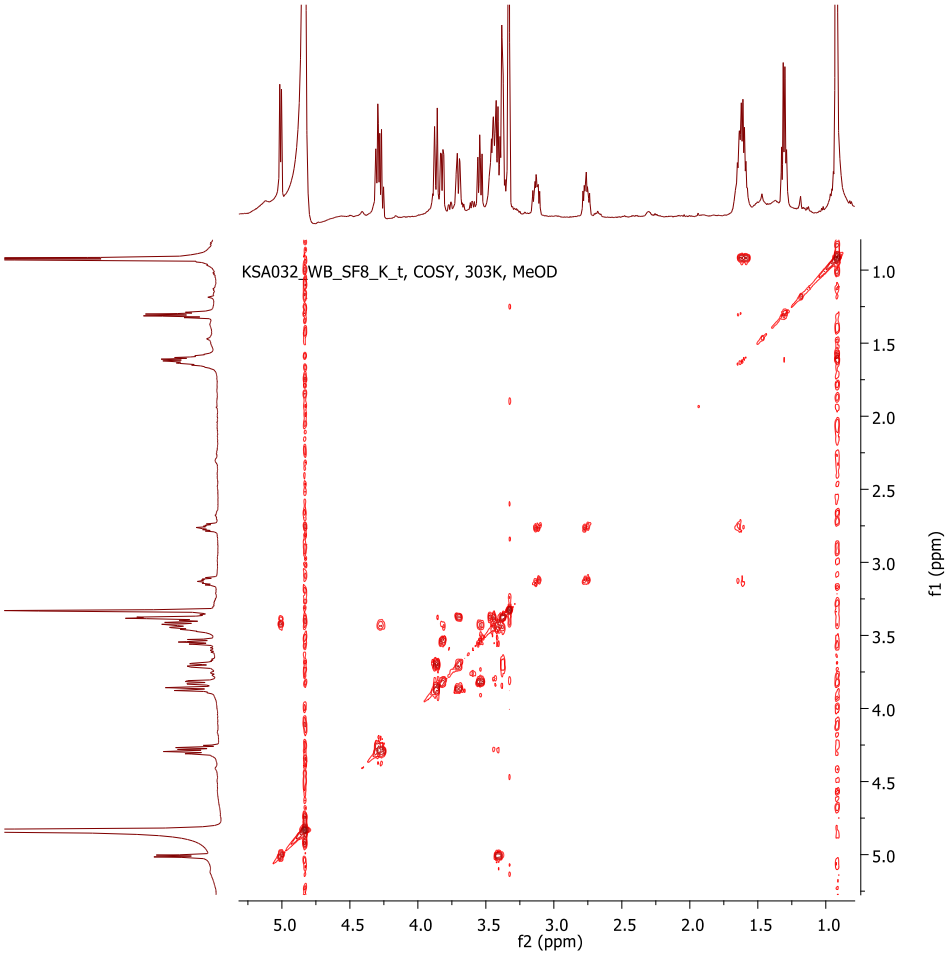

Figure S4.20. ^{1}H-^{1}H COSY spectrum (600MHz, MeOD, 303K) of compound **4.3**

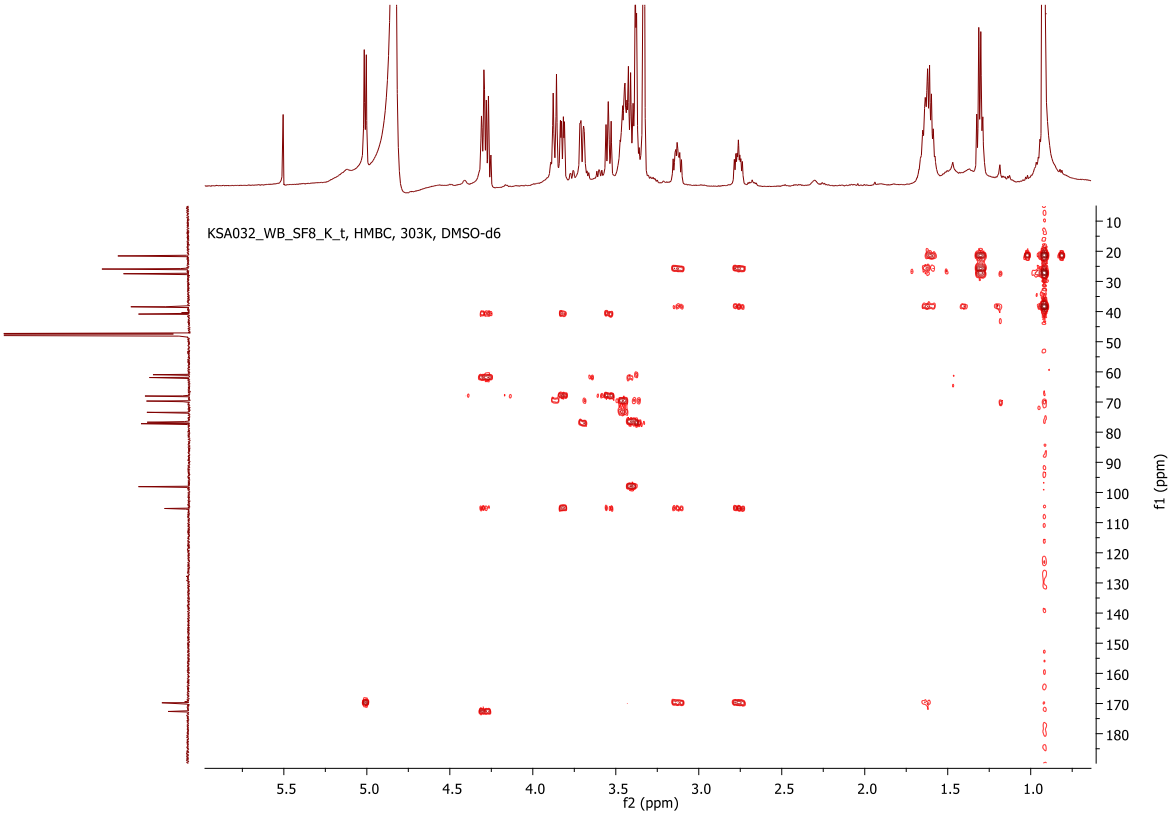

Figure S4.21. HMBC NMR spectrum (600MHz, MeOD, 303K) of compound **4.3**

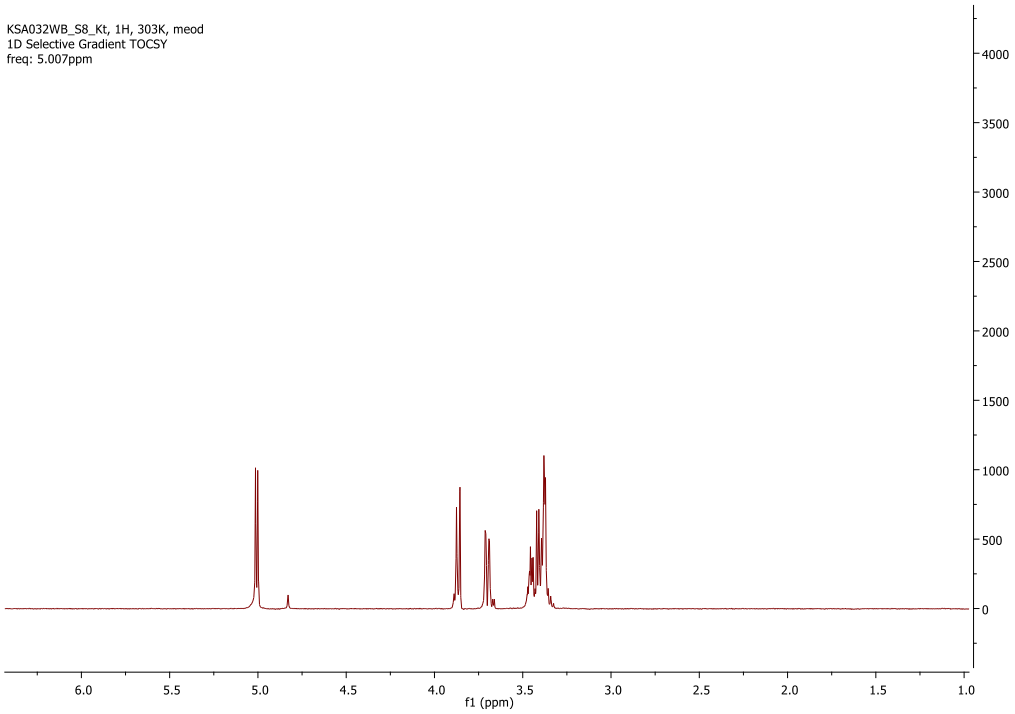

Figure S4.22. 1D selective gradient TOCSY freg. 5.007 ppm (600MHz, MeOD, 303K) of compound **4.3**

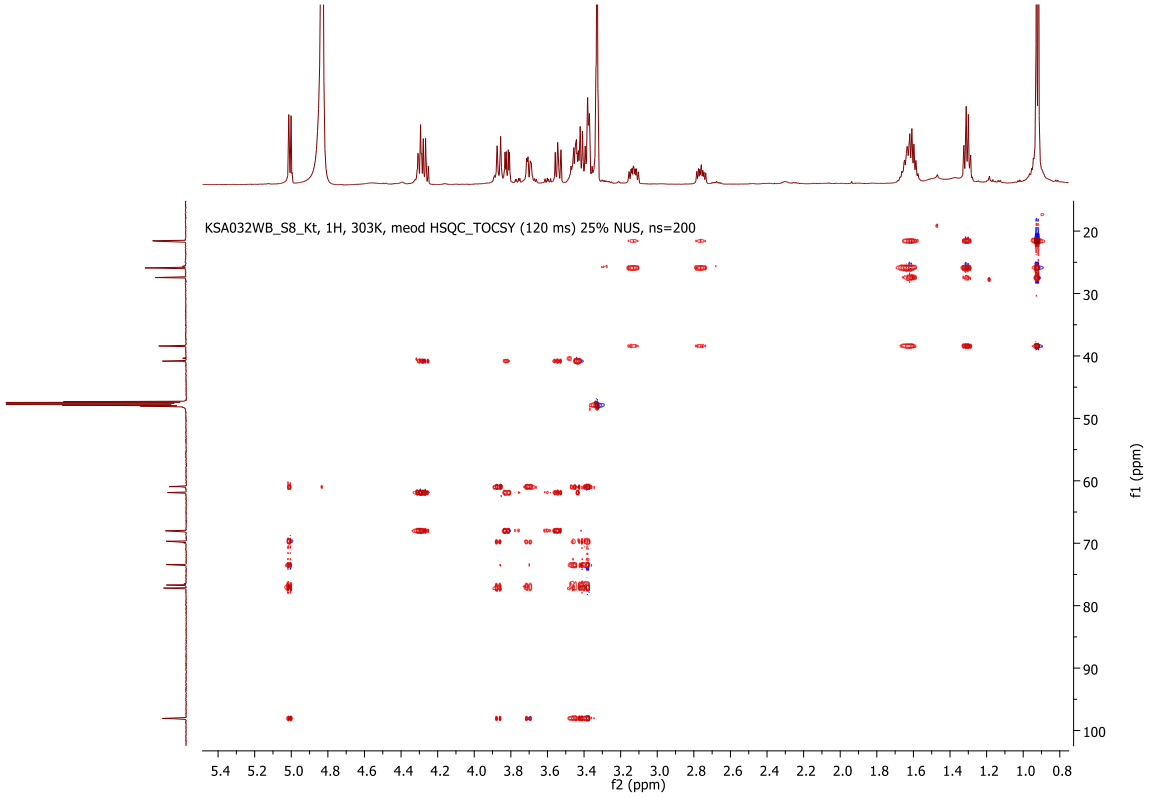

Figure S4.23. HSQC-TOCSY (120 ms) 25% NUS, ns=200 (600MHz, MeOD, 303K) of compound **4.3**

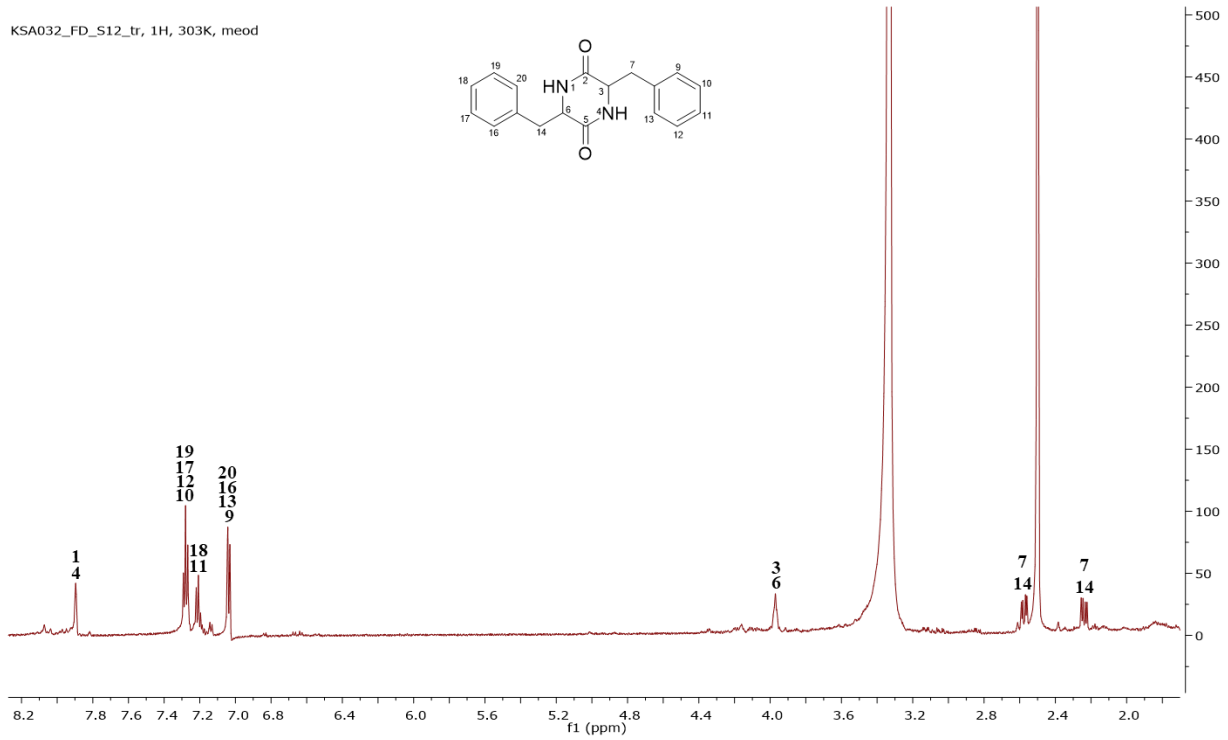

Figure S4.24. ^{1}H-NMR spectrum (600MHz, DMSO-d_6, 303K) of compound **4.4**

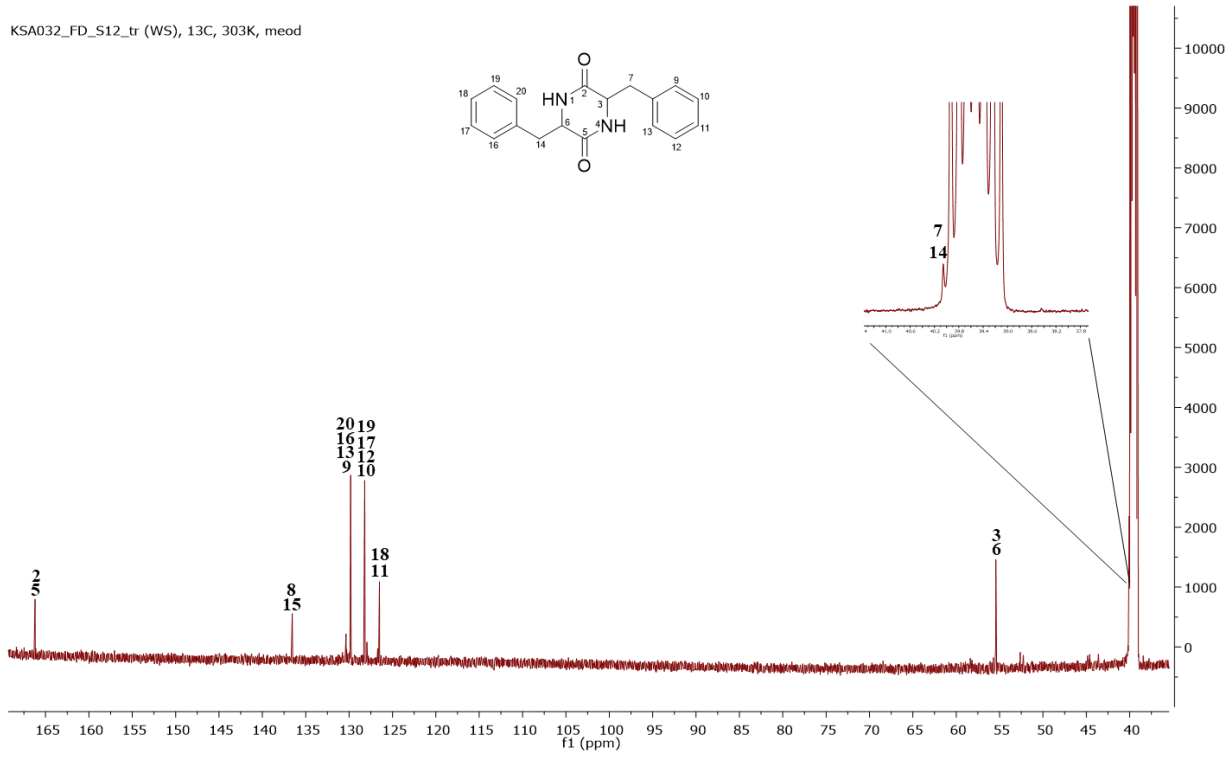

Figure S4.25. ^{13}C-NMR spectrum (150MHz, DMSO-d_6, 303K) of compound **4.4**

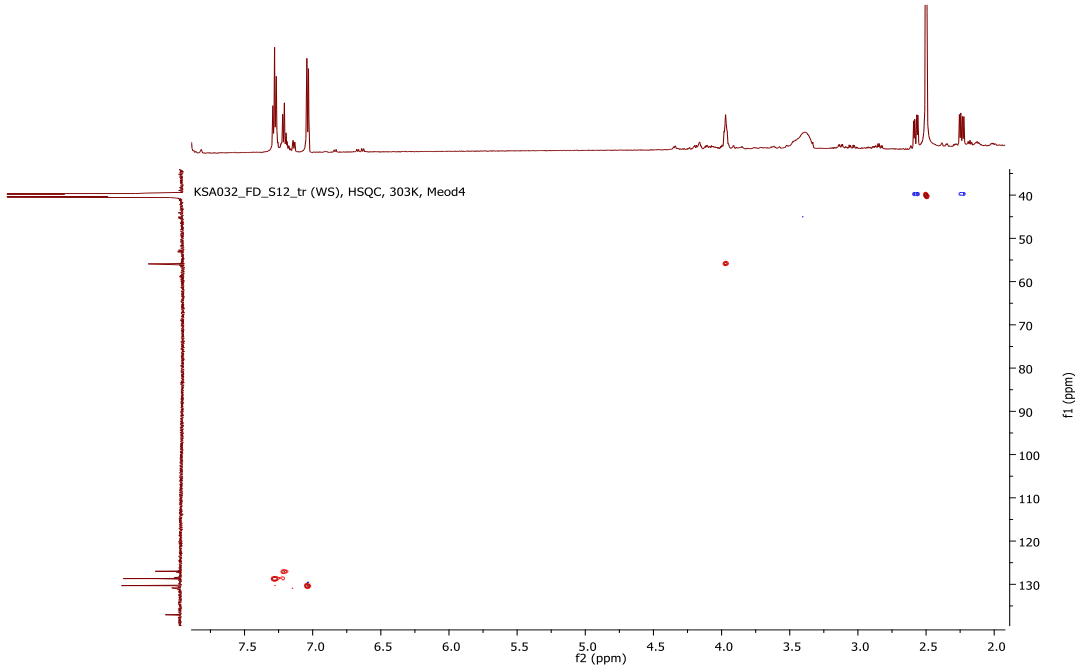

Figure S4.26. HSQC-DEPT NMR spectrum (600MHz, DMSO-d_6, 303K) of compound **4.4**

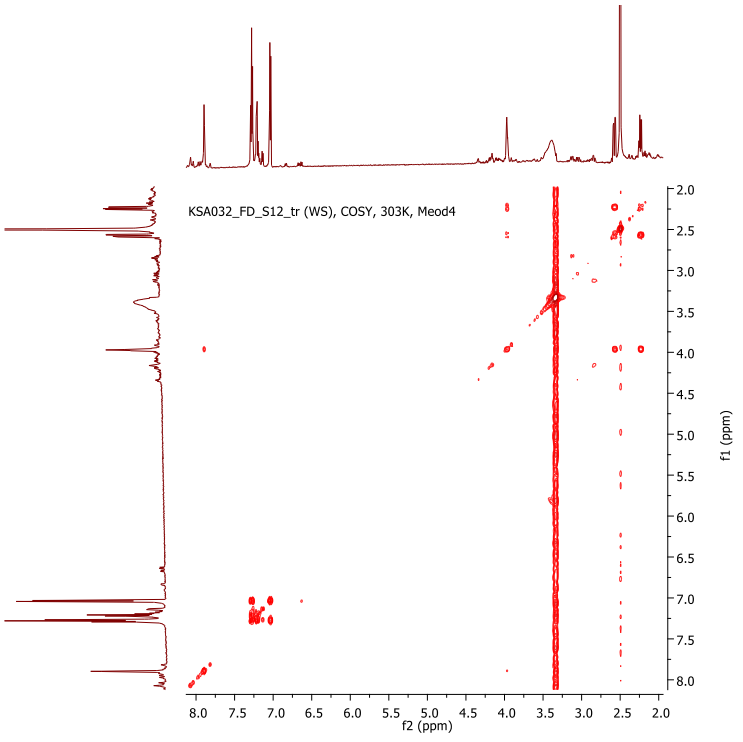

Figure S4.27. ^{1}H-^{1}H COSY spectrum (600MHz, DMSO-d_6, 303K) of compound **4.4**

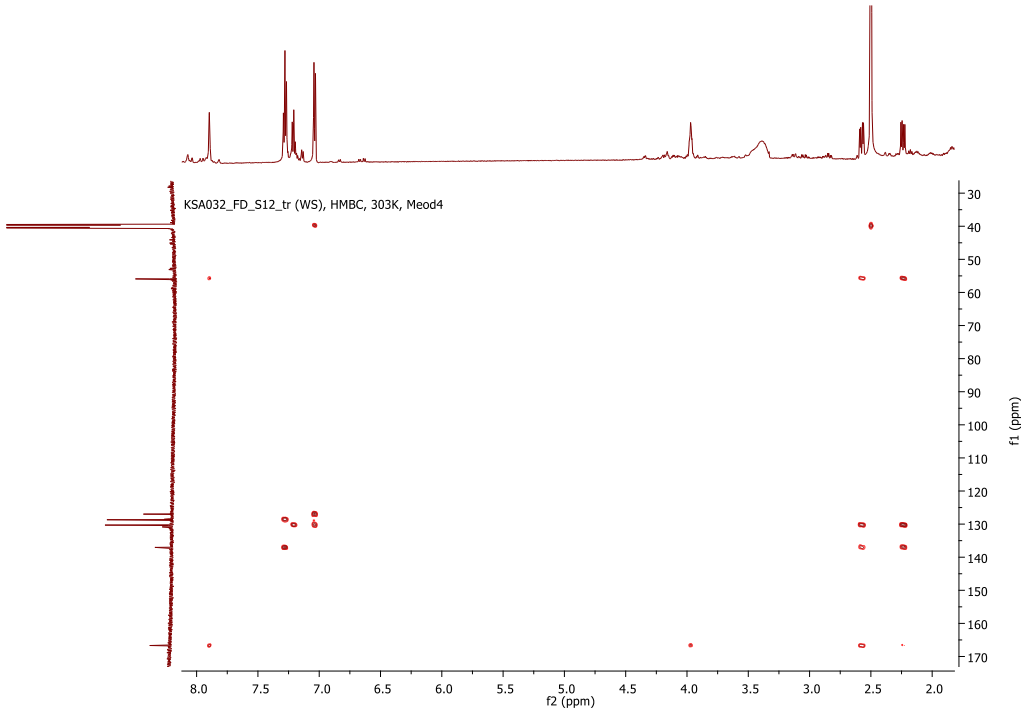

Figure S4.28. HMBC NMR spectrum (600MHz, DMSO-d_6, 303K) of compound **4.4**

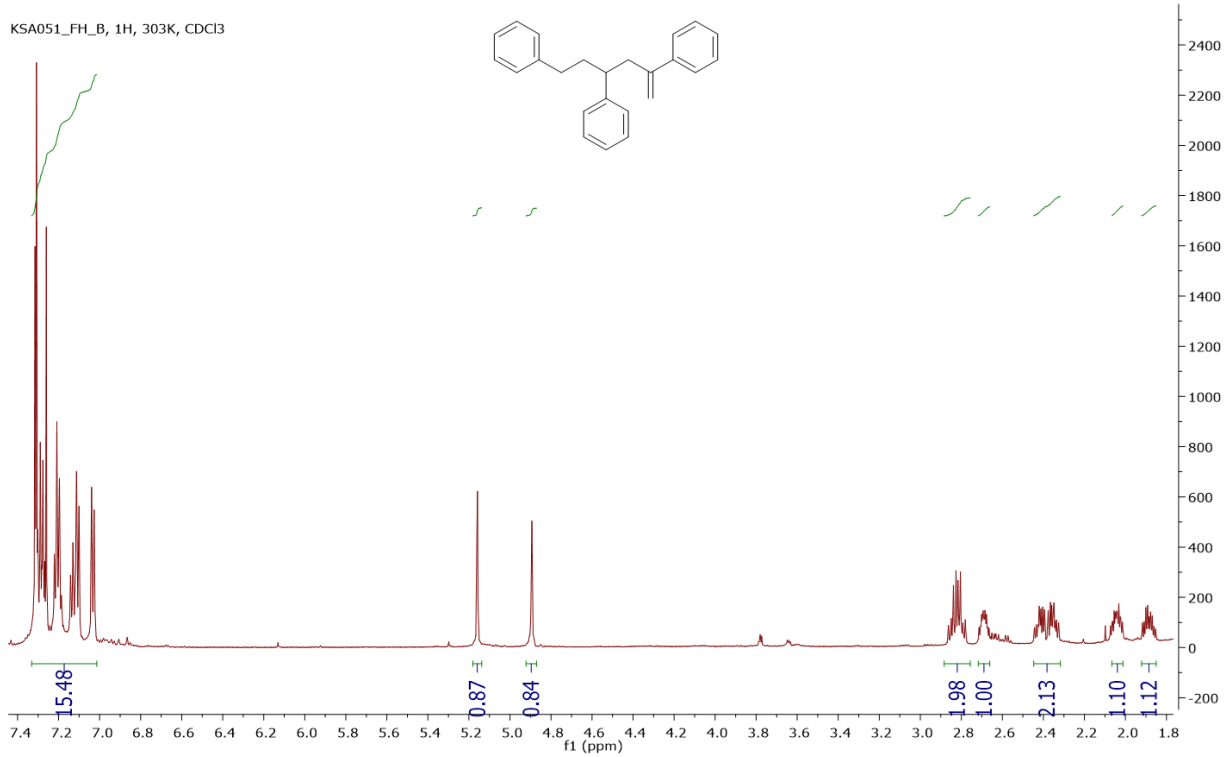

Figure S4.29. ^{1}H-NMR spectrum (600MHz, $CDCl_3$, 303K) of compound **4.5**

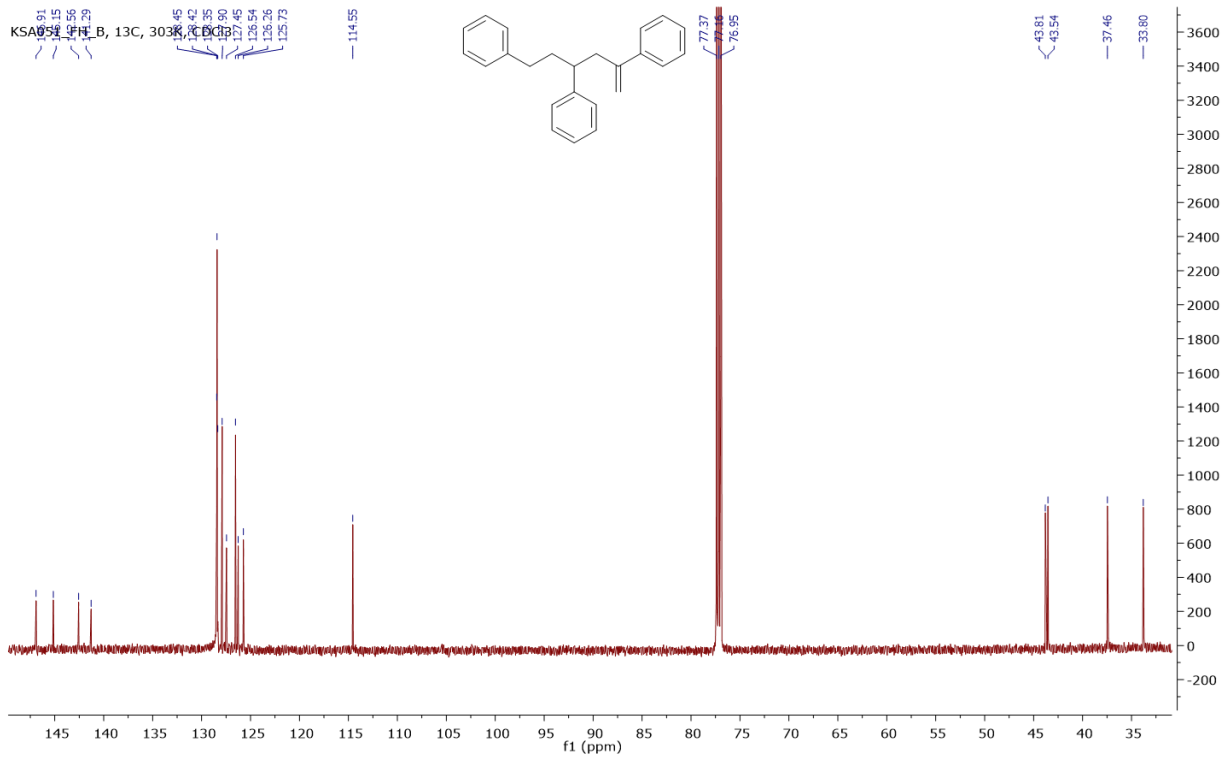

Figure S4.30. ^{13}C-NMR spectrum (150MHz, $CDCl_3$, 303K) of compound **4**

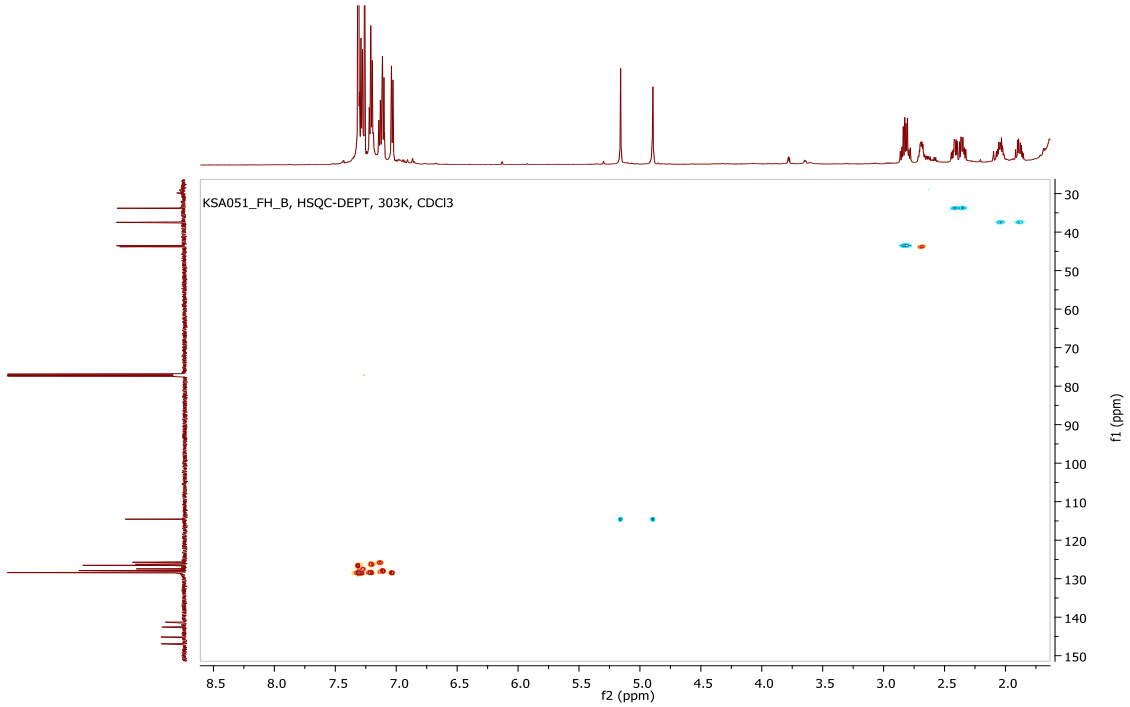

Figure S4.31. HSQC-DEPT NMR spectrum (600MHz, $CDCl_3$, 303K) of compound **4.5**

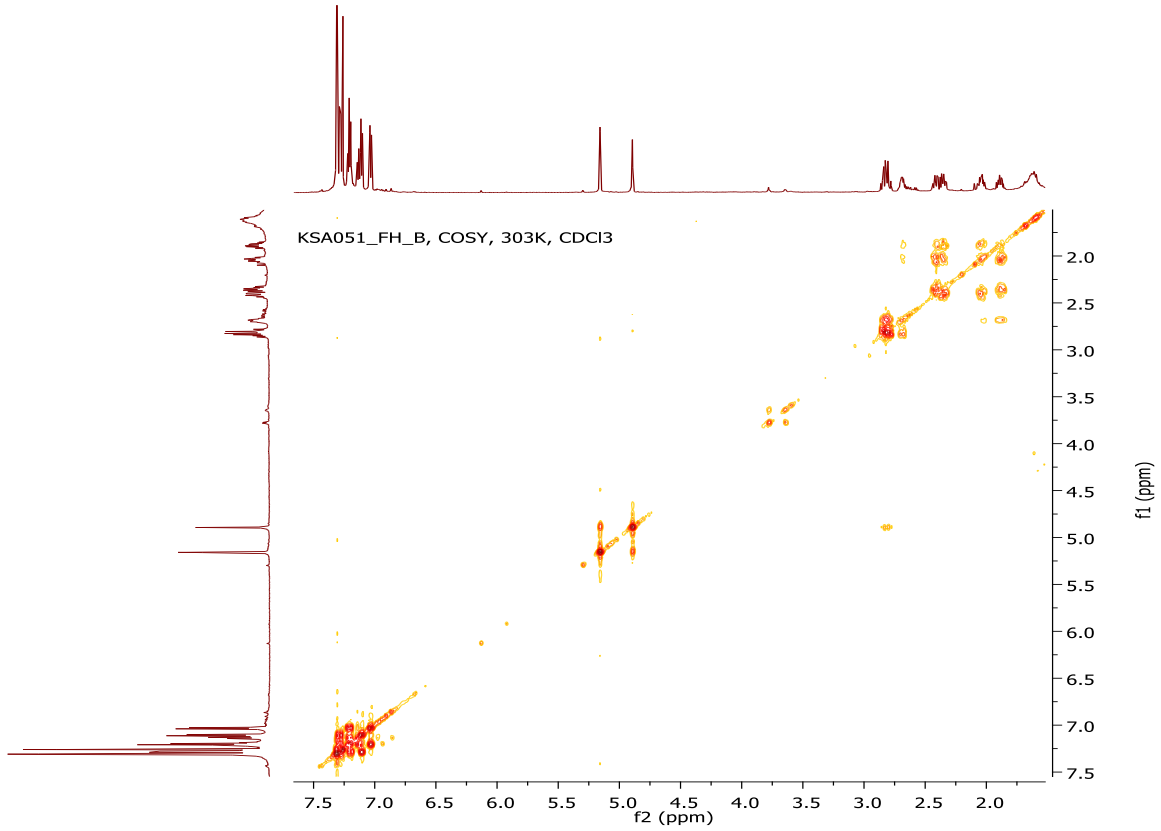

Figure S4.32. ^{1}H-^{1}H COSY spectrum (600MHz, $CDCl_3$, 303K) of compound **4.5**

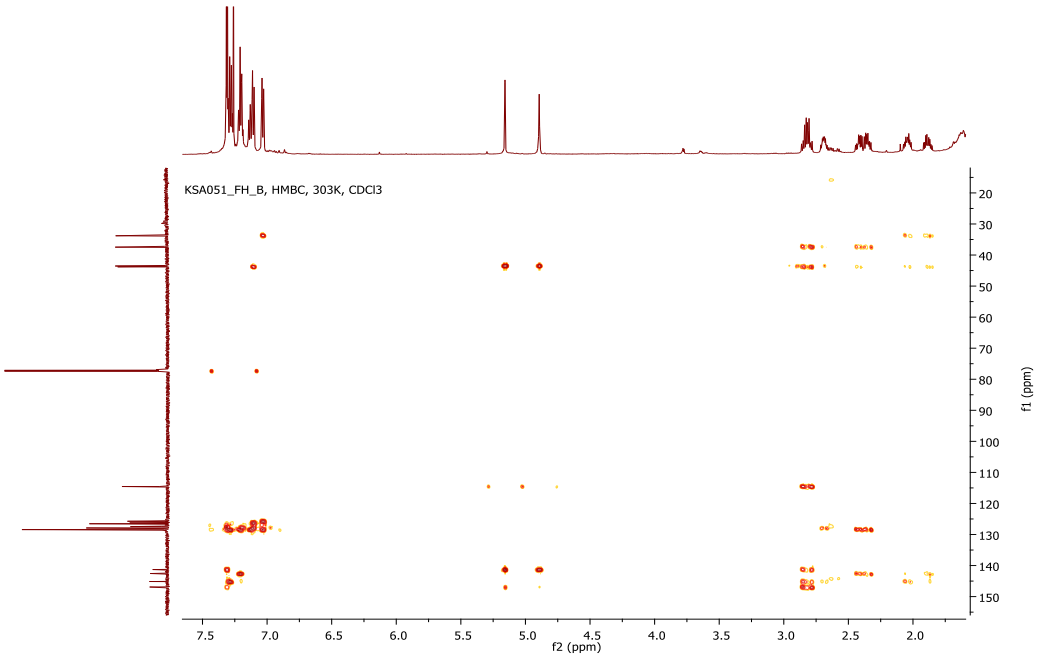

Figure S4.33. HMBC NMR spectrum (600MHz, $CDCl_3$, 303K) of compound **4.5**

Table S4.1. ^{1}H, ^{13}C, NMR data of isolated and synthesized compound **4.1** in DMSO. δ in ppm, *J* in Hz.

Compound **4.1**	Isolated		Literature	
Position	^{13}C	^{1}H mult (J, Hz)	^{13}C	^{1}H mult (J, Hz)
1	54.7, CH	4.43, m	56.1- 56.3	5.08, d (1)
2-N				
3	56.7, CH	3.62, m	56.1- 56.3	3.93-4.07, m
4	24.6, CH_2	3.04, dd (3.7, 14.7) 2.69, m	21.0 21.5	3.93-4.07, m 4.24-4.28, dd (4.76, 12.08)
4a	107.8, C		106.5, 107.3	
4b	126.5, C		124.6, 124.9, 125.2	
5	117.3, CH	7.42, d (7. 8)	117.3	7.54, d (7.69)
6	118.3, CH	6.98, t (7.4, 7.4)	119.0	7.12, dd (6.96, 8.06
7	120.7, CH	7.06, t (7.5, 7.5)	121.9	7.21, dd (6.96, 8.06)
8	111.2, CH	7.36, d (8.0)	110.7	7.43, d (8.06)
8a	136.1, C		136.1	
9-N		10.69, s		
9a	132.6, C		136.1	
1'	70.5, CH	4.18 dd, (4.0, 7. 7)	67.9, 68.4	4.54-4.56, dt (2.6, 4.3)
2'	62.9, CH_2	3.60, m 3.54, dd (5. 5, 10.8)	62.2, 62.8	3.05-3.22, m 3.4-3.51, m
3'	172.6, C		171.4, 175.1	

Table S4.1. ^{1}H, ^{13}C, NMR data of isolated and synthesized *N*-(2-phenylacetyl)-Serine **4.2** in DMSO. δ in ppm, *J* in Hz.

Compound **4.2**	Isolated		Literature
Position	^{13}C	^{1}H mult (J, Hz) isolated	^{1}H mult (J, Hz) literature
1	172.5, C		
2	55.1, CH	4.25, dt (4.9, 4.9, 7.9)	4.50, dd
3	61.9, CH_2	3.70, dd (5.3, 10.8) 3.61, m	4.00, d
4-N		8.18, d (7.8)	
1'	170.7, C		
2'	42.3, CH_2	3.52, s	3.44, s
3'	136.8, C		
4'/8'	128.6, CH	7.29, m	7.06–7.14, m
5'/7'	129.5, CH	7.28, m	7.06–7.14, m
6'	126.7, CH	7.21, m	7.06–7.14, m

Appendix for Chapter Five

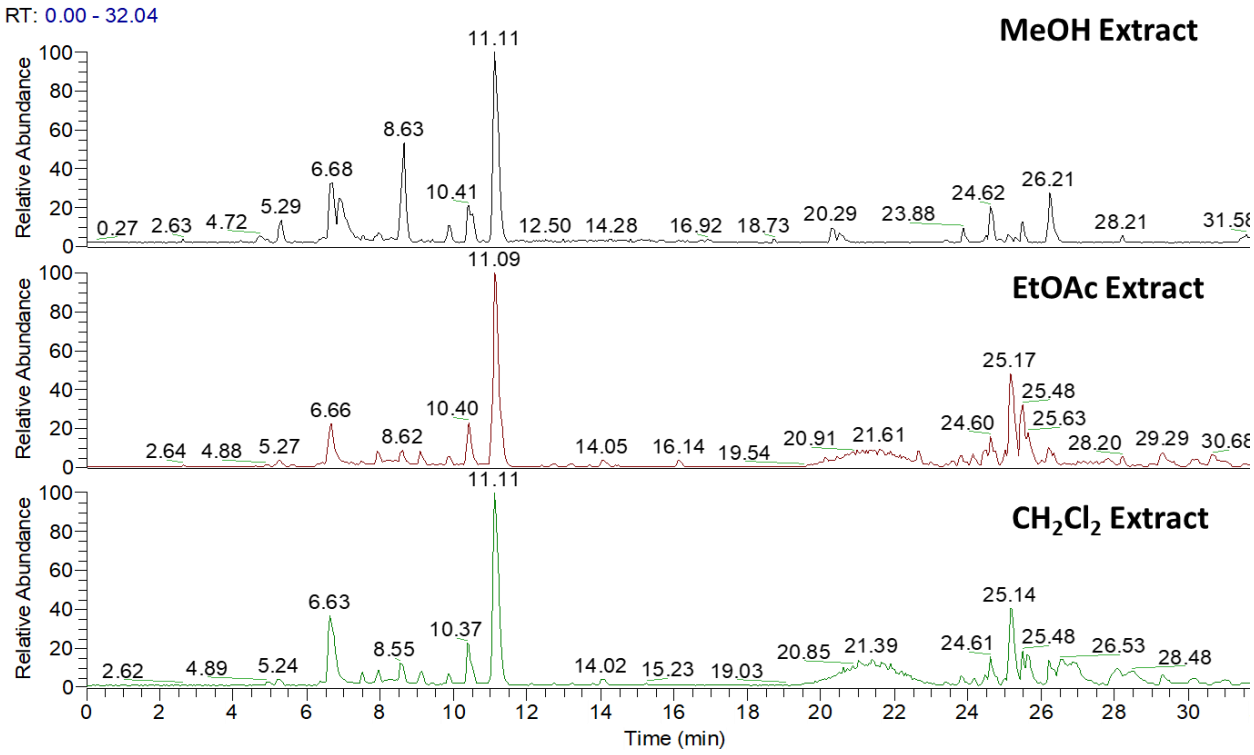

Figure S5.1. MS window of HPLC-DAD/HRESIMS profiles of MeOH (top), EtOAC (middle) and CH_2Cl_2 (bottom) extracts of the fermentation broth of *Kribbella speibonae* strain SK5 cultured in ISP2 liquid medium.

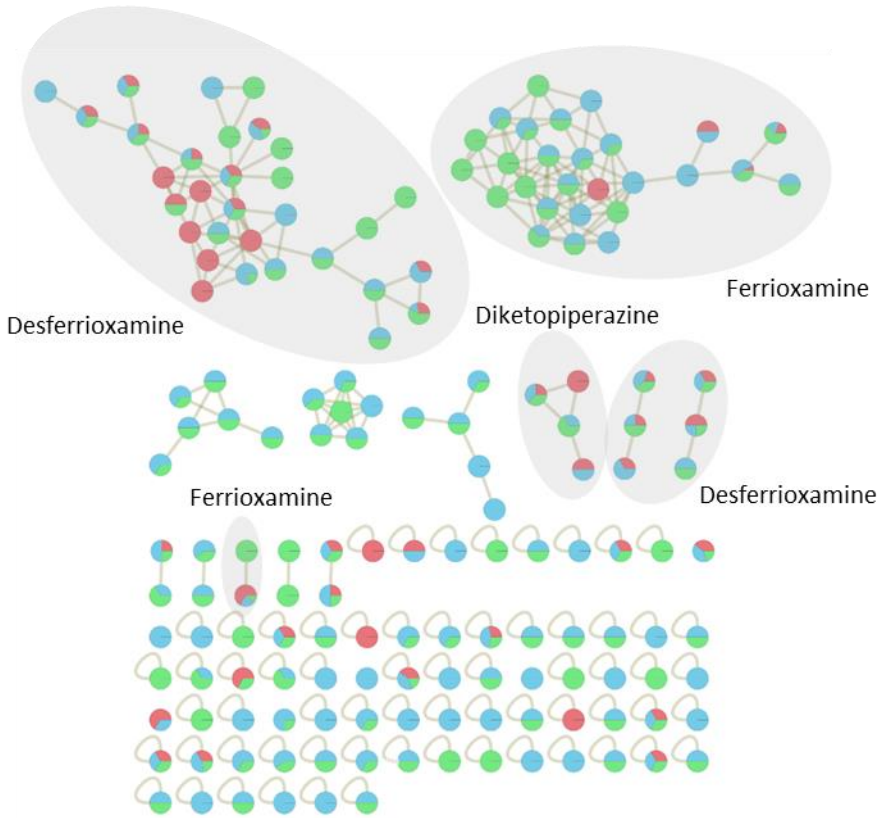

Figure S5.2. GNPS molecular network of the methanol (red nodes), ethyl acetate (blue nodes) and dichloromethane (green nodes) extracts of the fermentation broth of *K. speibonae* strain SK5. The molecular network contains 13 families with the highlighted families (desferrioxamines, ferrioxamines and diketopiperazines) containing some annotated nodes.

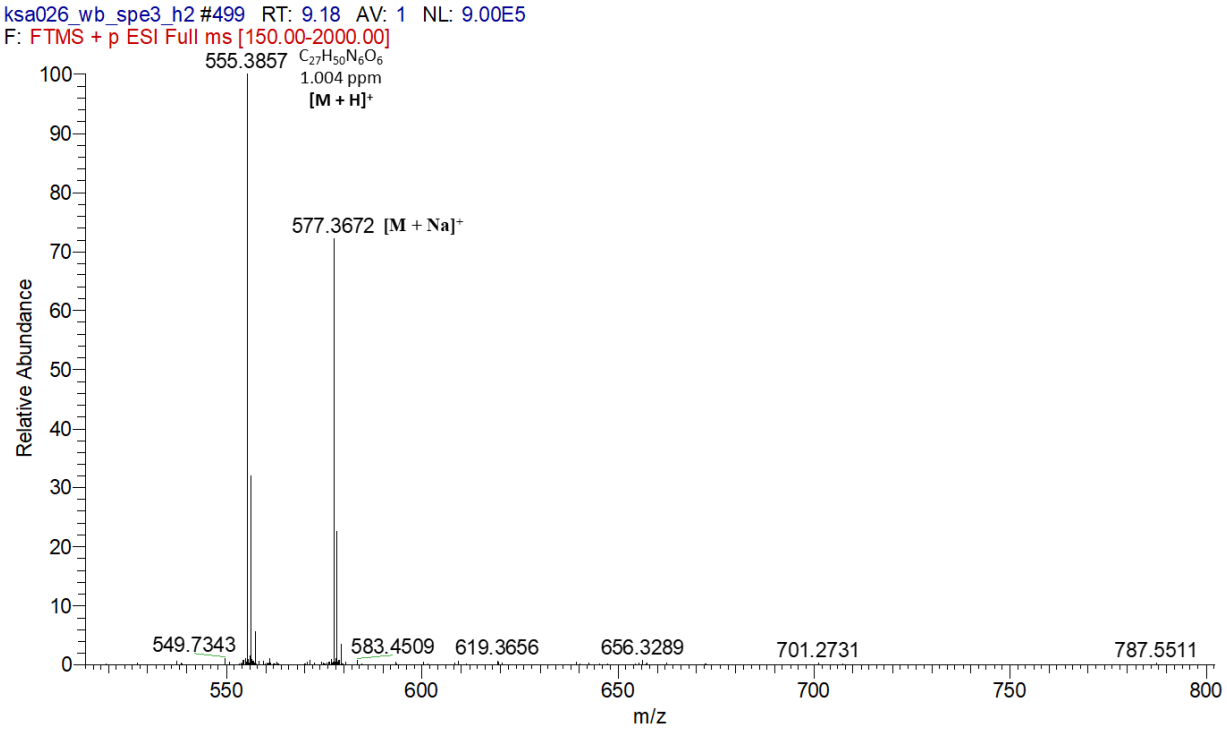

Figure S5.3. HR-ESI-MS spectrum of speibonoxamine (**5.1**)

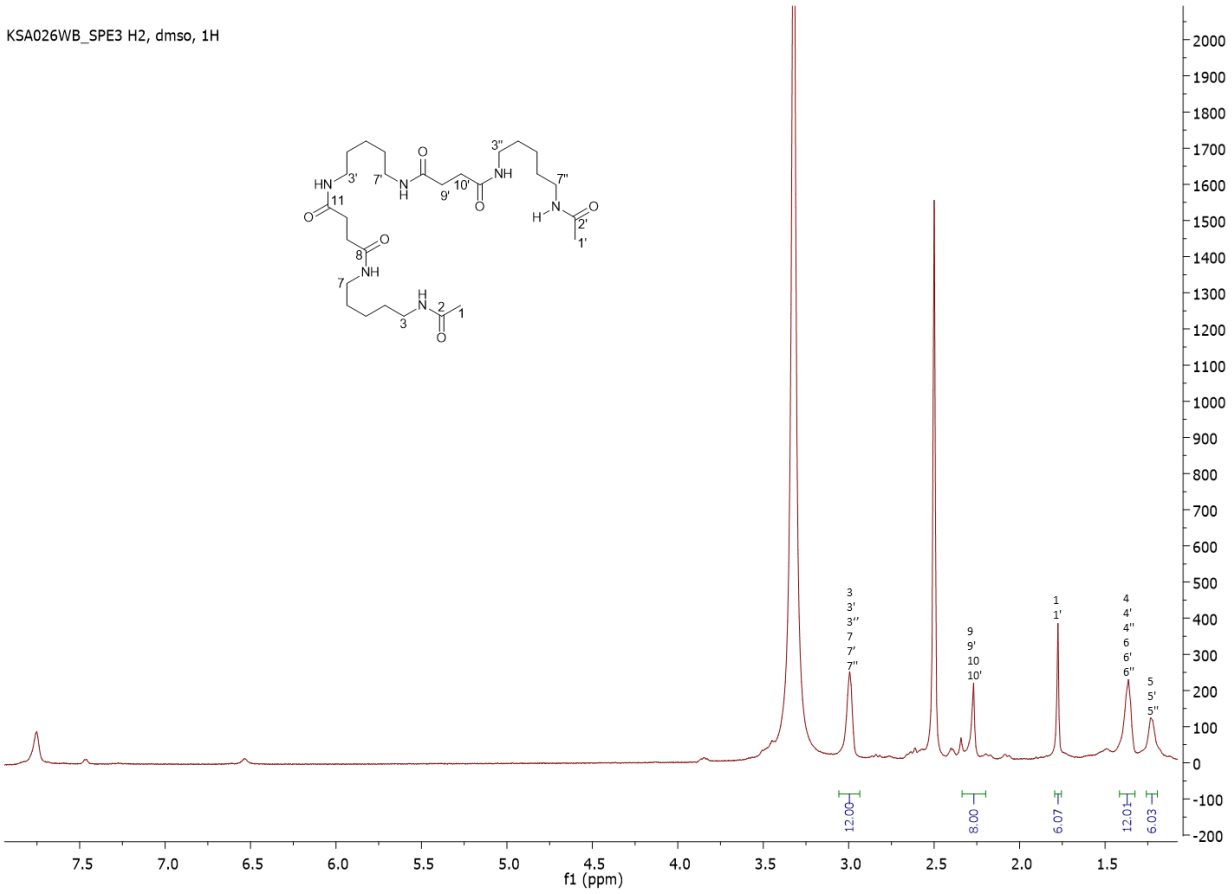

Figure S5.4. ^{1}H-NMR spectrum of speibonoxamine (**5.1**) in DMSO-d6 at 600 MHz.

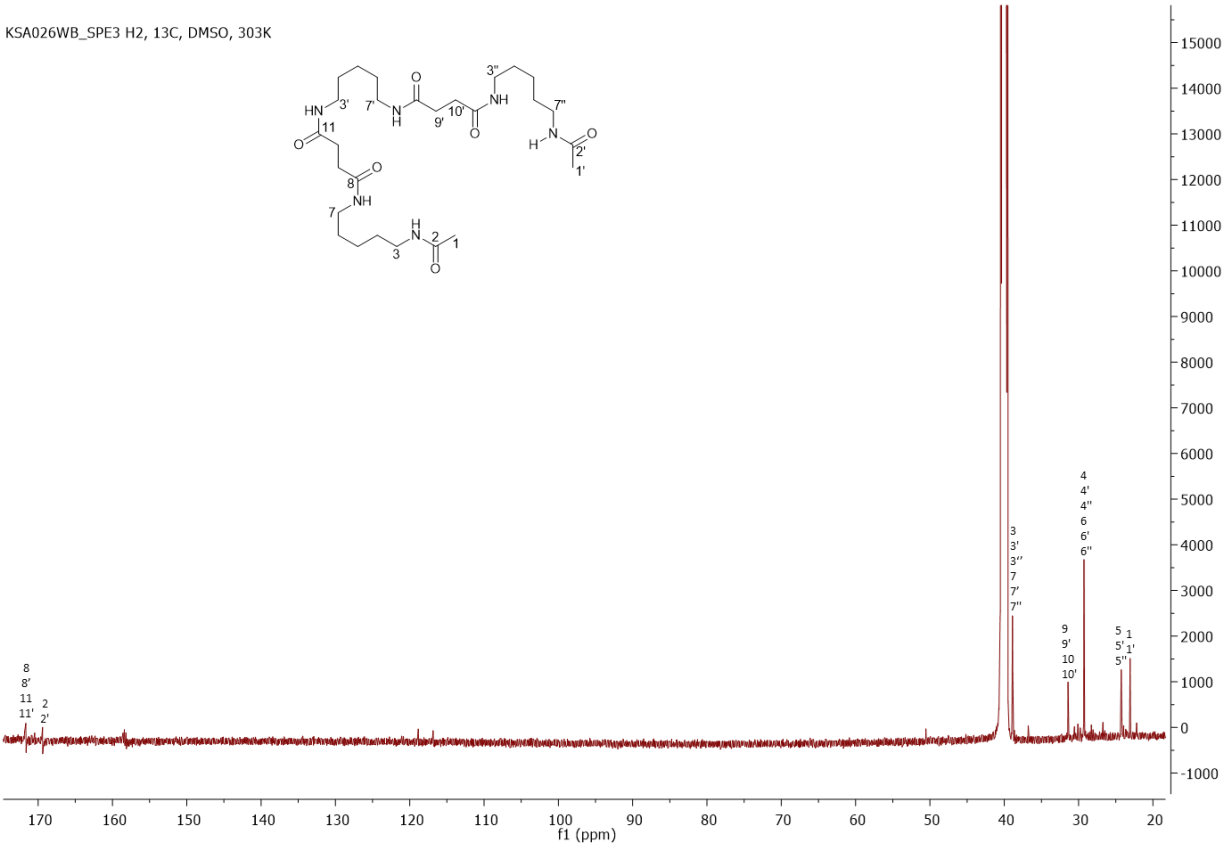

Figure S5.5. ^{13}C-NMR spectrum of speibonoxamine (**5.1**) in DMSO-d6 at 600 MHz.

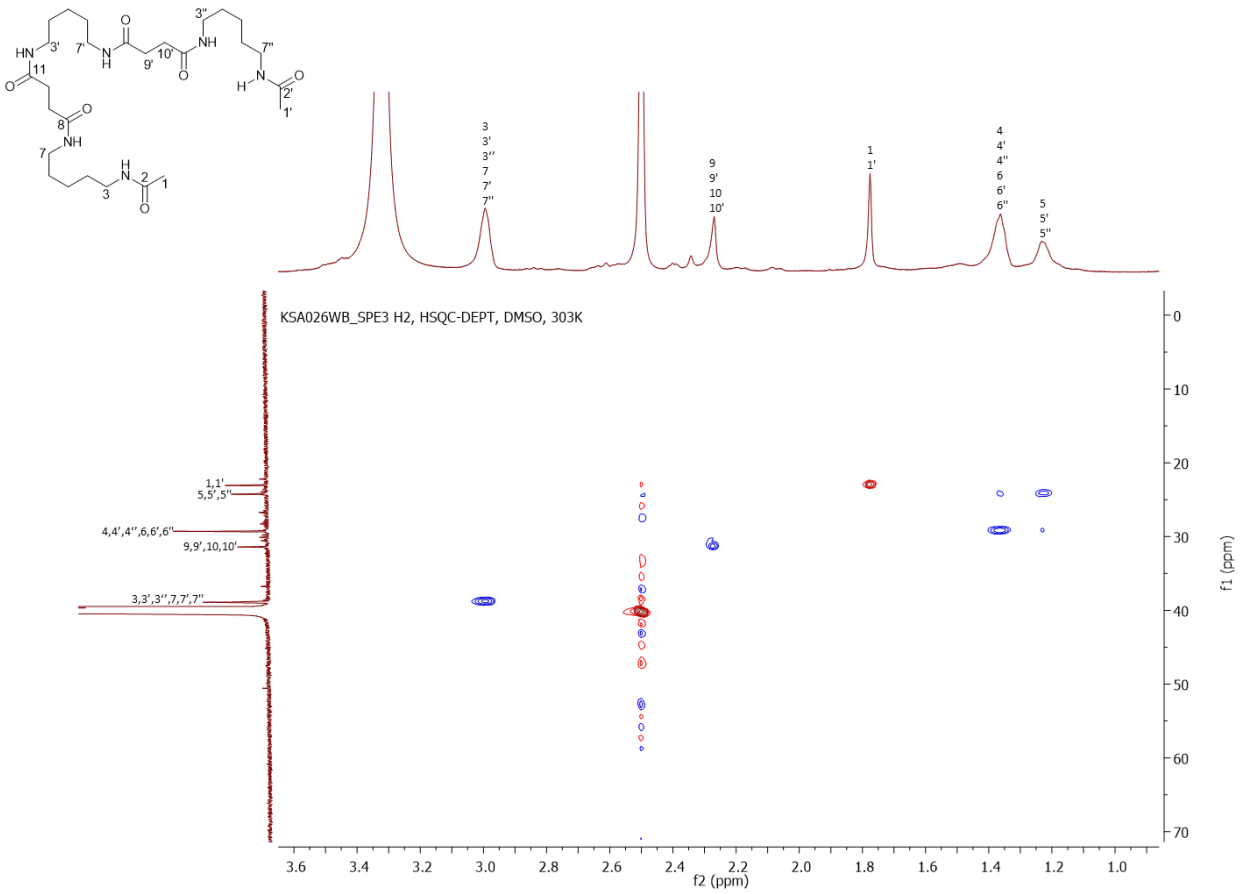

Figure S5.6. Multiplicity edited HSQC NMR spectrum of speibonoxamine (**5.1**) in DMSO-d6 at 600 MHz.

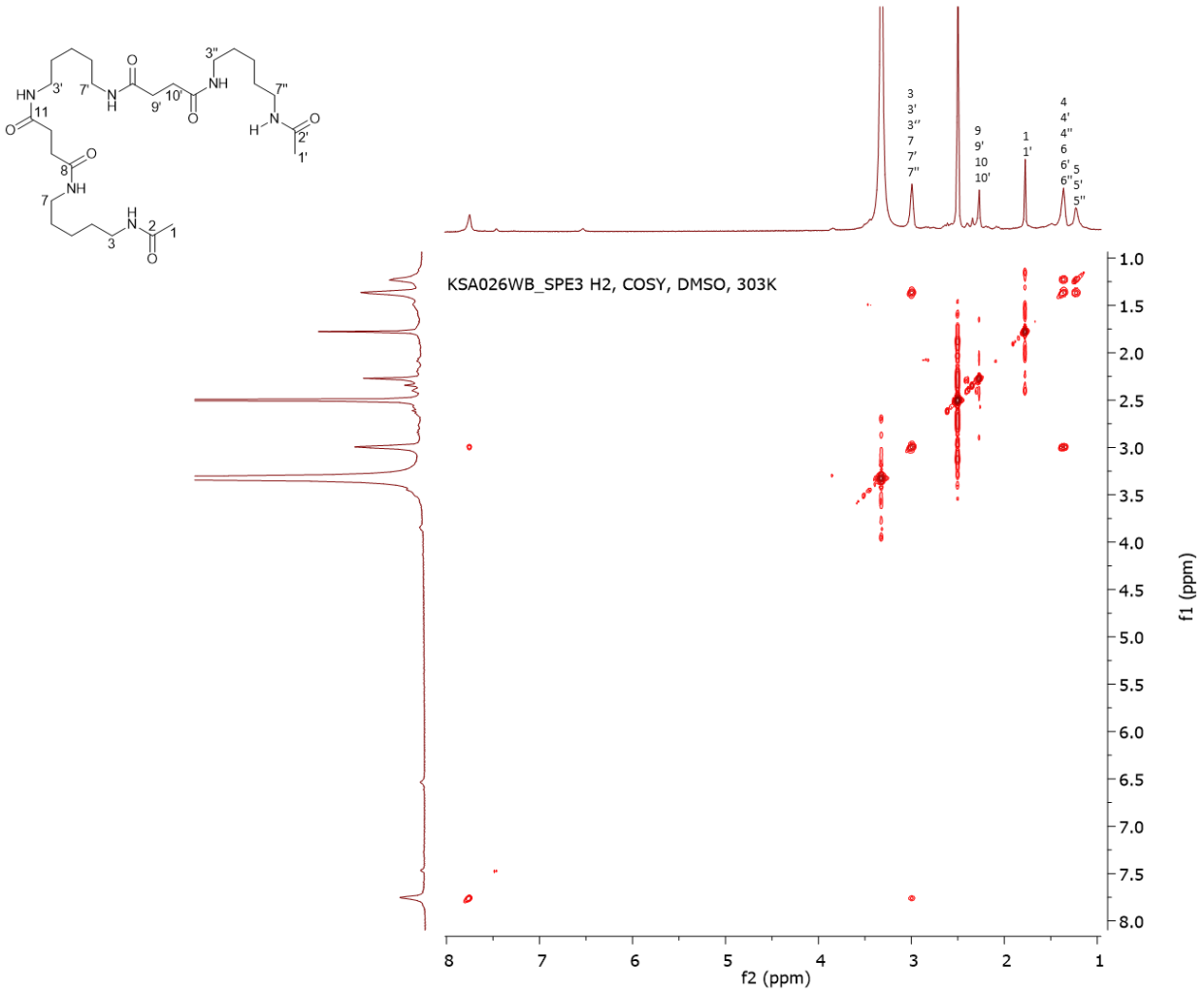

Figure S5.7. ^{1}H-^{1}H COSY spectrum of speibonoxamine (**5.1**) in DMSO-d6 at 600 MHz.

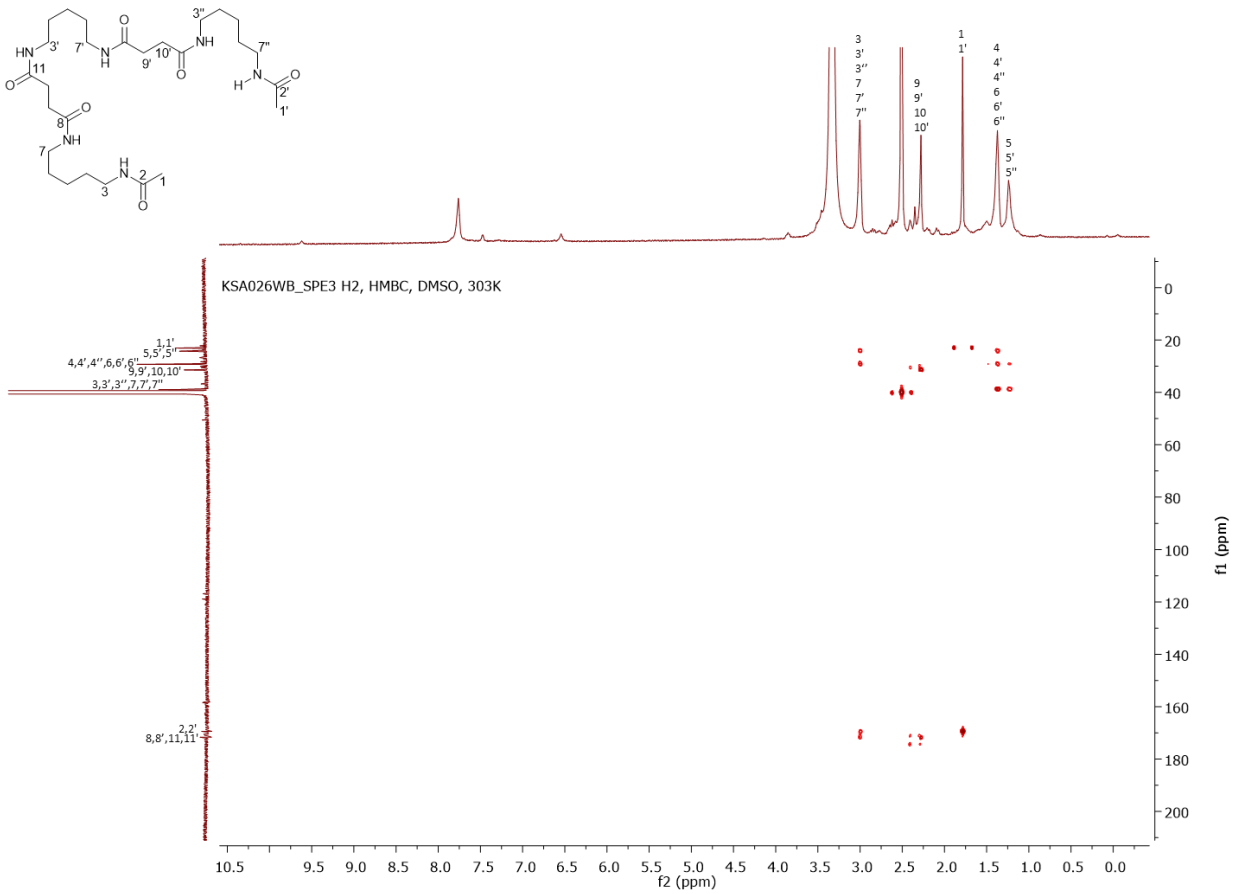

Figure S5.8. HMBC NMR spectrum of speibonoxamine (**5.1**) in DMSO-d6 at 600 MHz.

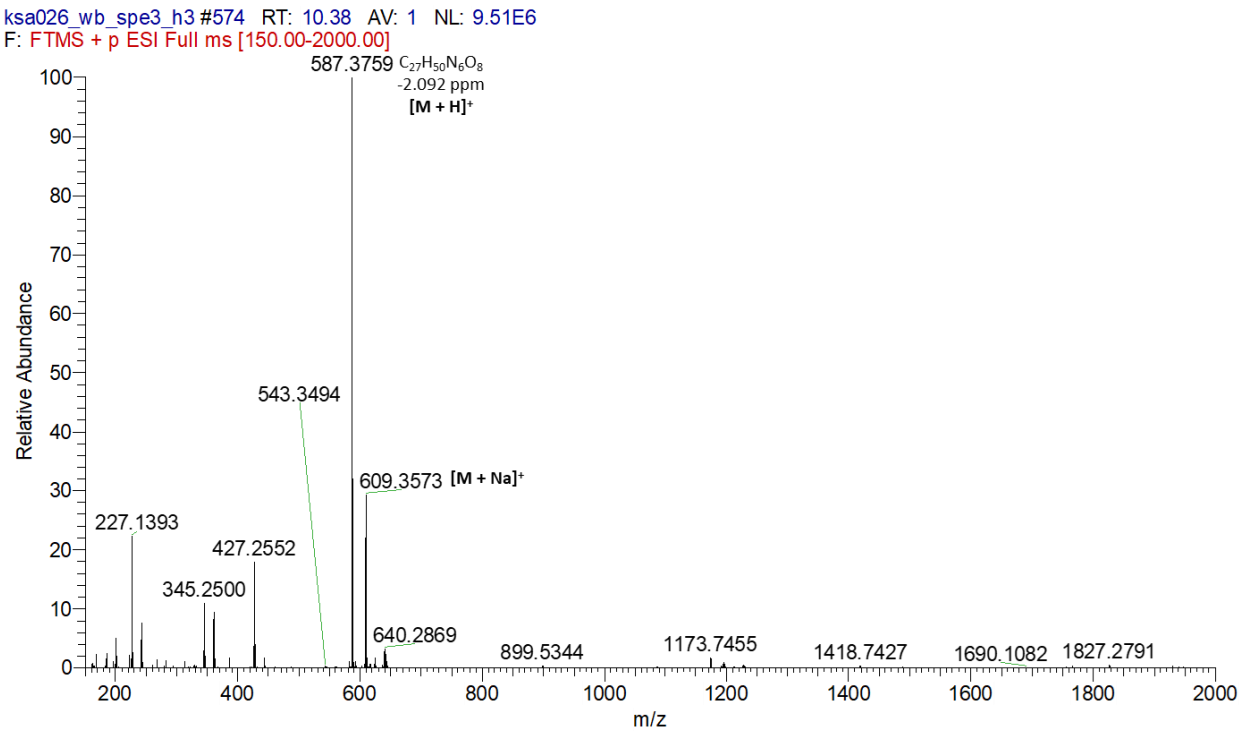

Figure S5.9. HR-ESI-MS spectrum of desoxy-desferrioxmaine D_1 (**5.2**)

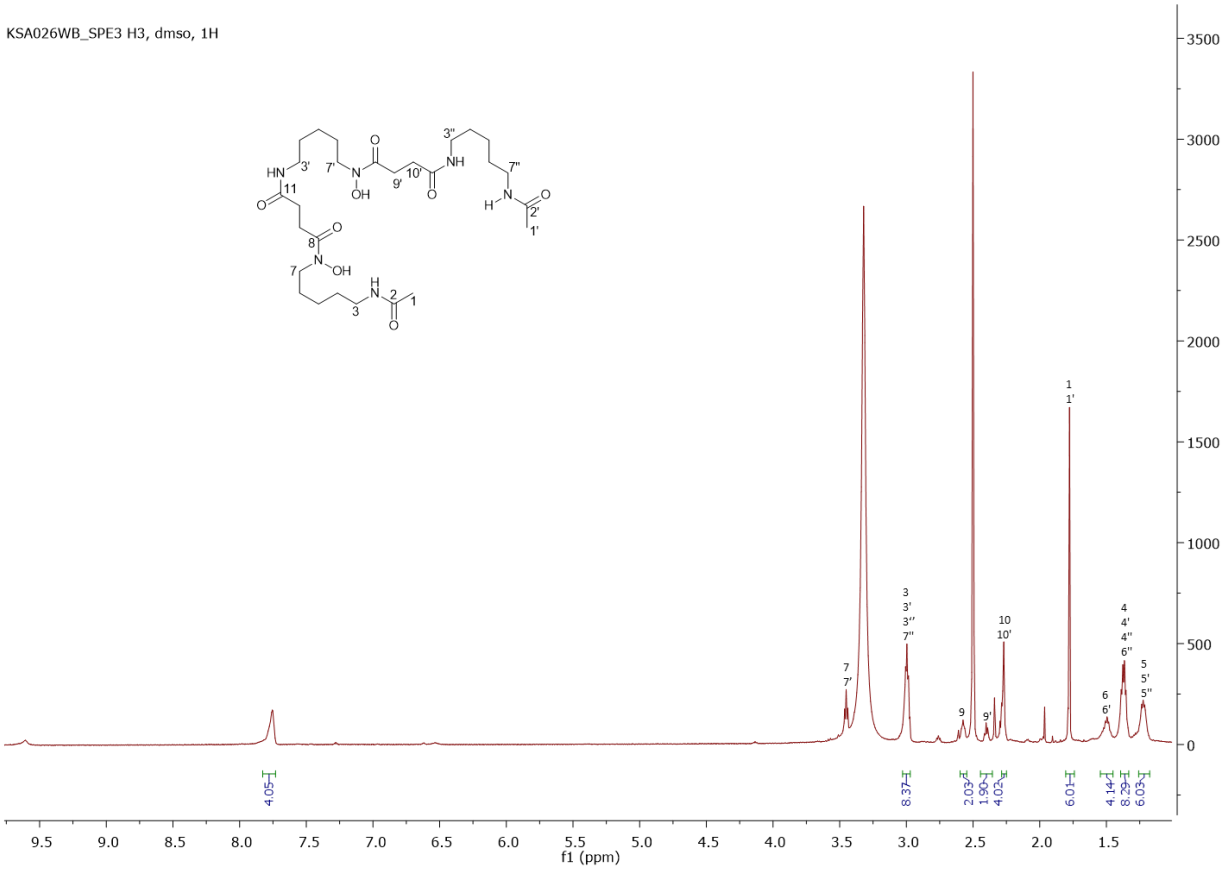

Figure S5.10. ^{1}H-NMR spectrum of desoxy-desferrioxmaine D_1 (**5.2**) in DMSO-d6 at 600 MHz.

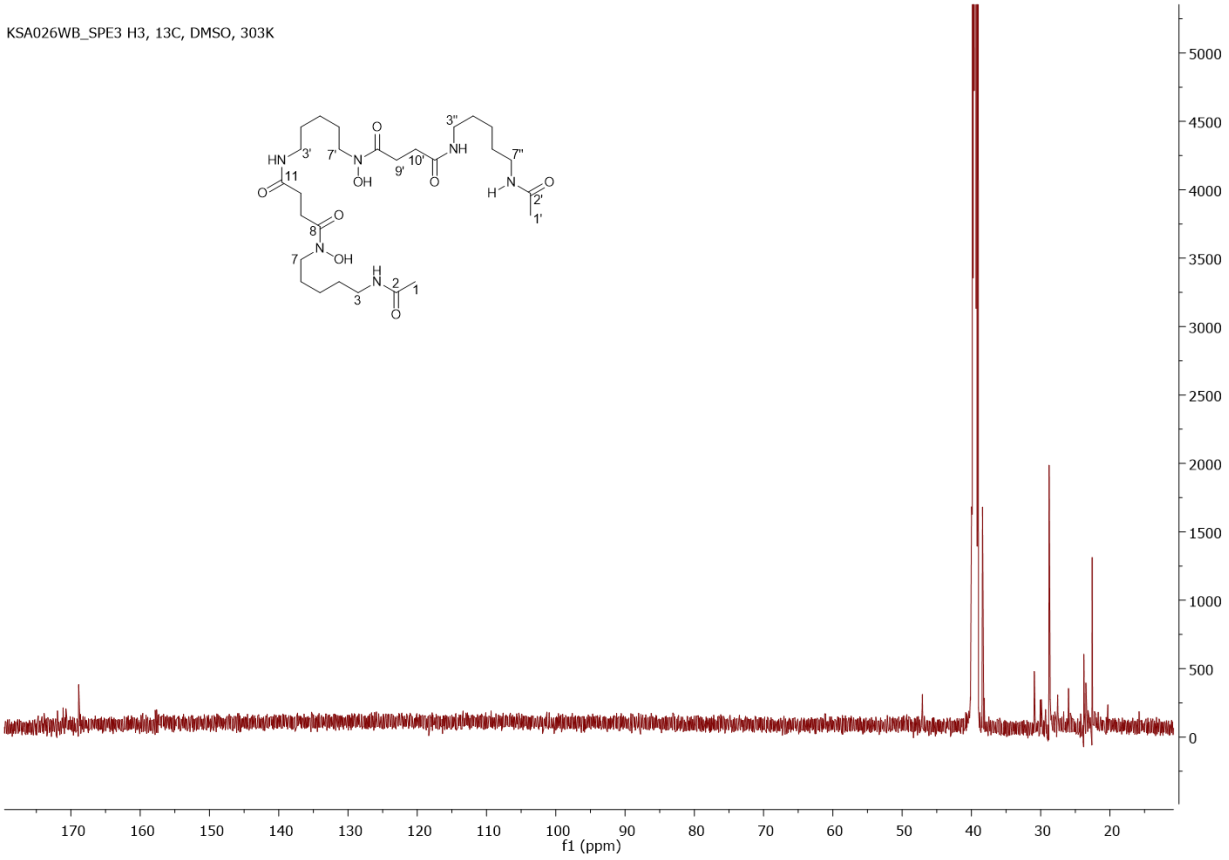

Figure S5.11. ^{13}C-NMR spectrum of desoxy-desferrioxmaine D_1 (**5.2**) in DMSO-d6 at 600 MHz.

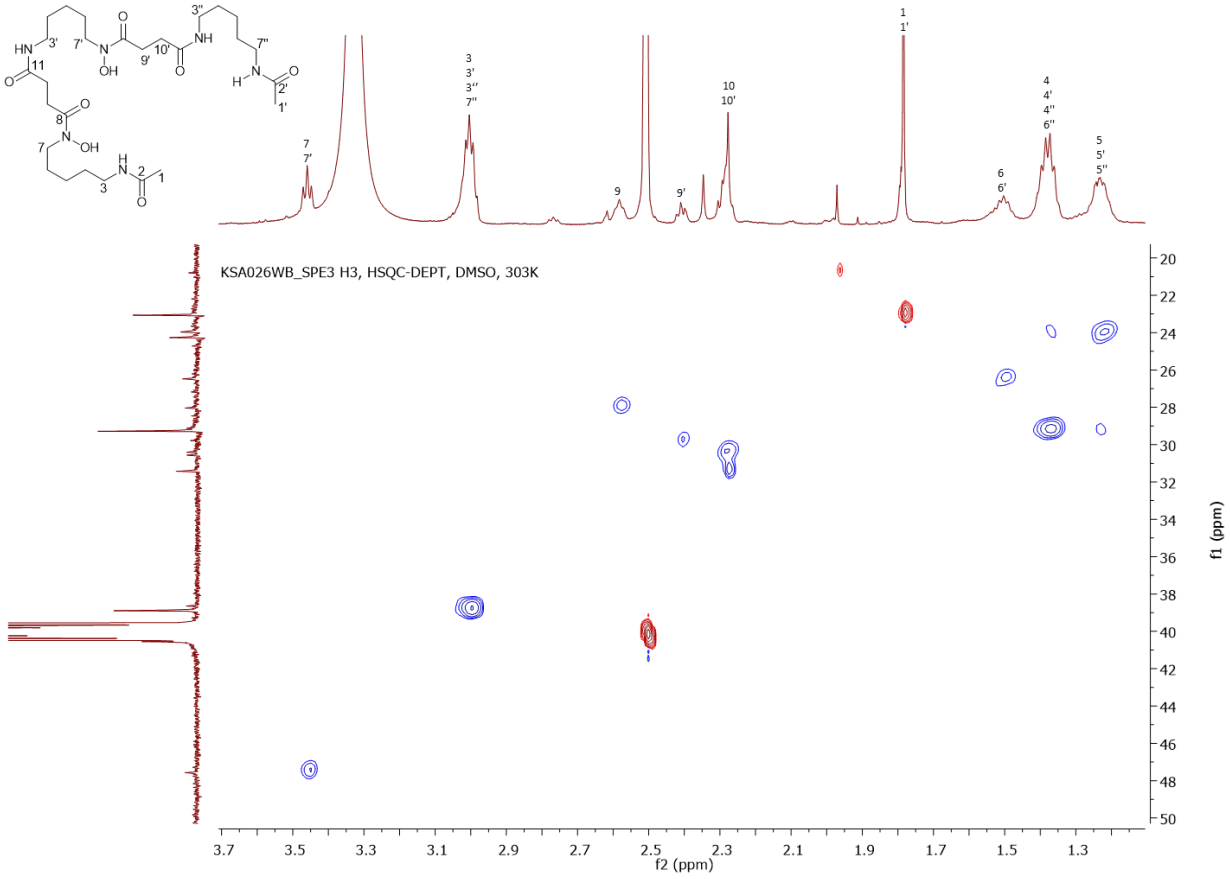

Figure S5.12. Multiplicity edited HSQC NMR spectrum of desoxy-desferrioxmaine D_1 (**5.2**) in DMSO-d6 at 600 MHz.

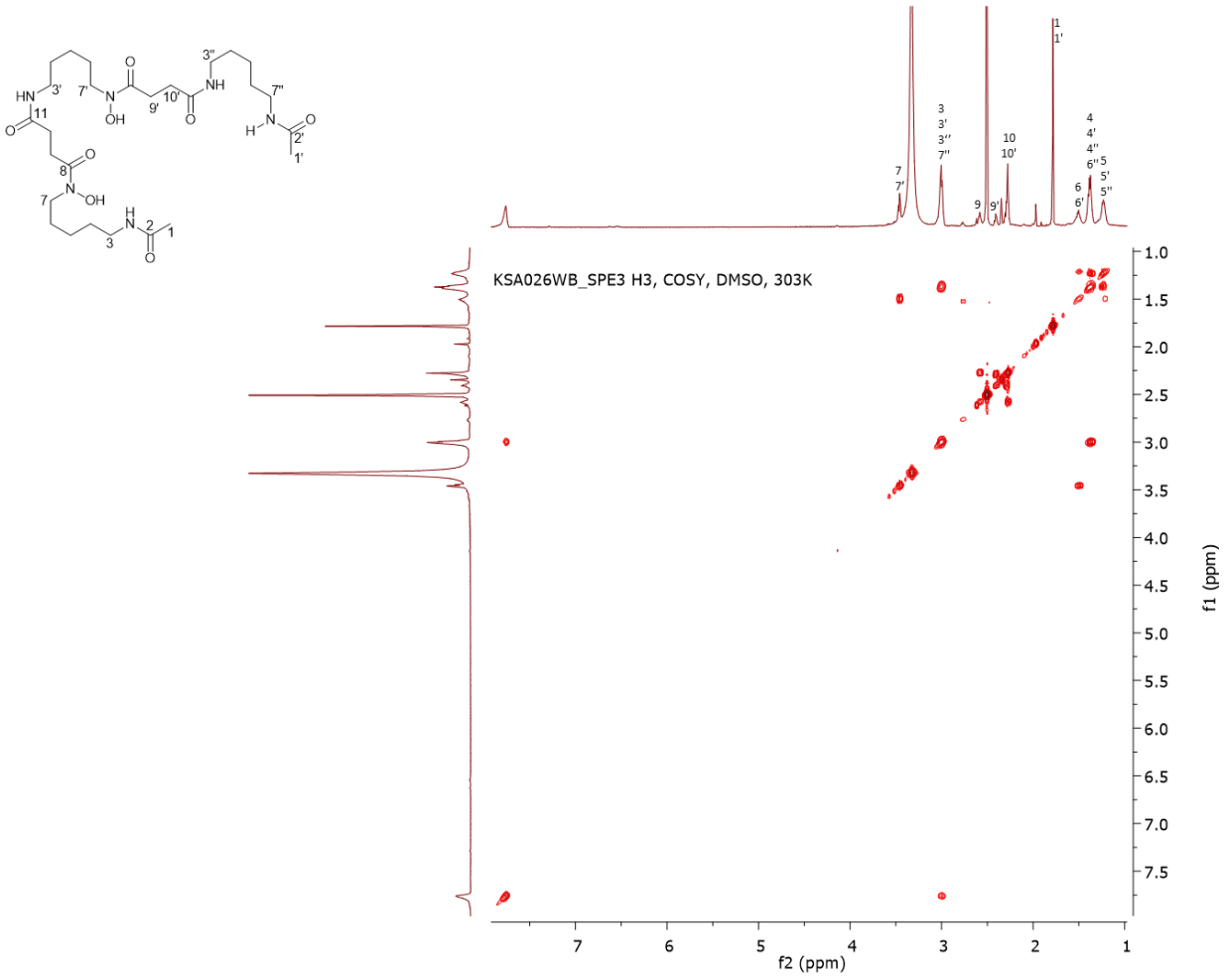

Figure S5.13. ^{1}H-^{1}H COSY spectrum of desoxy-desferrioxmaine D_1 (**5.2**) in DMSO-d6 at 600 MHz.

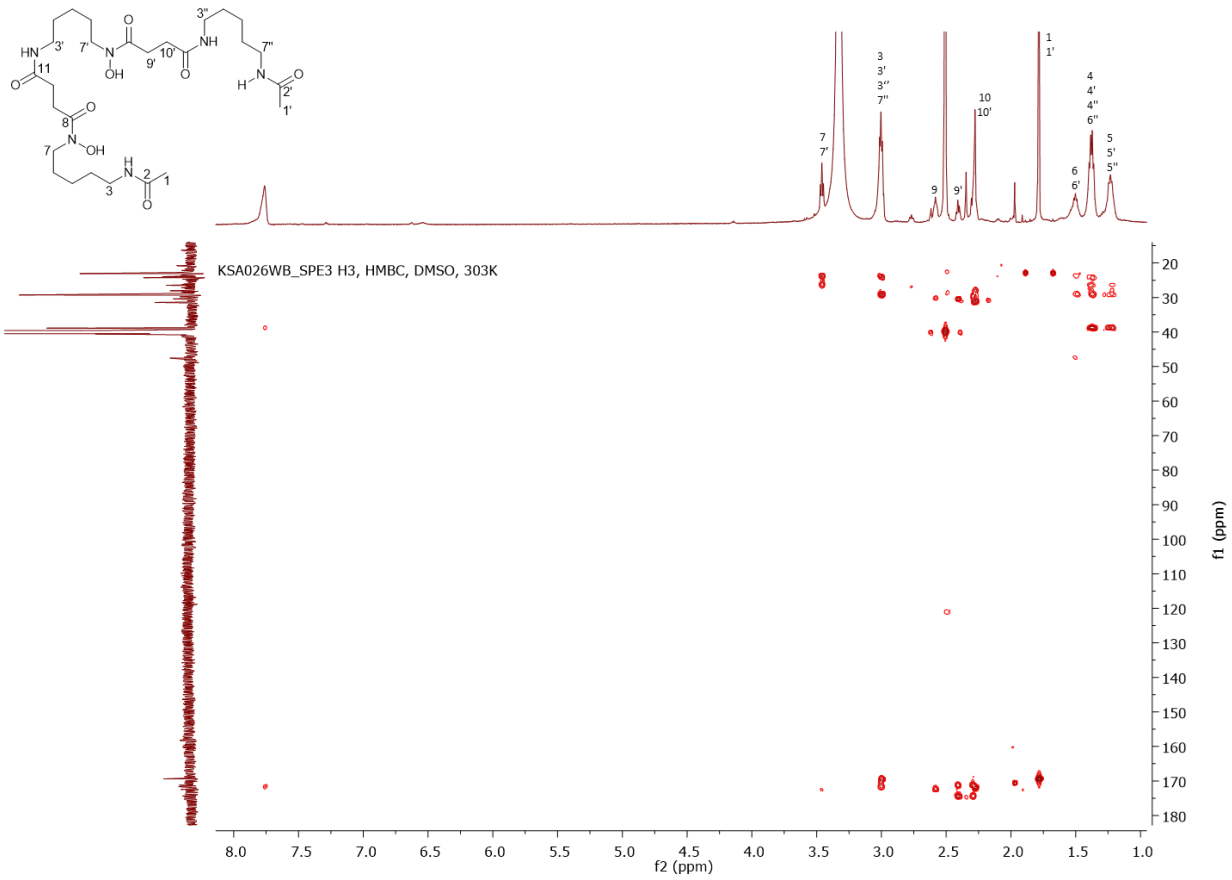

Figure S5.14. HMBC NMR spectrum of desoxy-desferrioxmaine D_1 (**5.2**) in DMSO-d6 at 600 MHz.

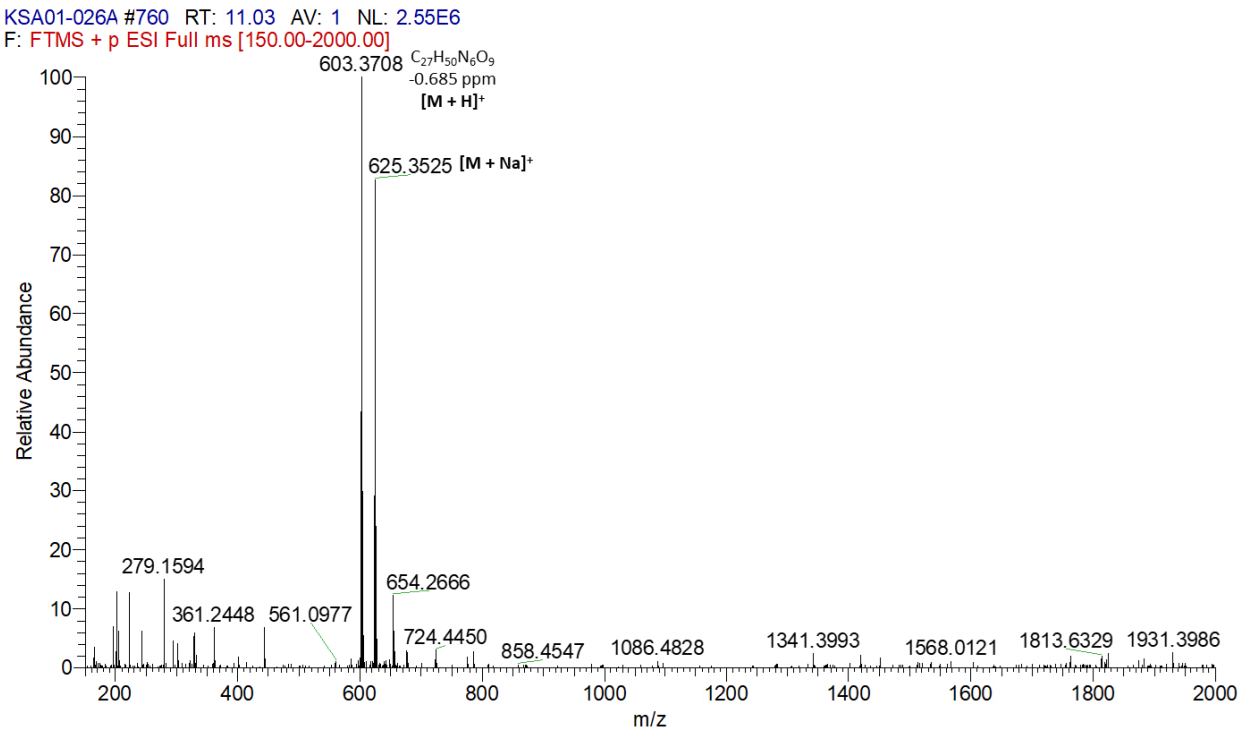

Figure S5.15. HR-ESI-MS spectrum of desferrioxamine D_1 (**5.3**)

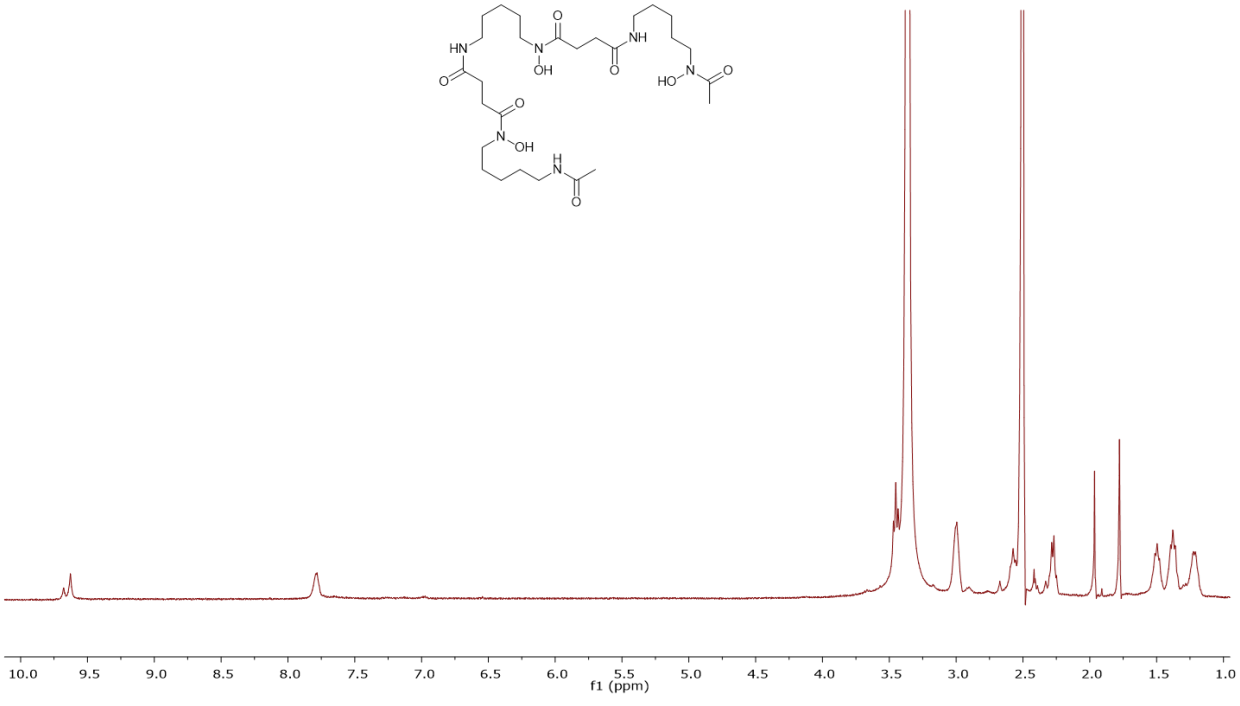

Figure S5.16. ^{1}H-NMR spectrum of desferrioxamine D_1 (**5.3**) in DMSO-d6 at 600 MHz.

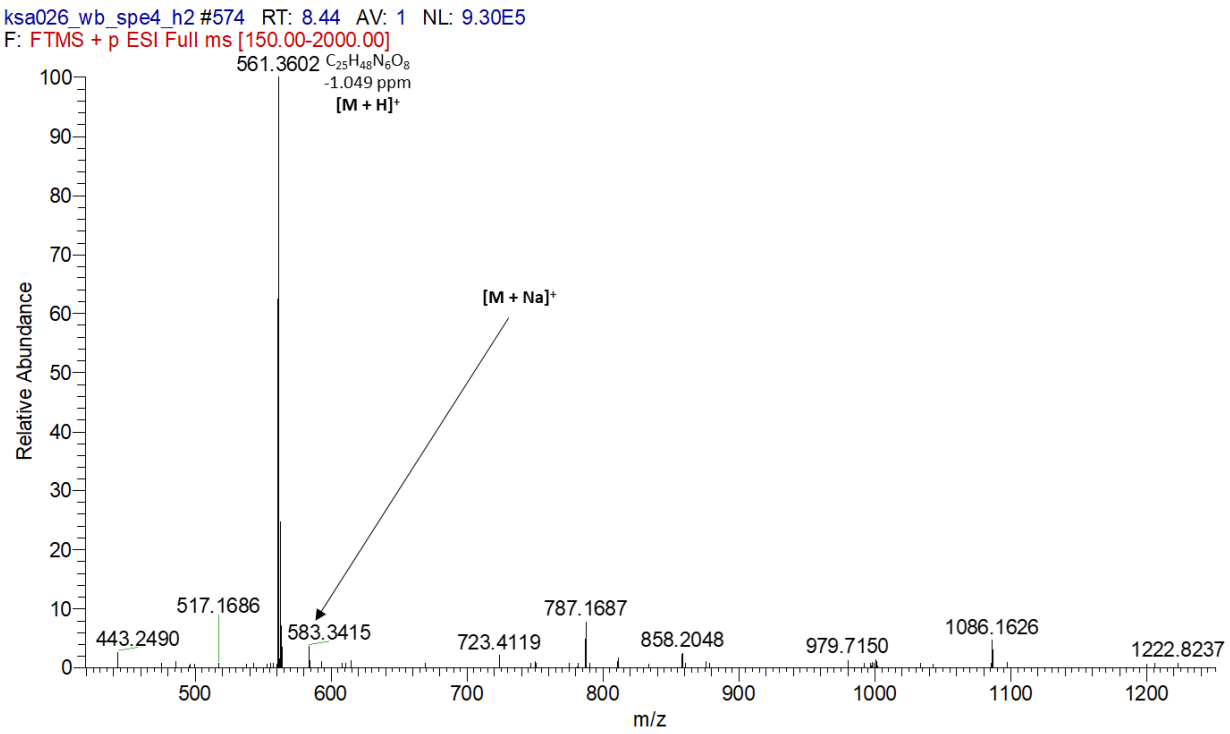

Figure S5.17. HR-ESI-MS spectrum of desferrioxamine B (**5.4**)

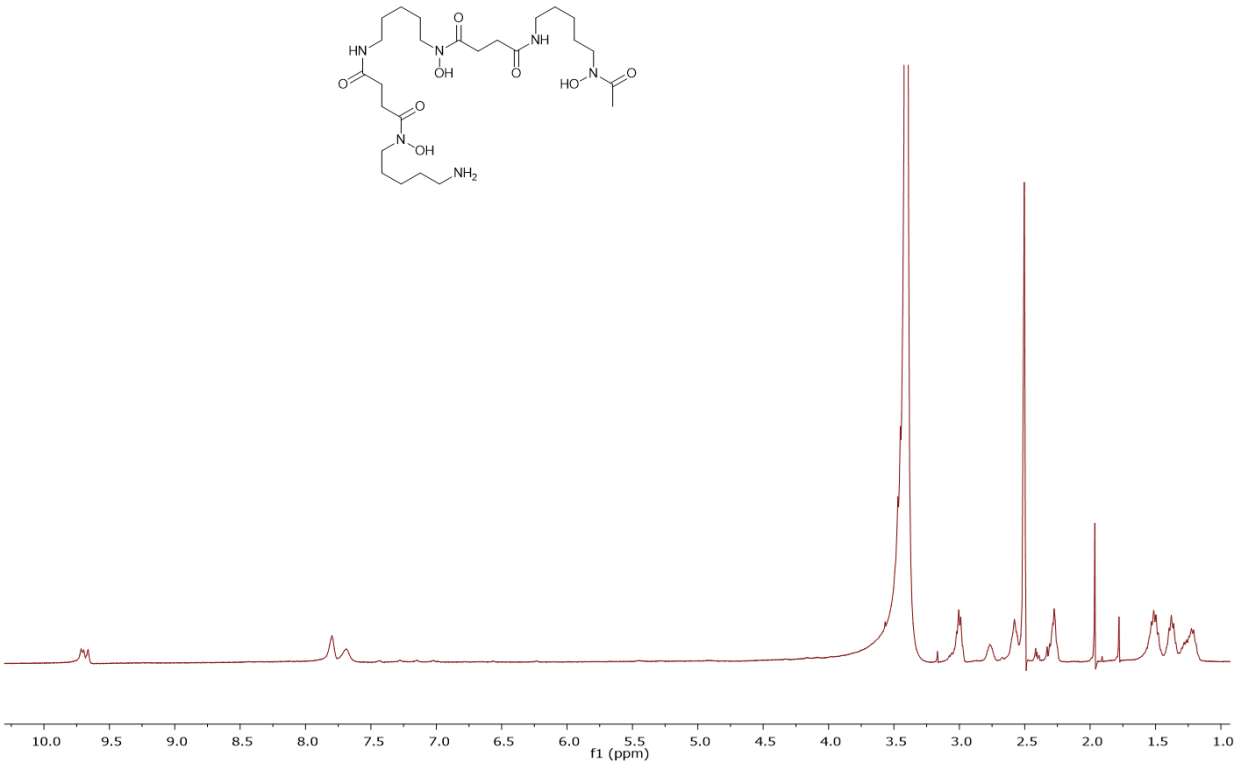

Figure S5.18. ^{1}H-NMR spectrum of desferrioxamine B (**5.4**) in DMSO-d6 at 600 MHz.

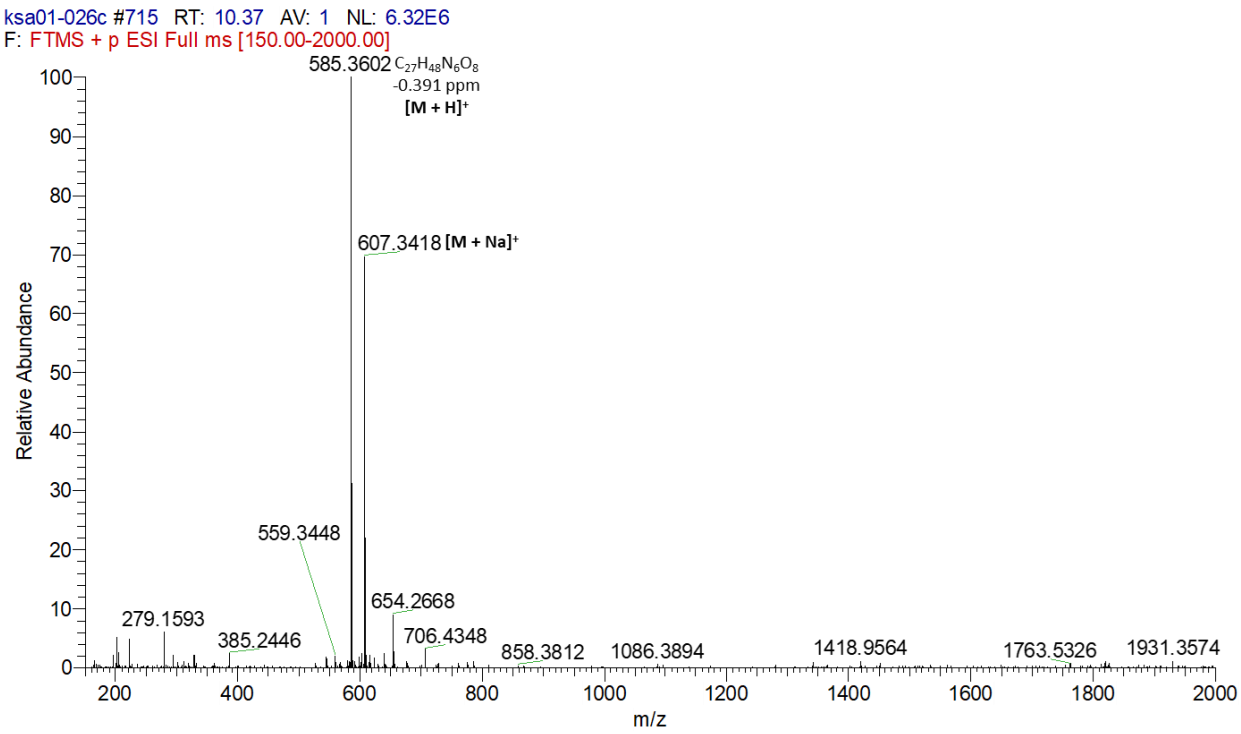

Figure S5.19. HR-ESI-MS spectrum of desoxynocardamine (**5.5**)

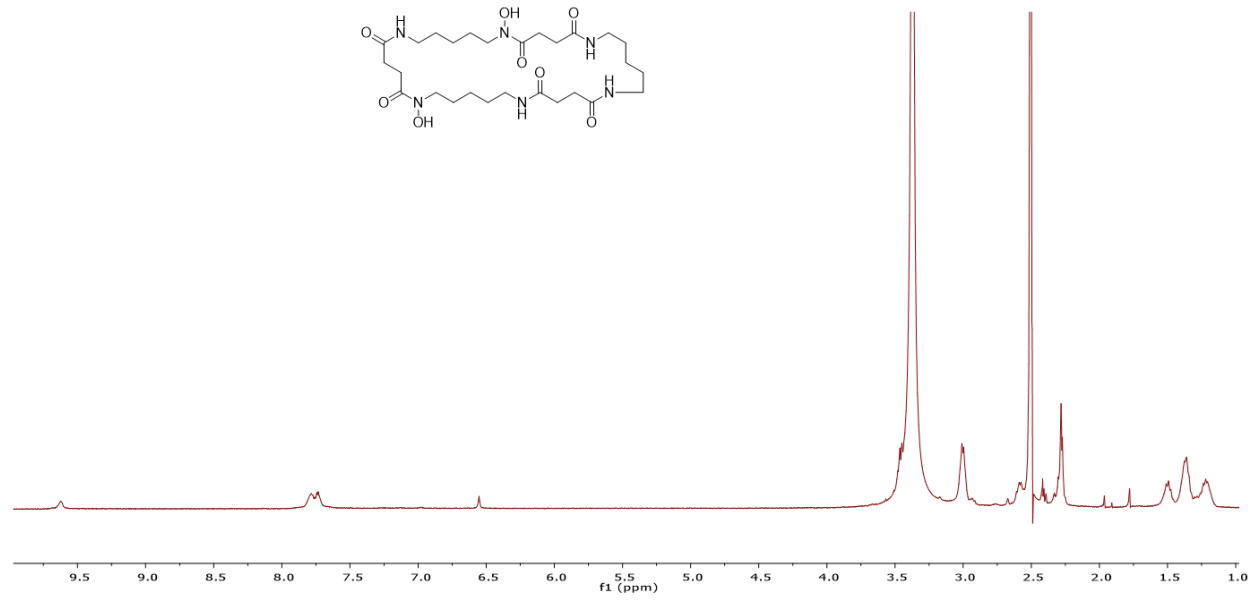

Figure S5.20. ^{1}H-NMR spectrum of desoxynocardamine (**5.5**) in DMSO-d6 at 600 MHz.

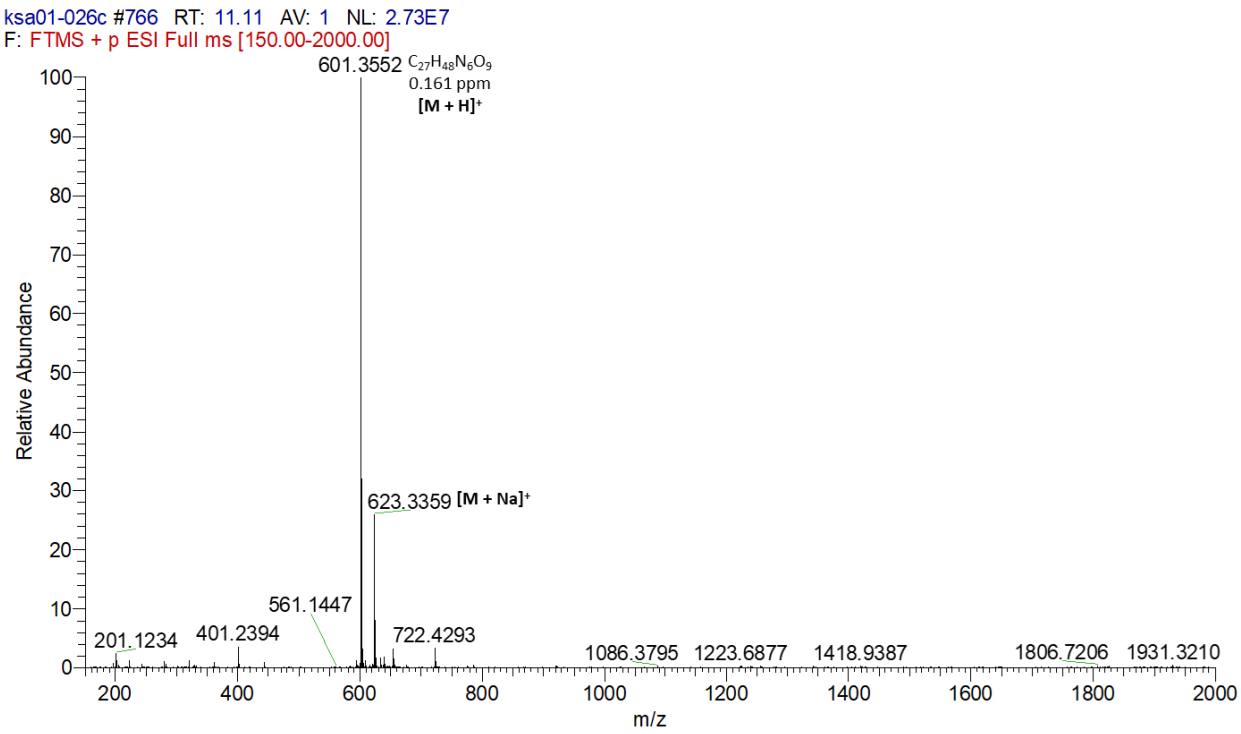

Figure S5.21. HR-ESI-MS spectrum of nocardamine (**5.6**)

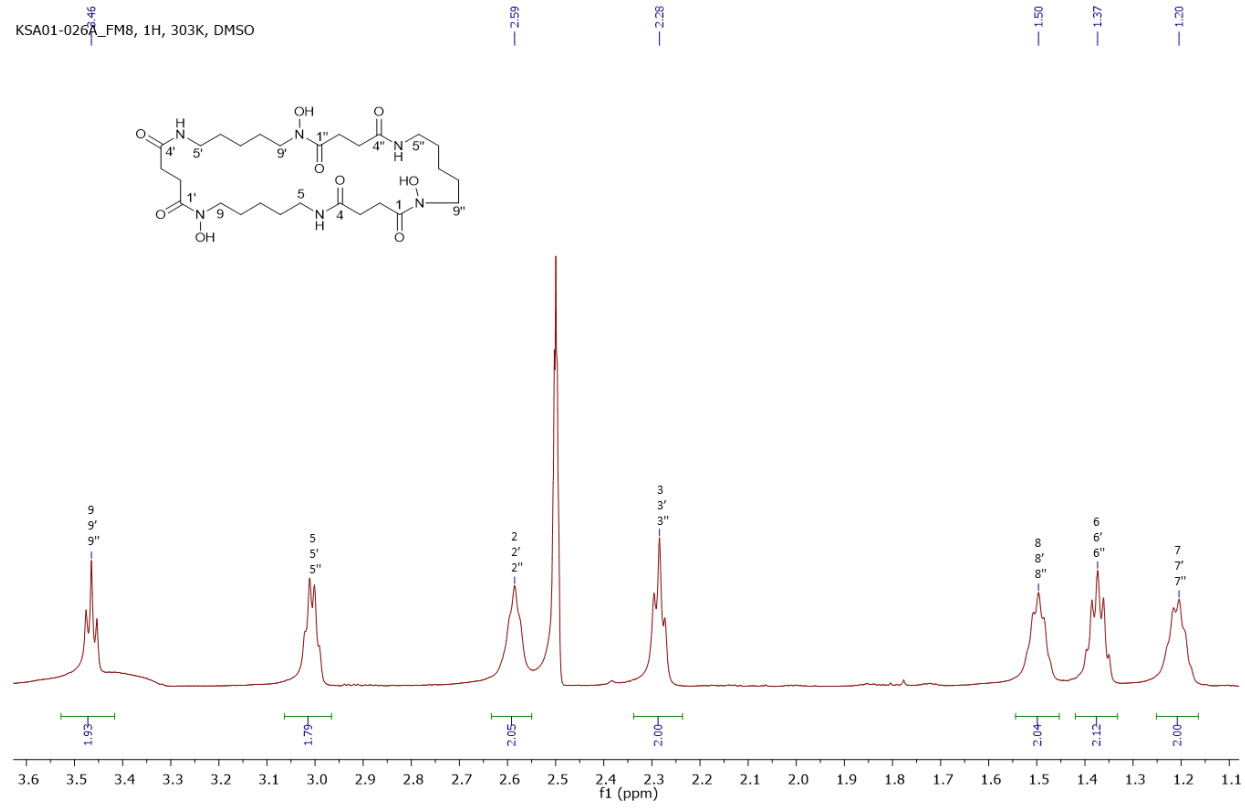

Figure S5.22. ^{1}H-NMR spectrum of nocardamine (**5.6**) in DMSO-d6 at 600 MHz.

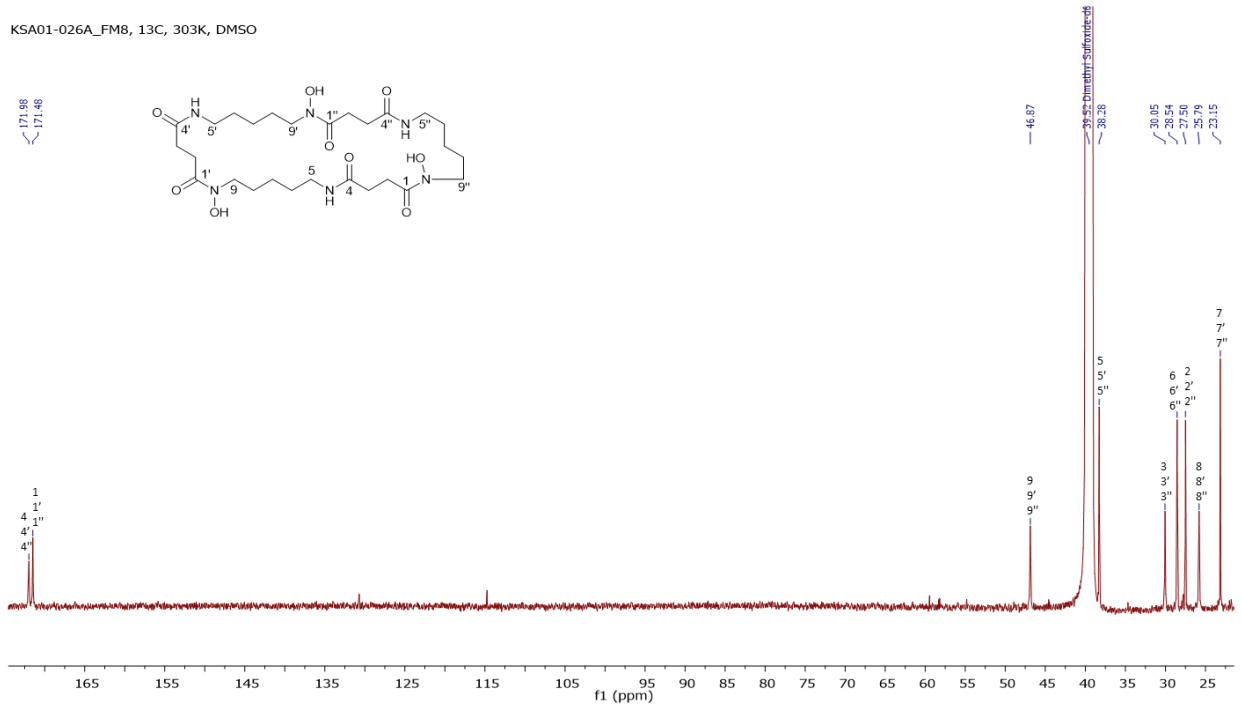

Figure S5.23. ^{13}C-NMR spectrum of nocardamine (**5.6**) in DMSO-d6 at 600 MHz.

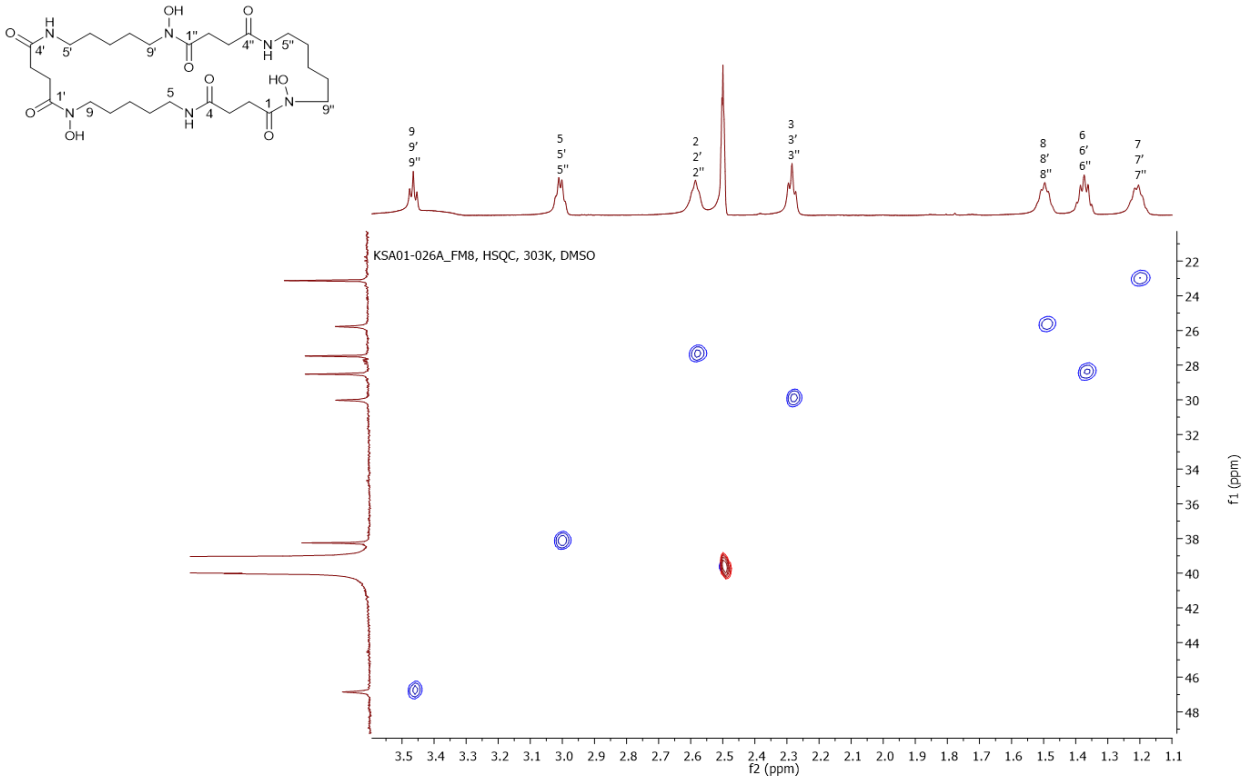

Figure S5.24. Multiplicity edited HSQC NMR spectrum of nocardamine (**5.6**) in DMSO-d6 at 600 MHz.

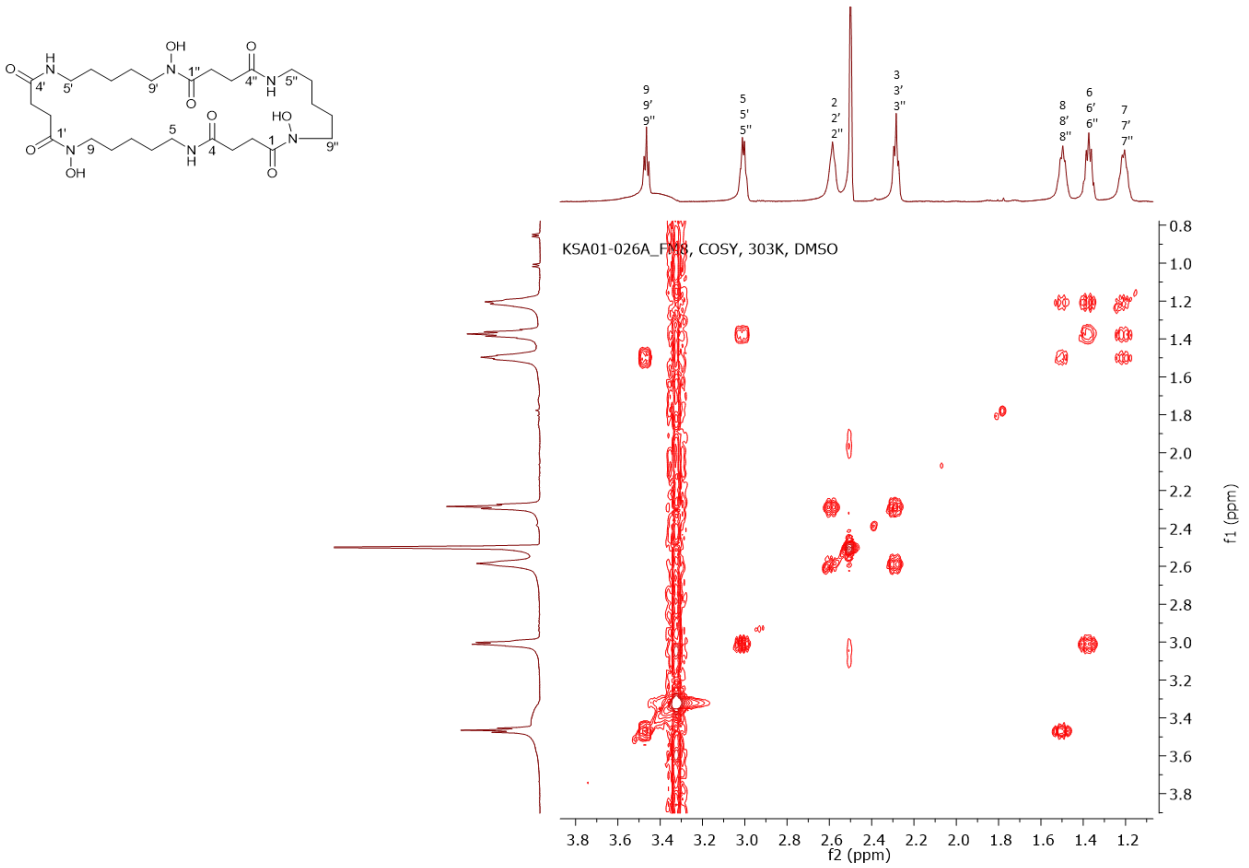

Figure S5.25. ^{1}H-^{1}H COSY spectrum of nocardamine (**5.6**) in DMSO-d6 at 600 MHz.

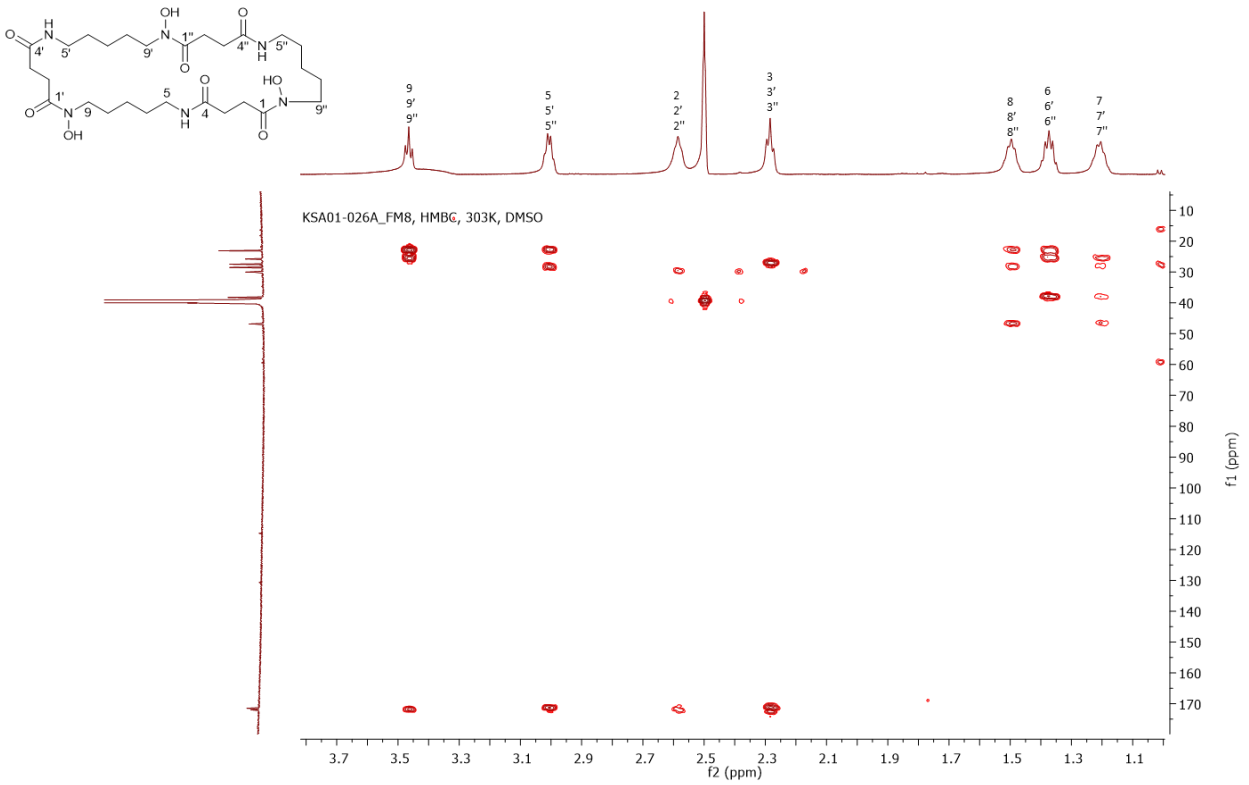

Figure S5.26. HMBC NMR spectrum of nocardamine (**5.6**) in DMSO-d6 at 600 MHz.

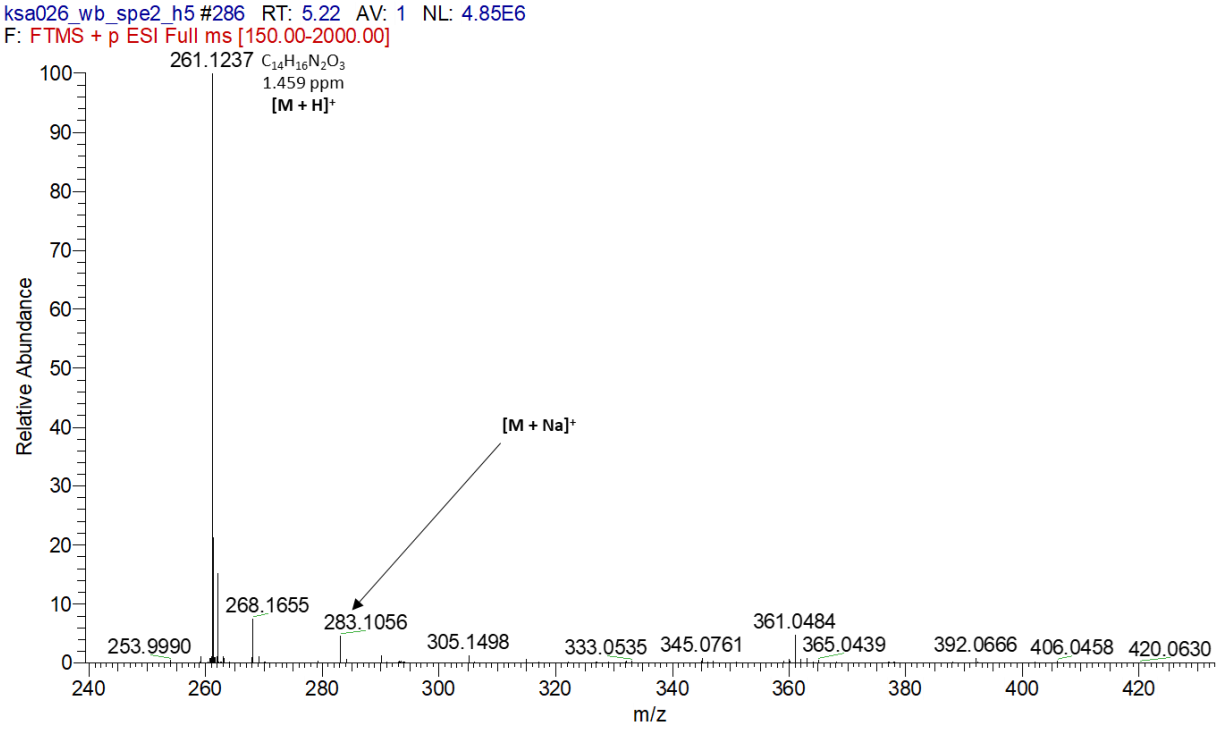

Figure S5.27. HR-ESI-MS spectrum of hexahydro-3-[(4-hydroxyphenyl)methyl]-Pyrrolo[1,2-a] pyrazine-1,4-dione (**5.7**)

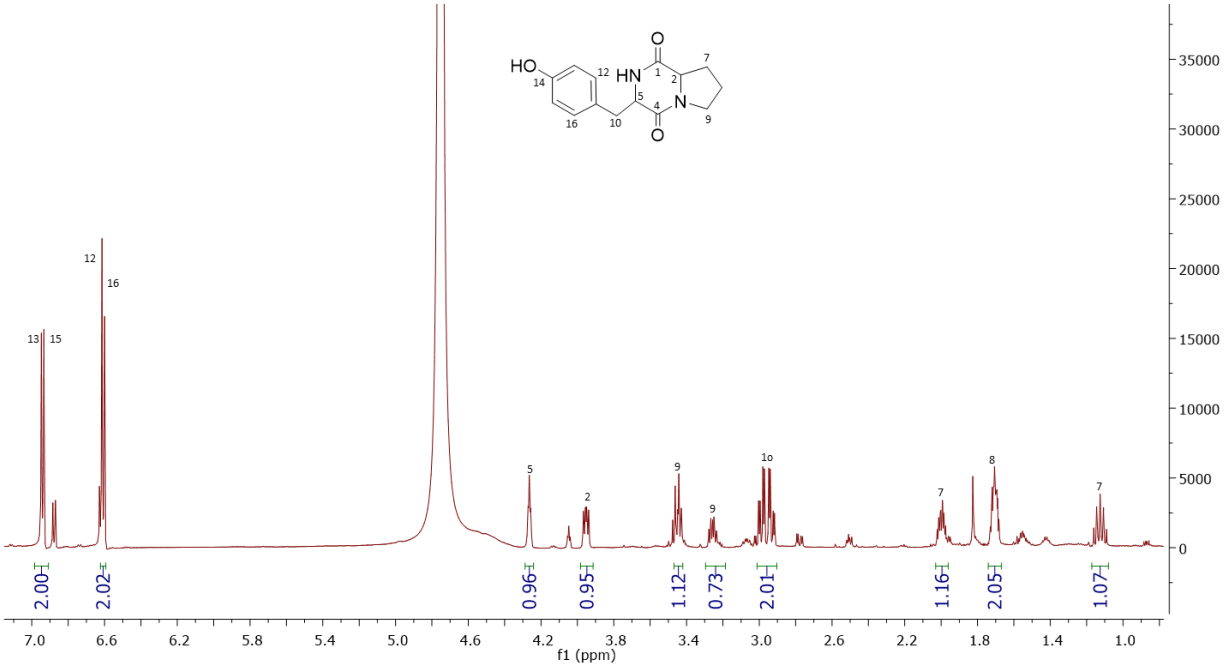

Figure S5.28. ^{1}H-NMR spectrum of hexahydro-3-[(4-hydroxyphenyl)methyl]-Pyrrolo[1,2-a] pyrazine-1,4-dione (**5.7**) in MeOD at 600 MHz

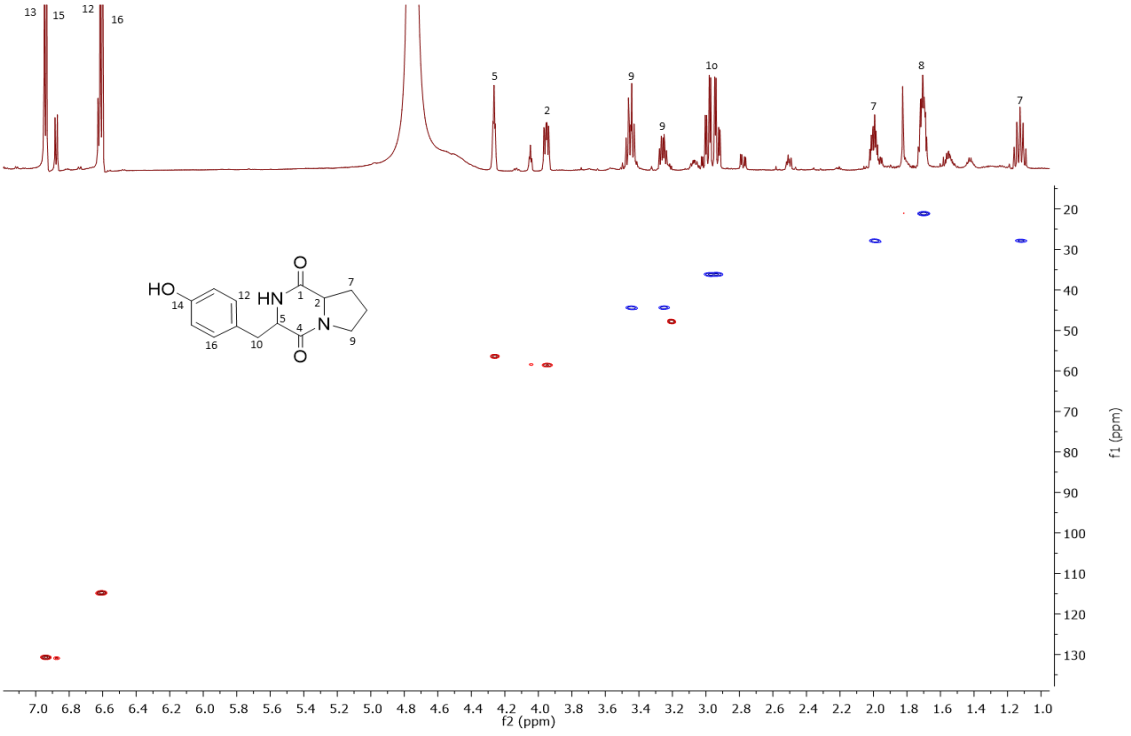

Figure S5.29. Multiplicity edited HSQC NMR spectrum of hexahydro-3-[(4-hydroxyphenyl)methyl]-Pyrrolo[1,2-a]pyrazine-1,4-dione (**5.7**) in MeOD at 600 MHz

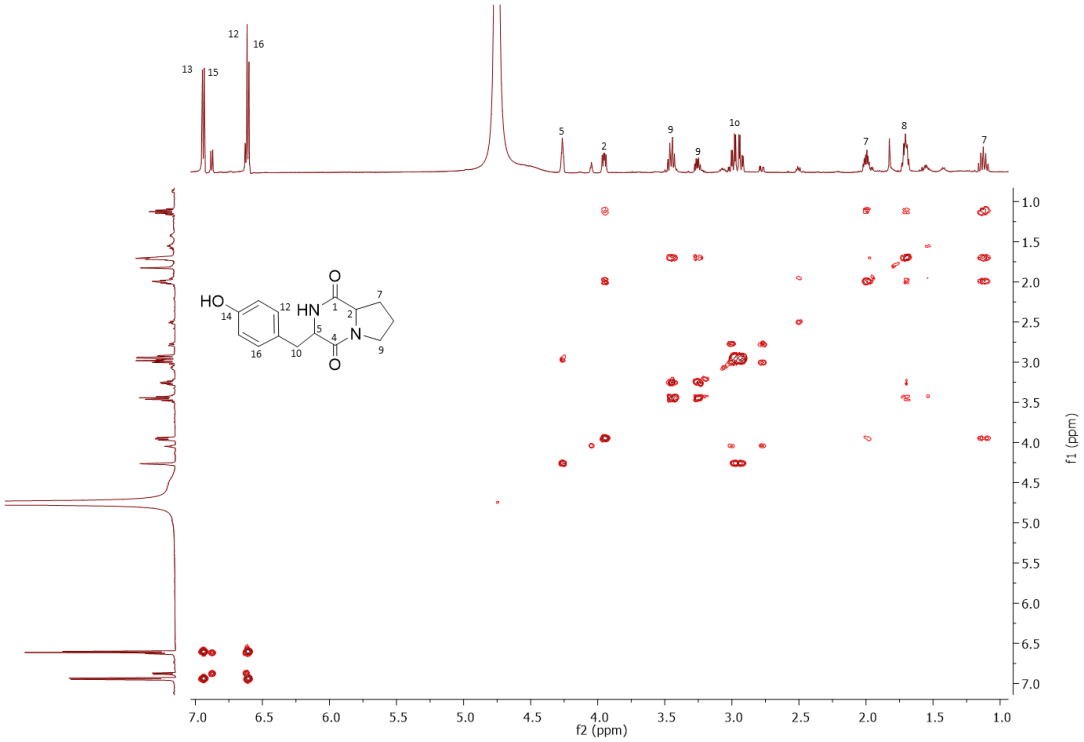

Figure S5.30. ^{1}H-^{1}H COSY spectrum of hexahydro-3-[(4-hydroxyphenyl)methyl]-Pyrrolo[1,2-a] pyrazine-1,4-dione (**5.7**) in MeOD at 600 MHz

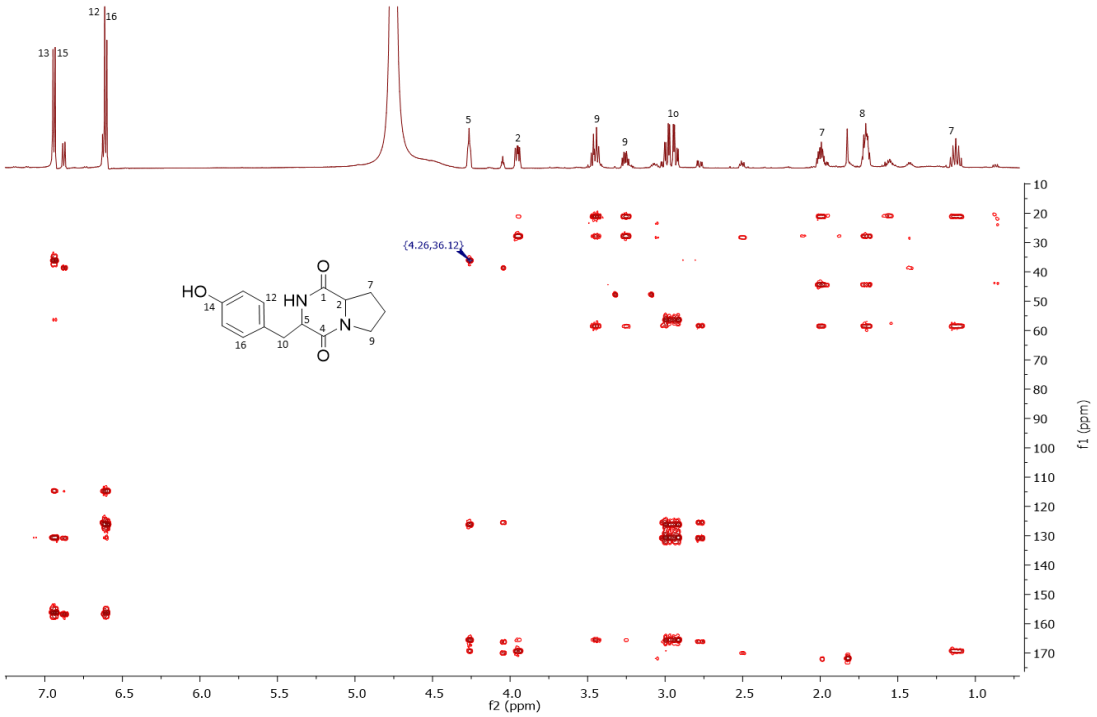

Figure S5.31. HMBC NMR spectrum of hexahydro-3-[(4-hydroxyphenyl)methyl]-Pyrrolo[1,2-a] pyrazine-1,4-dione (**5.7**) in MeOD at 600 MHz

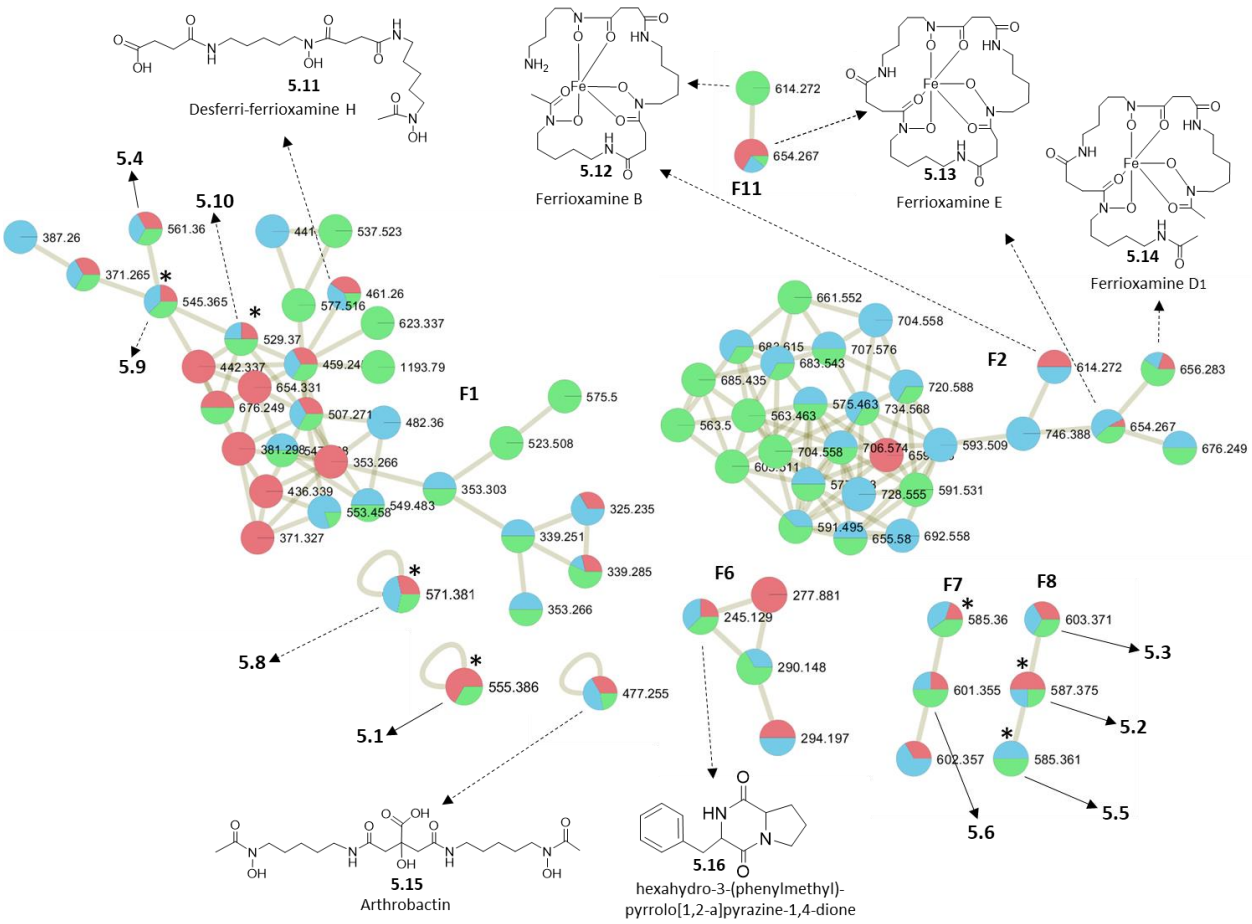

Figure S5.32. Molecular network of the molecular families F1, F2, F6-F8, F11 and the single nodes 477.2555 $[M+H]^+$, 555.3857 $[M+H]^+$ and 571.3807 $[M+H]^+$. Nodes of isolated compounds (**5.1**-**5.6**) are shown with solid arrowed lines while dereplicated nodes (**5.8**-**5.16**) are indicated by dotted arrowed lines. Nodes were represented as pie charts indicating their intensities or percentages in the methanol (red nodes), ethyl acetate (blue nodes) and dichloromethane (green nodes) extracts of the fermentation broth of *K. speibonae* strain SK5. Nodes with asterisk (*) indicate dehydroxylated desferrioxamines.

Figure S5.33. A MN showing a link between nodes *di*desoxy-desferrioxamine D_1 **5.8** (571.3807 $[M+H]^+$) and desoxy-desferrioxamine D_1 **5.2** (587.3754 $[M+H]^+$) when default parameters was used in generating the MN on the GNPS platform.

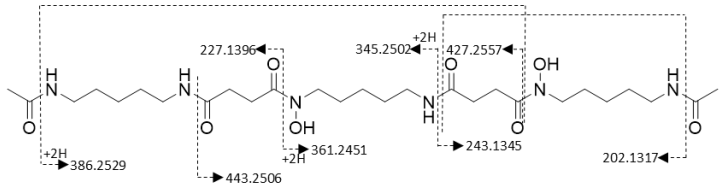

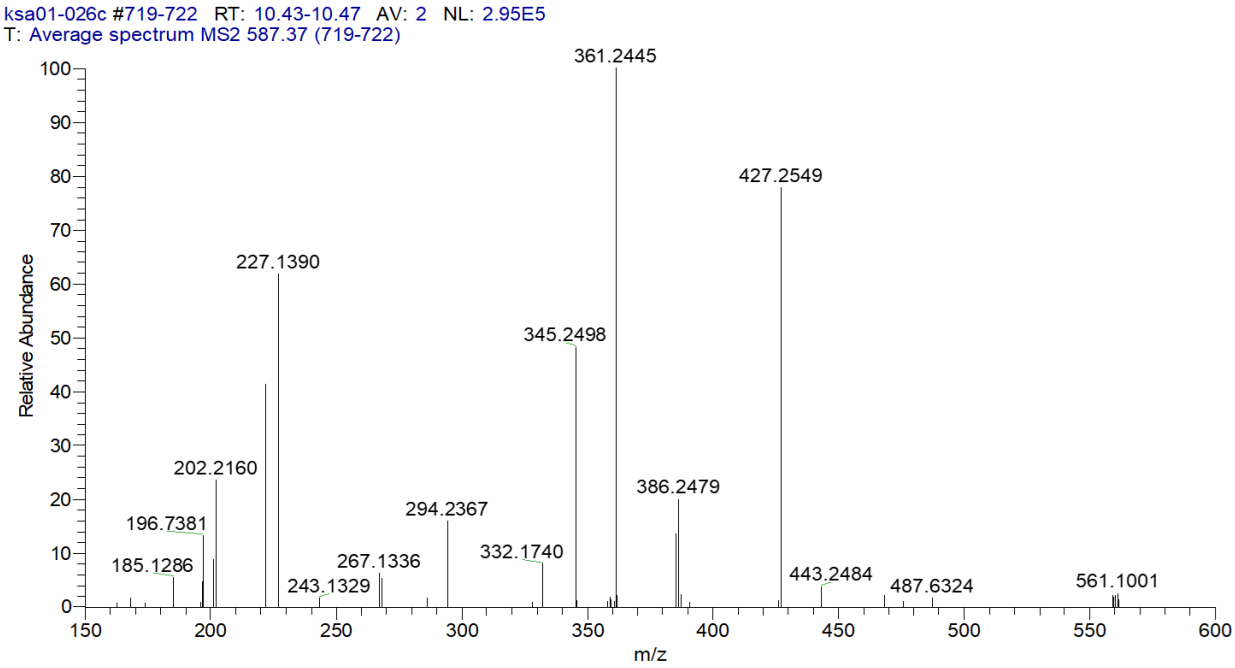

Figure S5.34. MS/MS spectrum of desoxy-desferrioxamine D_1 **5.2** (587.3754 $[M + H]^+$) with annotation in the structure.

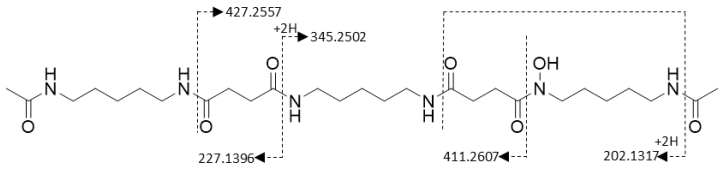

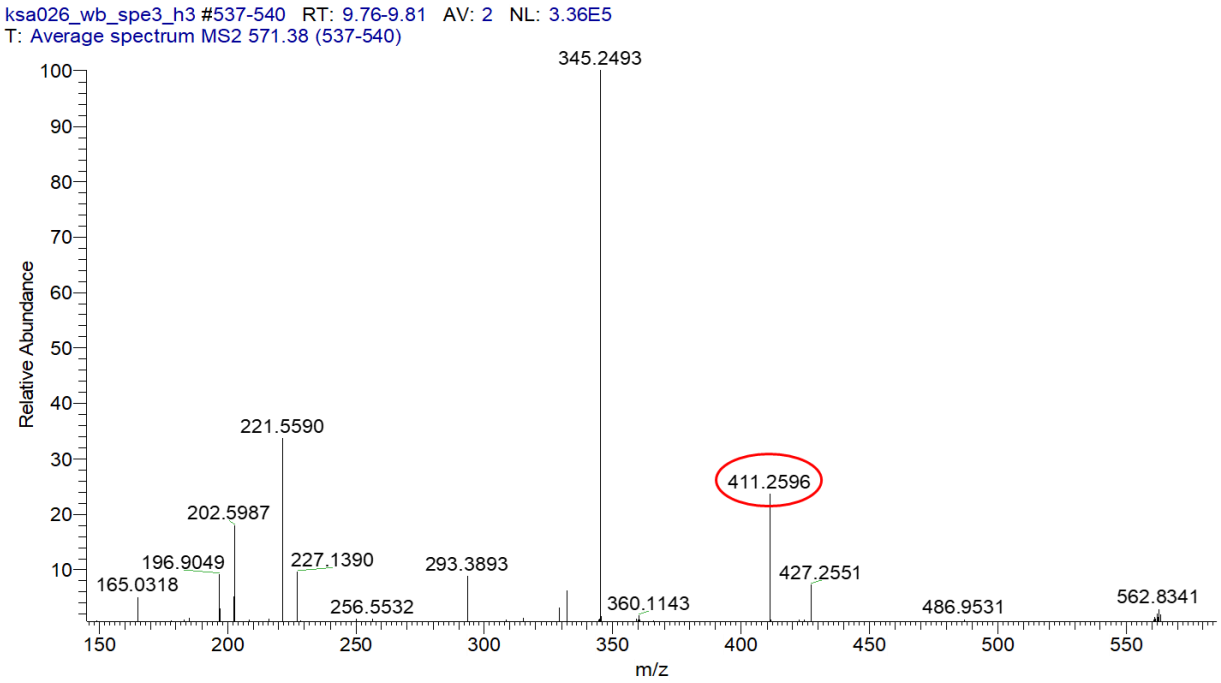

Figure S5.35. MS/MS spectrum of *di*desoxy-desferrioxamine D_1 **5.8** (571.3807 $[M + H]^+$) with annotation in the structure.

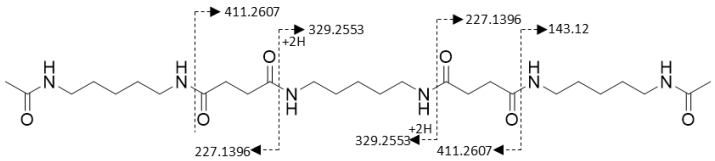

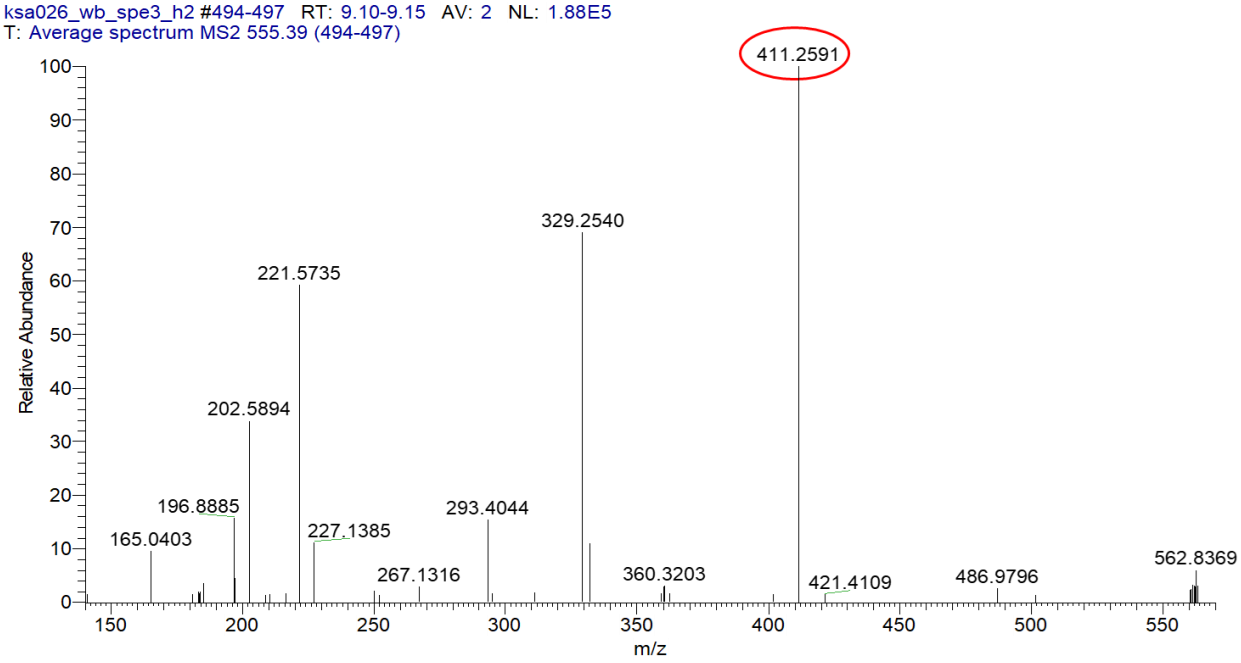

Figure S5.36. MS/MS spectrum of speibonoxamine **5.1** (555.3857 $[M + H]^+$) with annotation in the structure.

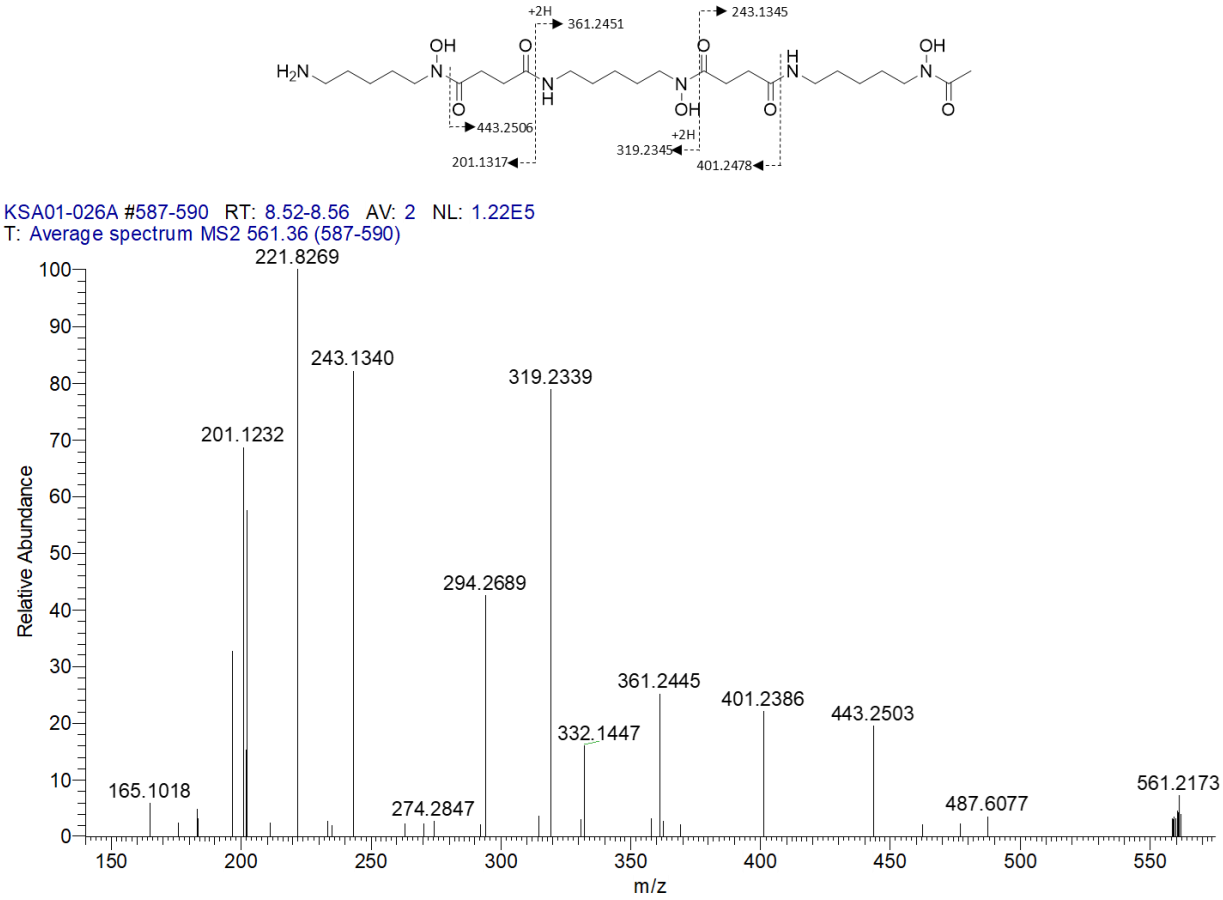

Figure S5.37. MS/MS spectrum of desferrioxamine B **5.4** (561.3606 $[M + H]^+$) with annotation in the structure.

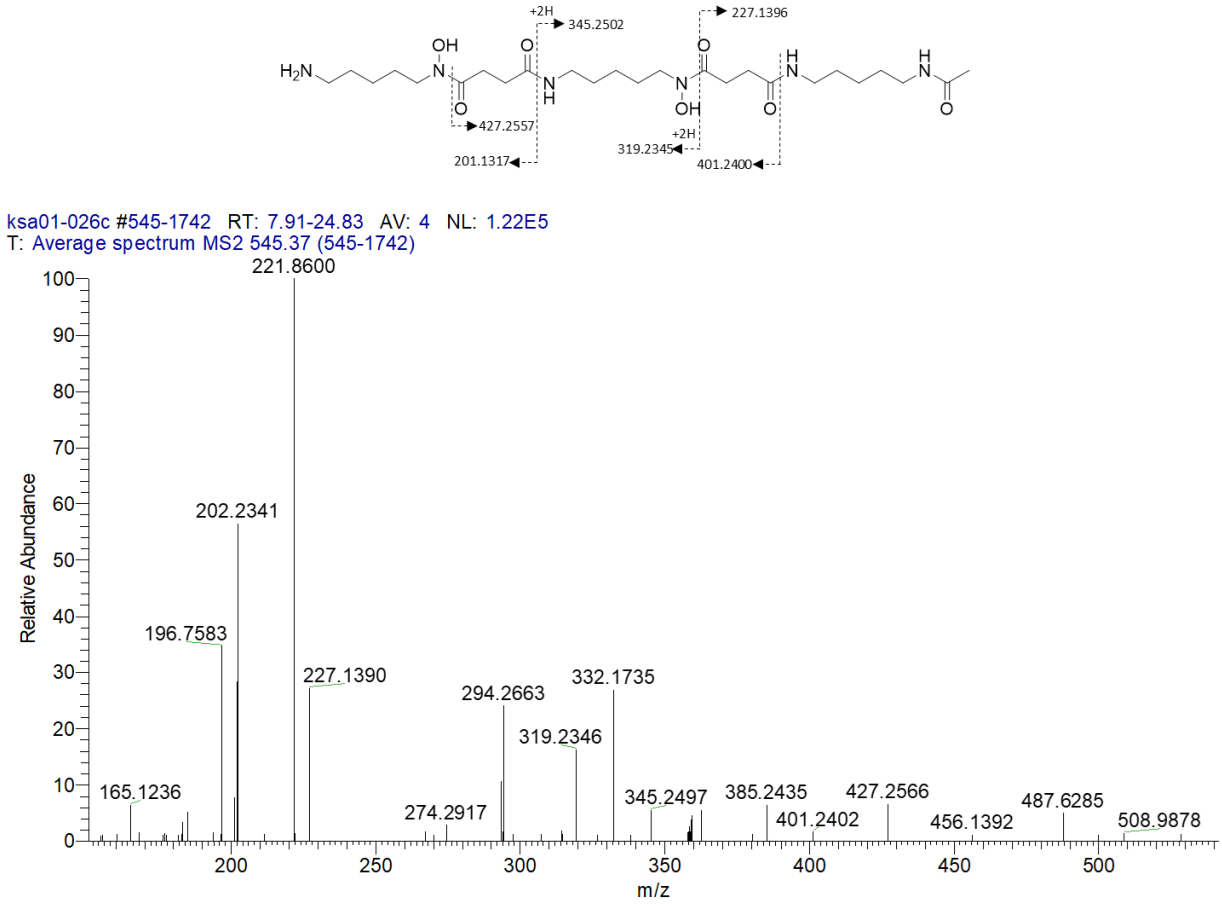

Figure S5.38. MS/MS spectrum desoxy-desferrioxamine B **5.9** (545.3654 $[M + H]^+$) with annotation in the structure.

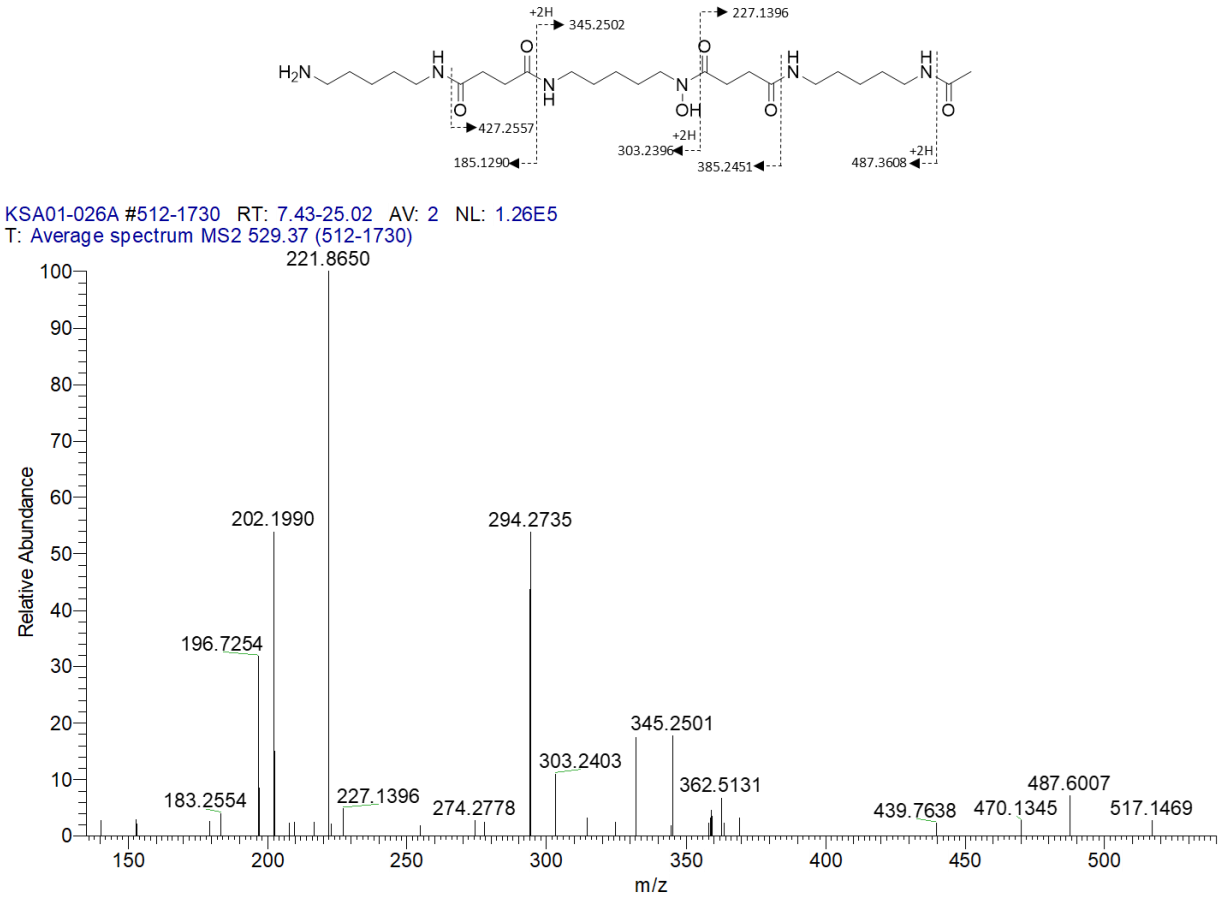

Figure S5.39. MS/MS spectrum *di*desoxy-desferrioxamine B **55.10** (529.3702 $[M + H]^+$) with annotation in the structure.

Table S5.1. Compounds isolated and tentatively identified in the molecular cluster and the MS chromatogram of the fermentation broth of *K. speibonae* strain SK5 with their corresponding masses, molecular formulae (MF), double bond equivalent (DBE), retention time (Rt) and mass error (ID (Δ ppm))

Compound	m/z ($[M+H]^+$)	m/z ($[M+H]^+$) Calculated	MF	DBE	Rt	ID Δ ppm
Speibonoxamine **5.1**	555.3857	555.3870	$C_{27}H_{50}N_6O_6$	6	9.13	1.004
Desoxy-desferrioxamine D_1 **5.2**	587.3754	587.3768	$C_{27}H_{50}N_6O_8$	6	10.41	-2.092
Desferrioxamine D_1 **5.3**	603.3712	603.3718	$C_{27}H_{50}N_6O_9$	6	11.03	-0.685
Desferrioxamine B **5.4**	561.3606	561.3612	$C_{25}H_{48}N_6O_8$	5	8.63	-1.049
Desoxynocardamine **5.5**	585.3606	585.3612	$C_{27}H_{48}N_6O_8$	7	10.40	-0.391
Desferrioxamine E **5.6**	601.3559	601.3561	$C_{27}H_{48}N_6O_9$	7	11.11	0.161
hexahydro-3-[(4-hydroxyphenyl)methyl]-pyrrolo[1,2-a]pyrazine-1,4-dione **5.7**	261.1235	261.1239	$C_{14}H_{16}N_2O_3$	8	5.29	1.459
*Di*desoxy-desferrioxamine D_1 **5.8**	571.3807	571.3819	$C_{27}H_{50}N_6O_7$	6	9.87	-1.005
Desoxy-desferrioxamine B **5.9**	545.3654	545.3663	$C_{25}H_{48}N_6O_7$	5	7.94	-0.668
*Di*desoxy-desferrioxamine B **5.10**	529.3702	529.3714	$C_{25}H_{48}N_6O_6$	5	7.40	-1.076
Desferri-ferrioxamine H **5.11**	461.2606	461.2611	$C_{20}H_{36}N_4O_8$	5	7.99	-0.608
Ferrioxamine B **5.12**	614.2720	614.2727	$C_{25}H_{45}FeN_6O_8$	5	4.89	0.370
Ferrioxamine E **5.13**	654.2670	654.2676	$C_{27}H_{45}FeN_6O_9$	7	6.64	0.330
Ferrioxamine D_1 **5.14**	656.2820	656.2832	$C_{27}H_{47}FeN_6O_9$	6	7.50	0.710
Arthrobactin **5.15**	477.2555	477.2561	$C_{20}H_{36}N_4O_9$		8.63	-0.849
hexahydro-3-(phenylmethyl)-pyrrolo[1,2-a]pyrazine-1,4-dione **5.16**	245.1288	245.1290	$C_{14}H_{16}N_2O_2$	8	9.11	0.961